A geochemical assessment of petroleum from underground oil storage caverns in relation to petroleum from natural reservoirs offshore Norway

Marie Østensen

Master thesis in Geosciences
Petroleum Geology and Geophysics
Department of Geosciences
University of Oslo
Spring 2005

Abstract

The aim of this study is to compare oils from known biodegraded fields offshore Norway to waxes and oils from an artificial cavern storage facility, to determine if the oil degradation processes observed in natural reservoirs offshore are in any way comparable to the processes occurring in oil storage facilities. The sample set contains wax and oil samples from an underground cavern crude oil storage facility and oils from the following fields: Svale, Heidrun, Falk, Draugen, Ula, Oseberg and one sample from the Gulf of Mexico. The analytical procedures used in this study are Iatroscan TLC-FID, GC-FID and GC-MS, and the chromatograms, chemical facies and maturity parameters are used to evaluate the origin and also the processes occurring in the storage tanks.

Wax deposition is a widespread and recurring problem that can occur during any stage of production, transportation and storage of crude oils. High molecular weight hydrocarbons ($>C_{40}$) are generally believed to have the most significant impact on wax deposition problems; and certain case studies have demonstrated that a minimum wax content of 2% in an oil can result in wax deposition.

The samples from the caverns show only a very moderate degree of biodegradation compared to the biodegraded samples from offshore Norway, and they have a rather normal oil composition, very typical for slightly biodegraded oils. The moderate degree of biodegradation may be due to limited access to oxygenated meteoric water, which results in anaerobe conditions. It is uncertain if there is purely inorganic processes, i.e. some sort of gravimetric segregation that leads to the formation of these waxes, or if anoxic bacteria may be involved in the formation of long chained waxy compounds.

This study illustrates that the processes that affects oils in natural reservoirs may not be active in artificial underground oil storage facilities.

Acknowledgements

I would like to thank my supervisor Dr. Dag A. Karlsen for giving me the opportunity to study what I find to be one of the most interesting fields in geology; petroleum geochemistry. I am thankful for all his help and support, and for always making me feel welcome to ask questions.

I would also like to thank Kristian Backer-Owe for his help and guidance in the lab. Jon Halvard Pedersen get my gratitude for data technical support in the final stage of this thesis, you saved me from a lot of last minute stress!

In addition, I would like to thank my family for their support and understanding. My son Kasper is my source of inspiration. Lots of thanks to Øyvind for being there for me and for distracting me with spectacular rock concerts. I would also like to thank my grandfather Jacob, for showing great interest in my studies, for correcting some of the chapters and for contributing to my mineral collection.

Lots of hugs to all my friends for being supportive and cheering me on this last part of my studies.

Last but not least; thanks to all my fellow students at the Department of Geosciences, we have had a lot of fun together!

Oslo, May 2005

Marie Østensen

Contents

1. Introduction

Petroleum geochemistry is the application of chemical principles to the study of the origin, migration, accumulation, and alteration of petroleum (oil and gas) and the use of this knowledge in exploring for and recovering petroleum (Hunt, 1996).

A biological marker, or biomarker, is a molecule synthesized by a plant or animal and unchanged, or having suffered only minor subsequent changes, with preservation of the carbon skeleton (Tissot and Welte, 1978). The biomarker is therefore representing a fingerprint of the geochemical input and the pH/Eh conditions of the palaeodepositional environments that resulted in organic matter becoming incorporated into the sediment. Petroleum contains a small amount (~1% and less) of biomarkers. The biomarkers can inform about the genetic relationship between petroleums, the amount of petroleum expelled and the quality and maturity of the source rock from which the petroleum originated.

Wax deposition is a widespread and recurring problem that can occur during any stage of production, transportation and storage of crude oils. High molecular weight hydrocarbons ($>C_{40}$) are generally believed to have the most significant impact on wax deposition problems; and certain case studies have demonstrated that a minimum wax content of 2% in an oil can result in wax deposition (Holder and Winkler, 1965; Tuttle, 1983; Ajienka and Ikoku, 1990).

The scope of this thesis is to investigate if oil degradation processes are in any way relevant to processes occurring in underground storage facilities on land (artificial traps in rock) to those observed in natural reservoirs offshore. Degradation in offshore environments is basically associated with bacterial oxidation and loss of normal alkanes which increases the viscosity and reduces the API of the oils, thereby reducing the price per barrel. In storage tanks is it possible that similar processes are operational, but access to moving oxygenated water may be a limiting factor, and more so than in natural reservoirs is gravitational segregation of heavy oil components - including wax formation – indicated to take place. Furthermore, it is possible that anoxic conditions exist in sub-surface cavern storage facilities for oil and that this has influenced

some of the oils in this data set. Samples from known biodegradated fields offshore Norway will be compared to oil and wax samples from an underground oil storage facility.

The analytical procedures used in this study are Iatroscan TLC-FID, GC-FID and GC-MS, and the chromatograms, chemical facies and maturity parameters are used to evaluate the origin and also the processes occurring in the storage tanks.

The work was undertaken within the time frame of a Master thesis (20 weeks).

2. The sample set

This chapter is a short description of the samples studied in this thesis.

The sample set consists of 4 waxy oil samples and 13 oil samples:

- 4 waxy oil samples and 2 oil samples from an underground crude oil storage facility
- 2 samples from the Svale field
- 4 samples from the Heidrun field
- 1 sample from the Falk discovery
- 1 sample from the Draugen field
- 1 sample from the Mexican Gulf
- 1 sample from the Ula field
- 1 sample from the Oseberg field (NSO-1)

Svale, Heidrun, Falk and Draugen are located in the Haltenbanken Area. Figure 2.1 is a map showing the locations of these fields.

The T samples

The T samples are from a natural rock cavity underground crude oil storage facility. The samples are from the residue left over after the cavern was emptied by pumping out most of the oil. The residue is composed of heavy oil and waxy deposits, lining the bottom of the cave. Piston coring allowed retrieval of the material.

Description of the core material:

Core T3-2: This sample is taken from the bottom layer, and consists of heavy and viscous bitumen. This sample is taken 60 cm up over the bottom of the core, which represent the bottom of the cave.

Core T4-1: This core contains a waxy bitumen deposit. The sample is taken from a point 15 cm below the top of the wax layer.

Core T5-2: This sample is a waxy bitumen. The sample is taken 20 cm down from the top level.
Core T6-1: This core contains a waxy bitumen, with a light H_2S smell. The sample is taken 50 cm below the top layer.

T4 and **T5** are oils that were floating on top of the cores.

Svale1 and Svale2

These samples are from the Svale field in the Haltenbanken area. See the location on figure 2.1.

6507/7-2 DST2, 6507/7-4 DST1, 6507/7-4 DST3 and 6507/7-5 DST2A

These samples are from the Heidrun field. H1 are produced from the Tilje Formation, while H2, H3 and H4 are produced from the Garn Formation (Karlsen et al., 1995).

6608/11-2

This sample is from the Falk discovery. The Falk discovery occurs near the Svale discovery in the Haltenbanken area, see figure 2.1.

6407/9-5 DST 1

This sample is from the Draugen field, and was produced from the Upper Jurassic Rogn Formation (Karlsen et al., 1995).

B IMP

This oil sample is from the Gulf of Mexico, and its origin is from the Cretaceous La Luna formation. It was taken from the giant Cantarell field in the Gulf of Mexico.

7/12-6 DST 1

This sample is from the Ula field, located in the Central Graben of the Norwegian Continental shelf, and was produced from the Upper Jurassic Ula Formation

NSO-1

This sample is from the Oseberg field, and is the North Sea Oil standard used by the Norwegian Petroleum Directorate. It is now used to calibrate laboratory instruments that are used to analyze petroleum (Weiss et al., 2000).

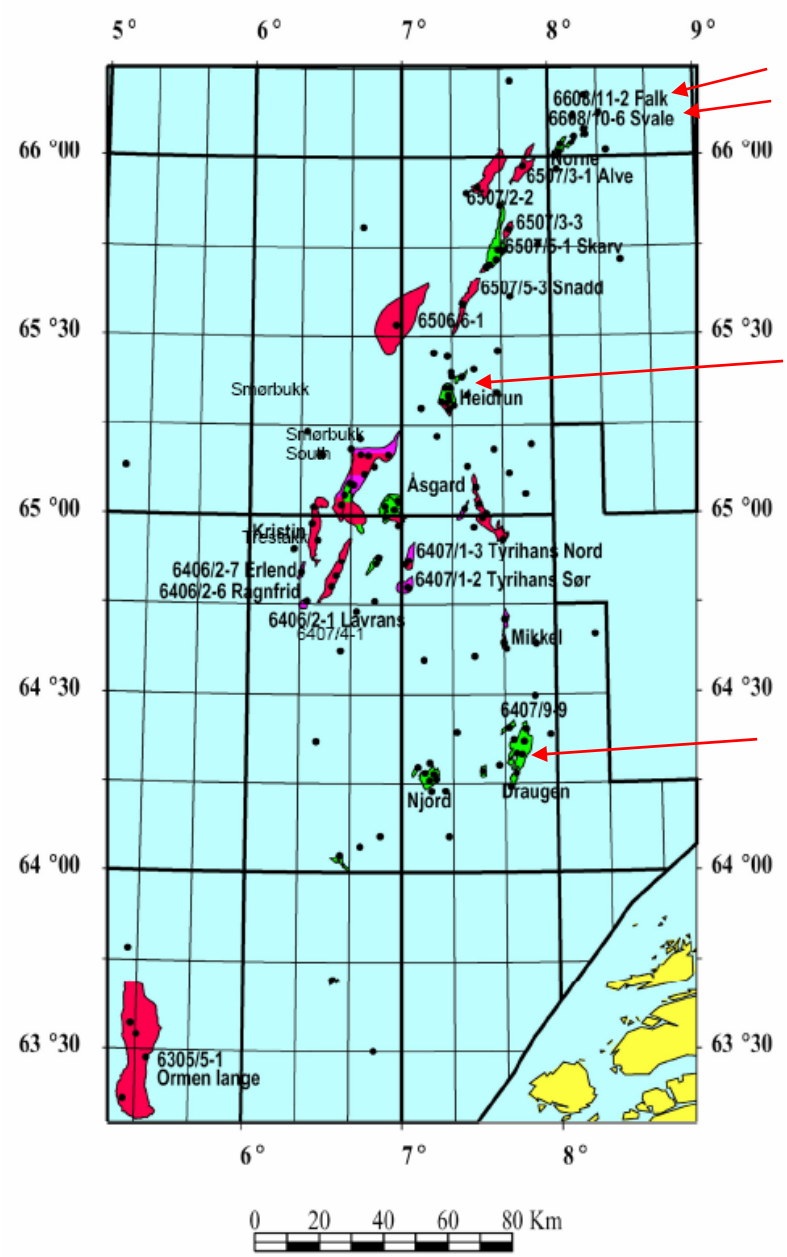

Figure 2.1. The fields in the Haltenbanken Area (Blystad et al., 1995). The red arrows show the fields in this study.

3. Analytical methods

The correlation techniques based on geochemical properties can be divided into two main groups; bulk parameters and specific properties. The bulk parameters describe gross composition properties of whole samples, in terms of either whole oil or total extracts, using for example percentage amount of aromatic hydrocarbons, polar compounds and saturated hydrocarbons (Iatroscan TLC-FID). The specific properties describe detailed chemical characteristics of either specific sample fractions or whole oils, using for example gas chromatography with flame ionization detector (GC-FID) or gas chromatography – mass spectrometry (GC-MS).

This chapter will describe the analytical methods used in this study.

3.1 Procedure of preparing samples

30 mg oil/wax (±5mg) was transferred to a 2 ml bottle with teflon lined plastic cork, and diluted with 1 ml dichloromethane. The sample set was analyzed by three different methods.

3.2 Iatroscan - Thin Layer Chromatography – Flame Ionization Detection (TLC-FID)

Iatroscan analysis involves thin layer chromatography and flame ionization detection (TLC-FID) of petroleum fractions (see figure 3.1). It provides a rapid and relatively accurate method for the quantification of saturated hydrocarbons, aromatic hydrocarbons and the polar fraction (resins and asphaltenes) in solvent extracts of petroleum source rocks, reservoir rocks and crude oils (Karlsen and Larter, 1989). The varying proportions of saturated and aromatic hydrocarbons and polar compounds can be used to characterize the petroleum populations in the reservoir (Bhullar

et al., 2000) and differentiate between migrated hydrocarbons, in-situ generated hydrocarbons and also diesel drilling fluids (Karlsen and Larter, 1991). This technique is suitable to screen large sample volumes from petroleum reservoirs to obtain information for selection of samples for high-resolution analysis.

The oil samples were analyzed by an Iatroscan TH-10, MK IV (Iatron inc., Tokyo) instrument equipped with a flame ionization detector (FID) and interfaced with an electric integrator (Perkin-Elmer LCI-100) used for rod scanning and quantification. The components were separated using silica rods, type Chromarods-S III (pore diameter 60 Å, particle size 5 μm).
All of the samples were applied (3 μl) to a fixed point near the base of the chromarod. 8 out of 10 rods were used for the samples (2 rods pr. sample), the remaining 2 were used for test runs, one blank and the other one with the NSO-1.
To develop the Chromarods, solvents of different polarity were used to separate saturated hydrocarbons, aromatic hydrocarbons and polar compounds. The rods were placed in normal-hexane for 35 minutes, causing the saturated hydrocarbons to rise to the uppermost part of the rods. After air drying the rods were placed in toluene for 6 minutes, causing the aromatic hydrocarbons to move to the middle of the rods. Then the Chromarods were dried at 60 ˚C (90 sec). Then the Chromarods were placed in the Iatroscan instrument, the scanning speed was 30 sec/scan, and pure grade hydrogen (180 ml/min) and air (2.1 l/min) supplied by a pump were used for the detector.

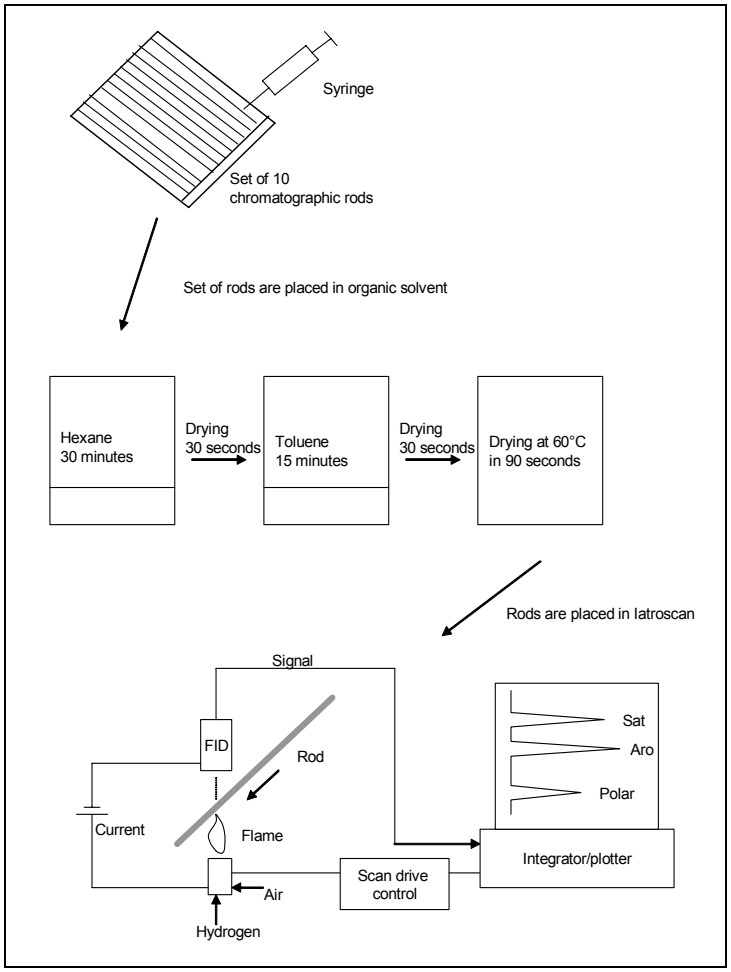

Figure 3.1. The key elements in the TLC-FID analysis for separating and quantifying saturated hydrocarbons, aromatic hydrocarbons plus resins and asphaltenes (polar compounds). (Pedersen, 2002)

3.3 Gas Chromatography- Flame Ionization Detector (GC-FID)

GC-FID methods allow identification and relative or absolute quantification (using internal standards) of individually separable major compounds in petroleum, such as n-alkanes, isoprenoids, toluene, hexane, xylene and more. The whole oil is injected and vaporized before entering a chromatographic column, in which the separation of the different molecules takes place. A film layer on the inside of the column acts as the stationary phase. The short-chained molecules travel quickly through the column, while longer or more branched molecules need a longer period of time to move through the entire column. An inert gas, like nitrogen (N_2) or helium (He), is used as carrier gas, and this is the mobile phase. The column is heated according to a program from 40ºC to 325ºC in 75 minutes, and is then kept on 325ºC for 20 minutes, i.e.

one run takes 95 minutes. This is to mobilize the compounds that have too low vapor pressure at ambient temperature. As the molecules exit the column they enter a flame ionization detector as described above. A computer records the signal from the FID, and the final gas chromatogram is edited and plotted using appropriate software. No preparation of the samples is needed.

The GC-FID instrument (see figure 3.2) used in this study was a Varian Capillary Gas Chromatograph Model 3500 with a 50 m length HP Ultra-1 column, which had a 0.2 mm internal diameter and 0.33 μm film thickness. Temperature programming was 80ºC for 1 min, then an increase of 4.5ºC/min to a final temperature of 320ºC held for 20 min (total time 79.33 min). Pressure was 45 psi, the split flow through the vent was 16 ml/min, the injector had a temperature of 300ºC and the detector temperature was 330ºC. The analysis was performed with nitrogen carrier gas and split injection.

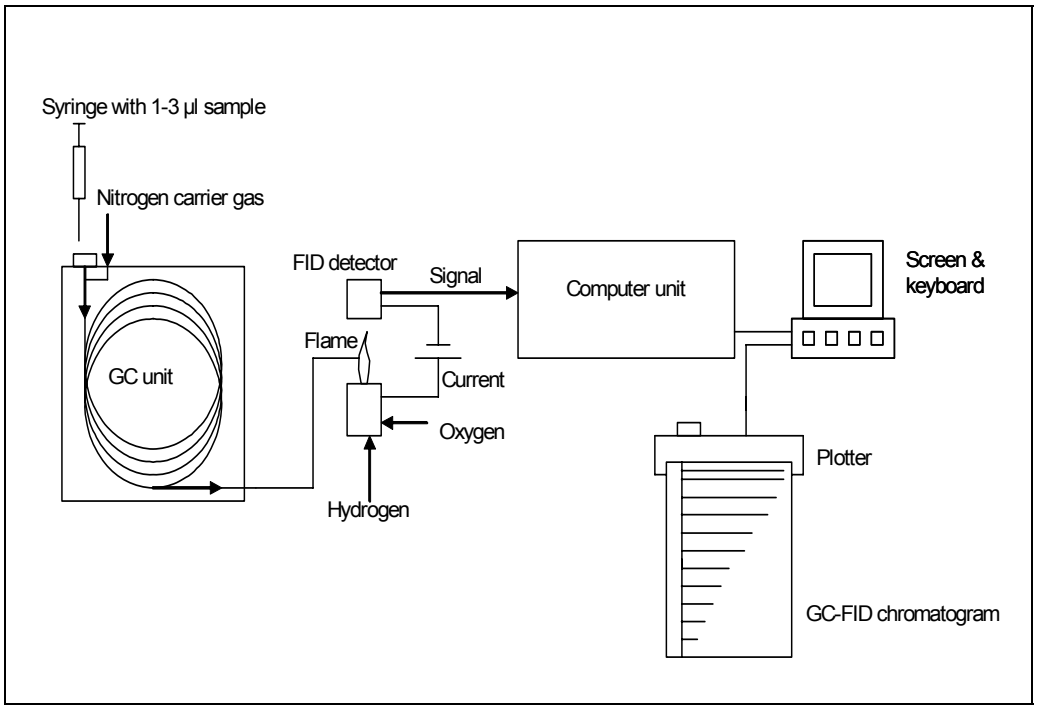

Figure 3.2. The GC-FID instrument (Pedersen, 2002)

Some of the most common parameters in organic petroleum geochemistry studies are based on data collected by the GC-FID. The parameters include:

- Carbon Preference Index (CPI) or Improved Odd Even Preference (OEP)
- Pristane/n-C_{17}
- Phytane/n-C_{18}
- Pristane/Phytane (Pr/Ph)

These parameters are mainly used as maturity and facies indicators, but GC-FID chromatograms may also be applied for general fingerprinting of the samples.

3.4 Gas Chromatography-Mass Spectrometry (GC-MS)

The GC-MS procedure allows identification and quantification of biomarkers. The separation of the molecules is done in the same manner as described above for the GC-FID procedure. After separation, a wolfram filament ionizes the molecules of the sample, before the ions are introduced to a quadropole analyzer. Here, the ions of interest are selected according to their mass before being detected. The different molecule fragments have different mass (m) and an electronic charge (z) equal to unit, and the ratio m/z is specific for many molecules of interest, such as biomarkers. Hopanes and triterpanes are for example found to have m/z = 191. The detector registers the m/z value and the relative abundance of the different ions. A PC program is used in recording and managing the data. The final plot shows the relative abundance of ions with the selected m/z ratio versus time elapsed (retention time).

3.4.1 Molecular Sieving

For many years organic geochemists have been using 5Å molecular sieves to separate n-alkanes from other saturated hydrocarbon components of petroleum (Eglinton and Murphy, 1969). The

main purpose for carrying out this separation is to remove the n-alkanes (straight chained hydrocarbons) and polar compounds from the sample. The n-alkanes comprise a major proportion of most petroleums and if present in the sample they will interfere with the signals from the biomarkers. By removing the n-alkanes the biomarker signals will be enhanced relative to the interference from n-alkane fragments. The molecular sieve is a special compound with a well defined molecular structure. In this study, a sieve made from zeolite, clay, alumina, amorphous silica and calcium oxide was used. The n-alkanes fit into the long, channel-like pores in the molecules and are trapped inside, while the bigger biomarkers are unaffected by the molecular sieve. When the sieve is separated from the sample, the biomarkers and aromatic compounds remain in the solution. In this way the sample is enriched in biomarkers and depleted in n-alkanes. In this study 5Å silicalite UOP MHS2-420LC (a synthetic zeolitic form of silica) was used.

About 0.18 g of molecular sieve was transferred into a 15 ml glass vial. 3 drops of sample were then mixed with the powder-like sieve using a pipette. The sample mixture was diluted with 2-2.5 ml cyclohexane and stirred thoroughly. Then the vial was centrifuged at 2000 rpm for 3 min in a Heraeus Sepatech Labofuge H, to settle the sieve. Subsequently, the sample was decanted into a new 15 ml glass vial, and about ¾ of the solvent evaporated by a flow of nitrogen. After the sample had been up-concentrated the procedure was repeated. After the final evaporation of cyclohexane, the sample was transferred to two 40X6 mm glass vials with a pipette and sealed with a teflon-lined cap.

3.4.2 GC-MS

A GC-MS system forms an instrument capable of separating mixtures into their individual components, identifying and then providing quantitative and qualitative information on the amount and chemical structure of each compound (McMaster and McMaster, 1998). The GC-MS is a combination of a gas chromatograph (GC) for compound separation and a mass spectrometer (MS) using ionization and mass analysis for detection and identification of the

components (see figure 3.3). The GC-MS uses the relative GC retention times, elution patterns and the mass spectral fragmentation patterns to detect and provisionally identify compounds.

The GC-MS instrument used in this study was a Fisons MD800 quadrupole-instrument with a 50 m long Chompack, WCOT, CP-sil 5 CB LOW BLEED/MS column, which had a 0.32 mm internal diameter and 0.40 μm film thickness. The injection was done using a CTC A200S autosampler with a sample volume of 4 μl. The starting temperature was 80ºC (1 min), then an increase of 10ºC/min to a temperature of 180ºC, and then 1.7ºC/min to a final temperature of 310ºC held for 30 min. The total time of the program was 120 min.

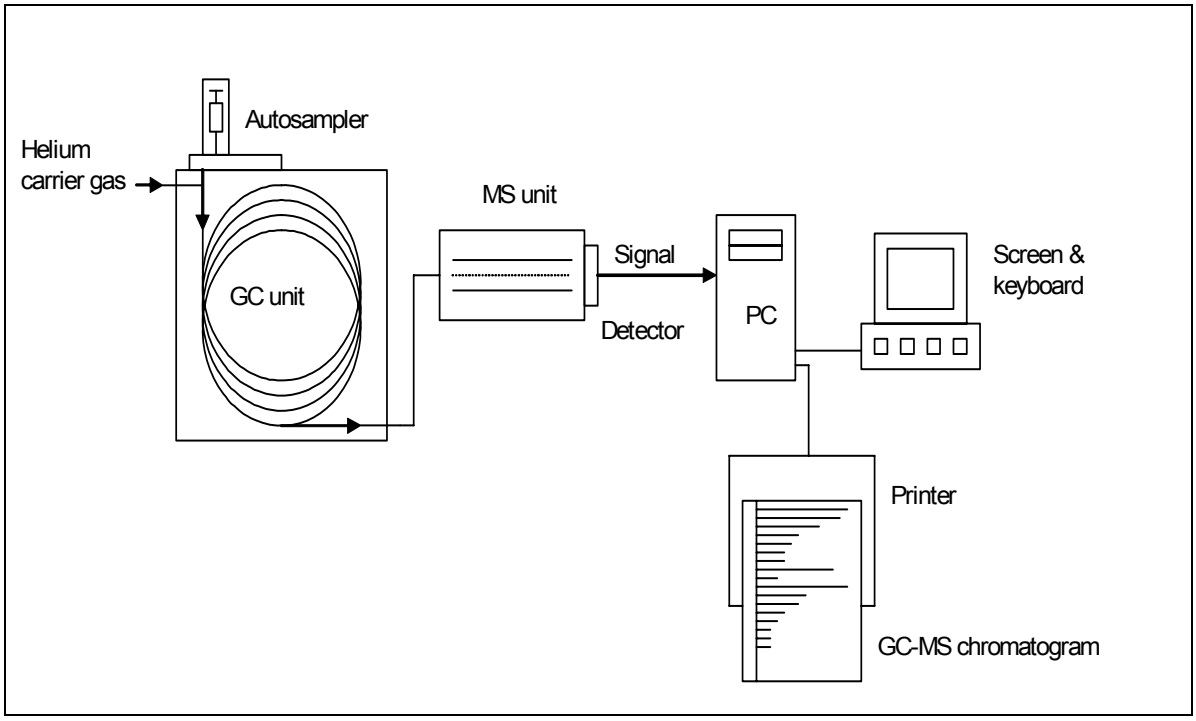

Figure 3.3. The GC-MS instrument (Pedersen, 2002)

The GC-MS was used in this study to monitor the ions with a mass/charge (m/z) ratio of 178, 191, 192, 217, 218, 231 and 253. Monitoring of these ions will give information about the n-alkane distribution and the most common biomarkers and related compounds used to establish the maturity, source and facies of the petroleums in this study.

4. Maturity and facies parameters

The various techniques described in the previous chapter yield a number of molecular parameters used to determine the maturity, facies and age of the petroleum samples. Below follows a description of the parameters used in this study concerning the following techniques:

4.1 Iatroscan TLC-FID
4.2 GC-FID
4.3 GC-MS

4.1 Iatroscan TLC-FID

Saturated hydrocarbons/aromatic hydrocarbons and polar compounds

The saturated hydrocarbons/aromatic hydrocarbons (SAT/ARO) mainly reflect source rock quality and maturity (Cornford et al., 1983; Clayton and Bostick, 1986). The ratio increase with increasing thermal maturity, but will also increase in the gas-phase of phase-fractionated petroleum during the migration to shallower depths. Polar compounds in oils reflect either low maturity or biodegradation. The concentration of these compounds is low in high maturity petroleums and condensates.

4.2. GC-FID

The GC-FID analyses of the oils have been used to analyze C_4 – C_{40} alkanes, with emphasis placed on the C_{15+} compounds (see figure 4.1). The n-alkane distribution together with Pristane/n-C_{17} and Phytane/n-C_{18} can give valuable information about source and depositional facies, maturity and biodegradation.

n-alkane patterns

The n-alkane patterns can be used to classify chromatograms and give information about the facies and maturity of the samples (Peters and Moldowan, 1993). In normal “North Sea” petroleums the peak height decreases asymptotically with increasing carbon number. This

creates a concave curve on the chromatogram. Bimodal extracts have chromatograms with two maxima groups of n-alkanes with a minimum between them. The GC-FID traces may also indicate if there is any biodegradation, in which case the unresolved complex mixture (UCM) of the compounds rises above the baseline, and the relative concentration of n-alkanes decrease compared to other compounds like isoprenoids and aromatics. The oil UCMs are amongst the most complex mixtures of organic compounds on Earth and extremely difficult to identify (Sutton et al., 2004).

Pristane/Phytane

Pristane and phytane are isoprenoid isoalkanes derived from phytol, a side chain of the chlorophyll molecule that separates from the porphyrine structure after deposition (Tissot and Welte, 1978). The depositional environment determines whether the phytol transforms into pristane or phytane. The parameter is therefore used to indicate what type of organic facies (kerogen) the sediments contain. Pr/Ph < 1 may indicate hypersaline, anoxic or carbonate setting, Pr/Ph > 3 indicates hydrocarbons from organic matter from a deltaic or humic dominated sediment deposited under dysoxic conditions, while intermediate values indicates normal marine sediments. These figures must be supported by other data to be conclusive. However, more recently, it has been suggested that pristane and in particular phytane also may have a bacterial origin (Peters and Moldowan, 1993). The ratio can also be used as a maturity indicator because it typically increases with increasing maturity (Alexander et al., 1981), but because pristane and phytane during diagenesis can be derived from other sources than phytol e.g. bacterial membranes (ten Haven et al., 1987) the ratio should be used together with other parameters.

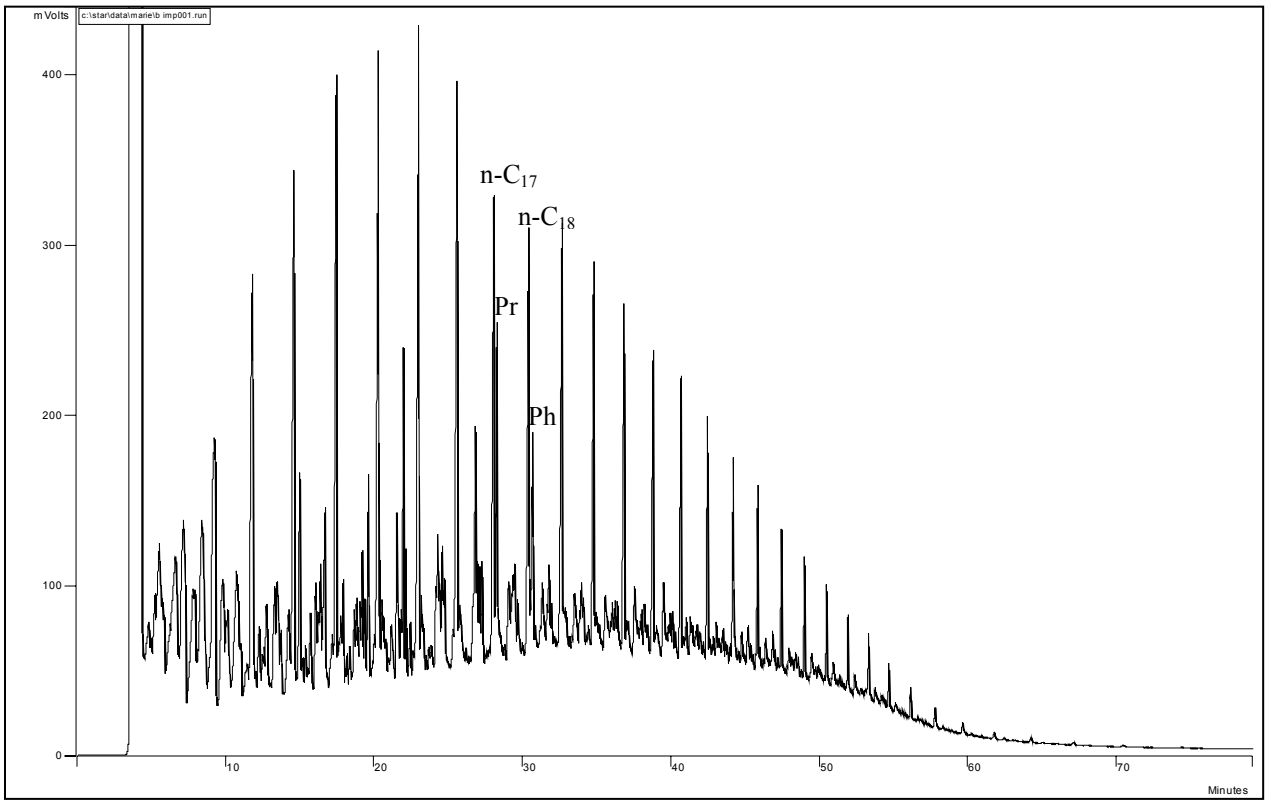

Figure 4.1. The GC-FID chromatogram for the B IMP sample, showing the peaks n-C_{17}, n-C_{18}, pristane (Pr) and phytane (Ph).

Pr/n-C_{17} and Ph/n-C_{18}

Pr/n-C_{17} and Ph/n-C_{18} ratios are used in addition to other parameters to determine source rock facies, maturity and the level of biodegradation of hydrocarbons. Low ratios indicate a more mature sample, because the isoprenoids will break down more readily than n-alkanes during maturation. The ratios can be used together with other parameters to rank related, non-biodegraded oils and bitumens based on thermal maturity. But care should be taken because organic input and biodegradation may affect the ratio (Peters and Moldowan, 1993).

Carbon Preference Index (CPI) and Odd/Even predominance (OEP)

The predominance of molecules with an odd number of carbon atoms can be measured by the Carbon Preference Index (CPI). That is the ratio, by weight, of odd to even molecules (Tissot and Welte, 1978).CPI was first introduced by Bray and Evans (1961) and can be used to indicate the thermal maturity of an oil or extract. CPI values significantly above or below 1.0 indicate that the oil or extract is thermally immature. Values close to 1.0 suggest, but do not prove an oil or extract to be thermally mature (Peters and Moldowan, 1993). Values below 1.0 indicate

carbonate facies, while values higher than 1.0 indicate lacustrine environment or silisiclastic source rock.

$CPI = 2(C_{23}+C_{25}+C_{27}+C_{29})/[C_{22}+2(C_{24}+C_{26}+C_{28})+C_{30}]$

$OEP = (C_{21}+6C_{23}+C_{25})/(4C_{22}+4C_{24})$

Long chained waxy n-alkanes in the C_{30} range

High molecular weight n-alkanes (>n-C_{20}) are responsible for high cloud points of certain crude oils. The cloud point corresponds to the appearance of a cloud of wax crystals when the oil is chilled. Oils of this type have a high wax content (Tissot and Welte, 1978). High molecular weight hydrocarbons are well preserved in oils and are relatively resistant to biodegradation (Hsieh et al., 2000). The presence of long-chained n-alkanes (waxes) can be observed in the GC-FID chromatograms.

4.3 GC-MS

The GC-MS method was used to monitor the ions with a mass/charge (m/z) ratio of 178, 191, 192, 198, 217, 218, 231 and 253. The following figures show the peaks that are identified from the chromatograms and the tables gives a short description of each peak (see figure 4.2 – 4.8 and table 4.1 – 4.7)

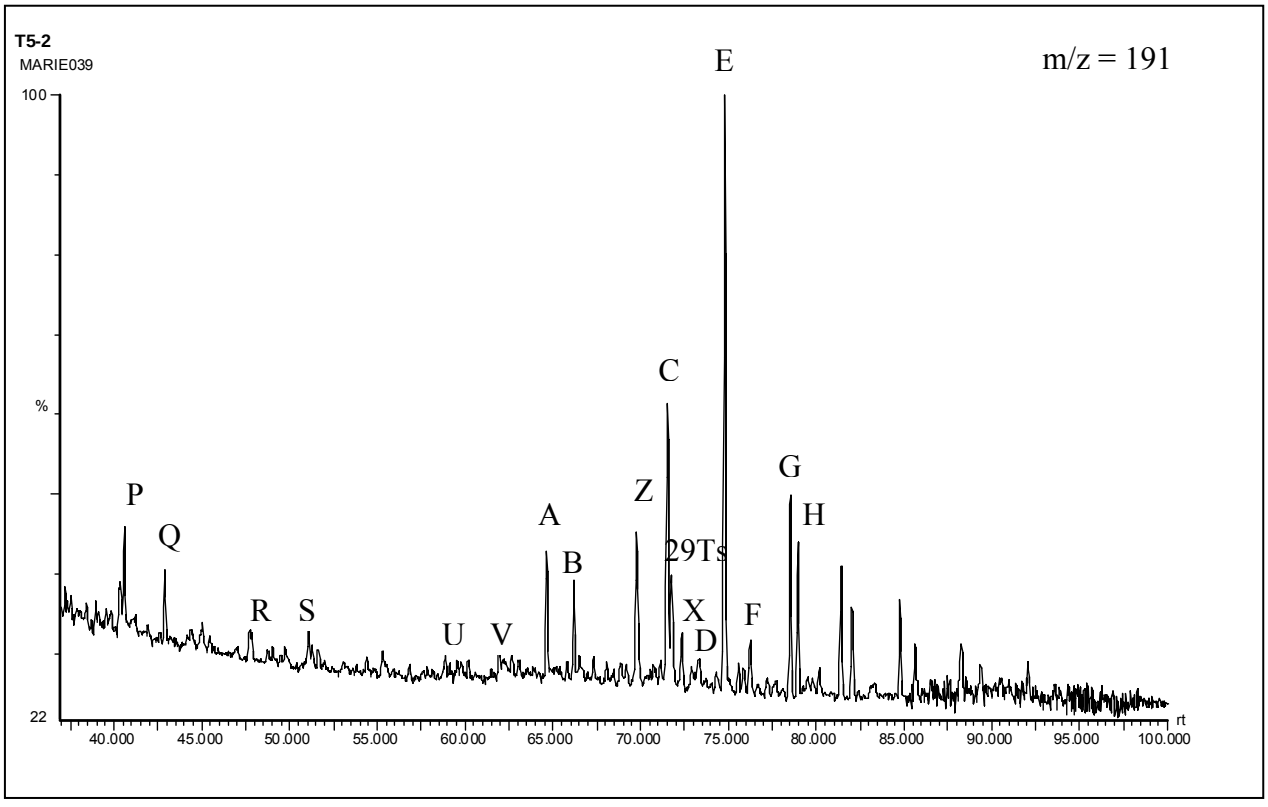

Peak	Stereochemistry	Identity	Composition
P		Tricyclic terpane	$C_{23}H_{42}$
Q		Tricyclic terpane	$C_{24}H_{44}$
R	(17R+17S)	Tricyclic terpane	$C_{25}H_{46}$
S		Tetracyclic terpane	$C_{24}H_{42}$
U		Tricyclic terpane	$C_{28}H_{48}$
V		Tricyclic terpane	$C_{29}H_{50}$
A		18α(H)-trisnorneohopane	C_{27}
B		17α(H)-trisnorhopane	C_{27}
Z		28,30-bisnorhopane	$C_{28}H_{48}$
C		17α(H), 21β(H)-norhopane	$C_{29}H_{50}$
29Ts		18α(H)-30-norneohopane	C_{29}
X		17α(H)-diahopane	$C_{30}H_{52}$
D		17α(H), 21β(H)-normoretane	$C_{29}H_{50}$
E		17α(H), 21β(H)-hopane	$C_{30}H_{52}$
F		17α(H), 21β(H)-moretane	$C_{30}H_{52}$
G	22S	17α(H), 21β(H)-homohopane	$C_{31}H_{54}$
H	22R	17α(H), 21β(H)-homohopane	$C_{31}H_{54}$

Table 4.1. Triterpanes identified from the m/z = 191 chromatogram (see figure 4.2).

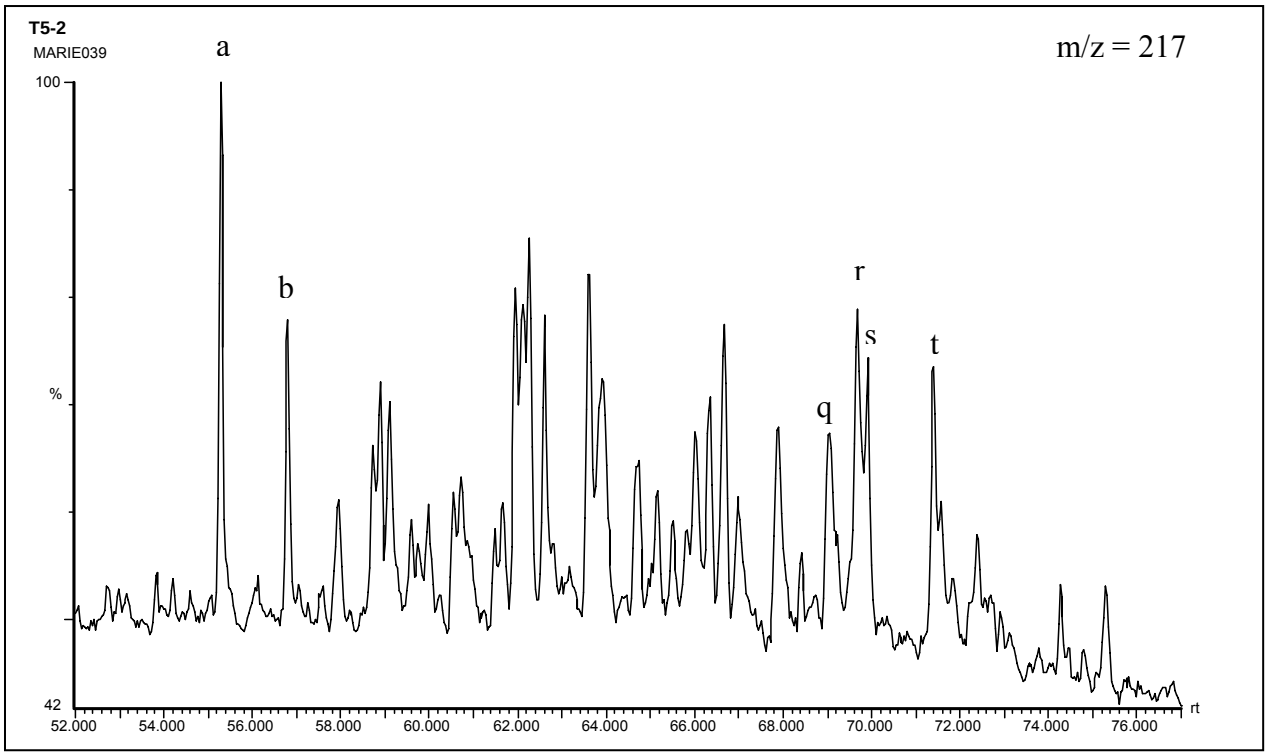

Figure 4.3. The m/z = 217 chromatogram from the T5-2 sample, showing the identified peaks of steranes (see table 4.2 for details).

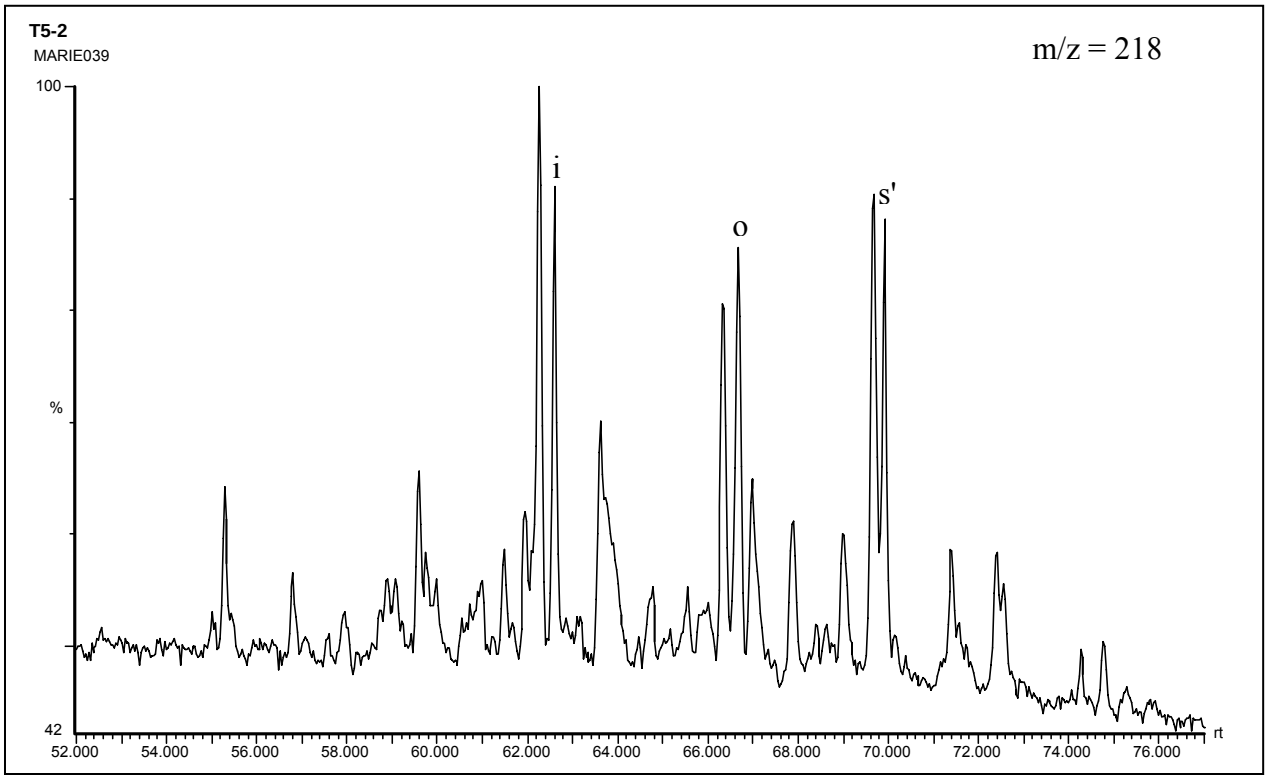

Figure 4.4. The m/z = 218 chromatogram from the T5-2 sample showing the identified peaks of C_{27}, C_{28} and C_{29} steranes (see table 4.3 for details).

Peak	Stereochemistry	Identity	Composition
a	20S	13β(H),17α(H)-dicholestane	$C_{27}H_{12}$
b	20R	13β(H),17α(H)-dicholestane	$C_{27}H_{48}$
q	20S	14α(H),17α(H)-24-ethyl-cholestane	$C_{29}H_{52}$
r	20R	14β(H),17β(H)-24-ethyl-cholestane	$C_{29}H_{52}$
s	20S	14β(H),17β(H)-24-ethyl-cholestane	$C_{29}H_{52}$
t	20R	14α(H),17α(H)-24-ethyl-cholestane	$C_{29}H_{52}$

Table 4.2. Steranes identified from the m/z = 217 chromatograms (see figure 4.3).

Peak	Identity
i	C_{27} regular sterane
o	C_{28} regular sterane
s’	C_{29} regular sterane

Table 4.3. Steranes identified from the m/z =218 chromatograms (see figure 4.4).

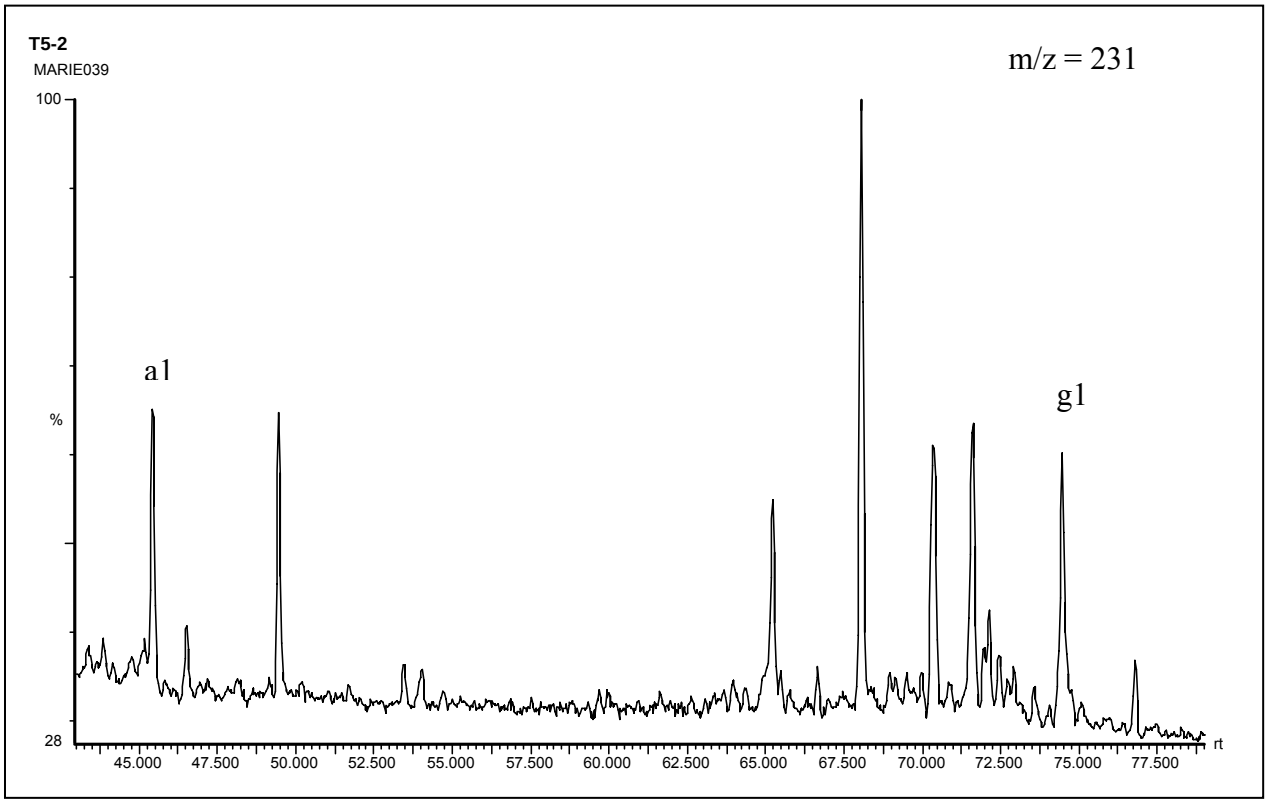

Figure 4.5. The m/z = 231 chromatogram from the T5-2 sample, showing the identified peaks of the triaromatic steroids (see table 4.4 for details).

Peak	Identity
a1	C_{20} triaromatic steroid (TA)
g1	C_{28} triaromatic steroid (TA)

Table 4.4. Triaromatic steroids identified from the m/z = 231 chromatograms (see figure 4.5).

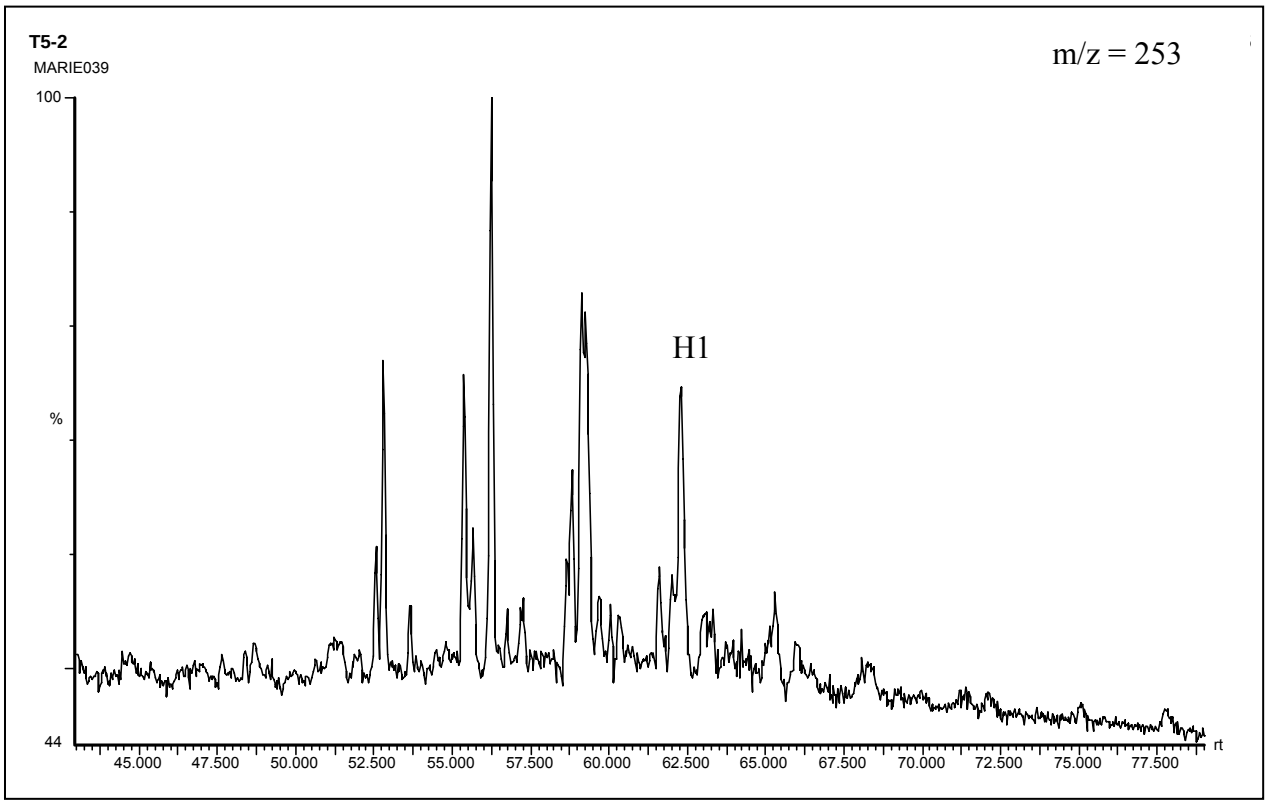

Figure 4.6. The m/z = 253 chromatogram from the T5-2 sample, showing the identified peak of the monoaromatic steroid (see table 4.5 for details).

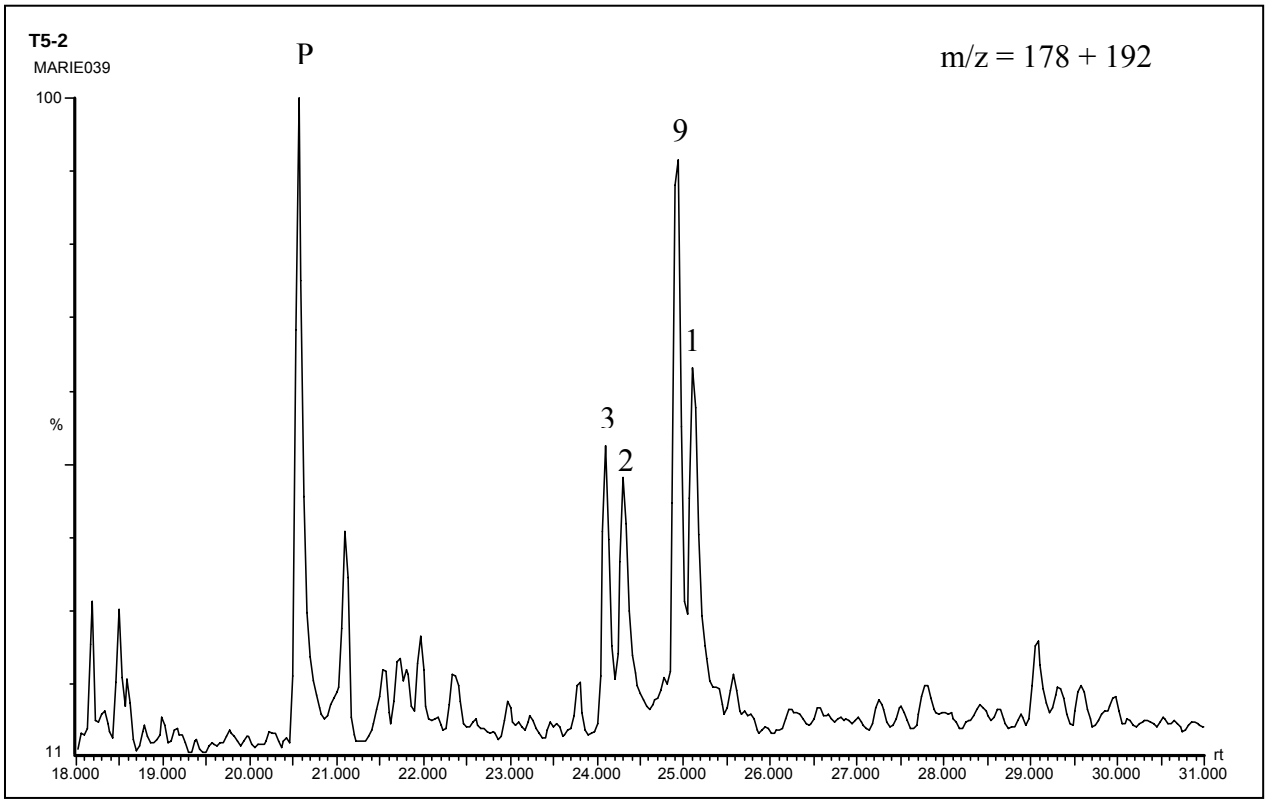

Figure 4.7. The m/z = 178 + 192 combined chromatograms from the T5-2 sample, showing the identified peaks of the phenanthrene and methylphenanthrene isomers (see table 4.6 for details).

Peak	Identity
H1	C_{29} monoaromatic steroid (MA)

Table 4.5. Monoaromatic steroid identified from the m/z = 253 chromatograms (see figure 4.6).

Peak	Identity
P	Phenanthrene
3	3-methylphenanthrene
2	2-methylphenanthrene
9	9-methylphenanthrene
1	1-methylphenanthrene

Table 4.6. Phenanthrene and methylphenanthrene identified from m/z = 178 and m/z = 192 chromatograms (see figure 4.7).

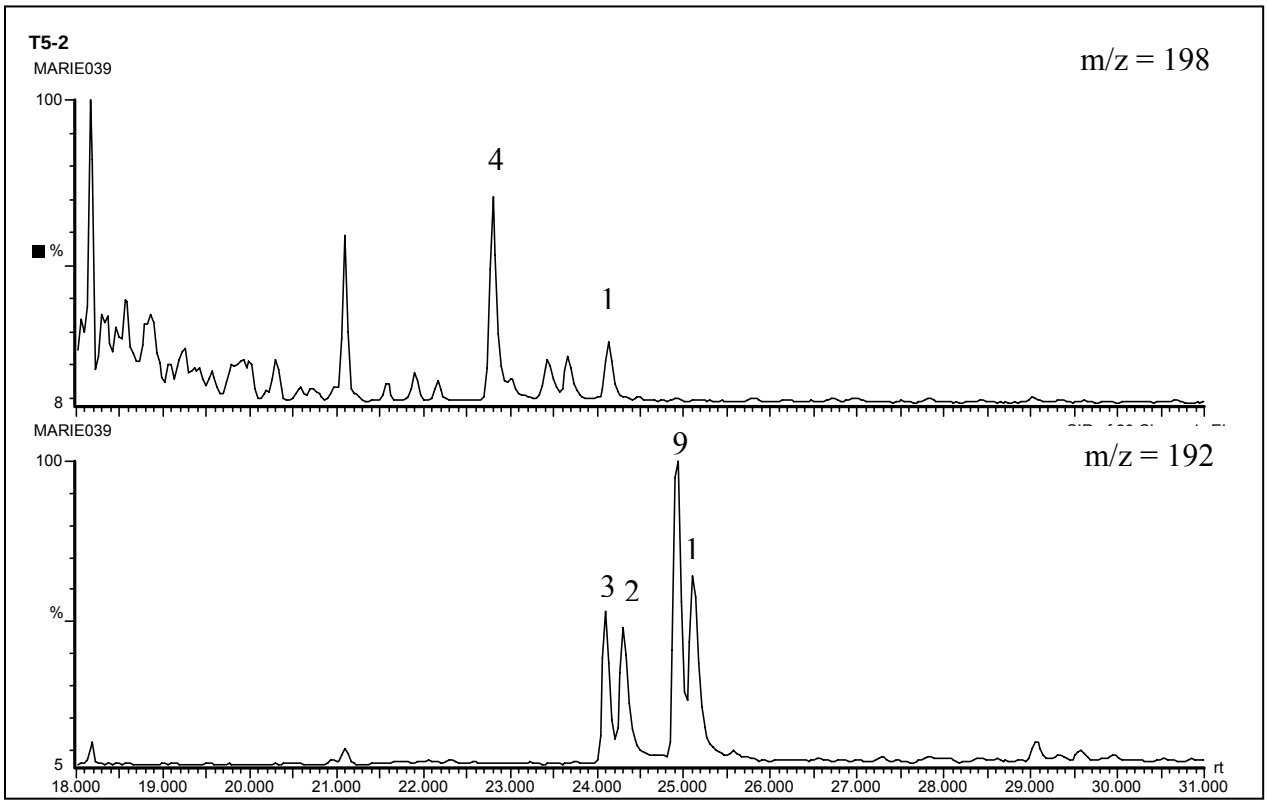

Figure 4.8. The m/z = 198 chromatogram compared with the m/z = 192 chromatogram (see table 4.7 for details).

Peak	Identity
4	4-methyldibenzothiophene
1	1- methyldibenzothiophene

Table 4.7. Dibenzothiophene identified from the m/z = 198 chromatogram (see figure 4.8).

The different peaks described above are used to calculate the following parameters:

1. 18α (H)-trisnorneohopane/ (18α (H)-trisnorneohopane+17α (H)-trisnorhopane) = Ts/(Ts+Tm). (Seifert and Moldowan, 1978: Mackenzie, 1984).

2. Diahopane/(diahopane+normoretane) (Cornford et al., 1986). Diahopane = hopane x (Moldowan et al., 1991).
3. 22S/(22S+22R) of C_{31} 17α(H), 21β(H)-hopanes
4. C_{30}-hopane/(C_{30}-hopane + C_{30}-moretane) (Mackenzie et al., 1985).
5. 29Ts/(29Ts + norhopane) (Moldowan et al., 1991).
6. Bisnorhopane/(bisnorhopane + norhopane) (Wilhelms and Larter, 1994).
7. C_{23}-C_{29} tricyclic terpanes/C_{30} αβ-hopane (modified from Mello et al., 1988).
8. C_{24} tetra cyclic terpanes/ C_{30} αβ-hopane (Mello et al., 1988).
9. Hopane/sterane from the C_{30} αβ-hopane and regular C_{29} sterane (Mackenzie et al., 1984).
10. ββ/(ββ + αα) of C29 (20R + 20S) sterane isomer (Mackenzie et al., 1980).
11. 20S/(20S+20R) of C_{29} 5α(H), 14α(H), 17α(H) steranes (Mackenzie et al., 1980).
12. Diasterane/(diasterane + regular sterane) (Mackenzie et al., 1985).
13. % C_{27} of C_{27} + C_{28} + C_{29} ββ-steranes (Mackenzie et al., 1985).
14. % C_{28} of C_{27} + C_{28} + C_{29} ββ-steranes (Mackenzie et al., 1985).
15. % C_{29} of C_{27} + C_{28} + C_{29} ββ-steranes (Mackenzie et al., 1985).
16. C_{20}/ (C_{20}+C_{28}) triaromatic steroids (TA) (Mackenzie et al., 1985).
17. C_{28} TA/(C_{28}TA + C_{29}MA) (Peters and Moldowan, 1993).
18. Methylphenanthrene ratio, MPR (Radke et al., 1982b).
19. Methylphenanthrene index 1, MPI 1 (Radke et al., 1982a).
20. Methylphenanthrene distribution factor (F1 or MPDF) (Kvalheim et al., 1987).
21. Methyldibenzothiophene ratio, MDR (Radke, 1988).
22. Calculated vitrinite reflectivity, $R_{m(1)}$= 1.1*log10 MPR + 0.95 (Radke, 1988).
23. Calculated vitrinite reflectivity, $\%R_c$ = 0.6*MPI 1 + 0.4 (Radke and Welte, 1983).
24. Calculated vitrinite reflectivity, $\%R_o$ =2.242*MPDF – 0.166 (Kvalheim et al., 1987).
25. Calculated vitrinite reflectivity, $R_{m(2)}$ =0.073*MDR + 0.51 (Radke, 1988).
26. 3-methylphenanthrene/ 4-methyldibenzotiophene (Radke et al., 2001).
27. MDBTs/MPs (Radke et al., 2001).

From chromatogram m/z = 191 it is possible to calculate the following parameters from identification of terpanes and triterpanes.

1: Ts/(Ts+Tm), maturity parameter, peaks A and B. The amount of Ts (C_{27} 18α(H)-trisnorneohopane) will increase compared to Tm (C_{27} 17α(H)-trisnorhopane) during maturation. Tm is believed to represent the biologically produced structure. The Ts/Tm ratio begins to decrease quite late during maturation (>0.9% R_o) (Waples and Machihara, 1991), but may be used through the entire oil window. This parameter may be influenced by the depositional environment, but it is a useful non-quantitative indicator of relative maturity when used on oils of uniform or common organic facies. The maximum ratio is 1.0 (Peters and Moldowan, 1993).

2: Diahopane/ (diahopane + normoretane), maturity parameter (peaks X and D). There is a relationship between maturity and this ratio; high ratios indicate high maturities (Peters and Moldowan, 1993). Peak X may also indicate terrestrial input.

3: 22S/(22S + 22R) of C_{31} 17α(H), 21β(H)- hopanes, maturity parameter (peaks G and H). The S and R isomers of C_{31} 17α(H), 21β(H)- hopanes behave differently during maturation. The 22S isomer is the most stable, and the ratio will therefore increase during maturation of the source rock. The equilibrium is reached fast, so the parameter is valid for immature to early mature petroleums. The maximum equilibrium ratio is 0.6 (Peters and Moldowan, 1993).

4: C30-hopane/(C30-hopane + C30-moretane), maturity parameter (peaks E and F). C30-hopane is thermally more stable than C30-moretane and the ratio will increase with increasing maturation. The range of the ratio is limited to immature samples and extracts, because the loss of C30-moretane occurs at relatively low maturity.

5: 29Ts/(29Ts+norhopane), maturity parameter (peaks 29Ts and C). The stability of the 29Ts compound is higher relative to norhopane, thus the ratio will increase with elevated temperature and maturity (Hughes et al., 1985).

6: Bisnorhopane/(bisnorhopane+norhopane), facies parameter (peaks Z and C). Bisnorhopane is believed to indicate anoxic conditions (Peters and Moldowan, 1993), and it is also affected by maturity. The amount of bisnorhopane is reduced through the oil window, while the norhopane

peak rises relative to bisnorhopane with increased maturation. Immature samples may therefore give a more anoxic impression than more mature samples.

7: C23-C29 tricyclic terpanes/ C30 αβ-hopane, maturity parameter (peaks P, Q, R, T, U, V and E). The amount of C23-C29 tricyclic terpanes will increase relative to the C30 αβ-hopane with increasing maturity. The parameter is valid through the entire oil window, but is strongly influenced by evaporative fractionation and phase fractionation (Karlsen et al., 1995).

8: C24 tetracyclic terpanes/ C30 αβ-hopane, maturity parameter (peaks S and E). The amount of C24 tetracyclic terpanes will increase relative to C30 αβ-hopane with thermal maturity (Peters and Moldowan, 1993).

Parameter 9 is calculated from chromatograms m/z = 191 and m/z = 217.

9: Hopane/sterane, facies parameter (peak E from chromatogram m/z = 191 and q, r, s and t from chromatogram m/z = 217). Hopanes are derived mainly from bacteria, while steranes are derived from algae and higher plants. A high hopane/sterane ratio indicate bacteria rich facies, bacterially reworked organic matter or a special terrestrial input, while a low ratio indicate marine, algae dominated organic matter (Peters and Moldowan, 1993). Hopanes are less thermally stable than steranes, so in a sample set with uniform organic facies, the hopane/sterane parameter will be somewhat more influenced by maturity in addition to the effect of facies.

From the m/z = 217 chromatogram it is possible to calculate the following parameters from identification of six isomers of diacholestanes and ethyl-cholestanes.

10: ββ/(ββ+αα) of the C_{29} (20R+20S) sterane isomers, maturity parameter (peaks q, r, s and t). The ββ-isomer increases with maturity compared to the αα-isomer. The parameter is valid up till peak oil generation, but it may be affected by the mineralogy in the rock. Maximum equilibrium ratio is 0.7 (Peters and Moldowan, 1993).

11: 20S/(20S+20R) of the C_{29} 5α(H), 14α(H), 17α(H) sterane isomers, maturity parameter (peaks q, r, s and t). The 20R isomer coverts to the 20S isomer during maturation and reaches equilibrium in the middle of the oil window. This parameter is affected by maturity, facies, biodegradation and weathering. Maximum equilibrium ratio is 0.55 (Peters and Moldowan, 1993).

12: Diasterane/(diasterane + regular sterane), facies and maturity parameter (peaks a, b, q, r, s and t). The amount of diasteranes will increase with thermal maturity relative to the regular steranes. The parameter is valid through the entire oil window. Maximum ratio is 1.0. Oils from carbonate source rocks may have lower ratios than oils from clastic source rocks (Peters and Moldowan, 1993). Presence of diasteranes indicates a silisiclastic source rock.

From the m/z = 218 chromatogram it is possible to calculate parameters 13 (peak i), 14 (peak o) and 15 (peak s'), which are the relative percentages of the C_{27}, C_{28} and C_{29} ββ-steranes. Plotted in a ternary diagram they indicate organic facies (Huang and Meinschein, 1979; Moldowan et al., 1985).

From the m/z = 231 and m/z = 253 chromatograms it is possible to calculate the following parameters:

16: C_{20}/ (C_{20}+C_{28}) triaromatic steroids (TA), maturity parameter (peaks a1 and g1). The amount of C_{20} increases relative to C_{28} during maturation. The parameter is valid through the entire oil window, but is very susceptible to phase fractionation (Karlsen et al., 1995). Maximum ratio is 1.0 (Peters and Moldowan, 1993).

17: C_{28} TA/(C_{28}TA + C_{29}MA), maturity parameter (peaks g1 and H1). Monoaromatics (MA) are rearranged to triaromatics (TA) during thermal maturation. The ratio between the two molecules is used to estimate maturity and possibly phase fractionation. The parameter is valid to peak oil generation. Maximum ratio is 1.0 (Peters and Moldowan, 1993).

Tricyclic aromatic hydrocarbons are identified from the m/z = 178+192 and m/z = 198 & 192 chromatograms, and utilized in the following parameters. They are calculated from the amount of phenanthrene and the four isomers of methylphenanthrene (peaks 1, 2, 3 and 9). The number assigns the location of the methyl group ($-CH_3$). 3-MP and 2-MP are the most thermally stable isomers, and the 1-MP and 9-MP isomers will be more rapidly depleted during maturation.

18: Methyl phenanthrene ratio (MPR), maturity parameter (peaks 1 and 2).
MPR = 2-MP/1-MP

19: Methyl phenanthrene index 1 (MPI 1), maturity parameter (peaks P, 1, 2, 3 and 9).
MPI 1 = 1,5(3-MP + 2-MP)/(P + 9-MP + 1-MP)

20: Methyl phenanthrene distribution factor (F1 or MPDF), maturity parameter (peaks 1, 2, 3 and9).
MPDF = (3-MP + 2-MP)/ (3-MP + 2-MP + 1-MP + 9-MP)

21: Methyl dibenzothiophene ratio (MDR), maturity and facies parameter (peaks 4 and 1).
MDR = 4-MDBT/ 1-MDBT
This parameter is based on the relationship between the two isomers of methyl dibenzothiophene, 4-MDBT and 1-MDBT. 4-MDBT is the most thermally stable isomer. The thiophene structure contains a sulphur atom, so the amount of MDBT in oils may indicate the sulphur contents in the oil/ source rock.

Vitrinite reflectance has been calculated based on measurements of phenanthrene, methyl phenanthrenes and methyl dibenzothiophene:

22: Calculated vitrinite reflection, maturity parameter, calculated from parameter 18.
$R_{m(1)}$ = 1.1*log10MPR + 0.95

23: Calculated vitrinite reflection, maturity parameter, calculated from parameter 19.
$\%R_c$ = 0.6*MPI 1 + 0.4

24: Calculated vitrinite reflection, maturity parameter, calculated from parameter 20.
$\%R_o = 2.242*MPDF - 0.166$

25: Calculated vitrinite reflection, maturity parameter, calculated from parameter 21.
$R_{m(2)} = 0.073*MDR + 0.51$

26: 3-methyl phenanthrene/ 4-methyl dibenzothiophene, facies parameter (peaks 3 and 4). This parameter can be used with a parameter like Pr/Ph to indicate different types of organic facies, e.g. carbonate and shale facies and the relative amount of sulfur in the source rock.

27: MDBTs/ MPs, facies parameter. The parameter is calculated from peak 1, 2, 3, 4 and 9 from chromatogram m/z = 178 + 192 and peak 1, 2+3 and 4 from the m/z = 192 chromatogram. Values above 1 indicate carbonate facies and values below 1 indicate shale facies.

5. Results

In this chapter the results from the analyses performed in the lab will be presented. This chapter also includes a presentation of scaled-down chromatograms for each sample (see figure 5.2-5.18). See chapter 2 for a detailed description of the methods used. The interpretations and discussions of the results follow in chapter 6.

5.1 Iatroscan TLC-FID

The data obtained from the Iatroscan analyses of the oils are presented in this section. Table 5.1 gives the relative percentages of saturated hydrocarbons, aromatic hydrocarbons and polar compounds, and the ratio of saturated to aromatic hydrocarbons. The numbers in the table represent the average of two Iatroscan runs. See table A.1 in the appendix for the gross compositions in terms of absolute yield and relative percentages for the two Iatroscan runs.

Sample	SAT%	ARO%	POL%	SAT/ARO
T3-2	37.6	46.8	15.6	0.8
T4-1	44.6	32	23.2	1.4
T5-2	40.7	33.8	25.6	1.25
T6-1	44.1	34.9	21	1.25
T4	56.8	20.6	22.7	2.75
T5	55.3	24.5	20.2	2.25
Svale1	54.4	37.1	8.6	1.45
Svale2	58.8	31.6	9.7	1.9
6507/7-2 DST2	40.4	24.7	35.1	1.65
6507/7-4 DST1	40.1	24.8	35.1	1.6
6507/7-4 DST3	54.3	22	23.8	2.55
6507/7-5 DST2A	60.4	17.1	22.6	3.55
Falk	42.2	25.5	32.4	1.65
Draugen	50.1	42.8	7.2	1.15
B IMP	73	14.4	12.7	5.15
7/12-6 DST1	80	13.9	6.2	5.95
NSO-1	56.9	20.7	22.4	2.8

Table 5.1. Relative percentages of the gross composition of the oils and SAT/ARO ratios. SAT = saturated hydrocarbons, ARO = aromatic hydrocarbons, POL = polar compounds. See table A.1 in the appendix for the complete results.

The T samples (sample T3-2, T4-1, T5-2, T6-1, T4 and T5)

The samples show a range in relative percentages from 37.6% (T3-2) to 56.8% (T4) saturated hydrocarbons, 20.6% (T4) to 46.8% (T3-2) aromatic hydrocarbons and 15.6% (T3-2) to 25.6% (T5-2) polar compounds. The SAT/ARO ratio varies from 0.8 (T3-2) to 2.75 (T4). The T3-2 sample has the lowest amount of saturated hydrocarbons, the highest amount of aromatic hydrocarbons and the lowest SAT/ARO ratio in the sample set.

Svale1 and Svale2

The Svale1 sample contains 54.4% saturated hydrocarbons, 37.1% aromatic hydrocarbons and 8.6% polar compounds. The SAT/ARO ratio is 1.45. The Svale2 sample contains 58.8% saturated hydrocarbons, 31.6% aromatic hydrocarbons and 9.7% polar compounds. The SAT/ARO ratio is 1.9.

Heidrun samples (sample 6507/7-2 DST2, 6507/7-4 DST1, 6507/7-4 DST3 and 6507/7-5 DST2A)

The samples from the Heidrun field show a range in relative percentages from 40.1% (6507/7-2 DST2) to 60.4% (6507/7-5 DST2A) saturated hydrocarbons, 17.1% (6507/7-5 DST2A) to 24.8% (6507/7-4 DST1) aromatic hydrocarbons and 22.6% (6507/7-5 DST2A) to 35.1% (6507/7-2 DST2 and 6507/7-4 DST1) polar compounds. This is the highest amount of polar compounds in the sample set. The SAT/ARO ratio varies from 1.6 (6507/7-4 DST1) to 3.55 (6507/7-5 DST2A).

Falk (6608/11-2)

The Falk sample contains 42.2% saturated hydrocarbons, 25.5% aromatic hydrocarbons and 32.4% polar compounds thus similar to the Heidrun samples. The SAT/ARO ratio is 1.65.

Draugen (6407/9-5)

The sample from the Draugen field contains 50.1% saturated hydrocarbons, 42.8% aromatic hydrocarbons and 7.2% polar compounds. The SAT/ARO ratio is 1.15.

B IMP

The B IMP sample contains 73% saturated hydrocarbons, 14.4% aromatic hydrocarbons and 12.7% polar compounds. The SAT/ARO ratio is 5.15, which is the second highest ratio in the sample set.

Ula (7/12-6 DST1)

The sample from the Ula field contains 80% saturated hydrocarbons, 13.9% aromatic hydrocarbons and 6.2% polar compounds. The SAT/ARO ratio is 5.95. This sample has the highest amount of saturated hydrocarbons, and the lowest amount of aromatic hydrocarbons and polar compounds. The SAT/ARO ratio is also the highest in the sample set.

NSO-1

The NSO-1 sample contains 56.9% saturated hydrocarbons, 20.7% aromatic hydrocarbons and 22.4% polar compounds. The SAT/ARO ratio is 2.8.

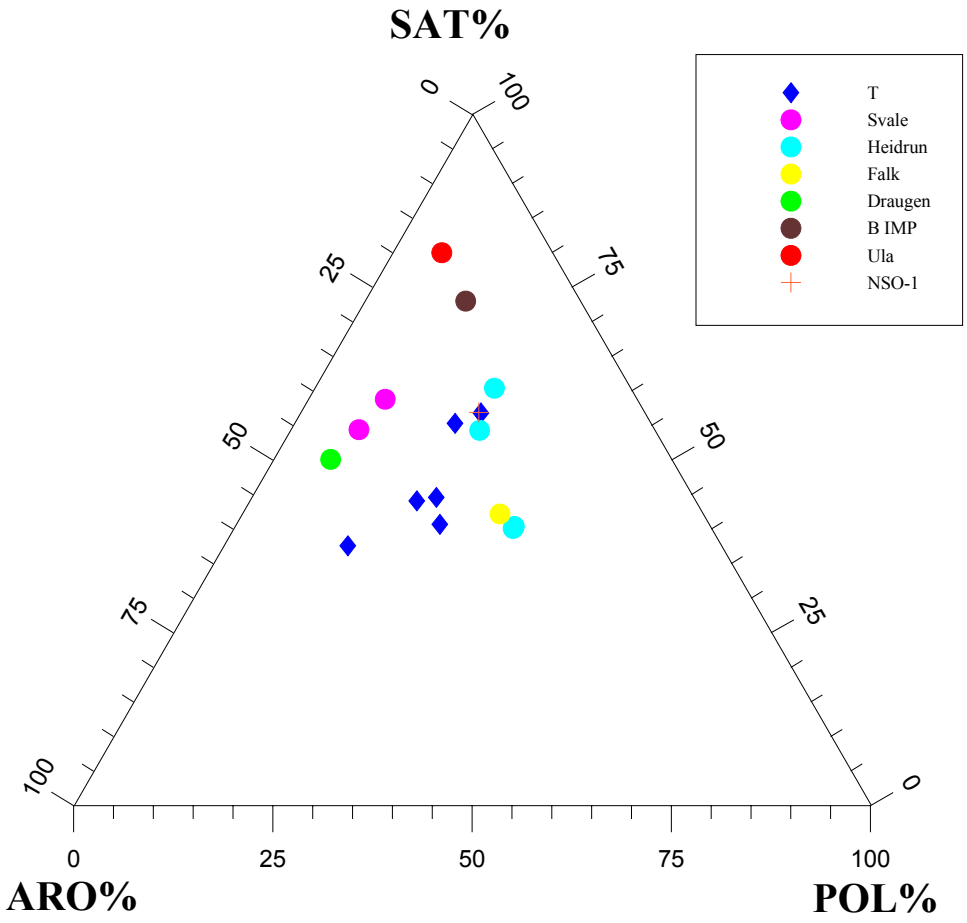

Figure 5.1. The relative SAP distribution of the samples plotted in a ternary diagram.

Figure 5.1 shows the relative Sat-Aro-Pol distribution of the samples plotted in a ternary diagram.

5.2 GC-FID

The samples were analyzed on the GC-FID instrument as described in chapter 2.3. This gives information about the n-alkane and isoprenoid distribution, and can give information about the maturity and source rock facies of the samples (Peters and Moldowan, 1993). In particular, this method also shows the relative proportion and the presence of waxes. The GC-FID traces may indicate if there is any biodegradation, in which case the unresolved complex mixture (UCM) of compounds rises above the baseline, and the relative concentration of n-alkanes decrease compared to other compounds like isoprenoids and aromatics. In normal North Sea oils the peak

height decreases asymptotically with increasing carbon number. This creates a concave curve on the chromatogram.

The results from the GC-FID analysis are presented in table 5.2, and the chromatograms are shown in figure 5.2-5.18.

Sample	Pr/Ph	Pr/n-C_{17}	Ph/n-C_{18}
T3-2	1.5	1.6	1.1
T4-1	1.4	4.2	3.6
T5-2	1.6	2.1	1.5
T6-1	1.5	9.6	13.7
T4	1.5	1.5	1.1
T5	1.5	1.2	0.9
Svale1	1.5	24.1	18.6
Svale2	1.7	2.2	1.1
6507/7-2 DST2	1.9	1.5	0.6
6507/7-4 DST1	1.6	1.2	0.9
6507/7-4 DST3	1.5	1.1	0.8
6507/7-5 DST2A	1.6	0.95	0.7
Falk	ND	ND	ND
Draugen	2	1.4	0.8
B IMP	1.5	0.7	0.5
Ula	1.3	0.5	0.4
NSO-1	1.7	0.7	0.5

Table 5.2. Data from the GC-FID chromatograms. ND = no data due to lack of peaks.

The T samples (T3-2, T4-1, T5-2, T6-1, T4 and T5)

All the T samples have high proportions of long-chained n-alkanes (waxes) out at 70 min as compared to the other oils (see figure 5.2- 5.18). The unresolved complex mixture (UCM) is generally not present or only partly present, and in a very low degree in T5-2 and T6-1. The T4-1 sample contain only limited amounts of n-alkanes in the C_{13} to C_{28} range, but have a tremendous hump of n-alkanes in the C_{30} to C_{38} range. In the T6-1 sample there are almost no n-alkanes in the n-C_{12} to n-C_{30} range, but at n-C_{30} the n-alkane waxy hump appears. In all the T samples the isoprenoids pristane (Pr) and phytane (Ph) are among the major peaks. The Pr/Ph ratios ranges

from 1.4 (T4-1) to 1.6 (T5-2).The Pr/n-C_{17} ranges from 1.2 (T5) to 9.6 (T6-1), while the Ph/n-C_{18} ratio ranges from 0.9 (T5) to 13.7 (T6-1).

Svale1 and Svale2

Significant UCM humps are observed in both samples, and also a depletion in n-alkanes (see figure 5.8-5.9). For Svale1, the Pr/Ph ratio is 1.5, Pr/n-C_{17} is 24.1, and Ph/n-C_{18} is 18.6. For Svale2 the Pr/Ph ratio is 1.7, Pr/n-C_{17} is 2.2 and Ph/n-C_{18} is 1.1.

Heidrun samples

All the samples have UCM humps present, 6507/7-2 DST2 as the most significant hump, H4 the least (see figure 5.10-5.13). 6507/7-2 DST2 shows the largest depletion of n-alkanes. The Pr/Ph ratio ranges from 1.5 (6507/7-4 DST3) to 1.9 (6507/7-2 DST2), the Pr/n-C_{17} ratio ranges from 0.95 (6507/7-5 DST2A) to 1.5 (6507/7-2 DST2) and the Ph/n-C_{18} ratio ranges from 0.6 (6507/7-2 DST2) to 0.9 (6507/7-4 DST1).

Falk (6608/11-2)

A huge UCM hump is dominating in the chromatogram representing the Falk discovery (see figure 5.14), the sample is obviously severely biodegraded, and it is not possible to detect any isoprenoids. The Pr/Ph ratio could therefore not be calculated.

Draugen (6407/9-5)

The chromatogram for the sample from the Draugen field shows a depletion of n-alkanes in the C_{15-} range (see figure 5.15). The Pr/Ph ratio is 2, which is the highest in the sample set. The Pr/n-C_{17} is 1.4 and the Ph/n-C_{18} is 0.8.

B IMP

The B IMP sample appears to have a low concentration of cyclic and aromatic compounds compared to n-alkanes (see figure 5.16). The pristane/phytane ratio is 1.5, the Pr/n-C_{17} is 0.7 and the Ph/n-C_{18} is 0.5.

Ula

The sample from the Ula field has a low concentration of cyclic and aromatic compounds compared to n-alkanes (see figure 5.17). The Pr/Ph ratio is 1.3, the Pr/n-C_{17} is 0.5, and the Ph/n-C_{18} is 0.4. These values are the lowest in the sample set.

NSO-1

The chromatogram for the NSO-1 sample illustrates nicely that the peak heights decrease with increasing carbon number, creating a concave curve (see figure 5.18). The Pr/Ph ratio is 1.65, the Pr/n-C_{17} is 0.68 and the Ph/n-C_{18} is 0.51.

5.3 GC-MS

The samples were analyzed on the GC-MS instrument as described in chapter 2.4. The technique makes it possible to study compounds present in only small concentrations in the complex matrix that make up the petroleum. The compounds of main interest in this study are generally referred to as "biomarkers" (Waples and Machihara, 1991). Methyl dibenzothiophenes and phenanthrenes compounds, which are not biomarkers, were also studied by GC-MS.

Several maturity and facies parameters have been calculated, based on measured selected peaks. See chapter 3.3 for a description of the parameters and for a description of the peaks. Some key numbers are given in the following section. The parameter values are given in table 5.3 and the chromatograms are shown in figure 5.2-5.18.

Sample	1	2	3	4	5	6	7	8	9	10	11	12	13
T3-2	0.56	0.67	0.62	0.90	0.28	0.37	0.68	0.11	1.78	0.50	0.43	0.45	35
T4-1	0.48	0.40	0.58	0.90	0.22	0.19	1.54	0.13	2.17	0.56	0.42	0.34	35
T5-2	0.56	0.67	0.57	0.92	0.28	0.36	0.66	0.09	1.59	0.54	0.43	0.43	35
T6-1	0.54	0.64	0.59	0.93	0.26	0.38	0.52	0.08	1.56	0.55	0.43	0.43	34
T4	0.60	0.63	0.59	0.90	0.31	0.39	0.78	0.11	1.50	0.50	0.47	0.48	38
T5	0.59	0.60	0.59	0.91	0.31	0.38	0.70	0.10	1.60	0.51	0.46	0.49	37
Svale1	0.46	0.65	0.57	0.91	0.22	0.21	0.90	0.18	2.84	0.63	0.42	0.53	33
Svale2	0.47	0.73	0.57	0.91	0.21	0.20	0.86	0.17	2.22	0.63	0.37	0.54	35
6507/7-2 DST2	0.70	0.86	0.57	0.92	0.43	0.30	1.86	0.19	1.53	0.70	0.51	0.76	39
6507/7-4 DST1	0.66	0.83	0.56	0.91	0.42	0.34	2.02	0.21	0.81	0.64	0.45	0.72	34
6507/7-4 DST3	0.71	0.83	0.58	0.92	0.41	0.34	1.91	0.22	1.30	0.67	0.46	0.72	35
6507/7-5 DST2A	0.69	0.82	0.60	0.92	0.42	0.32	1.78	0.18	1.05	0.64	0.49	0.72	35
6608/11-2	0.50	0.80	0.60	0.88	0.45	0.71	1.68	0.36	0.55	0.63	0.40	0.46	30
6407/9-5	0.60	0.75	0.59	0.91	0.31	0.39	0.69	0.12	1.53	0.63	0.45	0.53	35
B IMP	0.41	0.51	0.56	0.90	0.35	0.23	1.47	0.18	2.41	0.60	0.37	0.44	33
7/12-6 DST1	0.69	0.86	0.56	0.80	0.56	0.28	2.47	0.25	0.53	0.67	0.51	0.78	35
NSO-1	0.54	0.65	0.59	0.94	0.26	0.39	0.38	0.06	3.01	0.62	0.40	0.54	34

Table 5.3. Parameters calculated from the GC-MS chromatograms. See chapter 3.3 for description of the parameters.

Sample	14	15	16	17	18	19	20	21	22	23	24	25	26	27
T3-2	32	34	0.54	0.62	0.58	0.49	0.33	2.51	0.69	0.69	0.57	0.69	1.94	0.33
T4-1	29	36	0.55	0.71	0.79	0.56	0.37	3.82	0.84	0.74	0.67	0.79	2.15	0.28
T5-2	31	34	0.51	0.67	0.71	0.52	0.37	3.61	0.79	0.71	0.66	0.77	3.00	0.21
T6-1	32	34	0.50	0.62	0.80	0.50	0.39	3.26	0.85	0.70	0.70	0.75	1.92	0.37
T4	30	31	0.54	0.64	0.59	0.47	0.32	3.69	0.70	0.68	0.55	0.78	4.48	0.13
T5	31	32	0.49	0.61	0.58	0.46	0.32	2.13	0.69	0.68	0.55	0.67	2.11	0.31
Svale1	32	35	0.67	0.57	0.90	0.25	0.36	1.85	0.90	0.55	0.64	0.65	2.73	0.24
Svale2	29	36	0.70	0.54	1.43	0.33	0.43	2.00	1.12	0.60	0.81	0.66	2.73	0.24
6507/7-2 DST2	32	29	0.69	0.57	0.87	0.58	0.41	3.31	0.88	0.75	0.76	0.75	2.21	0.34
6507/7-4 DST1	33	33	0.69	0.59	0.80	0.60	0.40	3.70	0.85	0.76	0.72	0.78	2.49	0.27
6507/7-4 DST3	33	31	0.70	0.55	0.99	0.57	0.42	3.85	0.95	0.74	0.78	0.79	2.66	0.26
6507/7-5 DST2A	33	31	0.66	0.59	0.82	0.55	0.40	3.41	0.86	0.73	0.73	0.76	1.79	0.42
6608/11-2	32	38	0.54	0.63	1.05	0.74	0.41	0.24	0.97	0.85	0.76	0.53	1.64	1.13
6407/9-5	30	36	0.53	0.62	0.74	0.63	0.38	3.85	0.80	0.78	0.69	0.79	5.61	0.11
B IMP	32	35	0.63	0.40	1.38	0.89	0.52	1.35	1.10	0.93	1.01	0.61	2.03	0.61
7/12-6 DST1	32	33	0.89	0.54	0.55	0.44	0.29	5.75	0.66	0.66	0.49	0.93	6.61	0.06
NSO-1	33	32	0.46	0.68	0.87	0.56	0.41	3.60	0.88	0.74	0.76	0.77	3.11	0.24

Table 5.3 (continued). Parameters calculated from the GC-MS chromatograms.

The T samples (T3-2, T4-1, T5-2, T6-1, T4 and T5)

The T samples have Ts/(Ts+Tm) values ranging from 0.48 (T4-1) to 0.60 (T4). The 29Ts/(29Ts+norhopane) ratio ranges from 0.22 (T4-1) to 0.31 (T4 and T5). The diahopane/(diahopane+normoretane) ratio ranges from 0.40 (T4-1), which is the lowest in the sample set, to 0.67 (T3-2 and T5-2). The bisnorhopane/(bisnorhopane+norhopane) ratio ranges from 0.19 (T4-1), which is the lowest in the sample set, to 0.39 (T4). The amount of bisnorhopane in the T4-1 sample is significantly lower than in the other T samples.

Svale1 and Svale2

Svale1 has a Ts/(Ts+Tm) value of 0.46, and Svale2 has a value of 0.47. This is among the lowest in the sample set. The diahopane/(diahopane+normoretane) ratios are 0.65 (Svale1) and 0.73 (Svale2). The 29Ts/(29Ts+norhopane) ratios are 0.22 (Svale1) and 0.21 (Svale2), which are the lowest values in the sample set. The MPR ratios are 0.90 (Svale1) and 1.43 (Svale2), which is the highest value in the sample set. The MPI1 ratios are 0.25 (Svale1), which is the lowest in the sample set, and 0.33 (Svale2).

The Heidrun samples

The Ts/(Ts+Tm) values ranges from 0.66 (H2) to 0.71 (H3), which is the highest in the sample set. The 29Ts/(29Ts+norhopane) ratios ranges from 0.41 (H3) to 0.43 (H1).

Falk

The Ts/(Ts+Tm) ratio is 0.5, and the diasterane/(diasterane+regular sterane) ratio is 0.46. The bisnorhopane/(bisnorhopane+norhopane) ratio is 0.71, which is the highest value in the sample set. The MDR ratio is 0.24, which is the lowest in the sample set. The methyl dibenzothiophenes/methyl phenanthrene ratio is 1.13, which is a much higher value than for all the other samples.

Draugen

The Ts/(Ts+Tm) ratio is 0.60, and the diahopane/(diahopane+normoretane) ratio is 0.75. The 29Ts/(29Ts+norhopane) ratio is 0.31, and the bisnorhopane/ (bisnorhopane + norhopane) ratio is 0.39. The 3-methyl phenanthrene /4-methyl dibenzothiophene ratio is 5.61, which is the second highest value in the sample set.

B IMP

The Ts/(Ts+Tm) ratio is 0.41, which is the lowest value in the sample set. The 29Ts/(29Ts+norhopane) ratio is 0.35, and the bisnorhopane/(bisnorhopane+norhopane) ratio is 0.23. The MPI1 and MPDF (F1) ratios are 0.89 and 0.52 respectively, which are the highest values in the sample set.

Ula

The diahopane/(diahopane+normoretane) and 29Ts/(29Ts+norhopane) ratios are 0.86 and 0.56 respectively, which are the highest values in the sample set. The hopane/sterane ratio is 0.53, which is the lowest in the sample set.

NSO-1

The Ts/(Ts+Tm) ratio and the 29Ts(29Ts+norhopane) ratios are 0.54 and 0.26 respectively. The hopane/sterane ratio is 3.01, which is the highest in the sample set. The $C_{20}/(C_{20}+C_{28})$ triaromatic steroid ratio is 0.46, which is the lowest in the sample set.

5.4 Overview of the chromatograms

The following pages show all the compiled scaled-down chromatograms for each sample (see the appendix for the chromatograms in larger scale). The first chromatogram in each figure is from the GC-FID analysis, which represents the general isoprenoid and n-alkane distributions, and also gives information about biodegradation and source. The other chromatograms are from the GC-MS analysis, which indicate maturity and organic facies.

T3-2

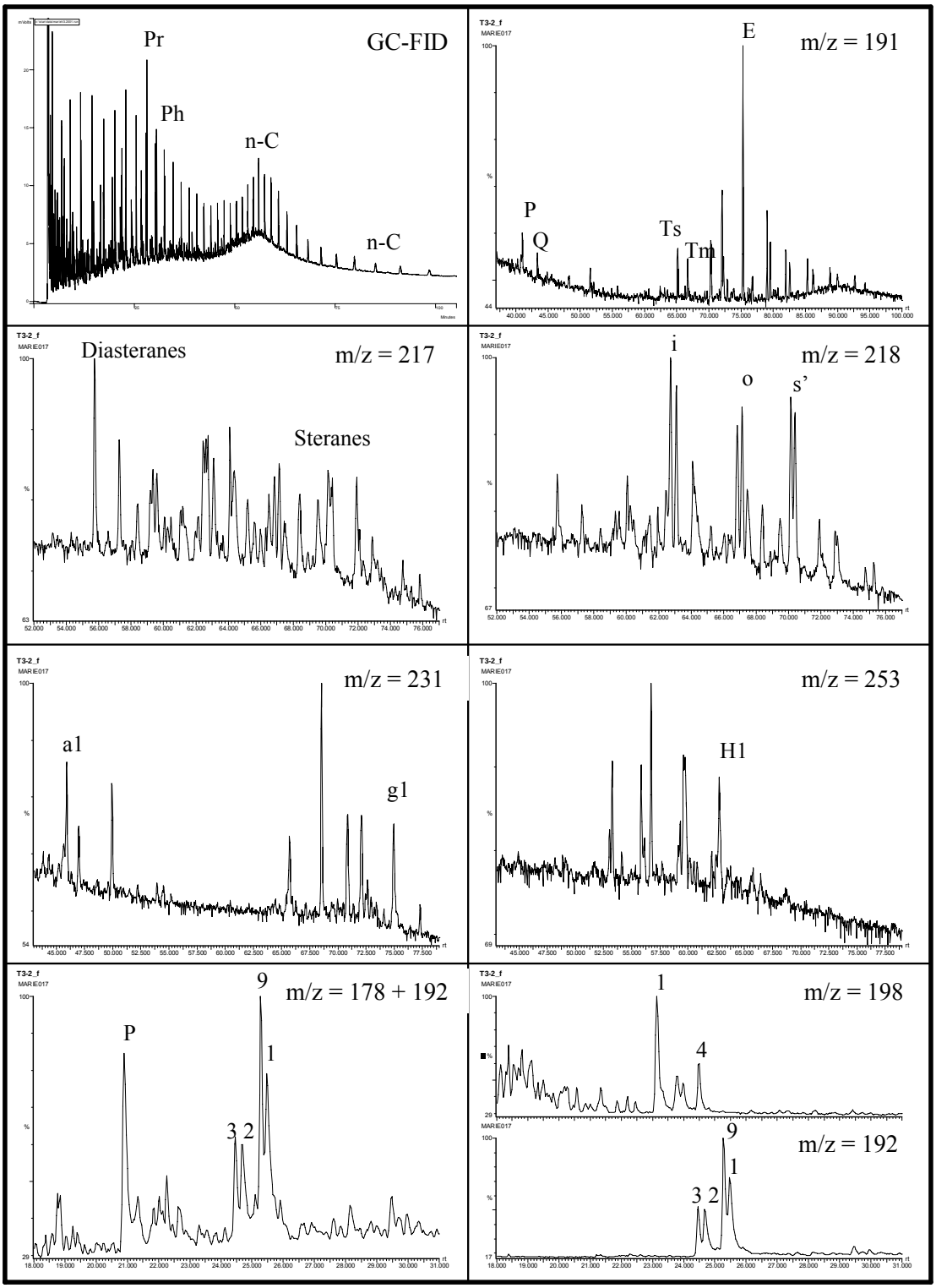

Figure 5.2. The chromatograms for the T3-2 sample.

T4-1

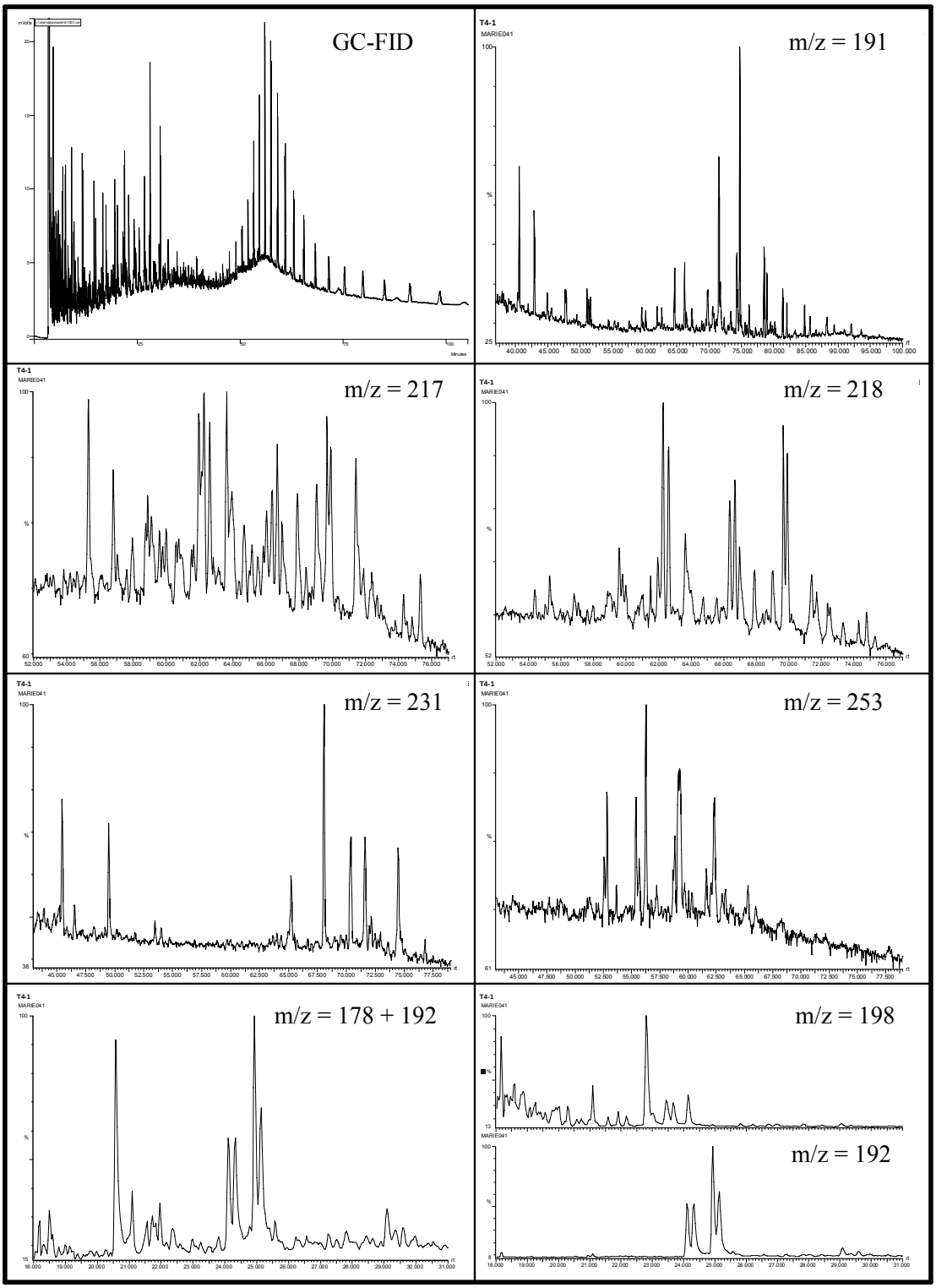

Figure 5.3. The chromatograms for the T4-1 sample.

T5-2

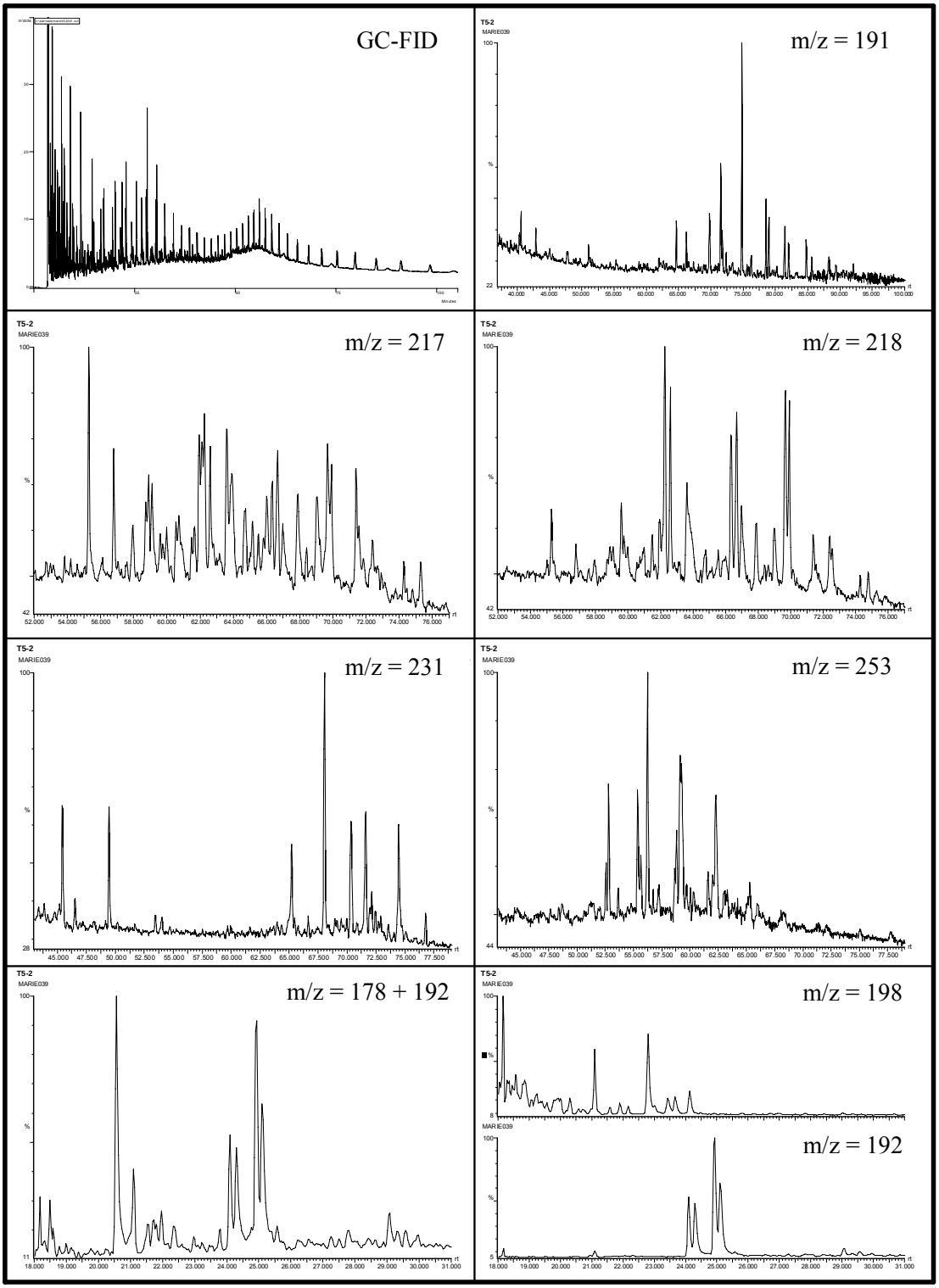

Figure 5.4. The chromatograms for the T5-2 sample.

T6-1

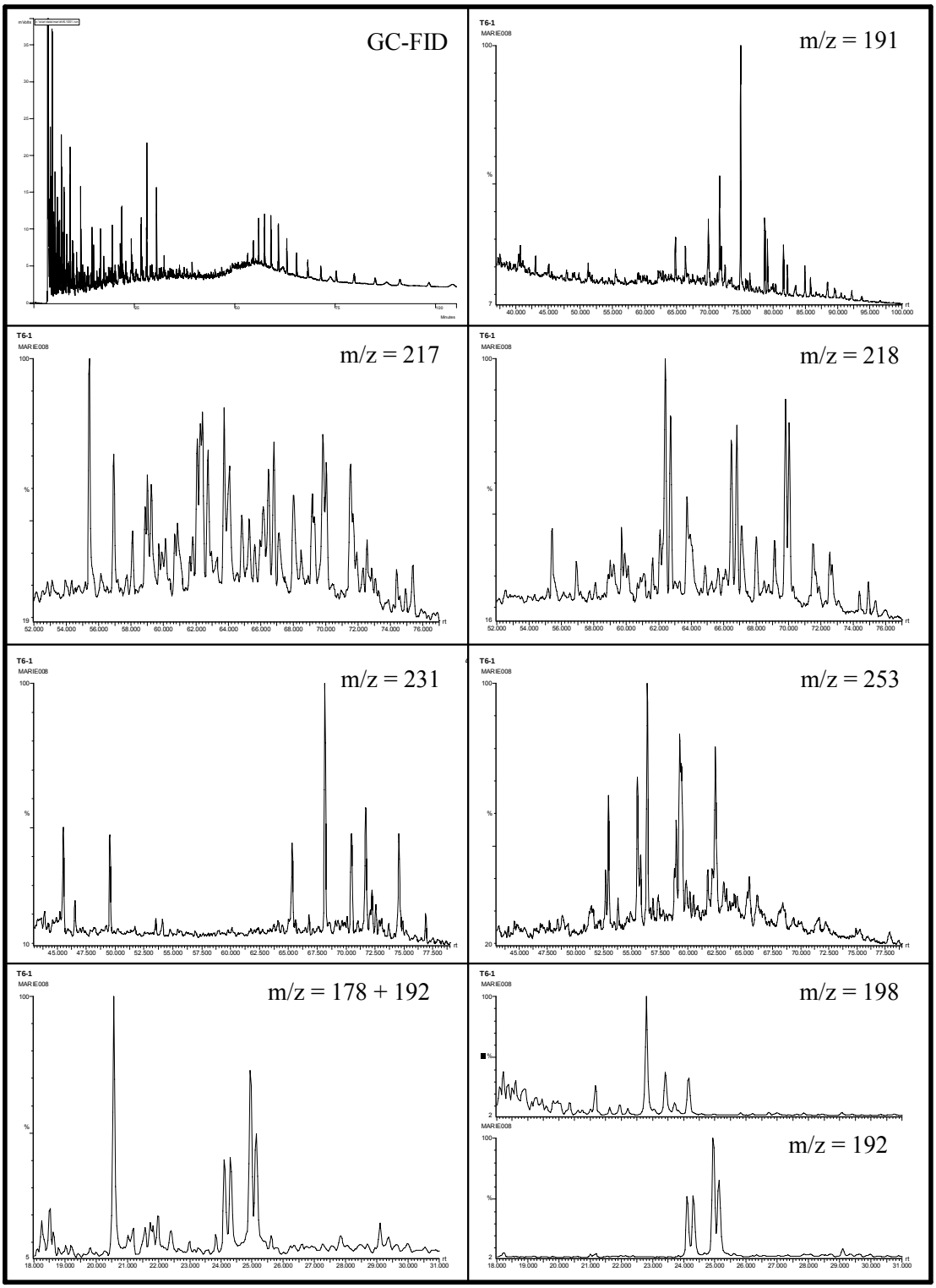

Figure 5.5. The chromatograms for the T6-1 sample.

T4

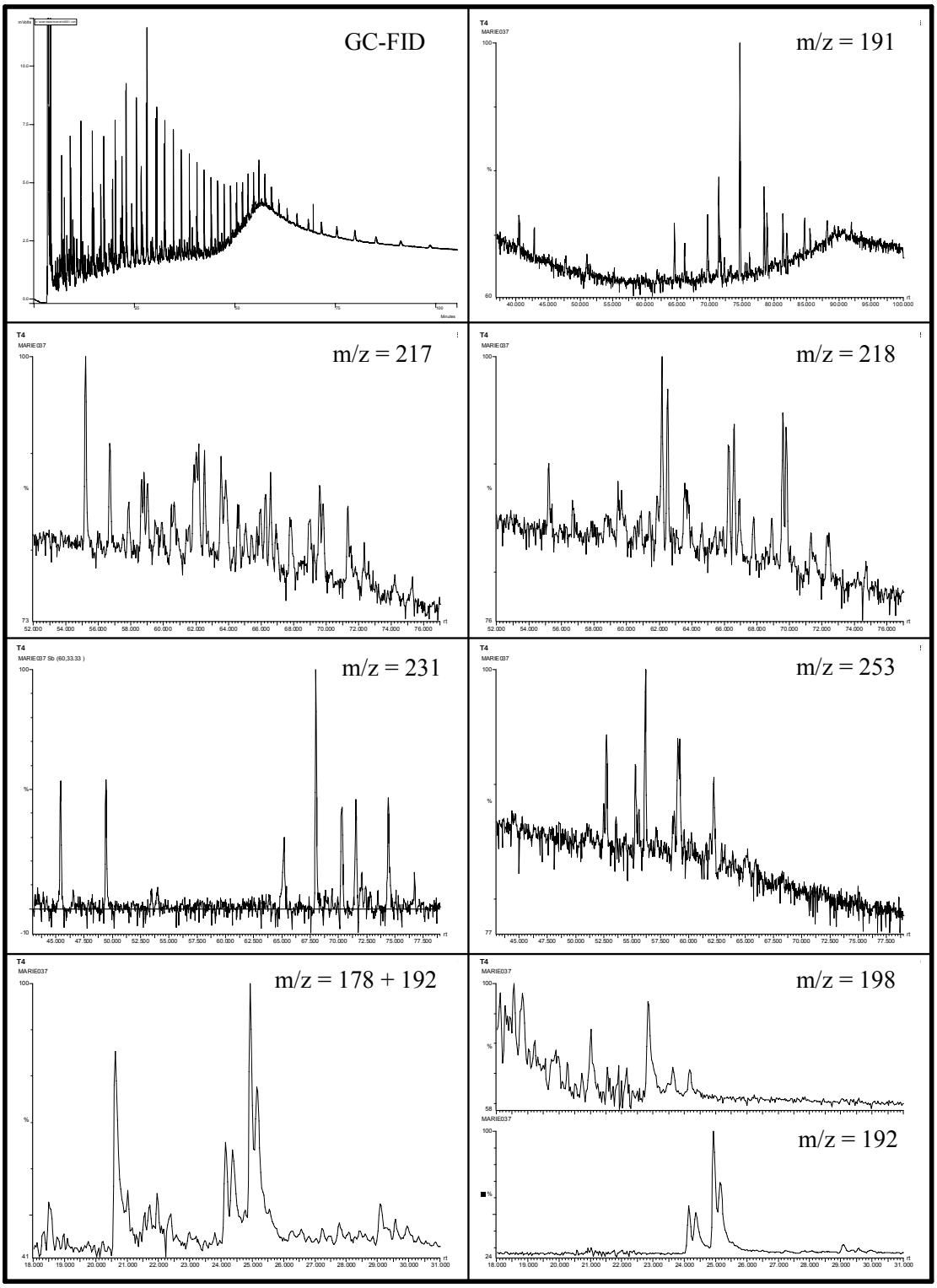

Figure 5.6. The chromatograms for the T4 sample.

T5

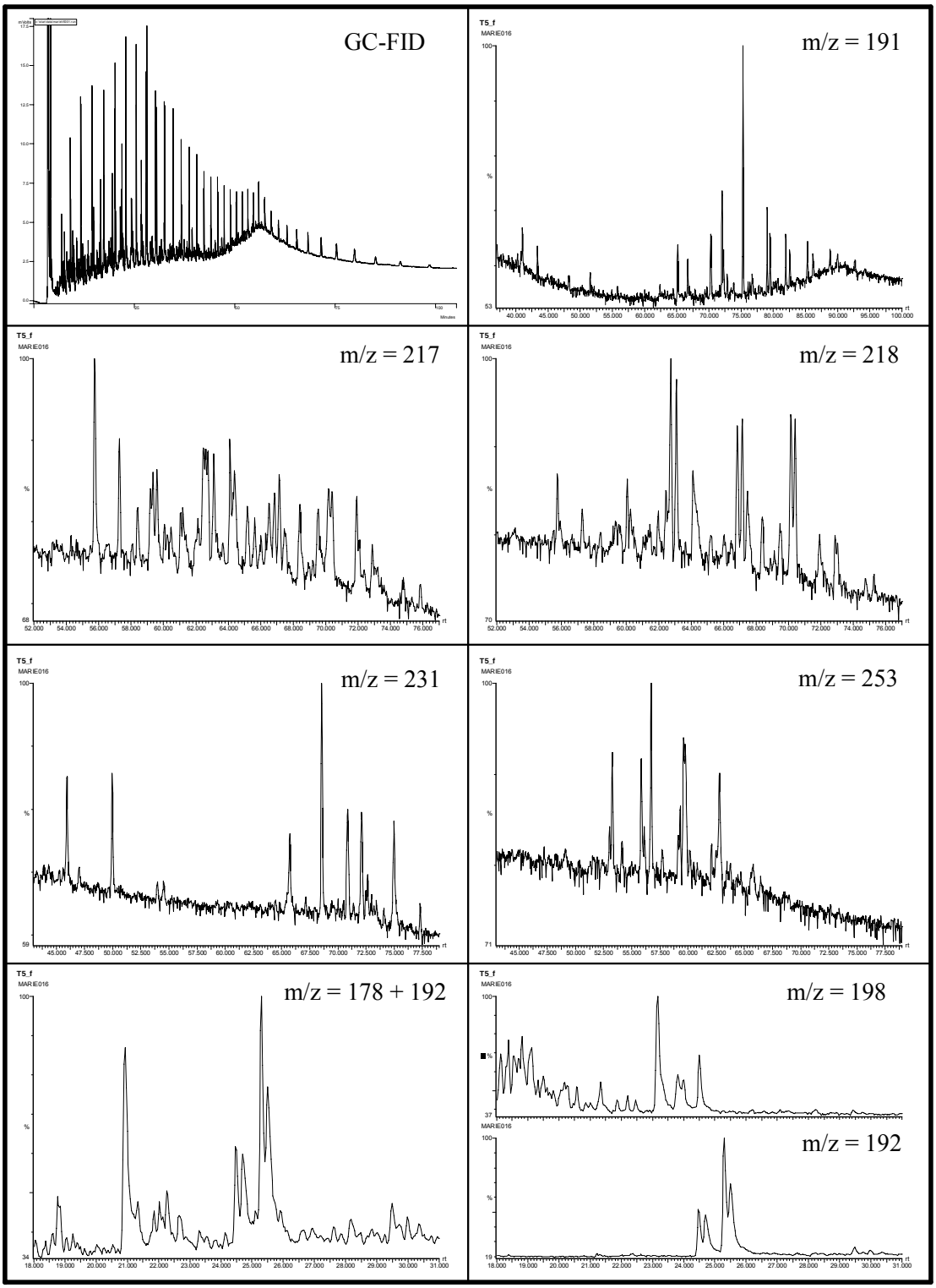

Figure 5.7. The chromatograms for the T5 sample.

Svale1

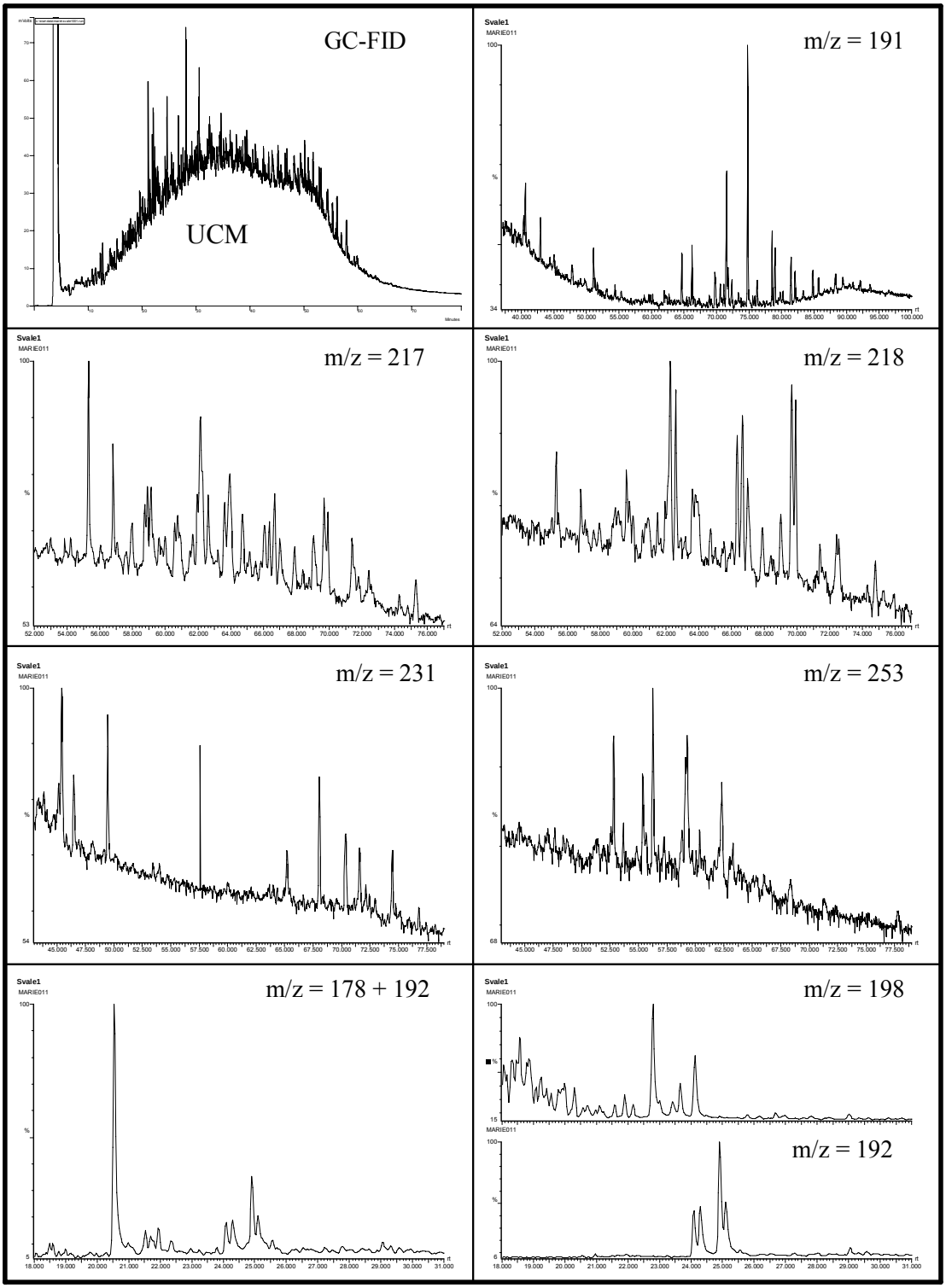

Figure 5.8. The chromatograms for the Svale1 sample.

Svale2

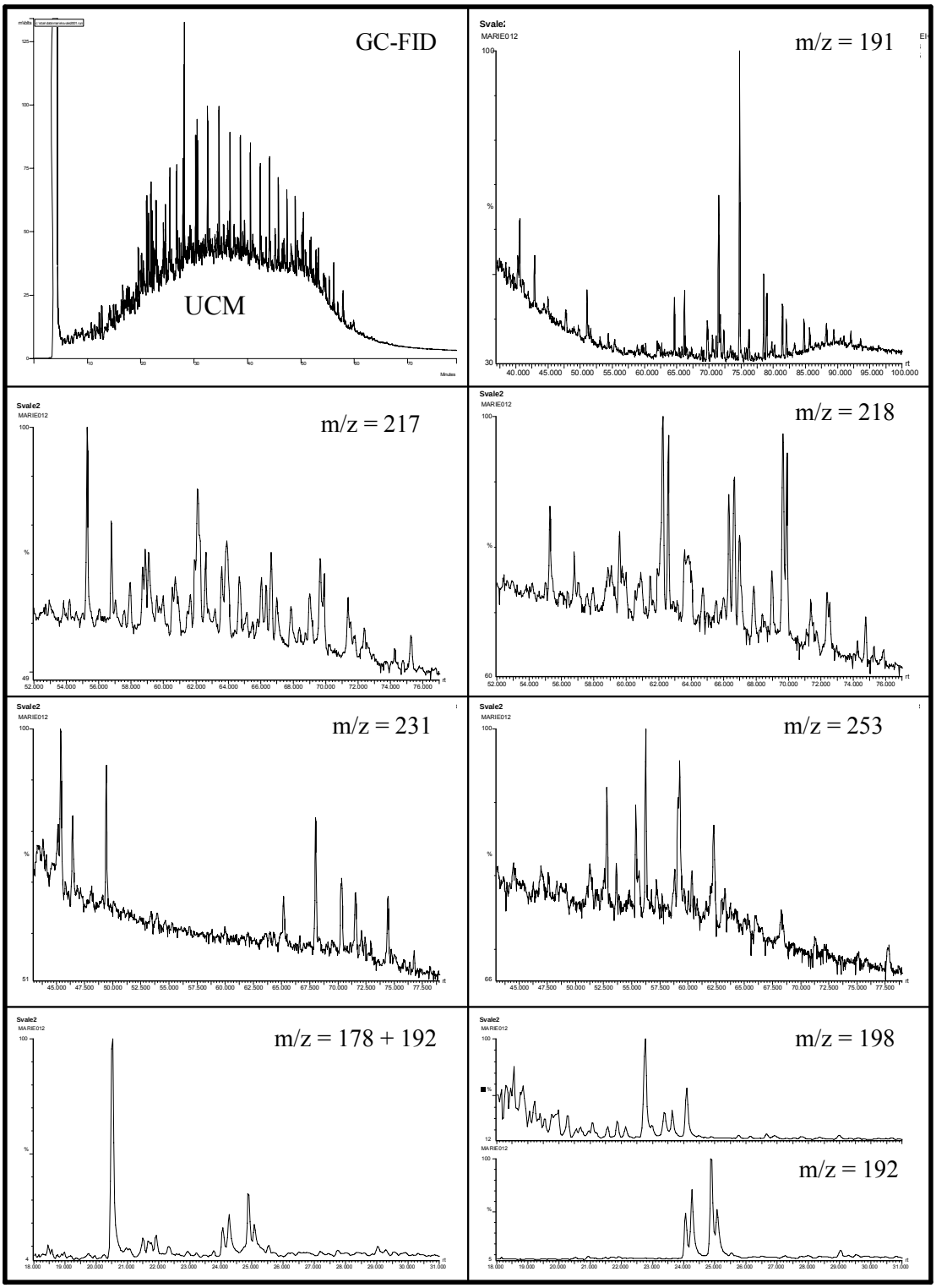

Figure 5.9. The chromatograms for the Svale2 sample.

6507/7-2 DST2

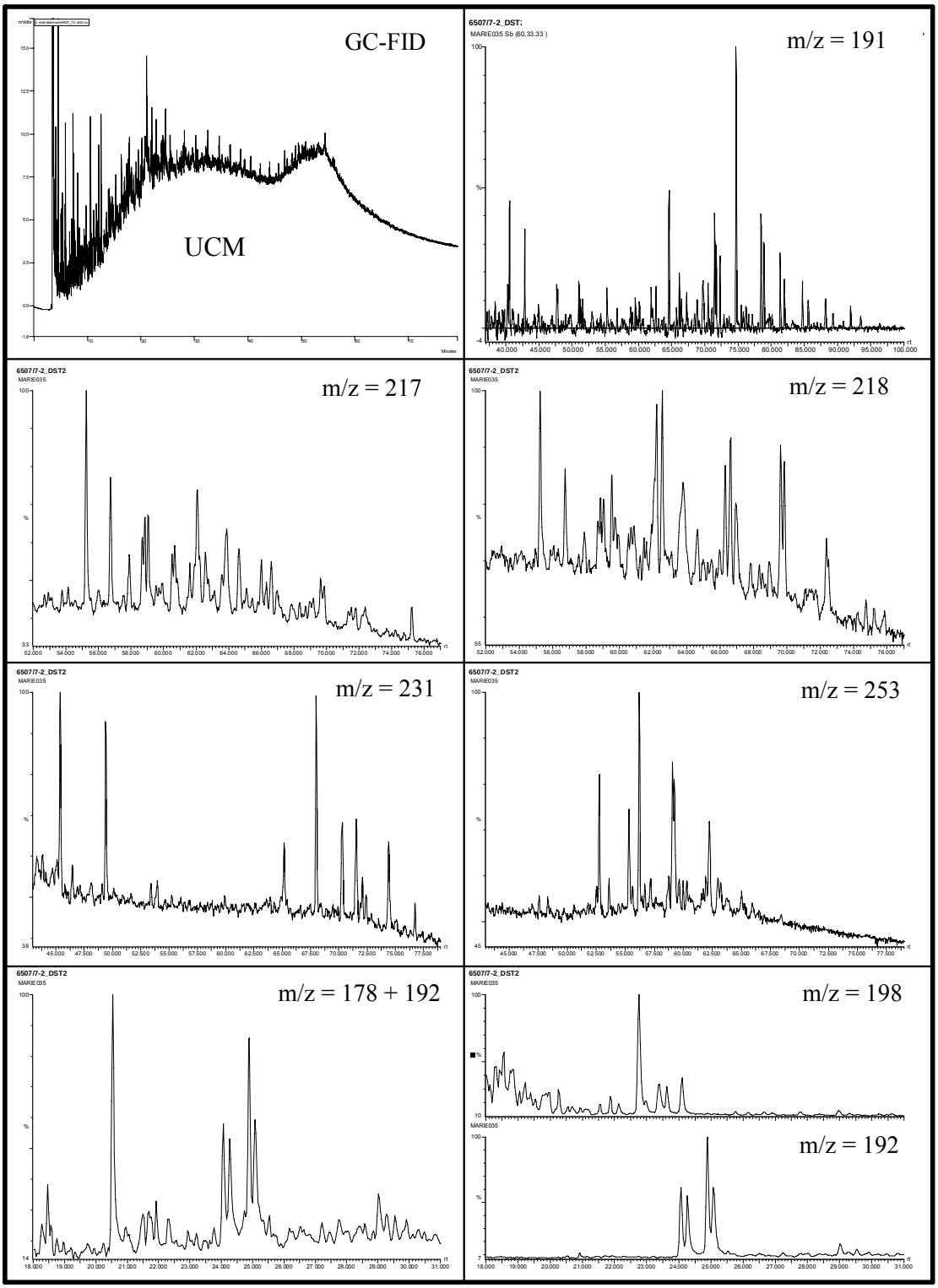

Figure 5.10. The chromatograms for the 6507/7-2 DST2 sample from the Heidrun field.

6507/7-4 DST1

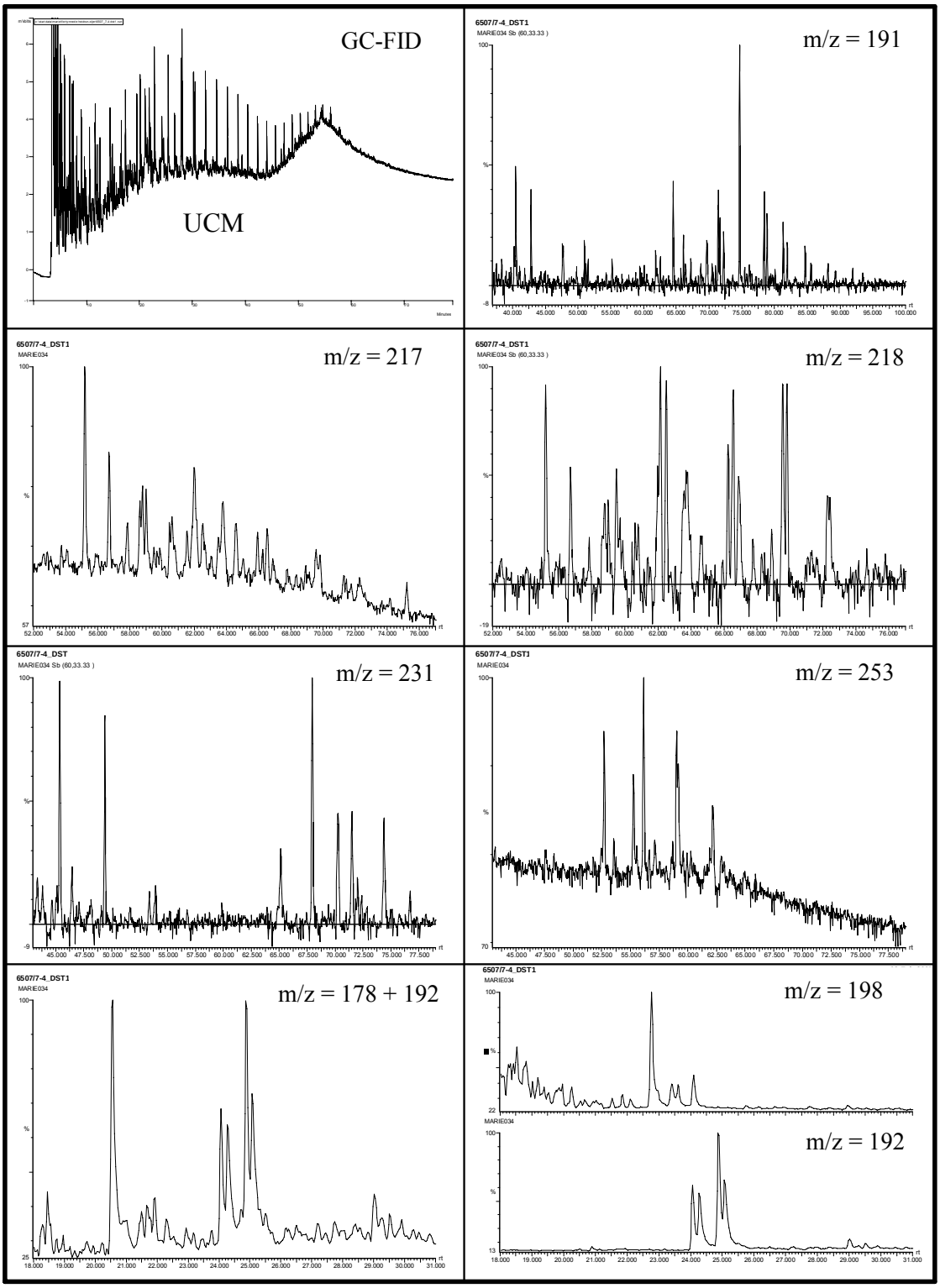

Figure 5.11. The chromatograms for the 6507/7-4 DST1 sample from the Heidrun field.

6507/7-4 DST3

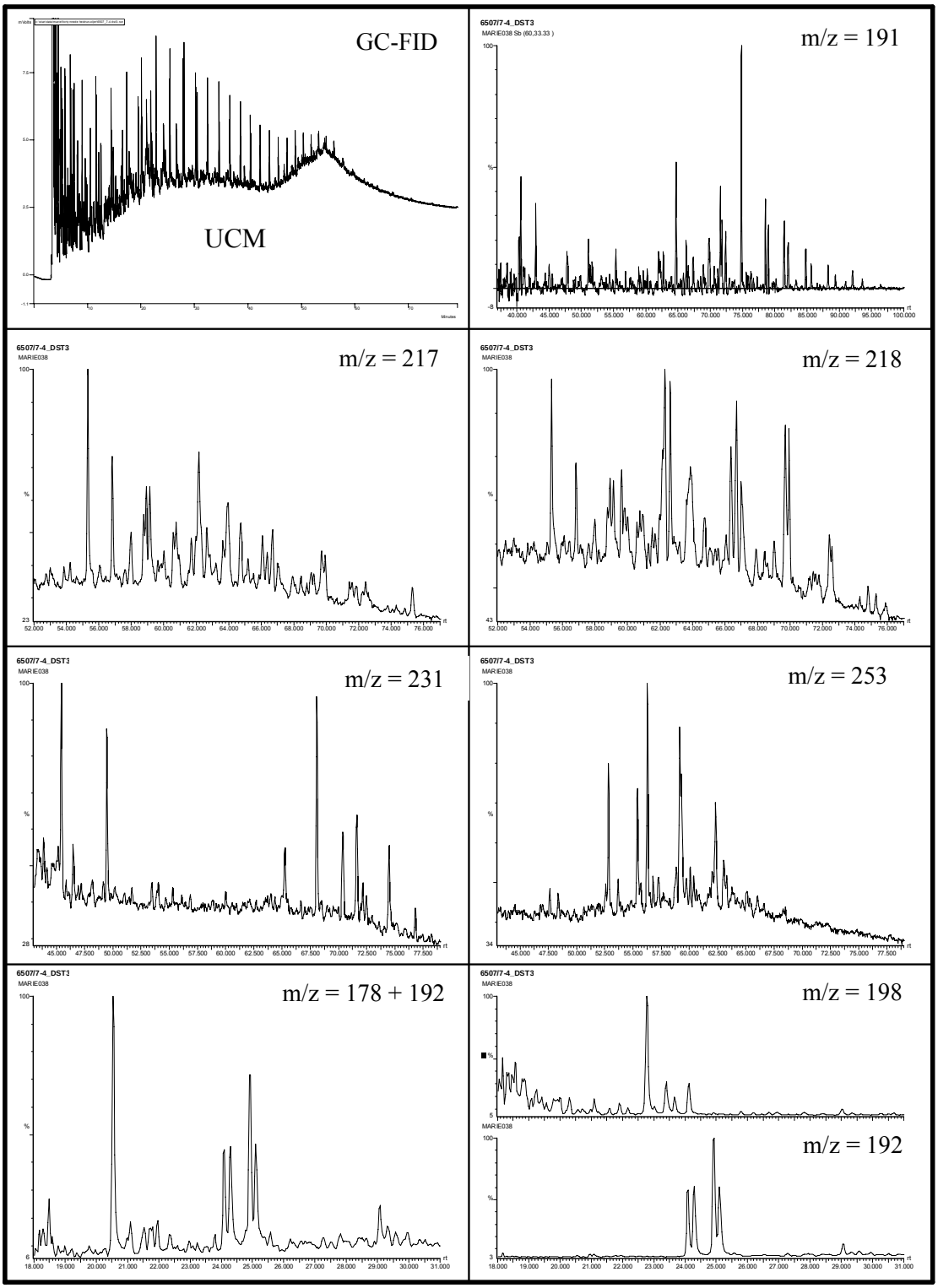

Figure 5.12. The chromatograms for the 6507/7-4 DST3 sample from the Heidrun field.

6507/7-5 DST2A

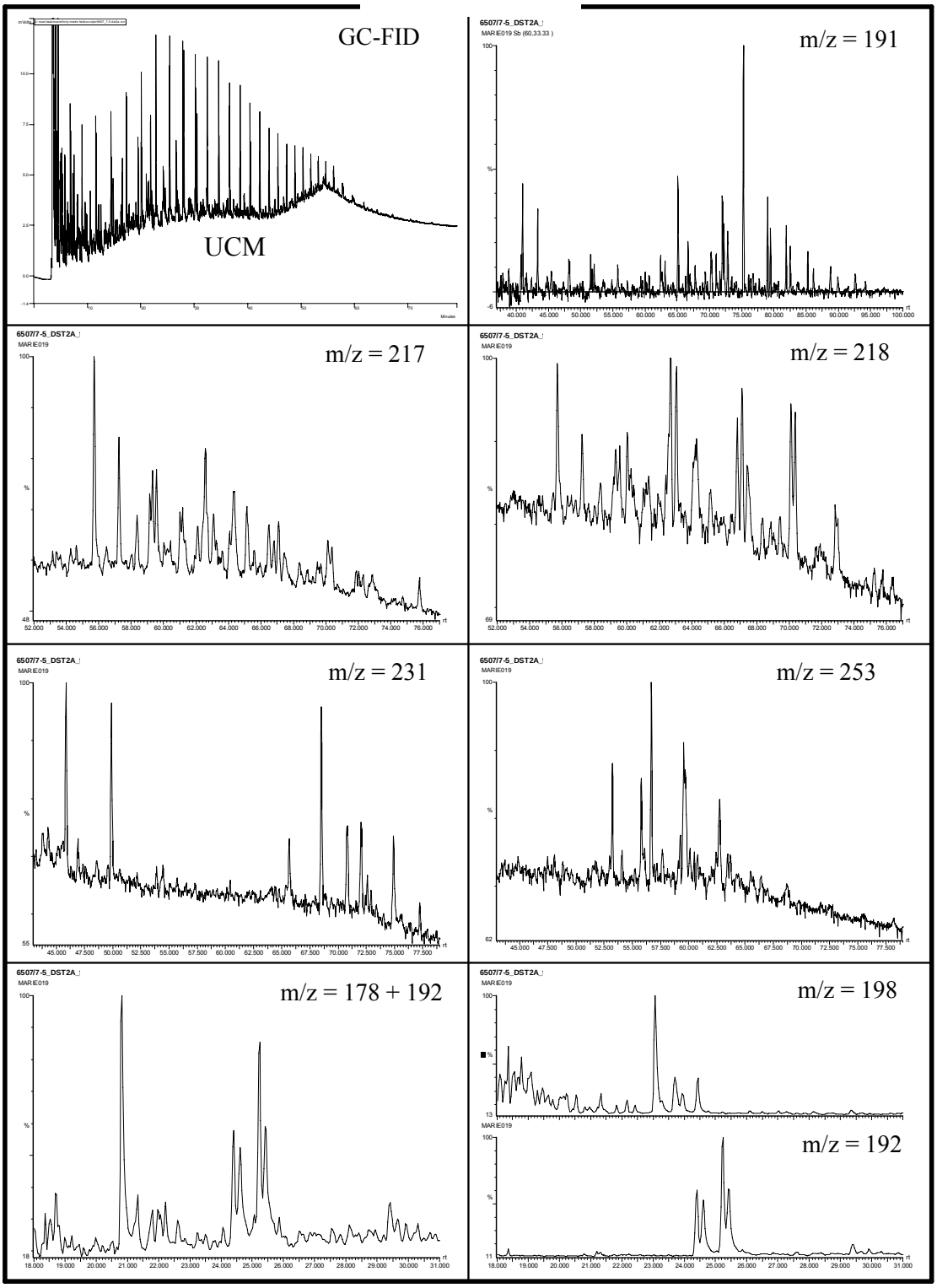

Figure 5.13. The chromatograms for the 6507/7-5 DST2A sample from the Heidrun field.

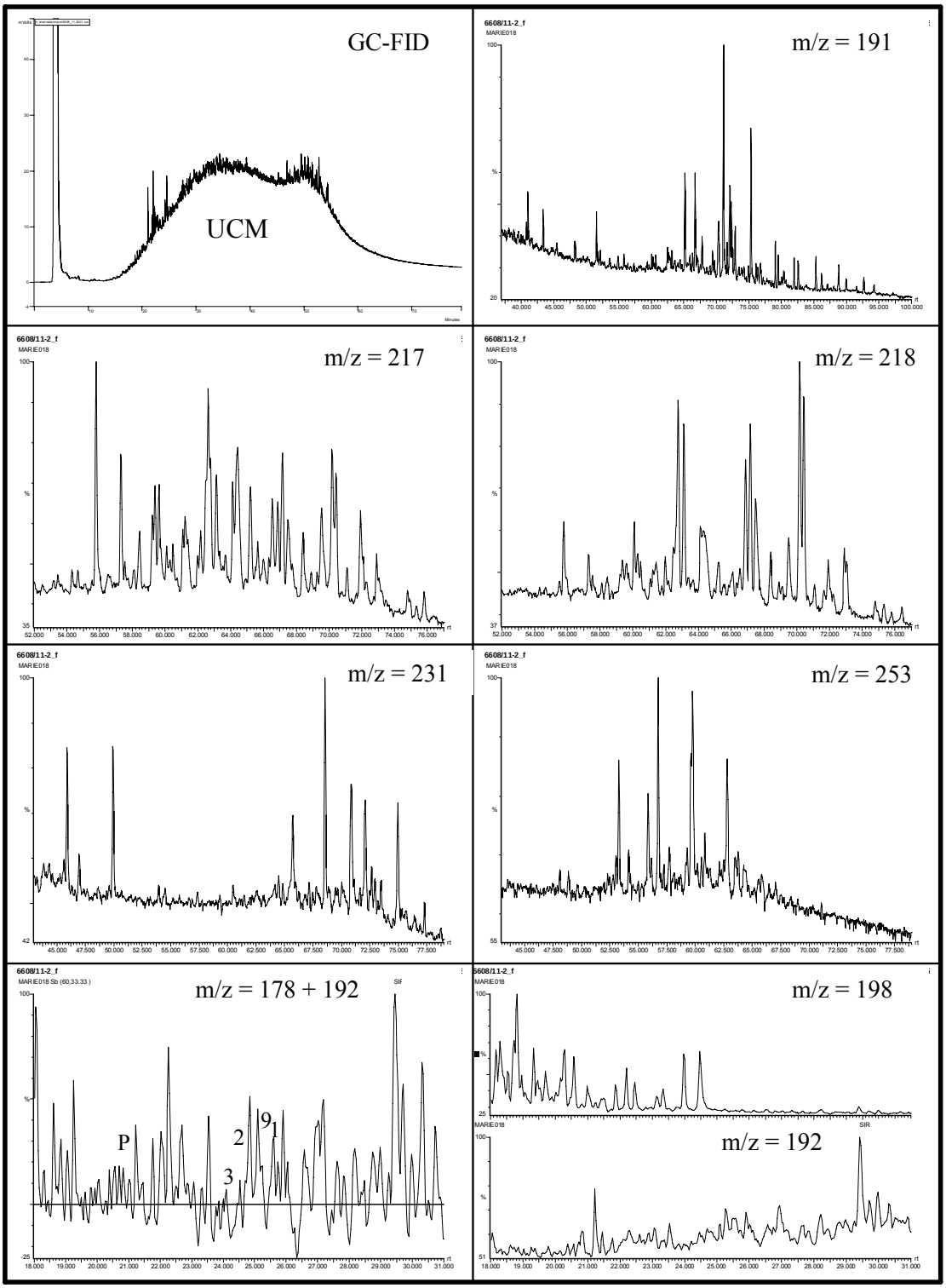

Figure 5.14. The chromatograms for the sample from the Falk field.

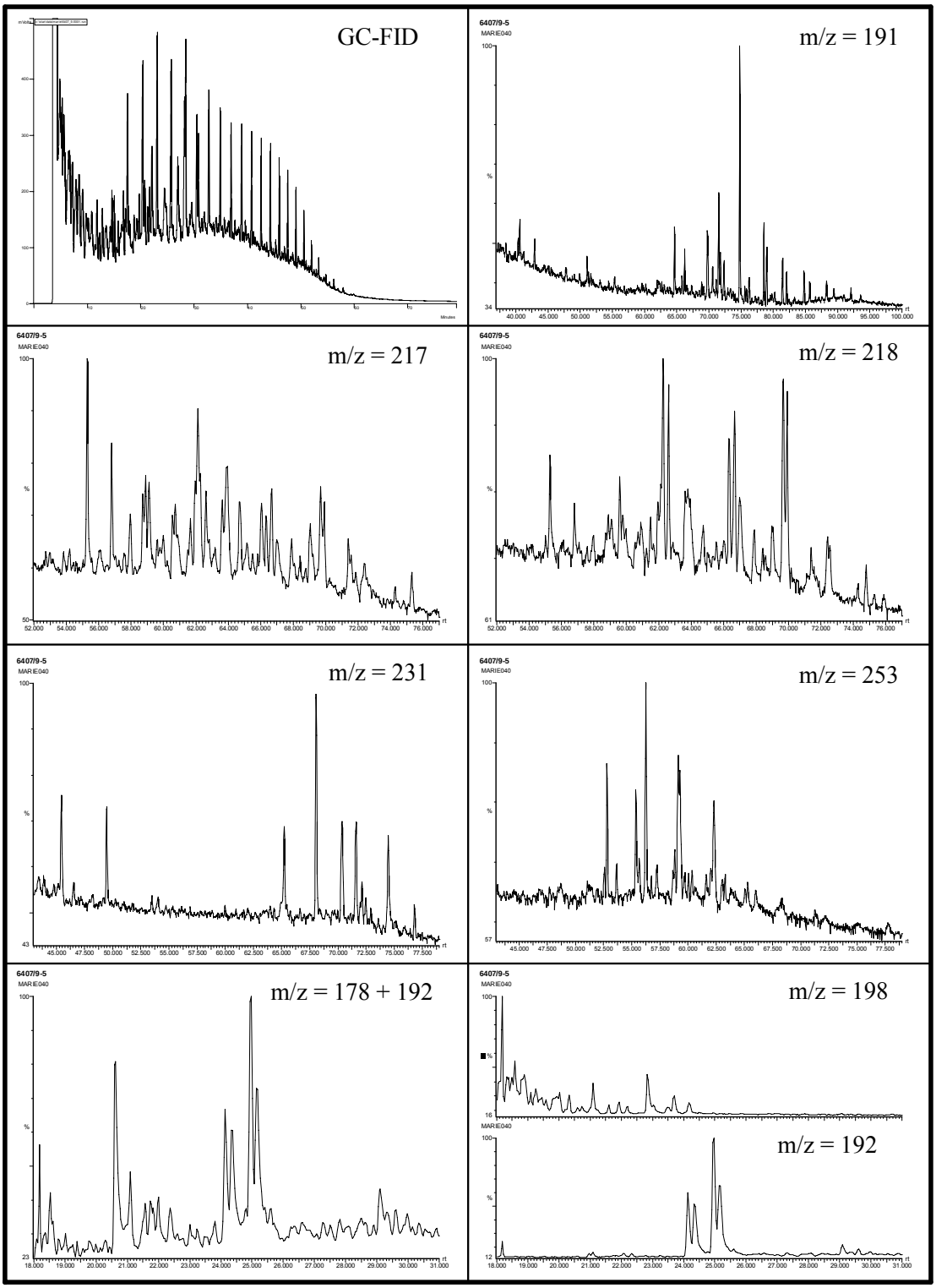

Figure 5.15. The chromatograms for the sample from the Draugen field.

B IMP

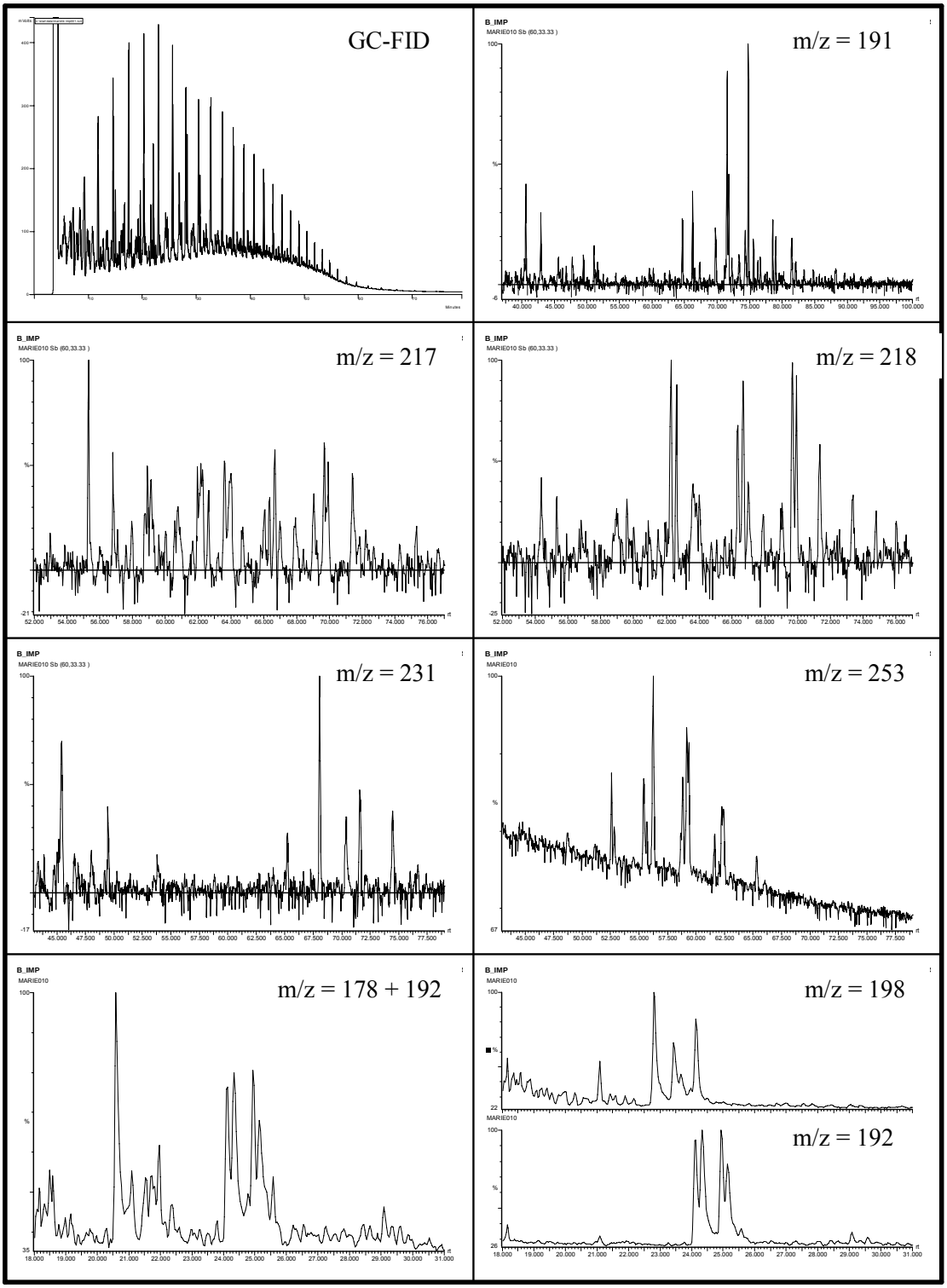

Figure 5.16. The chromatograms for the B IMP sample.

7/12-6 DST1

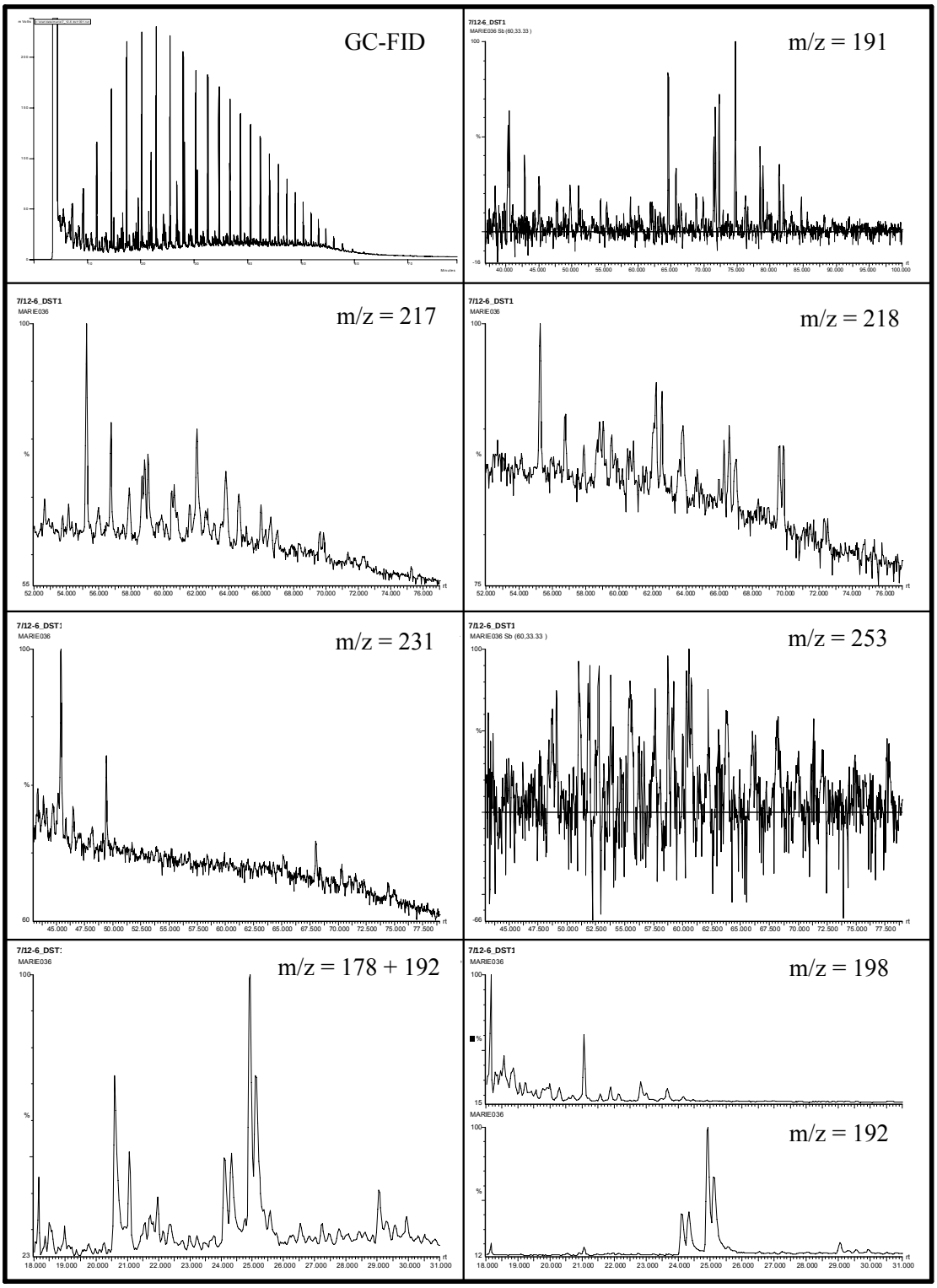

Figure 5.17. The chromatograms for the sample from the Ula field.

NSO-1

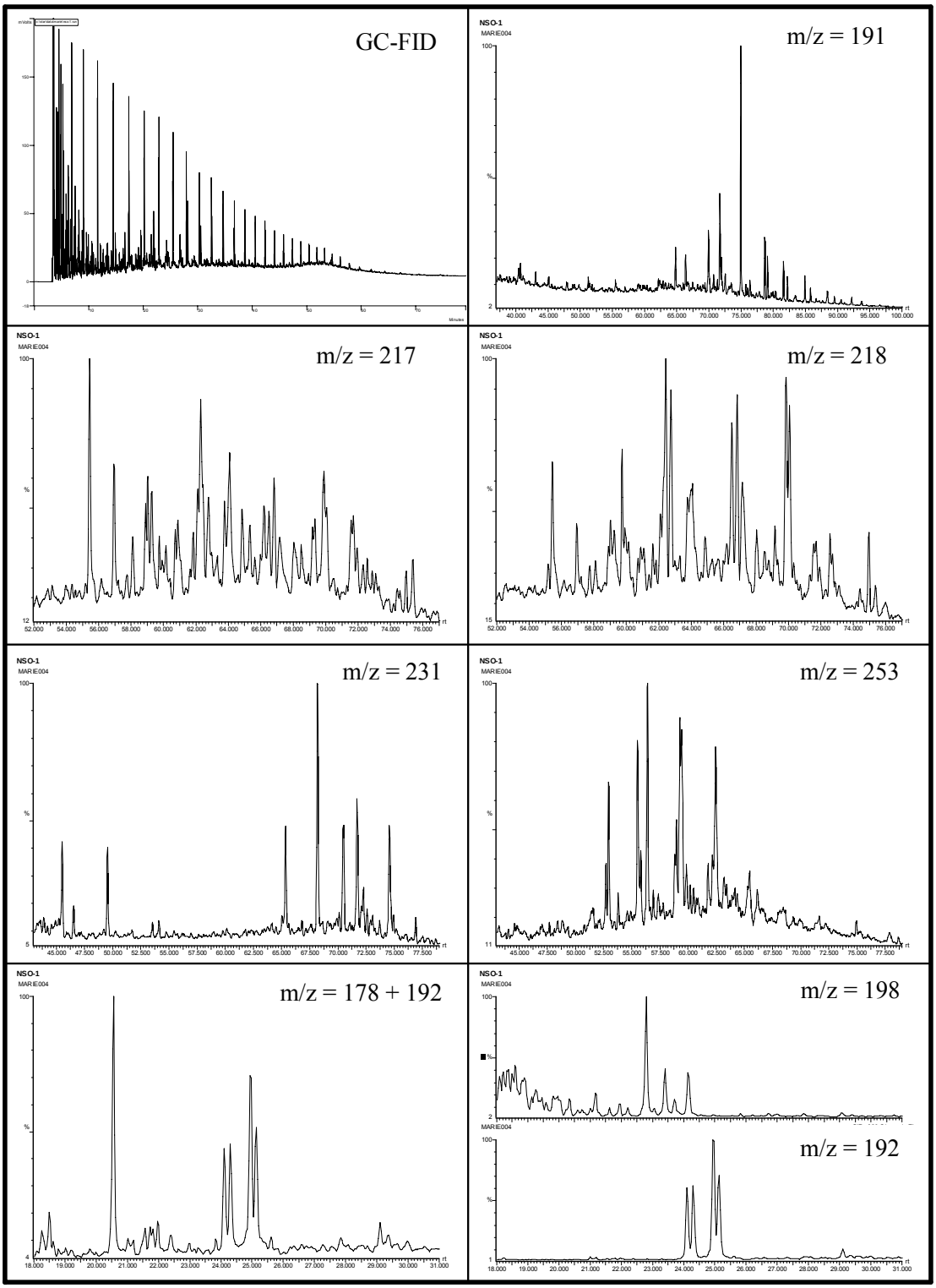

Figure 5.18. The chromatograms for the NSO-1 sample.

6. Discussions

In this chapter the results from chapter 5 will be evaluated. To illustrate maturity and organic facies, several plots have been generated. There will also be a discussion of the very apparent waxes in the T samples. Finally there will be a summary of the maturities and organic facies for the different samples.

6.1 Maturity

The maturity of a petroleum sample usually refers to the grade of heat experienced by the source rock until the petroleum became expelled. The maturity normally increases with burial depth. The oil window is the depth interval in which a petroleum source rock generates and expels most of its oil. The so called oil window occurs in the temperature range from 60ºC to 160ºC (Hunt, 1996), which typically corresponds to a depth interval of 2-5 km, given geothermal gradients in the range of 30-35°C.

The maturity of the samples is estimated using a variety of parameters, both from GC-FID and from GC-MS (biomarkers). There is generally in petroleums correspondence of the parameters for a given sample, but due to different source rock facies, migration histories, fractionation and degree of in-reservoir mixing, biodegradation, gas-stripping or water washing (Karlsen et al., 1993; 2004), parameters may in cases show varying trends for the individual samples in the sample set.

6.1.1 Medium range maturity parameters

The n-alkane distribution changes as a result of the maturity of the source rock. This change is often expressed by the CPI ratio (Peters and Moldowan, 1993; Philippi, 1965) in particular for low to medium maturity oils.

Based on the Pr/n-C_{17} and Ph/n-C_{18} ratios, which are cross-plotted in figure 6.8 and 6.13, the samples can be arranged into a sequence based on maturity. The most mature sample is the one from the Ula field, followed by B IMP → NSO-1 → Heidrun → Draugen → T samples → Svale.

The pristane/phytane ratio can also be used as a maturity parameter; the ratio will increase with increasing thermal maturity (Alexander et al., 1981). However, this ratio should be used with caution, because it can be affected both by diagenetic processes and organic facies. The ratio has high values in the sample from the Draugen field (see table 5.2 and figure 6.12). This may suggest that this sample came from a different source rock or depositional environment, since the sample generally show a medium maturity within the sample set.

6.1.2 Biomarker maturity parameters

Long chained biomarkers constitute the heavier part of the petroleum, and it is possible that these maturity indicators in some cases show contrasting maturities compared to the medium range parameters (Karlsen et al., 2004).

The maturity parameters for this sample set shows a quite uniform distribution of thermal maturities. All samples were generated from inside the oil window in terms of maturity, indicated by the 22S/(22S+22R) of the C_{31} hopane (see figure 6.1). This ratio reaches a maximum value of approximately 0.6 at the onset of oil generation (Peters and Moldowan, 1993) and does not evolve beyond this equilibrium value. However, the MPDF parameter on the phenanthrene has a larger dynamic range. The MPDF values in figure 6.1 illustrate the vertical distribution of maturity. This shows that the sample set covers the oil window from early, to peak and the late state of oil generation.

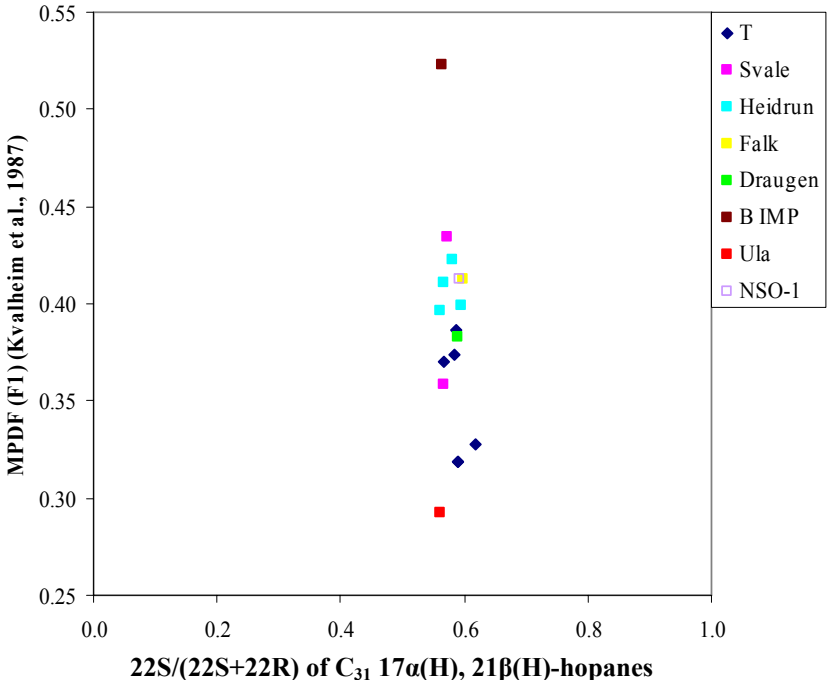

Figure 6.1. A cross plot of the MPDF (F1) parameter (parameter 20) versus 22S/(22S+22R) of C31 17α(H), 21β(H)-hopanes (parameter 3).

Figure 6.2 is a cross plot of the maturity parameters 20S/(20S+20R) and ββ/(ββ+αα) of the C_{29} steranes. This plot shows that all the samples are of medium maturity. The T samples have the lowest maturities, while the samples from the Heidrun and Ula fields show the highest maturities. The T samples are grouped together, which indicates that they are of almost the same maturity, and different to the Norwegian oils. Typically cited maximum values for these assumed izomerisation parameters are 0.7 for ββ/(ββ+αα) for C29 steranes (Peters and Moldowan, 1993) and 0.55 for 20S/(20S+20R) (Peters and Moldowan, 1993).

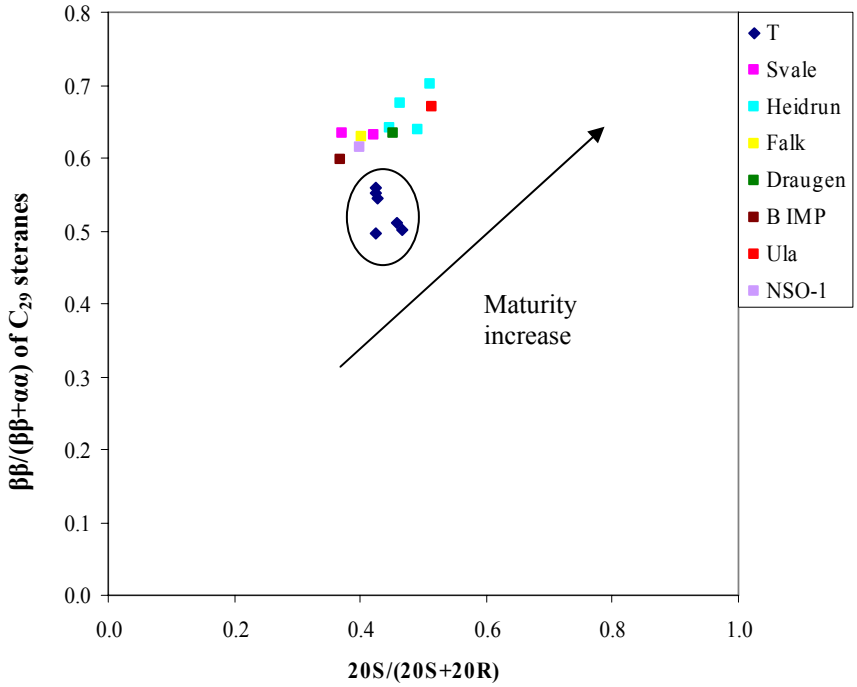

Figure 6.2. Cross plot of the maturity parameters 20S/(20S+20R) (parameter 11) and ββ/(ββ+αα) of C_{29} sterane (parameter 10). The T samples show lower maturities than the other samples, and plot separately in this diagram, forming a group. The samples from Heidrun and Ula show the highest maturities.

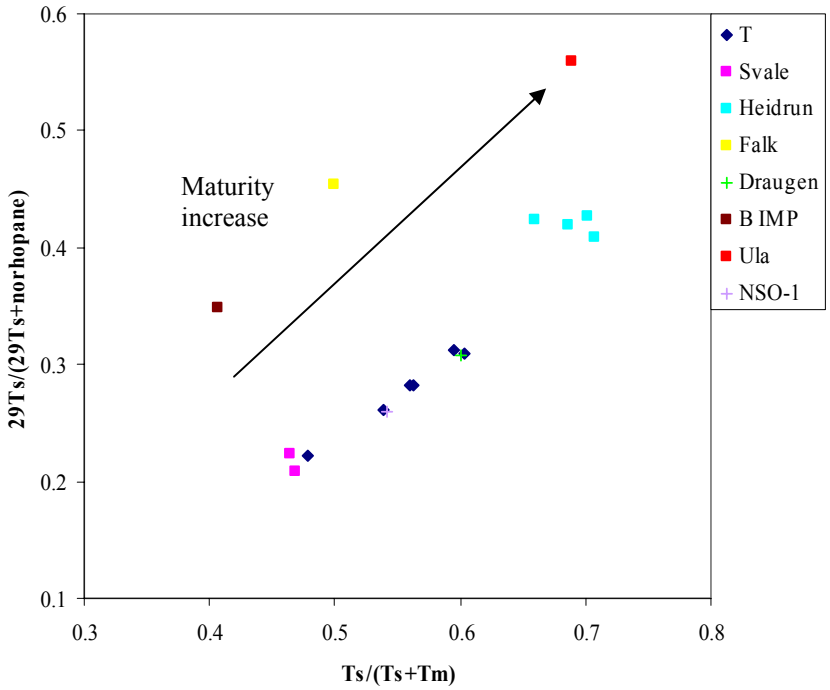

Figure 6.3. Maturity parameters Ts/(Ts+Tm) (parameter 1) and 29Ts/(29Ts+norhopane) (parameter 5) plotted together reflecting maturity differences within the sample set. The Ula sample shows the highest maturity, and the Svale samples show the lowest. The T samples are in this diagram distributed together with the other samples albeit towards the low maturity side.

The cross-plot of the parameters Ts/(Ts+Tm) and 29Ts/(29Ts+norhopane) in figure 6.3 illustrates the maturity difference in the sample set. The maturity trend is that the Ula sample is the most mature, followed by the Heidrun samples → Falk → Draugen → NSO-1 → B IMP → Svale. The T samples plots between the samples from Draugen and Svale.

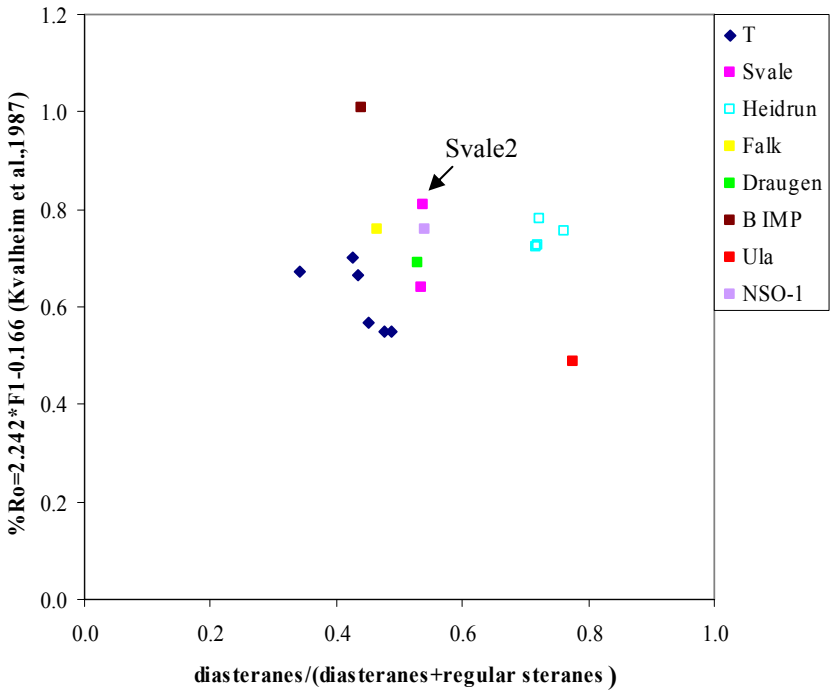

Figure 6.4. The maturity parameter diasteranes/(diasteranes+regular steranes) (parameter 12) plotted against maturity parameter Ro=2.242*F1-0.166 (parameter 24).

Figure 6.4 indicates that the samples from the Heidrun field are the most mature, followed by B IMP and Svale2, while the T samples have the lowest maturity. Note that diasteranes witherstand biodegradation better than do steranes (Ashan, 1993; Ashan et al., 1997) and that the Svale oils are severely biodegraded with large UCMs (figure 5.8 and 5.9). Hence, this may explain the high score for Svale in this parameter. The B IMP sample is from the Cretaceous La Luna formation which is a carbonate and carbonates generally contain less diasteranes than silisiclastic source rocks (Waples and Machihara, 1991).

Figure 6.5 show that the samples only have slight differences in thermal maturity. These differences reflect different degree of burial of the source rock and may represent different stages

of oil generation. Note again that the B IMP sample plus the biodegraded Falk sample from the Svale region deviate from the other samples.

The 22S/(22S+22R) ratio of hopanes has an equilibrium ranging from 0.57 to 0.62 (Seifert and Moldowan, 1986) corresponding to a vitrinite reflectance of 0.6%. This value reflects that the oils are migrated and not in-situ generated. The values of the samples in the sample set are close to equilibrium, which indicates that all the samples have reached or surpassed oil generation (see figure 6.6). The 20S/(20S+20R) ratio of steranes reaches equilibrium at 0.55 (Seifert and Moldowan, 1986), corresponding to a vitrinite reflectance of 0.8%. All the samples are close to reaching equilibrium, except Svale2 and B IMP, which both have ratios of 0.37. Both parameters indicate maturity in the peak oil level for all samples as shown in figure 6.6.

The Ts/(Ts+Tm) and the diasteranes/(diasteranes+regular steranes) ratios (see figure 6.7) illustrates the maturity differences in the sample set. The maturity trend for the oils indicate that the samples from the Heidrun and Ula fields are the most mature, followed by Draugen → NSO-1 → Svale → Falk → B IMP. The T samples plot somewhere between Draugen and Falk. The samples are generally indicated to have a somewhat lower maturity, i.e. early oil stage, than indicated by the other parameters. The diasteranes/(diasteranes+regular steranes) ratio may also be affected by facies as mentioned earlier; oils from carbonate source rocks may have lower ratios than oils from clastic source rocks (Peters and Moldowan, 1993). Note the relatively low ratio for the B IMP sample, which is originated from a carbonate source rock facies.

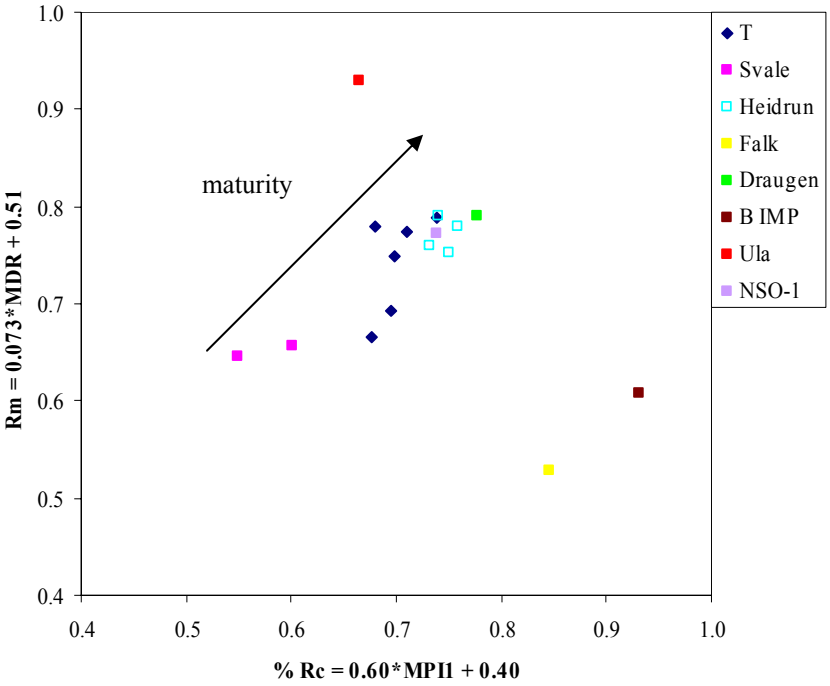

Figure 6.5. The maturity parameters %Rc = 0.60*MPI1 + 0.40 and Rm = 0.073*MDR + 0.51 plotted against each other to show the maturity distribution in the sample set.

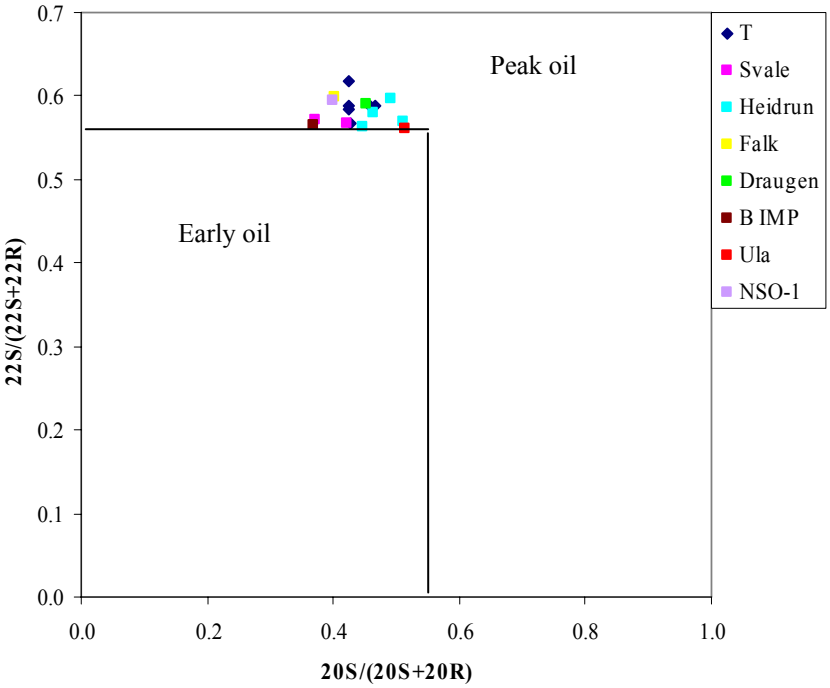

Figure 6.6. A cross plot of the 20S/(20S+20R) parameter and the 22S/(22S+22R) parameter describes maturity increases. The figure illustrates that all the samples from the sample set have reached peak oil generation.

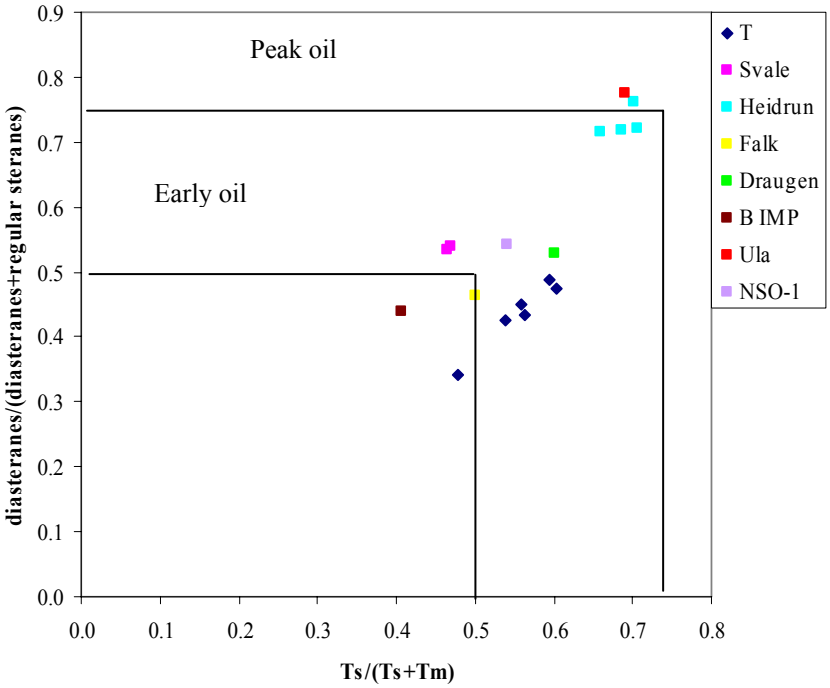

Figure 6.7. A cross plot of the parameters Ts/(Ts+Tm) and diasteranes/(diasteranes+regular steranes) indicating maturity, and may also be influenced by the organic source rock facies. The values increase with maturity, and are valid for the whole oil window.

6.1.3 Summary of maturities

The samples represent a wide span in maturity, ranging from petroleum generated early to late in the oil window. The 22S/(22S+22R) values of the samples in the sample set are close to equilibrium, which indicates that all the samples have reached or surpassed oil generation (see figure 6.6).

The suggested maturity trend is that the sample from the Ula field is the most mature followed by Heidrun → Draugen → NSO-1 → Falk → B IMP → Svale. The T samples generally plots between the sample from the Draugen field and B IMP. The Svale samples show a relatively high maturity for the diasterane/(diasterane+regular sterane) parameter. This is probably because diasteranes witherstand biodegradation better than do steranes, hence the Svale samples will be enriched with diasteranes.

6.2 Organic facies

6.2.1 Medium range facies parameters

The Pr/Ph ratios typical for type II marine shales are 0.6-1.6 (Elvsborg et al., 1985; Cohen and Dunn, 1987). Most of the samples fall into this category, except the sample from the Draugen field, Svale2 and 6507/7-2 DST2 from the Heidrun field. These samples have higher values, which may indicate a more terrestrial input. Figure 6.12 is a plot of Pr/Ph and hopane/sterane, which indicate that all the samples are derived from a marine source rock.

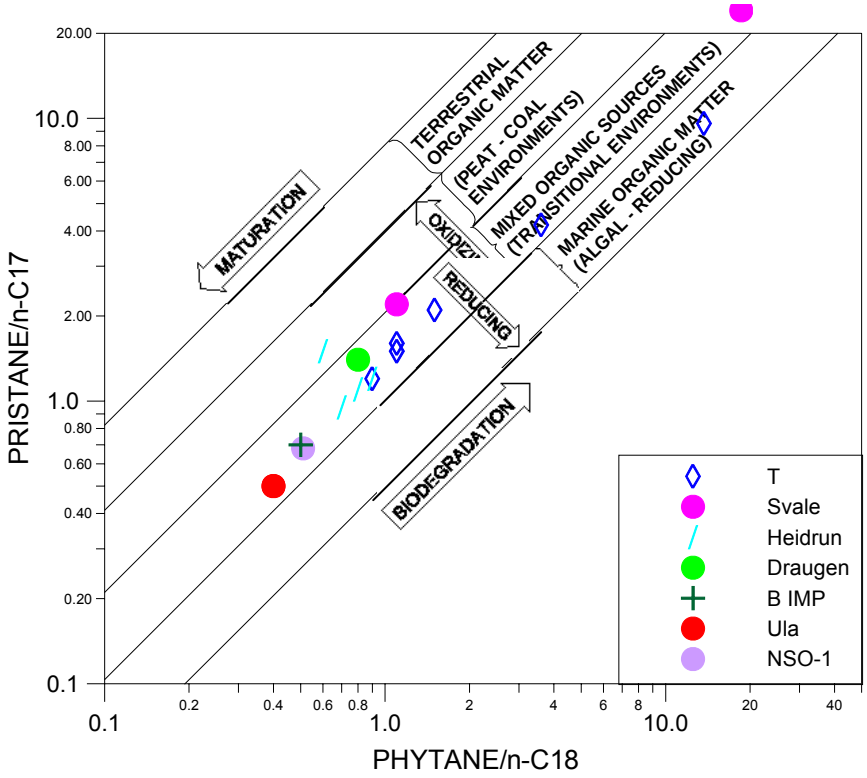

Figure 6.8. A cross plot of the Pristane/n-C_{17} versus Phytane/n-C_{18}. The Falk sample is not in the plot due to lack of data i.e. all n-alkanes were removed by biodegradation (from Shanmugam, 1984).

According to figure 6.8, most of the samples have originated from mixed organic sources. This is normal for transitional environments, which is also indicated in figure 6.10. Figure 6.8 shows that the sample from the Ula field is most mature, and the general trend for the T samples is one of lower maturity than for the other samples. Figure 6.8 could, with regard to the T samples, be taken to indicate that the T samples are biodegraded, but the GC-FID traces show that the

samples are only slightly biodegraded, as they probably not have been exposed to oxygenated meteoric water in the caverns. However, limited anaerobic oxidation might have occurred.

6.2.2 Biomarker facies parameters

The relationship between C_{27}, C_{28} and C_{29} ββ-steranes have been used to distinguish source rock facies of petroleum. Figure 6.9 is a ternary diagram showing the depositional environment (facies) of the samples. The diagram is divided into sub-areas where the individual areas are assigned to specific depositional environments (Shanmugam, 1984). It is indicated that all the samples originated from open marine source rock facies. The sample from the Falk discovery show a higher terrestrial input than the other samples.

The validity of the ternary diagram from Shanmugam (1984) is debated, and interpretation of source rock and its facies based entirely on sterane distributions alone is not recommended (Moldowan et al., 1985; Horstad, 1989). However, it is the case that most petroleums from the Norwegian Shelf plot in the same central indicated part of this diagram (Karlsen et al., 1993; 2004). Hence it is likely that the T samples are of marine type II origin.

All the samples are in the range Pr/Ph = 1-2 (figure 6.10), which indicate normal marine facies. Some of the T samples have the lowest 3-MP/ 4-MDTP ratios in the sample set, which indicates higher sulfur content (the thiophene 5-ring structure contains sulfur). Biodegradation may result in a sulfur enrichment, as benzothiphene derivates and high molecular weight heterocompounds are particularly resistant to bacterial degradation and hence they are selectively concentrated (Tissot and Welte, 1978).

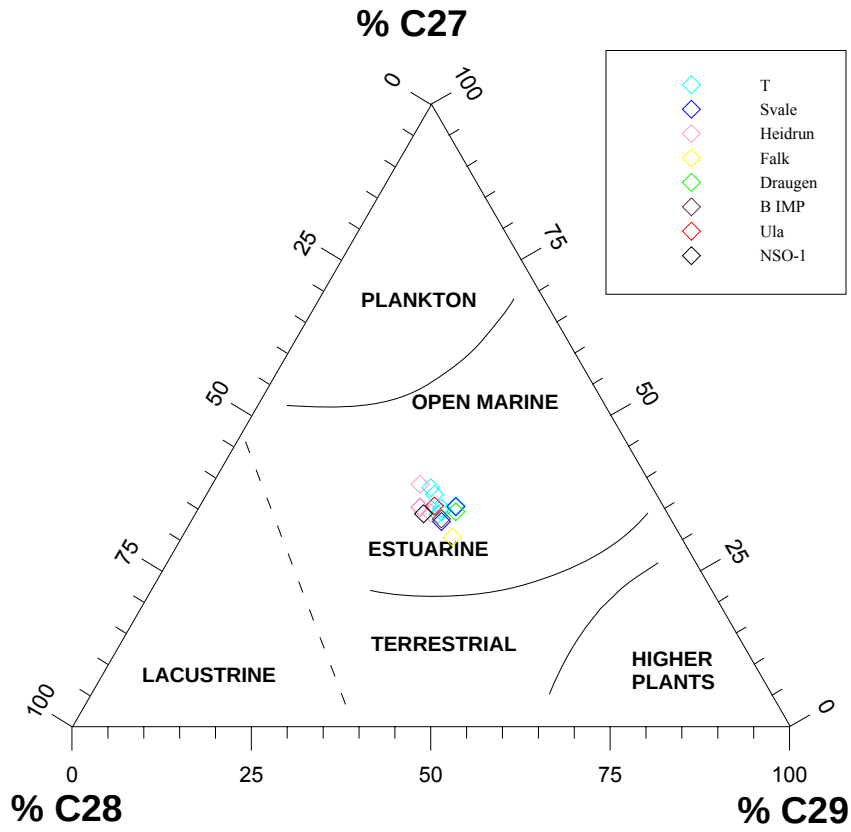

Figure 6.9. Ternary diagram after Shanmugam (1984), showing the relationship between the C_{27}, C_{28} and C_{29} ββ-steranes from the samples, illustrating the likely depositional environment.

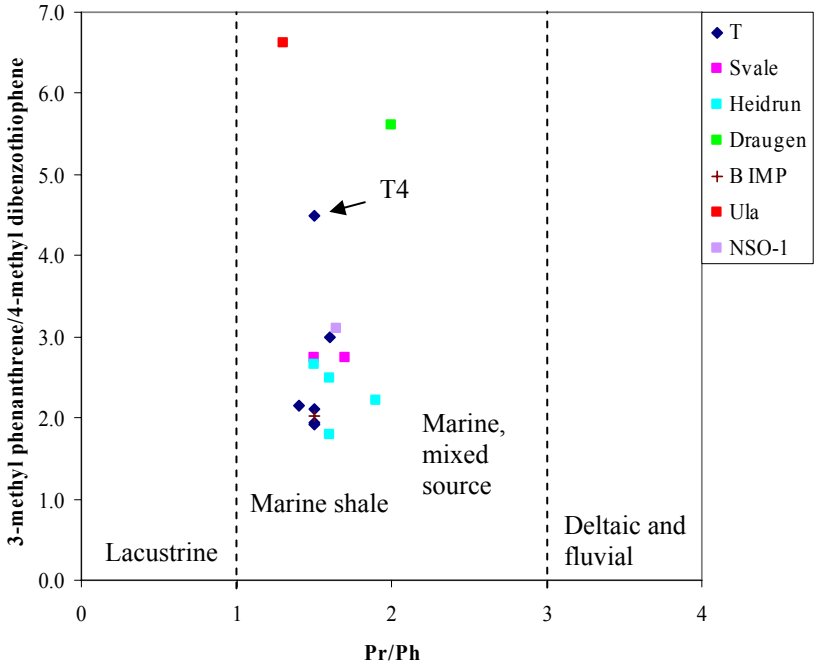

Figure 6.10. The Pr/Ph ratio plotted against the 3-MP/4-MDTP (parameter 26) ratio. This ratio can indicate the facies of petroleums. All the samples have Pr/Ph ratios between 1 and 2, but some of them, like the samples from the Ula field and the Draugen field, show high 3-MP/4-MDTP ratios. T4 stands out from the other T samples by having a rather high 3-MP/4-MDTP ratio (Modified from Hughes et al., 1995).

28, 30 bisnorhopane is present in all the samples, which indicates that the hydrocarbons have been generated from generally the same source rock facies (see figure 6.11).

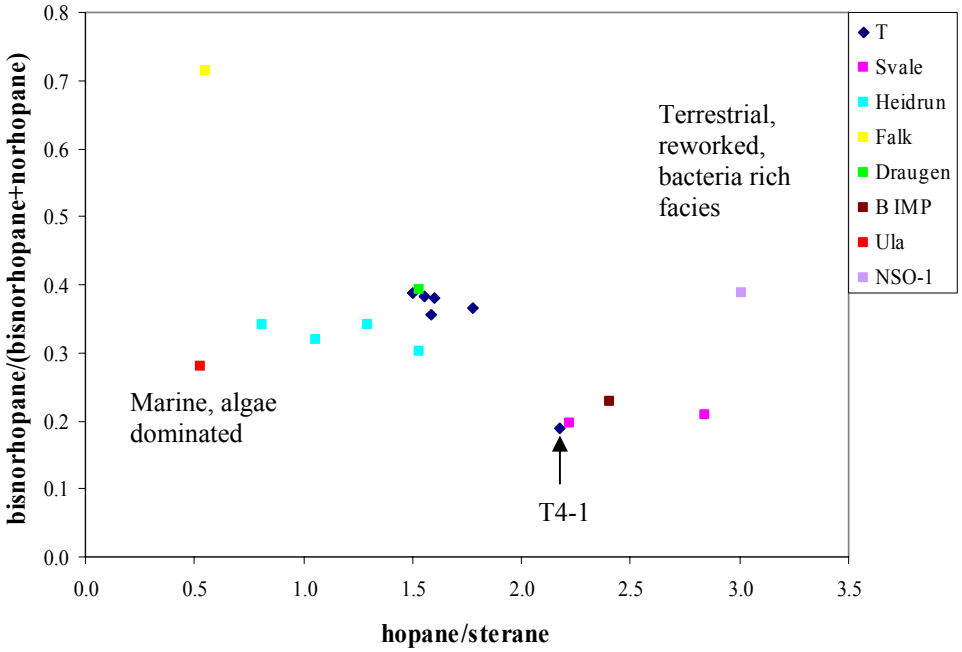

Figure 6.11. Cross-plot of the facies parameters hopane/sterane (parameter 9) versus bisnorhopane/(bisnorhopane + norhopane) (parameter 6). Note the high amount of bisnorhopane in the Falk sample.

Figure 6.11 shows a cross plot of the facies parameters hopane/sterane versus bisnorhopane/(bisnorhopane+norhopane). Low hopane/sterane ratios indicate marine, algae dominated organic matter, while higher ratios point to bacteria rich facies, bacterially reworked organic matter or a terrestrial input (Peters and Moldowan, 1993). The T samples are grouped together, except from the T4-1 sample which has a higher hopane/sterane ratio and lower amount of bisnorhopane.

The sample from the Falk discovery has a high amount of bisnorhopane (see figure 6.11). This is an indicator of anoxic conditions during deposition of the source rock (Peters and Moldowan, 1993). Several studies have confirmed this implication of the compound bisnorhopane (Dahl and Speers, 1985; Horstad, 1989), but anoxic source rocks have also been reported containing no bisnorhopane, and it is suggested that its occurrence is dependent upon a particular bacterial population or algal bloom (Waples and Machihara, 1991).

6.2.3 Summary of organic facies

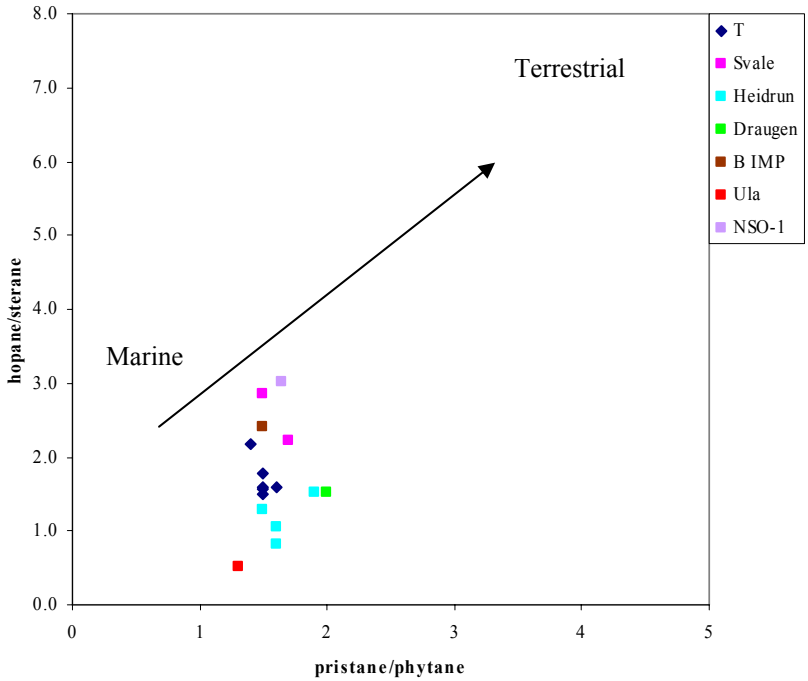

Figure 6.12. A cross plot of the facies parameters pristane/phytane versus hopane/sterane (parameter 9). A high value indicates strong terrestrial input, while lower values indicate normal marine facies.

Figure 6.12 combines medium range and biomarker facies parameters and all the samples plot in the marine area, but with a potentially different terrestrial influx. The NSO-1 and the Svale samples show the highest terrestrial influence followed by B IMP and the T samples. Draugen, Heidrun and Ula show the lowest terrestrial influence. This may indicate a more distal organic source rock facies.

The conclusion is that the depositional environment for the source rock that generated the petroleum in the samples is transitional, meaning it is marine with terrestrial input. Shanmugam (1984) described this to be typical for a proximal type II source rock (see figure 6.9 and 6.13).

The T samples and the samples from the Svale field show lower maturities than the other samples (see figure 6.13) but all the samples plot in the marine area.

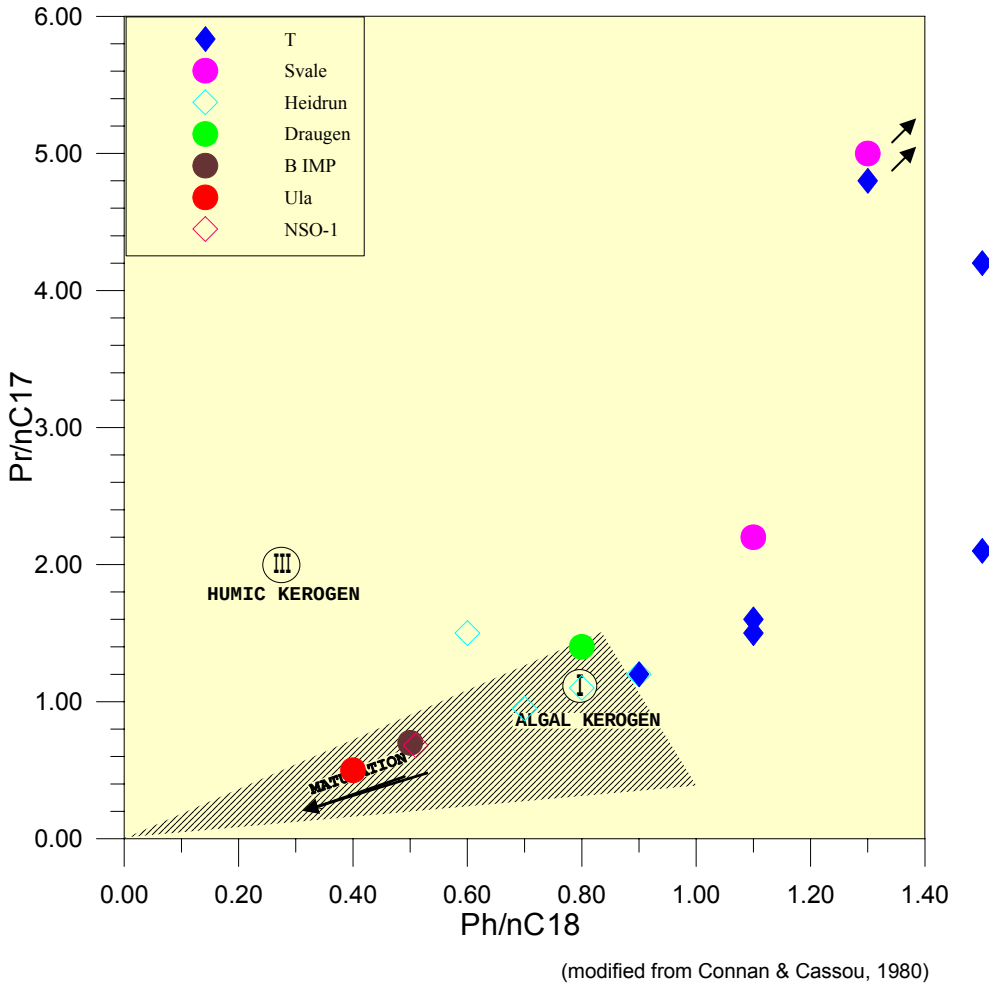

(modified from Connan & Cassou, 1980)

Figure 6.13. A plot of the Ph/n-C18 ratio versus the Pr/n-C17 ratio (modified from Connan and Cassou, 1980) indicating the maturity as well as the type of kerogen present in the source rock from where the petroleum originated.

6.3 Biodegradation of the samples

Biodegradation is the microbial alteration of crude oil, which occur if the there is access to meteoric water, temperature range less than 65-80ºC, absence of H_2S and proximity to an oil-water contact (Ahsan, 1993; Connan, 1984; Milner et al., 1977). Biodegradation results in partial or total removal of n-alkanes, followed by isoparaffins, napthenes (Such as steranes and terpanes), aromatics and eventually the polycyclic aromatics (Winters and Williams, 1969; Evans et al., 1971; Bailey et al., 1973; Chosson et al., 1992; Moldowan et al., 1992).

Biodegradation by loss of n-alkanes

Bacteria will remove n-alkanes prior to any other compound class (Winters and Williams, 1969), thus increasing the relative concentration of acyclic isoprenoids, like pristane and phytane, compared to n-C17 and n-C18 respectively, with increasing biodegradation.

The loss of n-alkanes is classified as moderate biodegradation, as observed in the Svale2 sample. The removal of pristane and phytane are classified as extensive biodegradation, as observed in Svale1 and the Falk sample. The Svale samples show increasing biodegradation with increasing depth. Svale1 is deeper, i.e. closer to the oil-water contact, than Svale2 and more biodegraded. All the n-alkanes are removed from the sample from the Falk discovery. The appearance of the unresolved complex mixture (UCM) hump is observed in both Svale samples, all the samples from the Heidrun field, and the Falk sample (see figure 5.8-5.14)

6.4 Wax

The presence of long-chained n-alkanes (waxes) has been observed in the GC-FID chromatograms for all of the T samples (see figure 6.14). In the T samples the unresolved complex mixture is either not present or only partly present, which indicates that there has been only a very moderate degree of biodegradation of the oils in the underground caverns. There may have been limited access to moving oxygenated water in the storage caverns, which may have led to less biodegradation or only partial anoxic degradation. Gravitational segregation of heavy oil components – including wax formation – has taken place in the storage tanks, as it was observed during sampling that the samples at the bottom of the caverns were solid and waxy: e.g. sample T3-2 in this study (pers. com. Dag A. Karlsen).

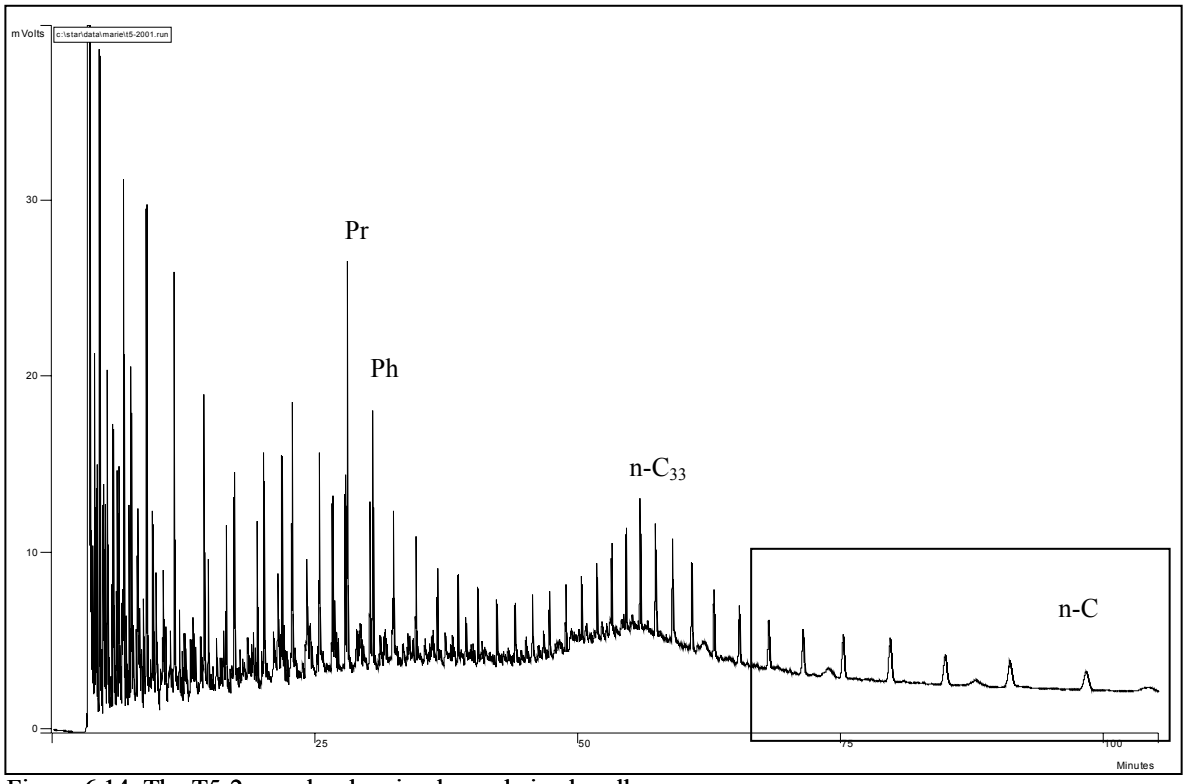

Figure 6.14. The T5-2 sample, showing long-chained n-alkanes.

6.5 Summary of the samples

The main difference in the chromatograms is that the T samples have long-chained n-alkanes (waxes) and show less evidence of biodegradation than e.g. the Heidrun, Svale and Falk samples. Some of the other samples are so severely biodegradated that many of the peaks are difficult to identify. The Falk sample has no detectable pristane nor phytane peaks. In the T samples the unresolved complex mixture (UCM) is not present to only partly present, and in a very low degree in samples T5-2 and T6-1. This testifies to the very moderate degree of biodegradation of the oils in the caverns.

The samples represent a wide span in maturity, ranging from petroleum generated early to late in the oil window. The general maturity trend is that the sample from the Ula field is the most mature, followed by Heidrun → Draugen → NSO-1 → Falk → B IMP and. Svale. The B IMP sample show a higher maturity trend in the medium range maturity parameters, which is

probably due to its carbonate source rock facies. The T samples show a higher maturity in the biomarker maturity parameters than in the medium range maturity parameters. This may be due to the anoxic conditions these samples are exposed to.

The depositional environment for the source rock that generated the petroleum in the samples is transitional, meaning it is marine with some terrestrial input (see figure 6.9). This is typical for a proximal type II source rock (Shanmugam, 1984).

7. Summary and conclusions

The sample set contains wax and oil samples from an underground cavern crude oil storage facility, Svale, Heidrun, Falk, Draugen, the Gulf of Mexico, Ula and Oseberg. The aim of this study was to compare oils from known biodegraded fields offshore Norway to waxes and oils from an artificial cavern storage facility, to determine if the oil degradation processes observed in natural reservoirs offshore are in any way comparable to the processes occurring in oil storage facilities.

The samples represent a wide span in maturity, ranging from petroleum generated early to late in the oil window, with the sample from the Ula field as the most mature and the samples from the Svale field the least mature. The T samples show maturities that generally plot in the middle of the sample set.

There are only small facies variations within the sample set, all the samples seem to have originated from mixed organic sources. Some of the samples (Draugen, NSO-1 and Svale) have a somewhat higher terrestrial input, and the Mexican sample is rich in sulfur compounds and low in diasteranes, typical for a carbonate source.

The samples from the caverns show only a very moderate degree of biodegradation compared to the biodegraded samples from offshore Norway, and they have a rather normal oil composition, very typical for slightly biodegraded oils. The moderate degree of biodegradation may be due to limited access to oxygenated meteoric water, which results in anaerobe conditions. It is uncertain if there is purely inorganic processes, i.e. some sort of gravimetric segregation that leads to the formation of these waxes, or if anoxic bacteria may be involved in the formation of long chained waxy compounds.

This study has illustrated that the processes that affects oils in natural reservoirs may not be active in artificial underground oil storage facilities.

8. References

Ajienka, J. A. and Ikoku, C. U., 1990: Waxy crude oil handling in Nigeria: practices, problems and prospects. Energy Sources 12, 463-478.

Ahsan, A, 1993: Petroleum biodegradation in the Tertiary Reservoirs of the North Sea. Cand. Scient. Thesis in Geology, Department of Geology, University of Oslo, Norway, 173 pp.

Ahsan, A., Karlsen, D. A. and Patience, R. L., 1997: Petroleum biodegradation in the Tertiary reservoirs of the North Sea. *Marine and Petroleum Geology,* **14,** 55-64.

Alexander, R., Kagi, R. I. and Woodhouse, G. W., 1981: Geochemical correlation of Windalia oil and extracts of Winning Group (Cretaceous) potential source rocks, Barrow Subbasin, Western Australia. *AAPG Bulletin,* **65,** 235-250.

Bhullar, A. G., Karlsen, D. A., Backer-Owe, K., Le Tran, K., Skålnes, E., Berchelmann, H. H. and Kittelsen, J. E., 2000: Reservoir characterization by combined micro extraction – micro thin-layer chromatography (Iatroscan) method: A calibration study with examples from the Norwegian North Sea. *Journal of Petroleum Geology,* **23,** 221-244.

Blystad, P., Brekke, H., Færseth, R. B., Larsen, B. T., Skogseid, J. and Tørudbakken, B., 1995: Structural elements of the Norwegian continental shelf. Part II: The Norwegian Sea Region. *Norwegian Petroleum Directorate Bulletin,* 1-45.

Bray, E. E. and Evans, E. D., 1961: Distribution of n-paraffins as a clue to recognition of source beds. Symposium on the chemical approaches to the recognition of petroleum source rocks., Pergamon, 2-15.

Chosson, P., Connan, J., Dessort, D. and Lanau, C., 1992: In vitro biodegradation of steranes and terpanes: A clue to understanding geological situations. Biological markers in sediments and petroleum., Moldowan, J. M. et al., Eds., Prentice Hall, Englewood Cliffs, N. J., 320-349.

Clayton, J. L. and Bostick, N. H., 1986: Temperature effects on kerogen and on molecular and isotopic composition of organic matter in Pierre Shale near an igneous dike. Advances in organic geochemistry, 1985; Part I; Petroleum geochemistry., Ruellkotter, J., Ed., Pergamon, 135-143.

Cohen, M. J. and Dunn, M. E., 1987: The hydrocarbon habitat of the Haltenbanken-Traenabank area, offshore Norway. Petroleum geology of north west Europe., Glennie Kenneth, W., Ed., Graham and Trotman, 1091-1104.

Connan, J., 1984: Biodegradation of crude oils in reservoirs. Advances in petroleum geochemistry., Brooks, J. and Welte, D. H., Eds., Academic press, London, Vol. 1, 299-335.

Connan, J. and Cassou, A. M., 1980: Properties of gases and petroleum liquids derived from terrestrial kerogen at various maturation levels. *Geochimica et Cosmochimica Acta,* **44,** 1-23.

Cornford, C., Morrow, J. A., Turrington, A., Miles, J. A. and Brooks, J., 1983: Some geological controls on oil composition in the U.K. North Sea. Petroleum geochemistry and exploration of Europe; International congress., Brooks, J., Ed., Geological Society of London, 175-194.

Cornford, C., Needham, C. E. J. and De Walque, L., 1986: Geochemical habitat of North Sea oils and gases. Habitat of hydrocarbons on the Norwegian continental shelf; proceedings of an international conference., Spencer, A. M., Ed., Graham & Trotman, 39-54.

Dahl, B. and Speers, G. C., 1985: Organic geochemistry of the Oseberg field. Petroleum geochemistry in exploration of the Norwegian Continental shelf, Thomas Bruce, M. E. A., Ed., Graham and Trotman, 185-195.

Eglinton, G. and Murphy, M. T. J., Eds., 1969: Organic geochemistry- methods and results, 781 pp.

Elvsborg, A., Hagevang, T. and Throndsen, T., 1985: Origin of the gas-condensate of the Midgard Field at Haltenbanken. Petroleum geochemistry in exploration of the Norwegian Shelf., Larsen Rolf, M., Ed., Graham and Trotman, 213-219.

Evans, C. R., Rogers, M. A. and Bailey, J. L., 1971: Evolution and alteration of petroleum in Western Canada. Chemical Geology, **8,** 147-170.

Holder, G. A. and Winkler, J., 1965: Wax crystallization from distillate fuels, Parts 1, 2 and 3. J. Inst. Petrol 51 (499), 228-252.

Horstad, I., 1989: Petroleum composition and heterogeneities within the Middle Jurassic reservoir in The Gullfaks field area, Norwegian North Sea, Department of Geology, University of Oslo.

Hsieh, M., Philp, R. P. and del Rio, J. C., 2000: Characterization of high molecular weight biomarkers in crude oils. *Organic Geochemistry,* **31,** 1581-1588.

Huang, W. Y. and Meinschein, W. G., 1979: Sterols as ecological indicators. *Geochimica et Cosmochimica Acta,* **59,** 739-745.

Hughes, W. B., Holba, A. G. and Dzou, L. I. P., 1995: The ratios of dibenzothiophene to phenanthrene and pristane to phytane as indicators of depositional environment and lithology of petroleum source rocks. *Geochimica et Cosmochimica Acta,* **59.7**, Elsevier Science Ltd, 3581-3598.

Hunt, J. M., 1996: Petroleum geochemistry and geology. W. H. Freeman and Company, 743 pp.

Karlsen, D. A. and Larter, S. R., 1989: A rapid correlation method for petroleum population mapping within individual petroleum reservoirs – applications to petroleum reservoir description. Correlation in Hydrocarbon Exploration, Haresnape, J., Ed., 77-85

Karlsen, D. A. and Larter, S. R., 1991: Analysis of petroleum fractions by TLC-FID; applications to petroleum reservoir description. *Organic Geochemistry,* **17,** 603-617.

Karlsen, D. A., Nedkvitne, T., Larter, S. R. and Bjørlykke, K., 1993: Hydrocarbon composition of authigenic inclusions, Application to elucidation of petroleum reservoir filling history, *Geochimica et Cosmochimica Acta,* **57,** 3641-3659.

Karlsen, D. A., Nyland, B., Flood, B., Ohm, S. E., Brekke, T., Olsen, S. and Backer-Owe, K., 1995: Petroleum geochemistry of the Haltenbanken, Norwegian continental shelf. *The geochemistry of reservoirs.,* Cubitt, J. M. and England, W. A., Eds., Geological Society, London, Special Publications, **86,** 203-256.

Karlsen, D. A., Skeie, J. E., Backer-Owe, K., Bjørlykke, K., Olstad, R., Berge, K., Cecchi, M., Vik, E. and Schaefer, R. G., 2004: Petroleum migration, faults and overpressure. Part II. Case history: The Haltenbanken Petroleum Province, offshore Norway. *Understanding Petroleum Reservoirs: towards an Integrated Reservoir Engineering and Geochemical Approach.* Cubitt, J. M., England, W. A. and Larter, S., Eds., Geological Society, London, Special Publications, **237,** 305-372.

Kvalheim, O. M., Telnaes, N., Bjorseth, A. and Christy, A. A., 1987: Interpretation of multivariate data; relationship between phenanthrenes in crude oils. Multivariate statistical workshop for geologists and geochemists., Kvalheim, O. M., Ed., Elsevier, 149-153.

Mackenzie, A. S., 1984: Applications of biological markers in petroleum geochemistry. Advances in petroleum geochemistry; Volume 1., Welte, D. H., Ed., Acad. Press, 115-214.

Mackenzie, A. S., Maxwell, J. R., Coleman, M. L. and Deegan, C. E., 1984: Biological marker and isotope studies of North Sea crude oils and sediments. *Proceedings – World Petroleum Congress = Actes et Documents – Congres Mondial du Petrole,* **11,** 45-56.

Mackenzie, A. S., Rullkoetter, J., Welte, D. H. and Mankiewicz, P., 1985: Reconstruction of oil formation and accumulation in North Slope, Alaska, using quantitative gas chromatography-

mass spectrometry. Alaska North Slope oil-rock correlation study; analysis of North Slope crude., Claypool, G. E., Ed., American Association of Petroleum Geologists, 319-377.

Mackenzie, A. S., Quirke, J. M. E. and Maxwell, J. R., 1980: Molecular parameters of maturation in the Toarcian shales, Paris Basin, France; II, Evolution of metalloporphyrins. Advances in organic geochemistry 1979., Maxwell, J. R., Ed., Pergamon, 239-248.

McMaster, M. and McMaster, C., 1998: GC/MS – A Practical User's Guide. Wiley – VCH, 189 pp.

Mello, M. R., Telnaes, N., Gaglianone, P. C., Chicarelli, M. I., Brassell, S. C. and Maxwell, J. R., 1988: Organic geochemical characterization of depositional palaeoenvironments of source rocks and oils in Brazilian marginal basins. Advances in organic geochemistry 1987; Part I, Organic geochemistry in petroleum exploration; proceedings of the 13th international meeting on organic geochemistry., Novelli, L., Ed., Pergamon, 31-45.

Milner, C. W. D., Rogers, M. A. and Evans, C. R., 1977: Petroleum transformations in reservoirs. *Journal of Geochemical exploration,* **7,** 101-153.

Moldowan, J. M., Fago, F. J., Carlson, R. M. K., Young, D. C., Van, D. G., Clardy, J., Schoell, M., Pillinger, C. T. and Watt, D. S., 1991: Rearranged hopanes in sediments and petroleum. *Geochimica et Cosmochimica Acta,* **55,** 3333-3353.

Moldowan, J. M., Seifert, W. K. and Gallegos, E. J., 1985: Relationship between petroleum composition and depositional environment of petroleum source rocks. *American Association of Petroleum Geologists Bulletin,* **69,** 1255-1268.

Moldowan, J. M., Sundararaman, P., Salvatori, T., Alajberg, A., Gjukic, B., Lee, C. Y. and Demaison, G. J., 1992: Source correlation and maturity assessment of selected oils and rocks from the Central Adriatic Basin (Italy and Yugoslavia). Biological markers in sediments and petroleum, Moldowan et al., Eds., Prentice Hall, Englewood Cliffs, N. J., 370-401.

Pedersen, J. H., 2002: Atypical oils, unusual condensates and bitumens of the Norwegian Continental Shelf: an organic geochemical study, Cand. Scient. Thesis in Geology, Department of Geology, University of Oslo.

Peters, K. E. and Moldowan, J. M., 1993: The biomarker guide – Interpreting molecular fossils in petroleum and ancient sediments. Prentice Hall, Englewood Cliffs, New Jersey 07632, 363 pp.

Philippi, G. T., 1965: On the depth, time and mechanism of petroleum generation. *Geochimica et Cosmochimica Acta,* **29,** 1021-1049.

Radke, M., 1988: Application of aromatic compounds as maturity indicators in source rocks and crude oils. *Marine and Petroleum Geology,* **5,** 224-236.

Radke, M., Vriend, S. P. and Schaefer, R. G., 2001: Geochemical characterization of Lower Toarcian source rock from NW Germany: Interpretation of aromatic and saturated hydrocarbons in relation to depositional environment and maturation effects. *Journal of Petroleum Geology,* **24(3),** 287-307.

Radke, M. and Welte, D. H., 1983: The methylphenanthrene index (MPI); a maturity parameter based on aromatic hydrocarbons. Advances in organic geochemistry 1981., Speers, G., Ed., Wiley & Sons, 504-512.

Radke, M., Welte, D. H. and Willsch, H., 1982a: Geochemical study on a well in the western Canada Basin; relation of the aromatic distribution pattern to maturity of organic matter. *Geochimica et Cosmochimica Acta,* **46,** 1-10.

Radke, M., Willsch, H., Leythaeuser, D. and Teichmueller, M., 1982b: Aromatic components of coal; relation of distribution pattern to rank. *Geochimica et Cosmochimica Acta,* **46,** 1831-1848.

Seifert, W. K. and Moldowan, J. M., 1978: Applications of steranes, terpanes and monoaromatics to the maturation, migration and source of crude oils. *Geochimica et Cosmochimica Acta,* **42,** 77-95.

Shanmugam, G., 1984: Significance of terrestrial environments and related organic matter in generating commercial quantities of oil, Gippsland Basin, Australia. Society of Economic Paleontologists and Mineralogists First annual midyear meeting. Society of Economic Paleontologists and Mineralogists, 73.

Sutton, P.A., Lewis, C. A. and Rowland, S. J., 2004: Isolation of individual hydrocarbons from the unresolved complex hydrocarbon mixture of a biodegraded crude oil using preparative capillary gas chromatography. *Organic Geochemistry,* **36 (2005),** 963-970.

ten Haven, H. –L., De Leeuw, J. W., Rullkoetter, J. and Sinninghe Damste, J. S., 1987: Restricted utility of the pristane/phytane ratio as a palaeoenvironmental indicator. *Nature (London),* **330,** 641-643.

Tissot, B. P. and Welte, D. H., 1978: Petroleum formation and occurrence: a new approach to oil and gas exploration. Springer- Verlag, 538 pp.

Tuttle, R. N., 1983: High-pour-point and asphaltic crude oils and condensates. J. Petrol. Tech. **35,** 1192-1197.

Waples, D. W. and Machihara, T., 1991: Biomarkers for geologists – A practical guide to the application of steranes and triterpanes in petroleum geology. Vol. 9, *AAPG Methods in Exploration,* AAPG, 91 pp.

Weiss, H. M., Wilhelms, A., Mills, N., Scotchmer, J., Hall, P. B., Lind, K. and Brekke, T., 2000: NIGOGA – The Norwedian Industry Guide to Organic Geochemical Analyses [online]. Norsk Hydro, Statoil, Geolab Nor, SINTEF Petroleum Research and the Norwegian Petroleum Directorate. Available from World Wide Web: http://www.npd.no/ **4.0**, 1-102.

Wilhelms, A. and Larter, S. R., 1994: Origin of tar mats in petroleum reservoirs; Part II, Formation mechanisms for tar mats. *Marine and Petroleum Geology,* **11,** 442-456.

Winters, J. C. and Williams, J. A., 1969: Microbiological alteration of crude oil in the reservoir. American Chemical Society, division of petroleum chemistry, New York Meeting Preprints, **14(4),** E22-E31.

Appendix Contents

Sample	Rod	SAT	ARO	POL	SAT/ARO	SAT%	ARO%	POL%
T3-2	1	9,6216	12,4498	3,6537	0,8	37,4	48,4	14,2
	2	9,347	11,1659	4,1961	0,8	37,8	45,2	17
T4-1	1	8,4969	6,2259	4,8377	1,4	43,4	31,8	24,7
	2	10,174	7,0483	4,7614	1,4	46,3	32,1	21,7
T5-2	1	10,07	7,4004	4,7747	1,4	45,3	33,3	21,5
	2	8,9243	8,4811	7,3136	1,1	36,1	34,3	29,6
T6-1	1	8,4455	6,3397	3,7086	1,3	45,7	34,3	20
	2	5,8881	4,924	3,0451	1,2	42,5	35,5	22
T4	1	5,3514	2,0349	2,1641	2,6	56	21,3	22,7
	2	5,4134	1,876	2,1275	2,9	57,5	19,9	22,6
T5	1	9,173	3,8459	2,8863	2,4	57,7	24,2	18,1
	2	7,3998	3,4737	3,1248	2,1	52,9	24,8	22,3
Svale1	1	5,81	4,341	0,896	1,3	52,6	39,3	8,1
	2	4,9684	3,0716	0,7979	1,6	56,2	34,8	9,1
Svale2	1	5,3873	3,0728	0,9684	1,8	57,1	32,6	10,3
	2	6,5342	3,2901	0,9769	2	60,5	30,5	9
6507/7-2 DST2	1	1,1503	0,7214	1,1404	1,6	38,2	24	37,9
	2	1,4995	0,8958	1,1357	1,7	42,5	25,4	32,2
6507/7-4 DST1	1	0,6107	0,3968	0,605	1,5	37,9	24,6	37,5
	2	2,141	1,2662	1,6563	1,7	42,3	25	32,7
6507/7-4 DST3	1	3,558	1,7123	1,3653	2,1	53,6	25,8	20,6
	2	2,0212	0,67	0,9889	3	54,9	18,2	26,9
6507/7-5 DST2A	1	2,0765	0,5666	0,7984	3,7	60,3	16,5	23,2
	2	2,8278	0,8258	1,0311	3,4	60,4	17,6	22
Falk	1	2,1432	1,4039	1,5715	1,5	41,9	27,4	30,7
	2	1,9745	1,0914	1,5801	1,8	42,5	23,5	34
Draugen	1	19,4503	16,0897	2,8889	1,2	50,6	41,9	7,5
	2	19,9916	17,6043	2,7799	1,1	49,5	43,6	6,9
B IMP	1	15,053	3,4104	2,4762	4,4	71,9	16,3	11,8
	2	13,6278	2,297	2,4879	5,9	74	12,5	13,5
7/12-6 DST1	1	3,7379	0,7644	0,2973	4,9	77,9	15,9	6,2
	2	4,3302	0,6228	0,3243	7	82,1	11,8	6,1
NSO-1	1	1,5513	0,4768	0,6052	3,2	58,9	18,1	23
	2	2,1759	0,9223	0,8647	2,4	54,9	23,3	21,8

Table A.1. Gross composition in terms of absolute yield and relative percentages of the samples. SAT = saturated hydrocarbons, ARO = aromatic hydrocarbons, POL = polar compounds. The units are given in (mg/ml DCM).

T3-2

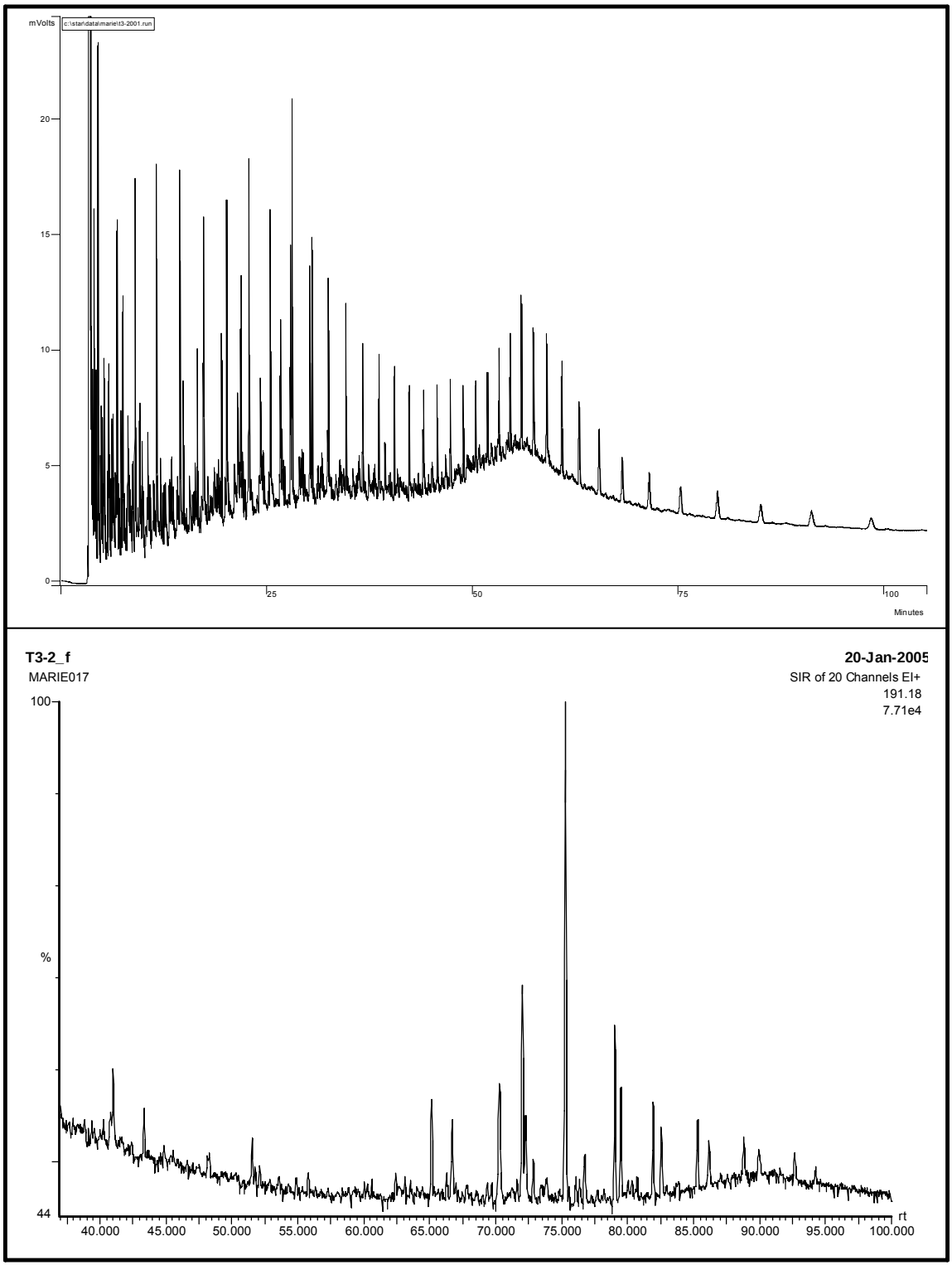
mVolts
c:\star\data\mariet3-2001.run
20
15
10
5
0
25
50
75
100
Minutes
T3-2_f
MARIE017
20-Jan-2005
SIR of 20 Channels EI+
191.18
7.71e4
100
%
44
40.000
45.000
50.000
55.000
60.000
65.000
70.000
75.000
80.000
85.000
90.000
95.000
100.000
rt

T3-2

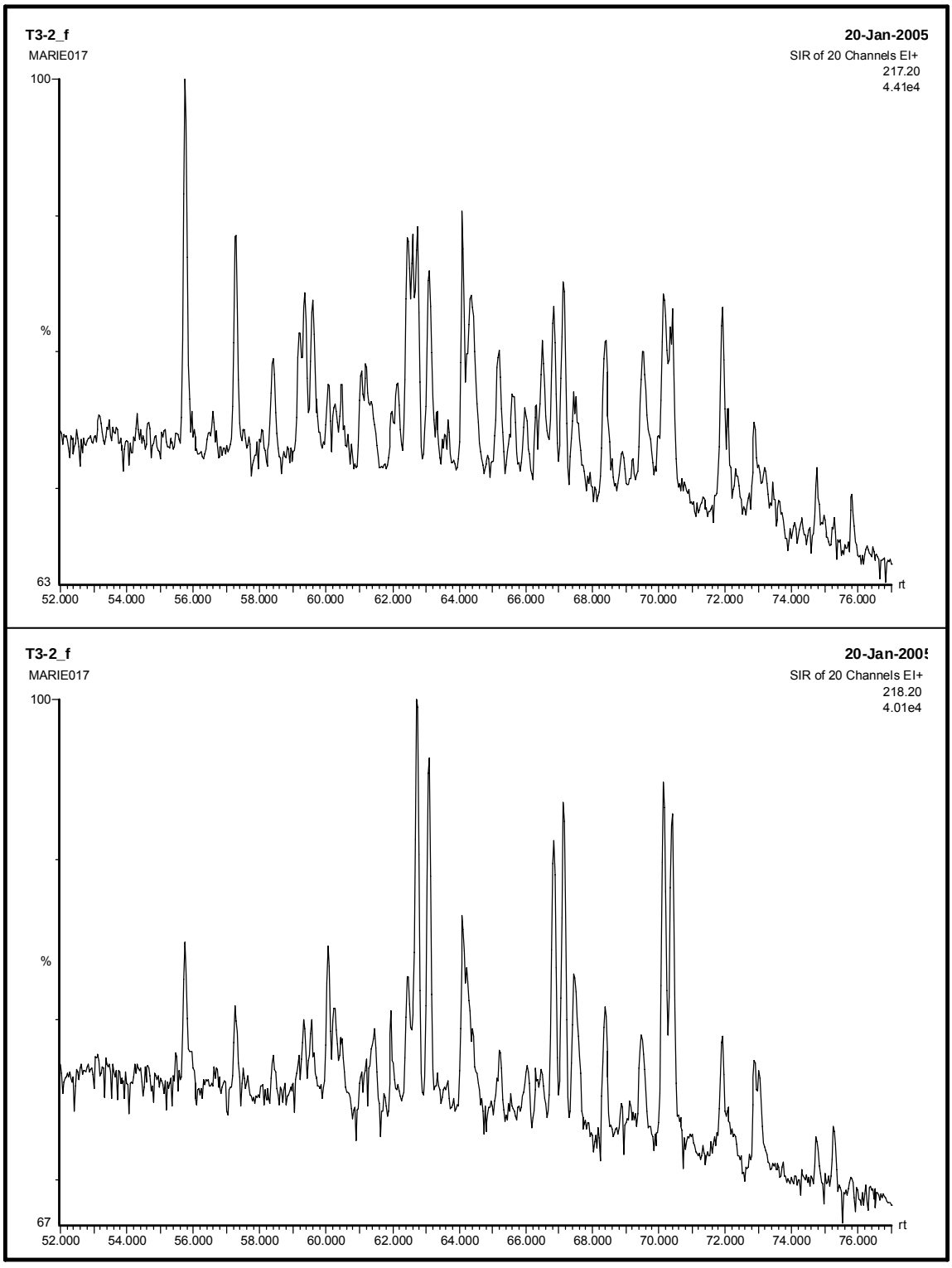
T3-2_f
MARIE017
20-Jan-2005
SIR of 20 Channels EI+
217.20
4.41e4
100
%
63
52.000
54.000
56.000
58.000
60.000
62.000
64.000
66.000
68.000
70.000
72.000
74.000
76.000
rt
T3-2_f
MARIE017
20-Jan-200
SIR of 20 Channels EI+
218.20
4.01e4
100
%
67
52.000
54.000
56.000
58.000
60.000
62.000
64.000
66.000
68.000
70.000
72.000
74.000
76.000
rt

T3-2

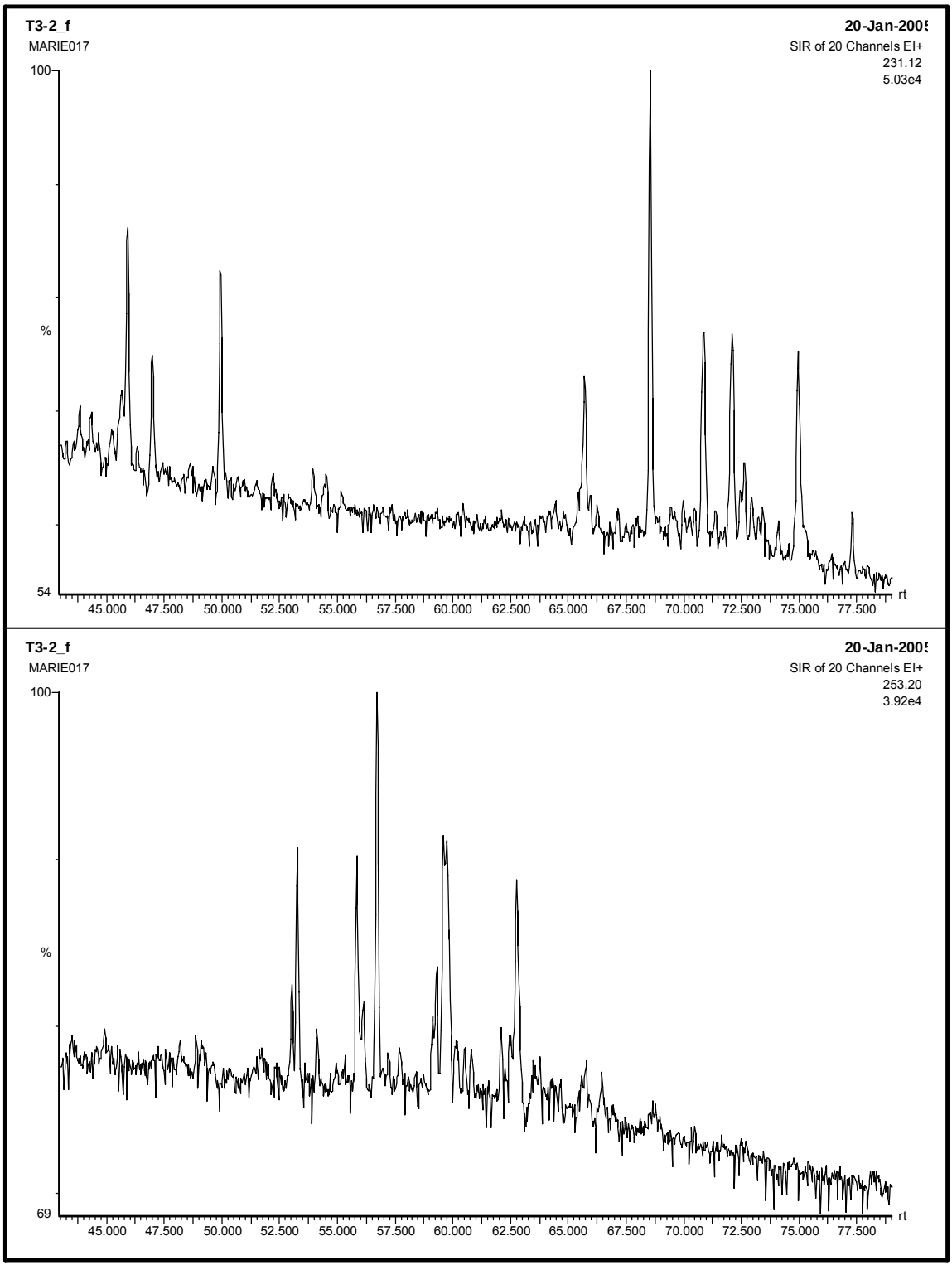
T3-2_f
MARIE017
20-Jan-200
SIR of 20 Channels EI+
231.12
5.03e4
100
%
54
45.000 47.500 50.000 52.500 55.000 57.500 60.000 62.500 65.000 67.500 70.000 72.500 75.000 77.500
rt
T3-2_f
MARIE017
20-Jan-200
SIR of 20 Channels EI+
253.20
3.92e4
100
%
69
45.000 47.500 50.000 52.500 55.000 57.500 60.000 62.500 65.000 67.500 70.000 72.500 75.000 77.500
rt

T3-2

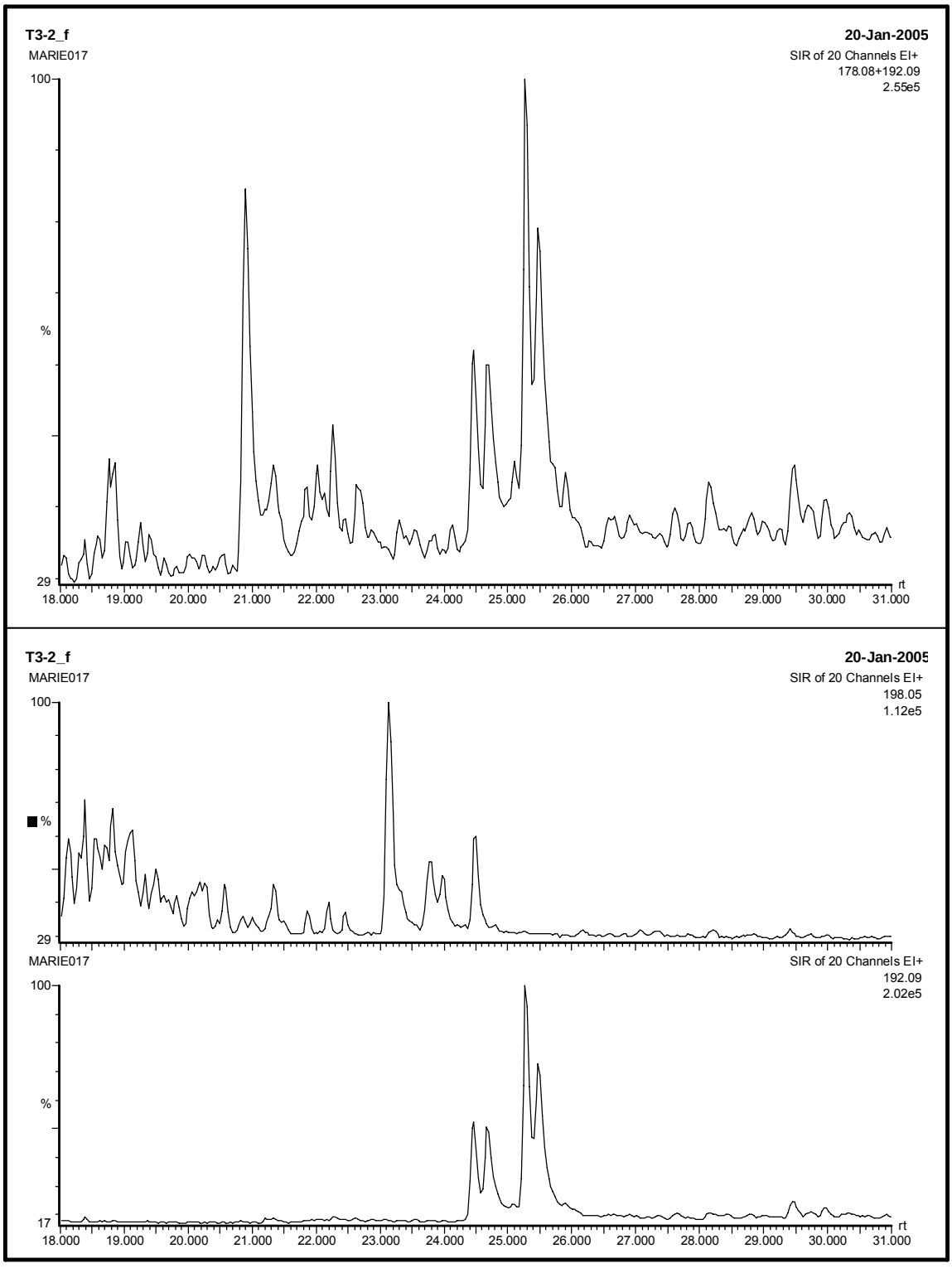
T3-2_f
MARIE017
20-Jan-2005
SIR of 20 Channels EI+
178.08+192.09
2.55e5
100
%
29
18.000
19.000
20.000
21.000
22.000
23.000
24.000
25.000
26.000
27.000
28.000
29.000
30.000
31.000
rt
T3-2_f
MARIE017
20-Jan-2005
SIR of 20 Channels EI+
198.05
1.12e5
100
%
29
MARIE017
SIR of 20 Channels EI+
192.09
2.02e5
100
%
17
18.000
19.000
20.000
21.000
22.000
23.000
24.000
25.000
26.000
27.000
28.000
29.000
30.000
31.000
rt

T4-1

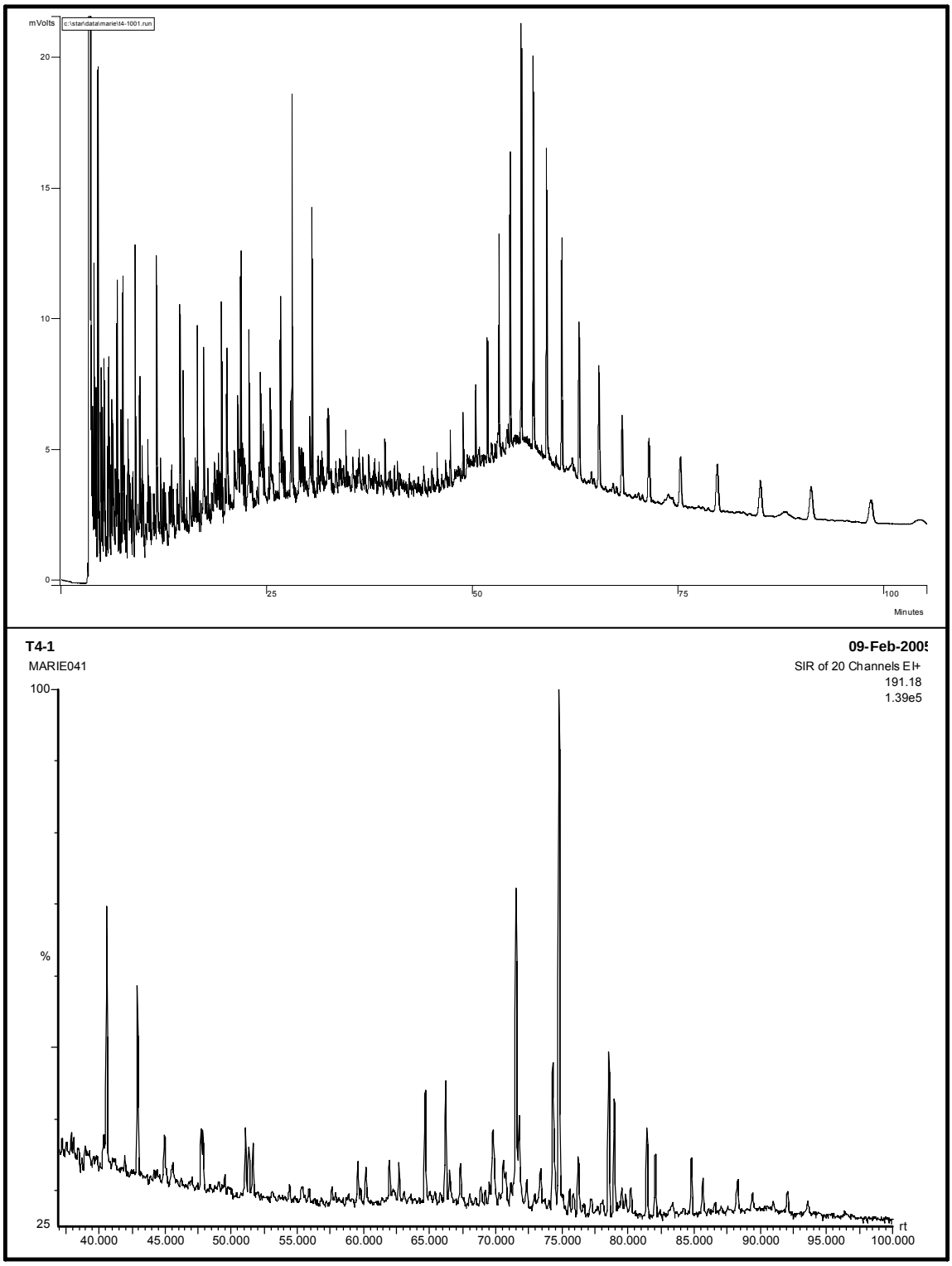
mVolts
c:\star\data\mariet\t4-1001.run
20
15
10
5
0
25
50
75
100
Minutes
T4-1
MARIE041
09-Feb-200
SIR of 20 Channels EI+
191.18
1.39e5
100
%
25
40.000
45.000
50.000
55.000
60.000
65.000
70.000
75.000
80.000
85.000
90.000
95.000
100.000
rt

T4-1

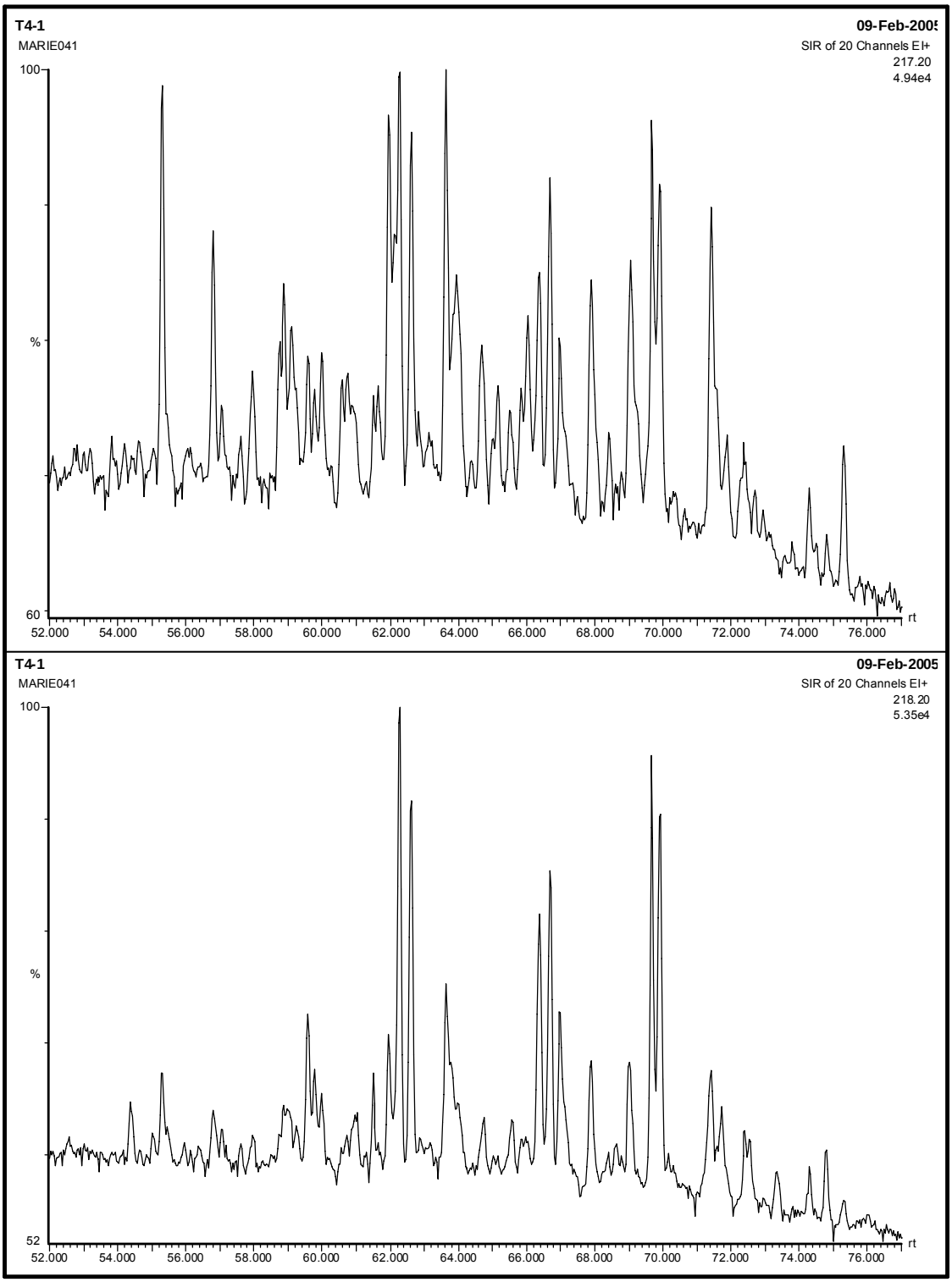
T4-1
09-Feb-200
MARIE041
SIR of 20 Channels EI+
217.20
4.94e4
100
%
60
52.000
54.000
56.000
58.000
60.000
62.000
64.000
66.000
68.000
70.000
72.000
74.000
76.000
rt
T4-1
09-Feb-2005
MARIE041
SIR of 20 Channels EI+
218.20
5.35e4
100
%
52
52.000
54.000
56.000
58.000
60.000
62.000
64.000
66.000
68.000
70.000
72.000
74.000
76.000
rt

T4-1

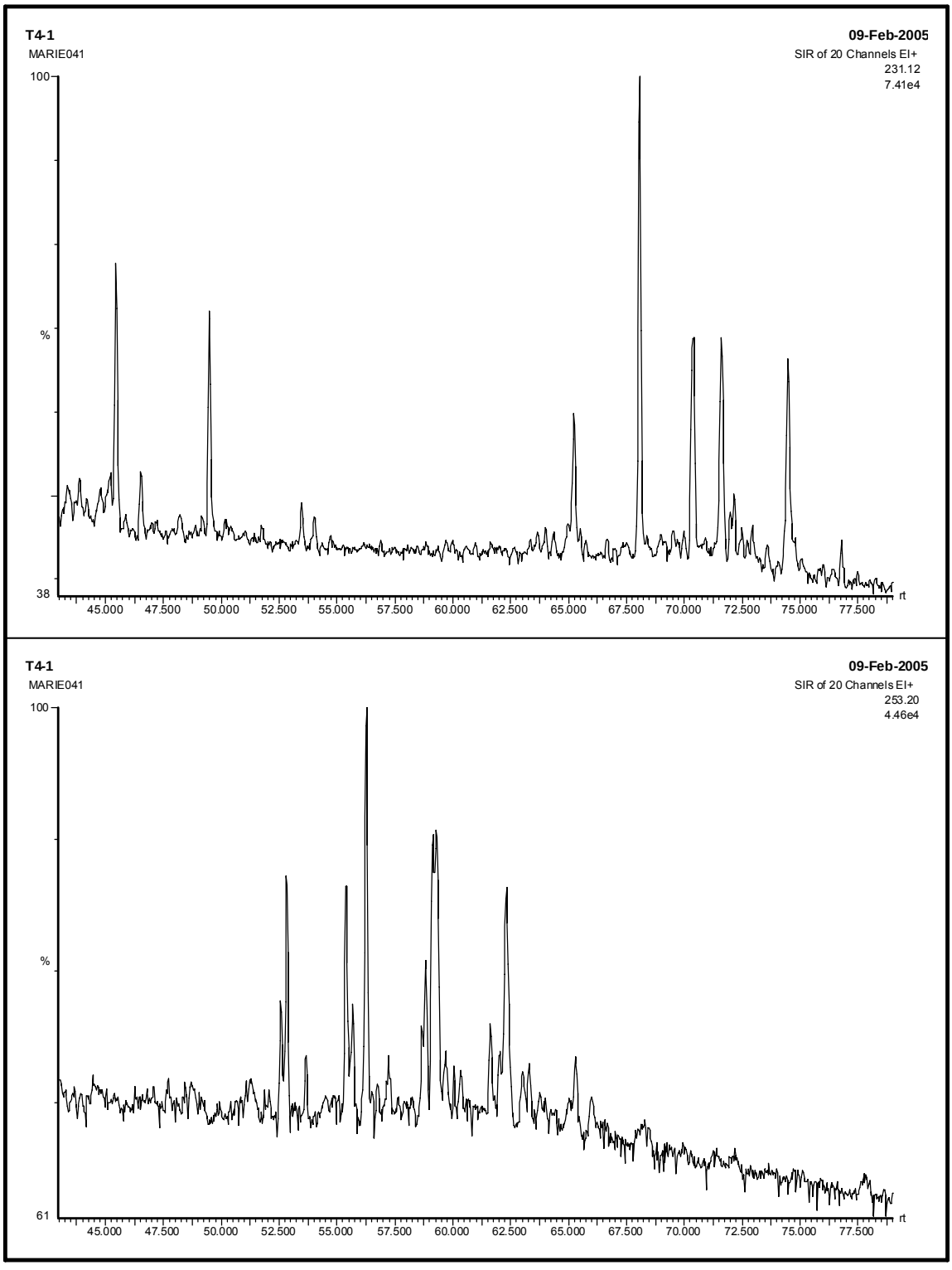
T4-1
MARIE041
09-Feb-2005
SIR of 20 Channels EI+
231.12
7.41e4
100
%
38
45.000 47.500 50.000 52.500 55.000 57.500 60.000 62.500 65.000 67.500 70.000 72.500 75.000 77.500
rt
T4-1
MARIE041
09-Feb-2005
SIR of 20 Channels EI+
253.20
4.46e4
100
%
61
45.000 47.500 50.000 52.500 55.000 57.500 60.000 62.500 65.000 67.500 70.000 72.500 75.000 77.500
rt

T4-1

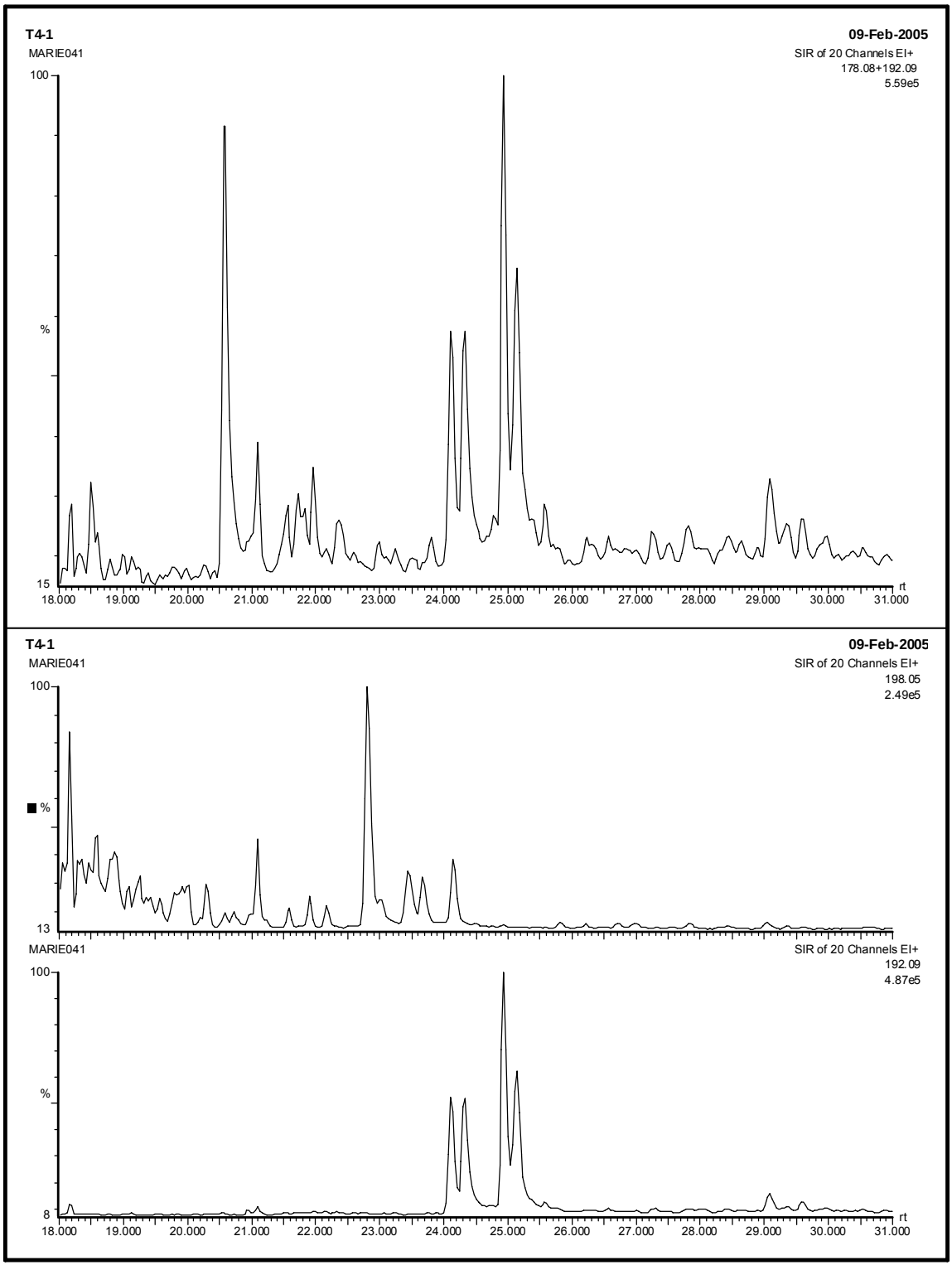
T4-1
MARIE041
09-Feb-2005
SIR of 20 Channels EI+
178.08+192.09
5.59e5
100
%
15
18.000
19.000
20.000
21.000
22.000
23.000
24.000
25.000
26.000
27.000
28.000
29.000
30.000
31.000
rt
T4-1
MARIE041
09-Feb-2005
SIR of 20 Channels EI+
198.05
2.49e5
100
%
13
MARIE041
SIR of 20 Channels EI+
192.09
4.87e5
100
%
8
18.000
19.000
20.000
21.000
22.000
23.000
24.000
25.000
26.000
27.000
28.000
29.000
30.000
31.000
rt

T5-2

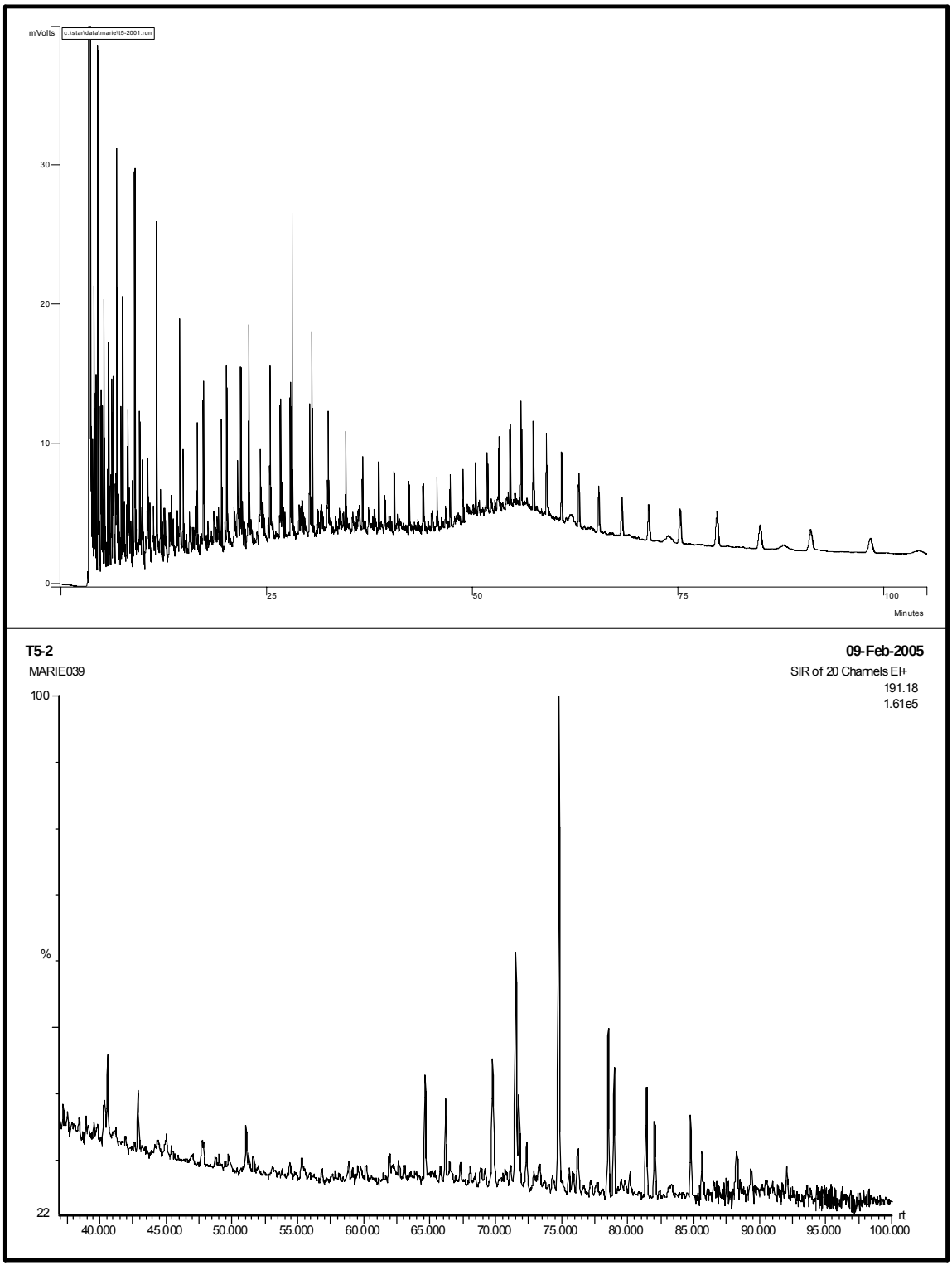
mVolts
c:\star\data\marie\t5-2001.run
30
20
10
0
25
50
75
100
Minutes
T5-2
MARIE039
09-Feb-2005
SIR of 20 Channels EI+
191.18
1.61e5
100
%
22
40.000
45.000
50.000
55.000
60.000
65.000
70.000
75.000
80.000
85.000
90.000
95.000
100.000
rt

T5-2

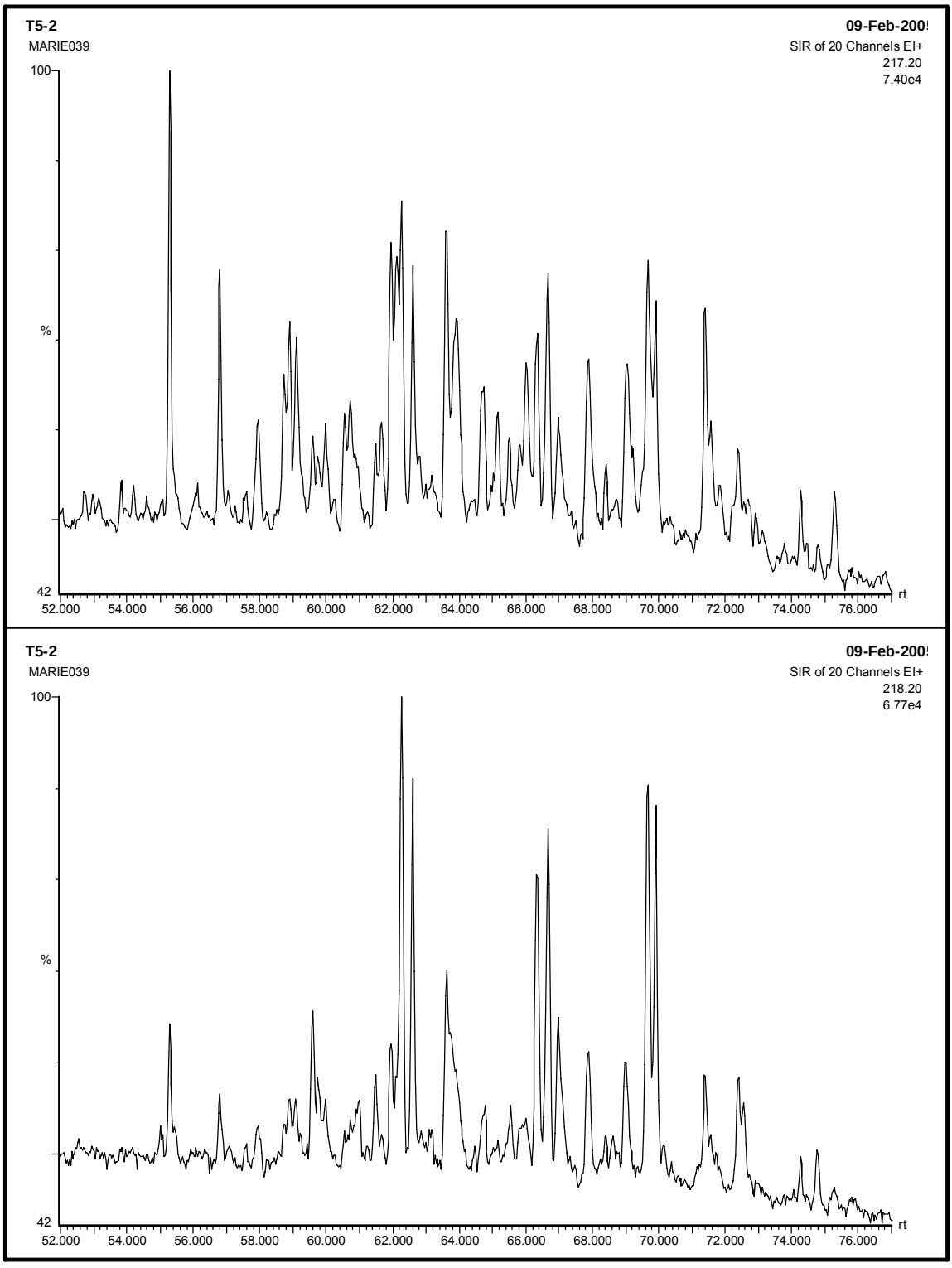
T5-2
MARIE039
09-Feb-200
SIR of 20 Channels EI+
217.20
7.40e4
100
%
42
52.000
54.000
56.000
58.000
60.000
62.000
64.000
66.000
68.000
70.000
72.000
74.000
76.000
rt
T5-2
MARIE039
09-Feb-200
SIR of 20 Channels EI+
218.20
6.77e4
100
%
42
52.000
54.000
56.000
58.000
60.000
62.000
64.000
66.000
68.000
70.000
72.000
74.000
76.000
rt

T5-2

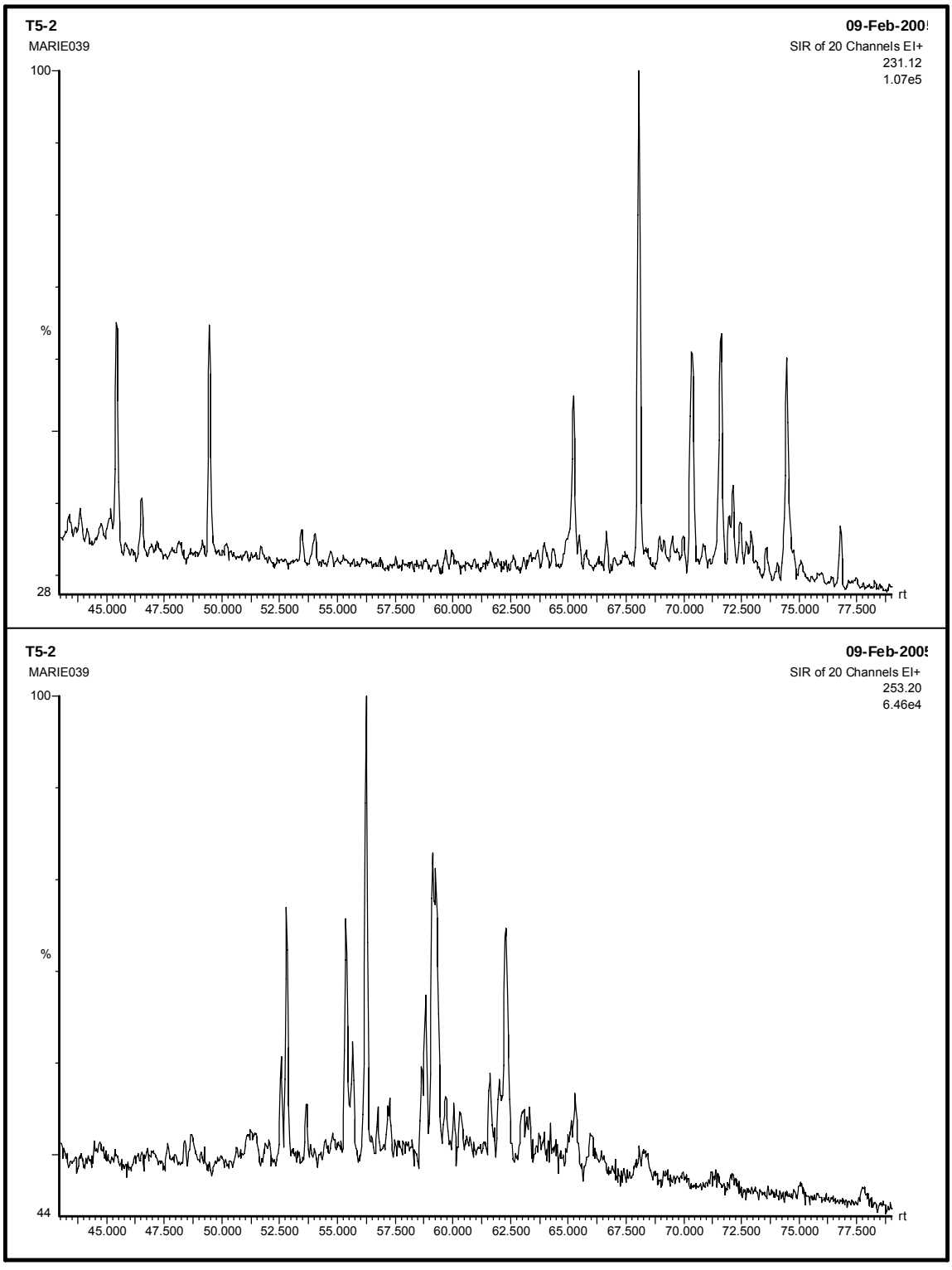
T5-2
MARIE039
09-Feb-200
SIR of 20 Channels EI+
231.12
1.07e5
100
%
28
45.000 47.500 50.000 52.500 55.000 57.500 60.000 62.500 65.000 67.500 70.000 72.500 75.000 77.500
rt
T5-2
MARIE039
09-Feb-200
SIR of 20 Channels EI+
253.20
6.46e4
100
%
44
45.000 47.500 50.000 52.500 55.000 57.500 60.000 62.500 65.000 67.500 70.000 72.500 75.000 77.500
rt

T5-2

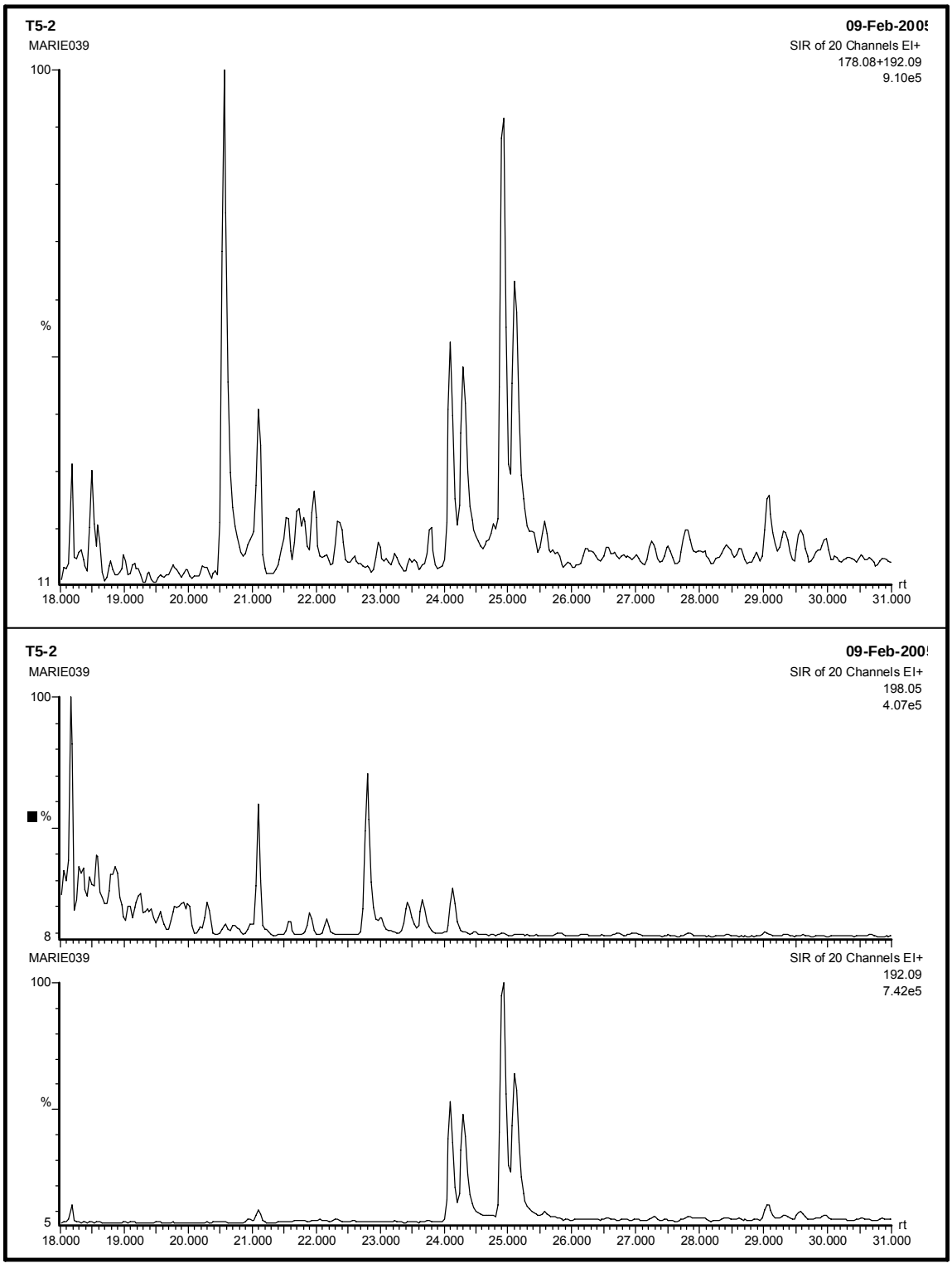
T5-2
MARIE039
09-Feb-200
SIR of 20 Channels EI+
178.08+192.09
9.10e5
100
%
11
18.000
19.000
20.000
21.000
22.000
23.000
24.000
25.000
26.000
27.000
28.000
29.000
30.000
31.000
rt
T5-2
MARIE039
09-Feb-200
SIR of 20 Channels EI+
198.05
4.07e5
100
%
8
MARIE039
SIR of 20 Channels EI+
192.09
7.42e5
100
%
5
18.000
19.000
20.000
21.000
22.000
23.000
24.000
25.000
26.000
27.000
28.000
29.000
30.000
31.000
rt

T6-1

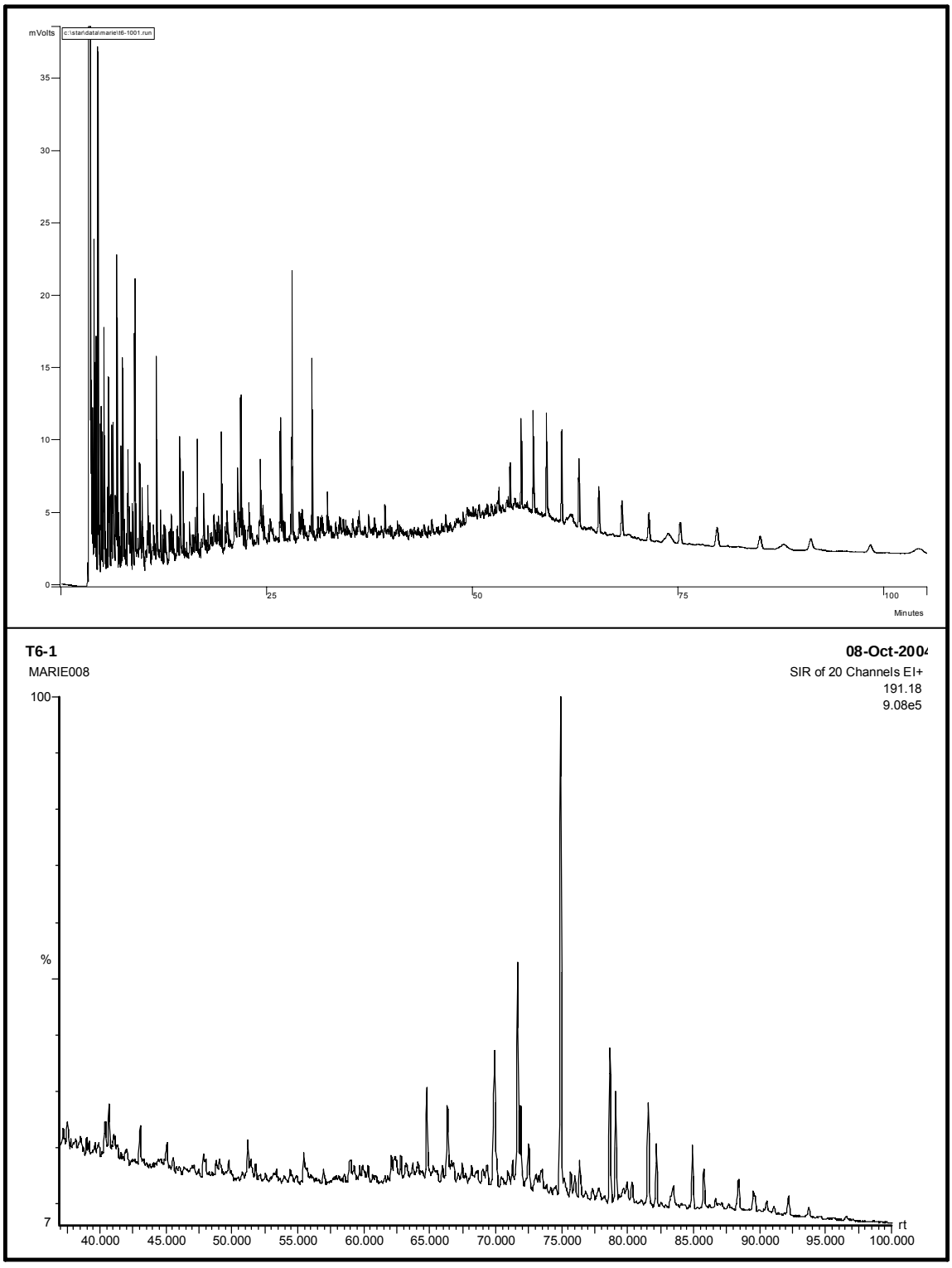
mVolts
c:\star\data\marie\t6-1001.run
35
30
25
20
15
10
5
0
25
50
75
100
Minutes
T6-1
MARIE008
08-Oct-200
SIR of 20 Channels EI+
191.18
9.08e5
100
%
7
40.000
45.000
50.000
55.000
60.000
65.000
70.000
75.000
80.000
85.000
90.000
95.000
100.000
rt

T6-1

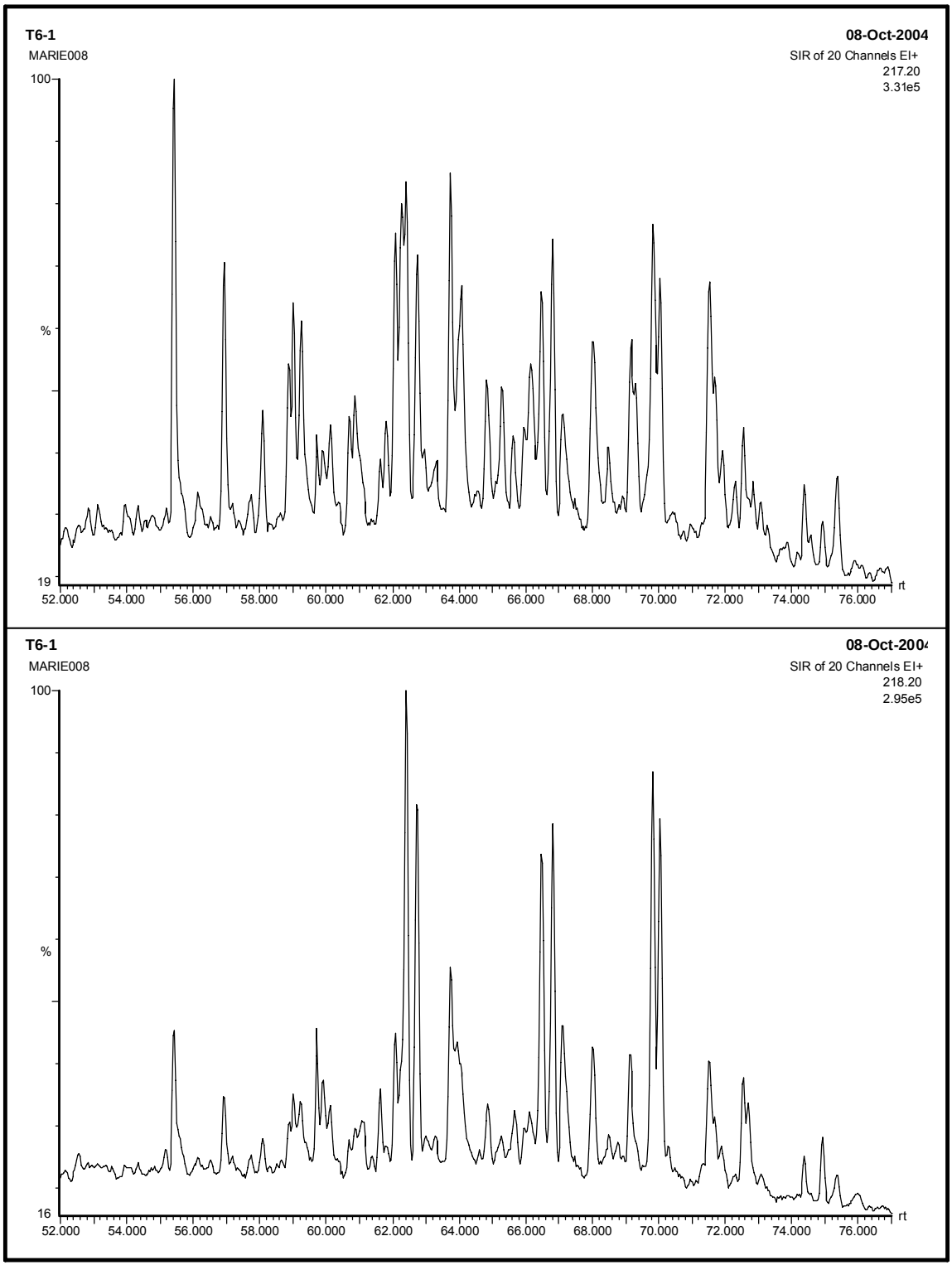
T6-1
MARIE008
08-Oct-2004
SIR of 20 Channels EI+
217.20
3.31e5
100
%
19
52.000 54.000 56.000 58.000 60.000 62.000 64.000 66.000 68.000 70.000 72.000 74.000 76.000
rt
T6-1
MARIE008
08-Oct-200
SIR of 20 Channels EI+
218.20
2.95e5
100
%
16
52.000 54.000 56.000 58.000 60.000 62.000 64.000 66.000 68.000 70.000 72.000 74.000 76.000
rt

T6-1

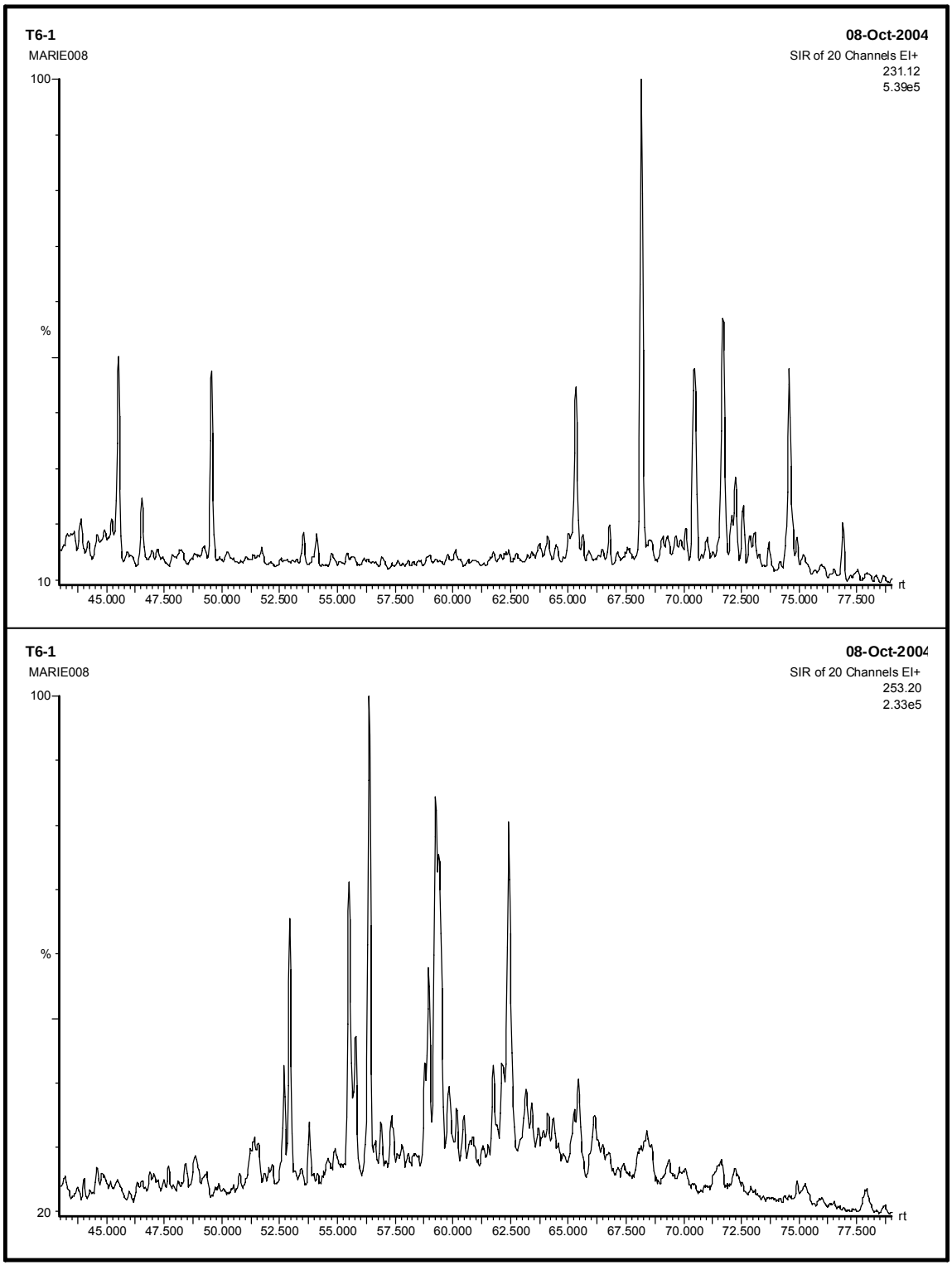
T6-1
MARIE008
08-Oct-2004
SIR of 20 Channels EI+
231.12
5.39e5
100
%
10
45.000 47.500 50.000 52.500 55.000 57.500 60.000 62.500 65.000 67.500 70.000 72.500 75.000 77.500
rt
T6-1
MARIE008
08-Oct-2004
SIR of 20 Channels EI+
253.20
2.33e5
100
%
20
45.000 47.500 50.000 52.500 55.000 57.500 60.000 62.500 65.000 67.500 70.000 72.500 75.000 77.500
rt

T6-1

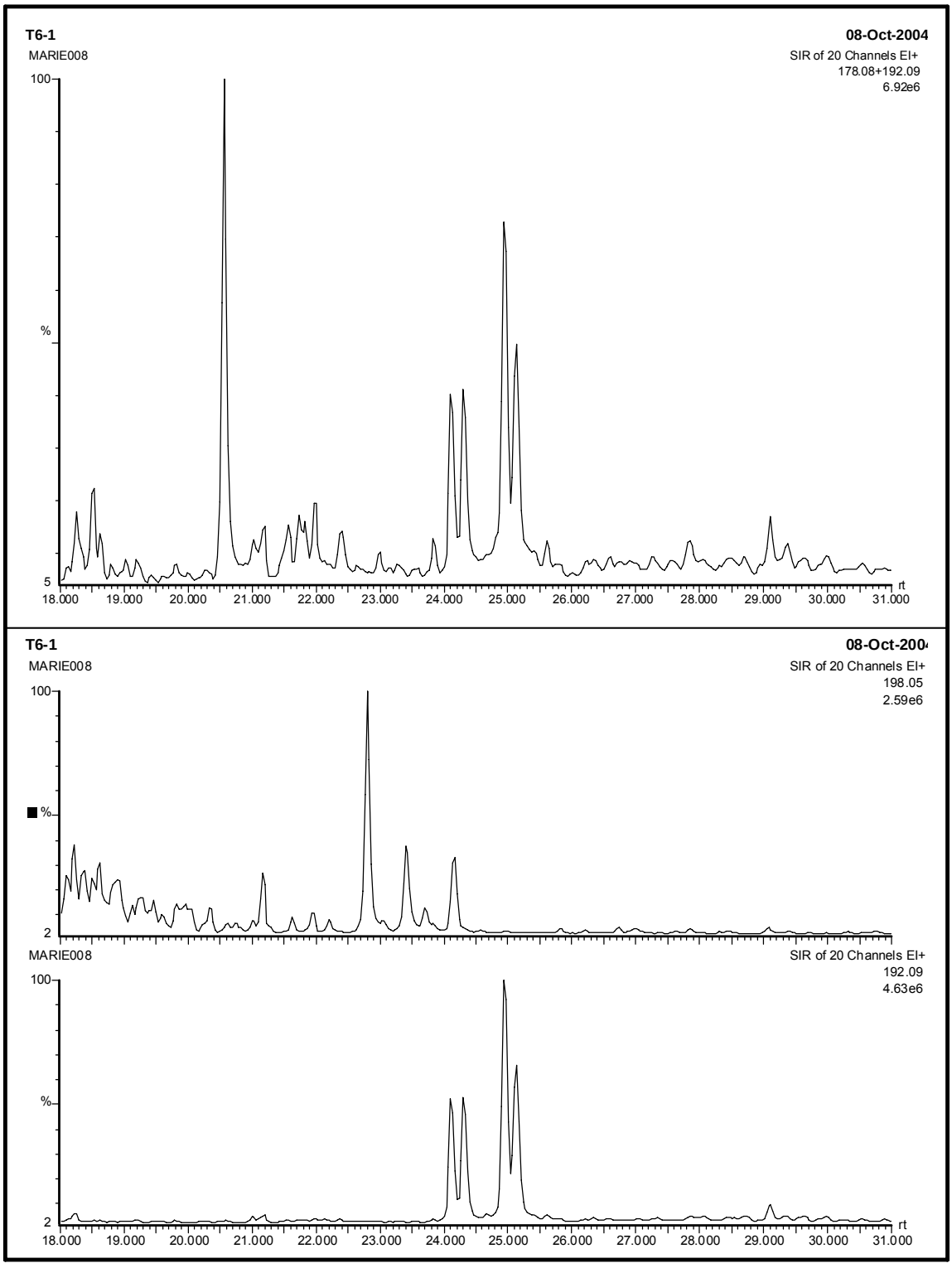
T6-1
08-Oct-2004
MARIE008
SIR of 20 Channels EI+
178.08+192.09
6.92e6
100
%
5
18.000 19.000 20.000 21.000 22.000 23.000 24.000 25.000 26.000 27.000 28.000 29.000 30.000 31.000
rt
T6-1
08-Oct-200
MARIE008
SIR of 20 Channels EI+
198.05
2.59e6
100
%
2
MARIE008
SIR of 20 Channels EI+
192.09
4.63e6
100
%
2
18.000 19.000 20.000 21.000 22.000 23.000 24.000 25.000 26.000 27.000 28.000 29.000 30.000 31.000
rt

T4

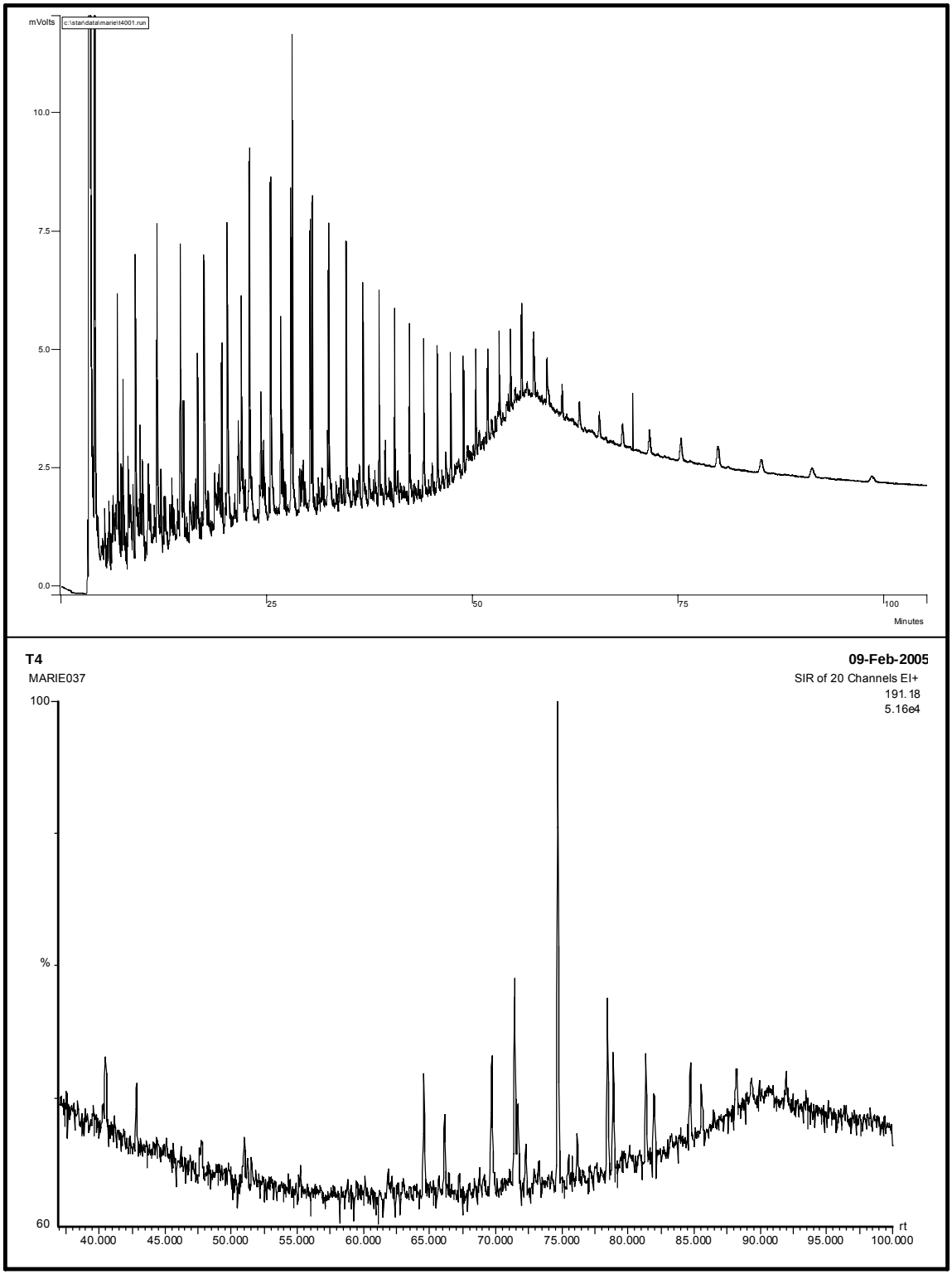
mVolts
c:\star\data\mariet4001.run
10.0
7.5
5.0
2.5
0.0
25
50
75
100
Minutes
T4
MARIE037
09-Feb-2005
SIR of 20 Channels EI+
191.18
5.16e4
100
%
60
40.000
45.000
50.000
55.000
60.000
65.000
70.000
75.000
80.000
85.000
90.000
95.000
100.000
rt

T4

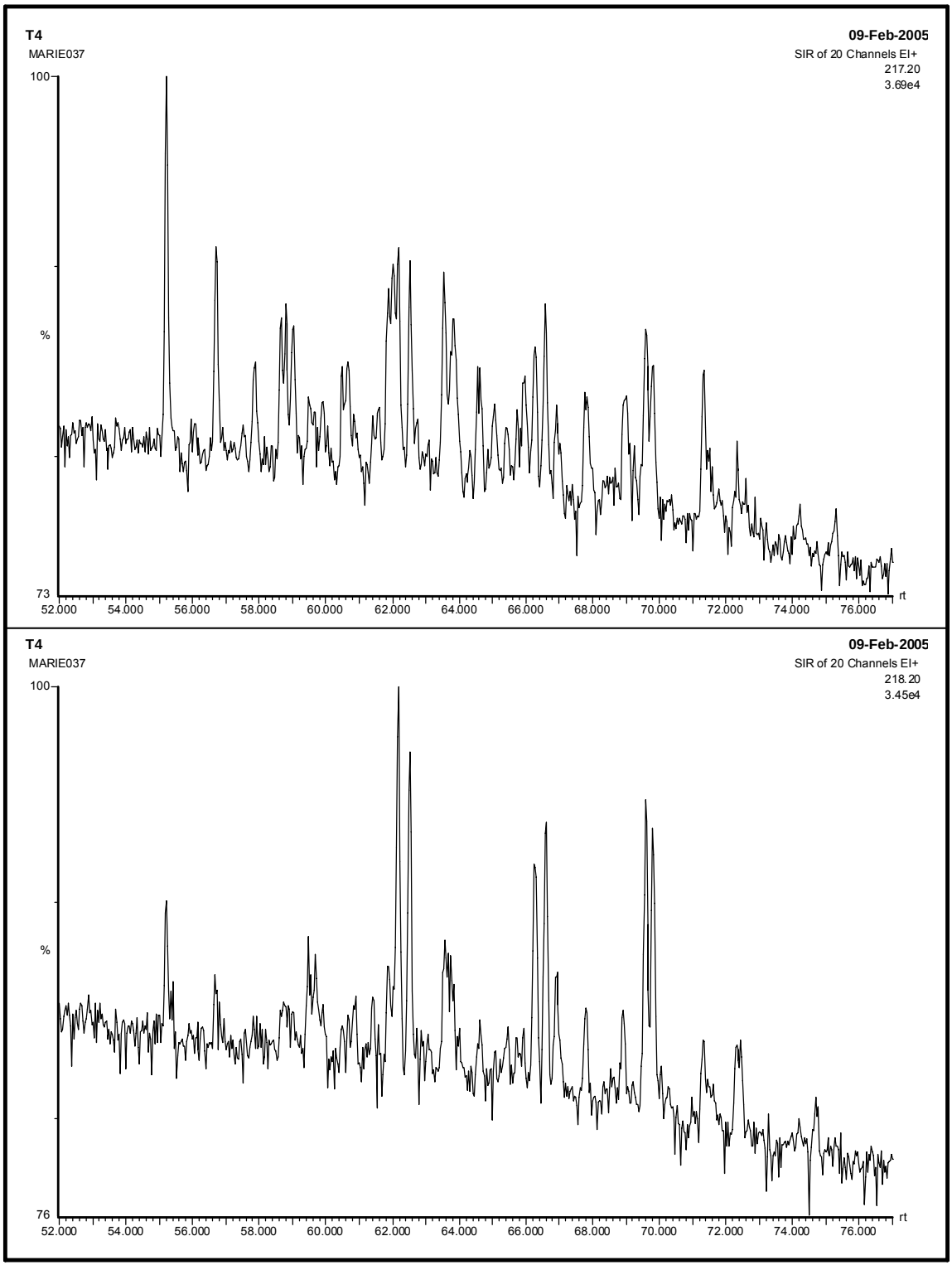
T4
MARIE037
09-Feb-2005
SIR of 20 Channels EI+
217.20
3.69e4
100
%
73
52.000
54.000
56.000
58.000
60.000
62.000
64.000
66.000
68.000
70.000
72.000
74.000
76.000
rt
T4
MARIE037
09-Feb-2005
SIR of 20 Channels EI+
218.20
3.45e4
100
%
76
52.000
54.000
56.000
58.000
60.000
62.000
64.000
66.000
68.000
70.000
72.000
74.000
76.000
rt

T4

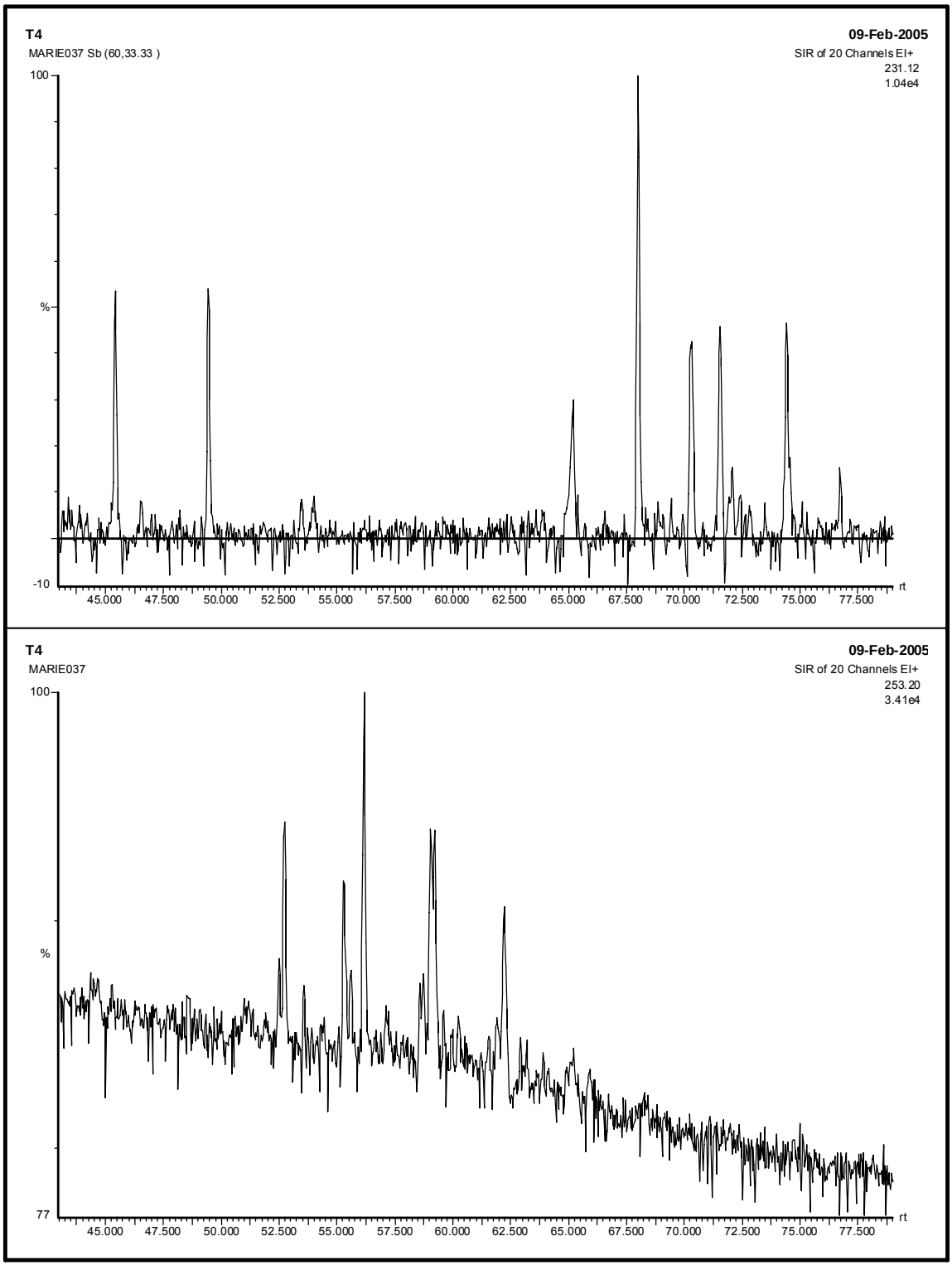
T4
MARIE037 Sb (60,33.33)
09-Feb-2005
SIR of 20 Channels EI+
231.12
1.04e4
100
%
-10
45.000 47.500 50.000 52.500 55.000 57.500 60.000 62.500 65.000 67.500 70.000 72.500 75.000 77.500
rt
T4
MARIE037
09-Feb-2005
SIR of 20 Channels EI+
253.20
3.41e4
100
%
77
45.000 47.500 50.000 52.500 55.000 57.500 60.000 62.500 65.000 67.500 70.000 72.500 75.000 77.500
rt

T4

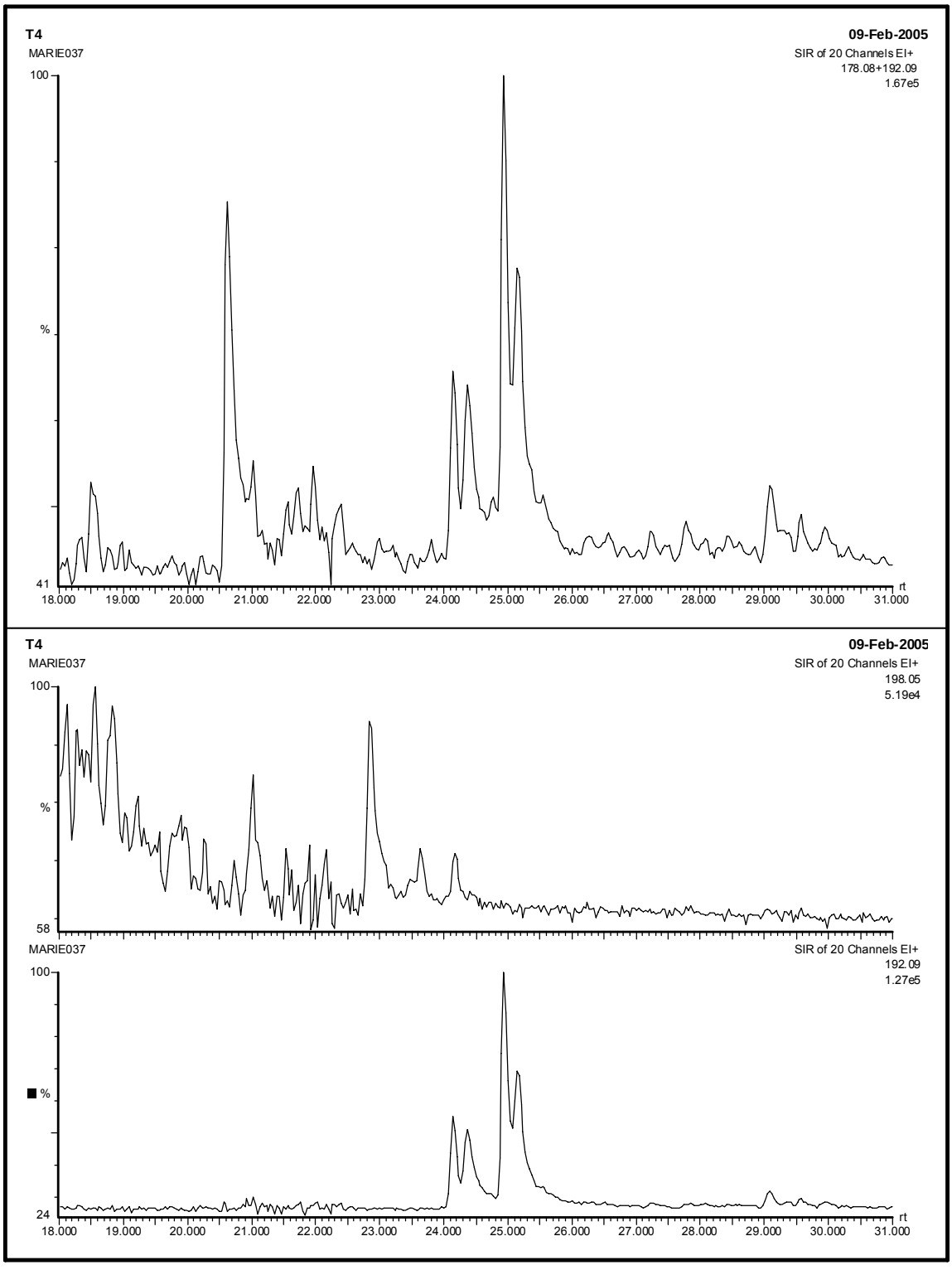
T4
09-Feb-2005
MARIE037
SIR of 20 Channels EI+
178.08+192.09
1.67e5
100
%
41
18.000 19.000 20.000 21.000 22.000 23.000 24.000 25.000 26.000 27.000 28.000 29.000 30.000 31.000
rt
T4
09-Feb-2005
MARIE037
SIR of 20 Channels EI+
198.05
5.19e4
100
%
58
MARIE037
SIR of 20 Channels EI+
192.09
1.27e5
100
%
24
18.000 19.000 20.000 21.000 22.000 23.000 24.000 25.000 26.000 27.000 28.000 29.000 30.000 31.000
rt

T5

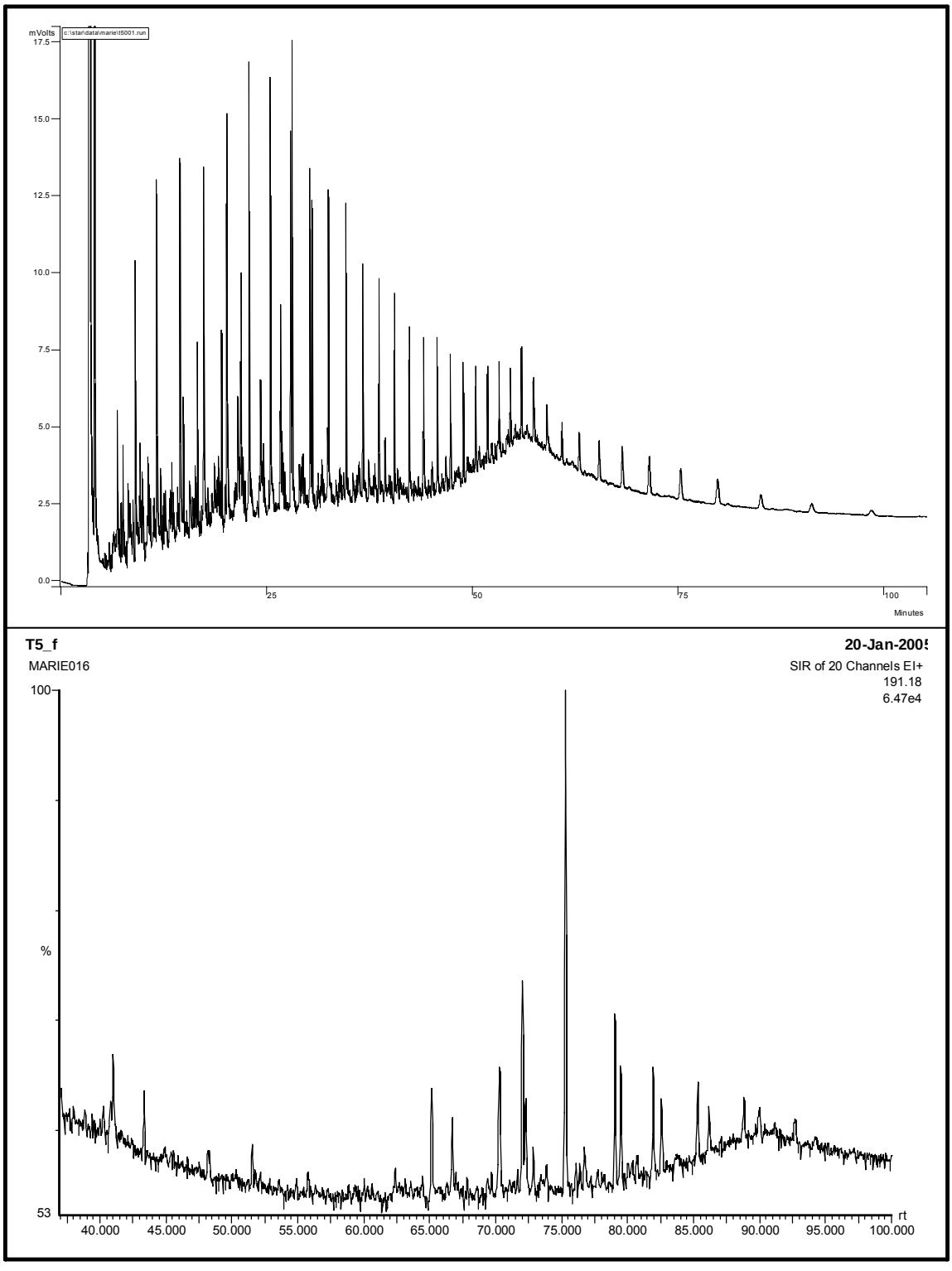
mVolts
c:\star\data\marie\t5001.run
17.5
15.0
12.5
10.0
7.5
5.0
2.5
0.0
25
50
75
100
Minutes
T5_f
MARIE016
20-Jan-200
SIR of 20 Channels EI+
191.18
6.47e4
100
%
53
40.000
45.000
50.000
55.000
60.000
65.000
70.000
75.000
80.000
85.000
90.000
95.000
100.000
rt

T5

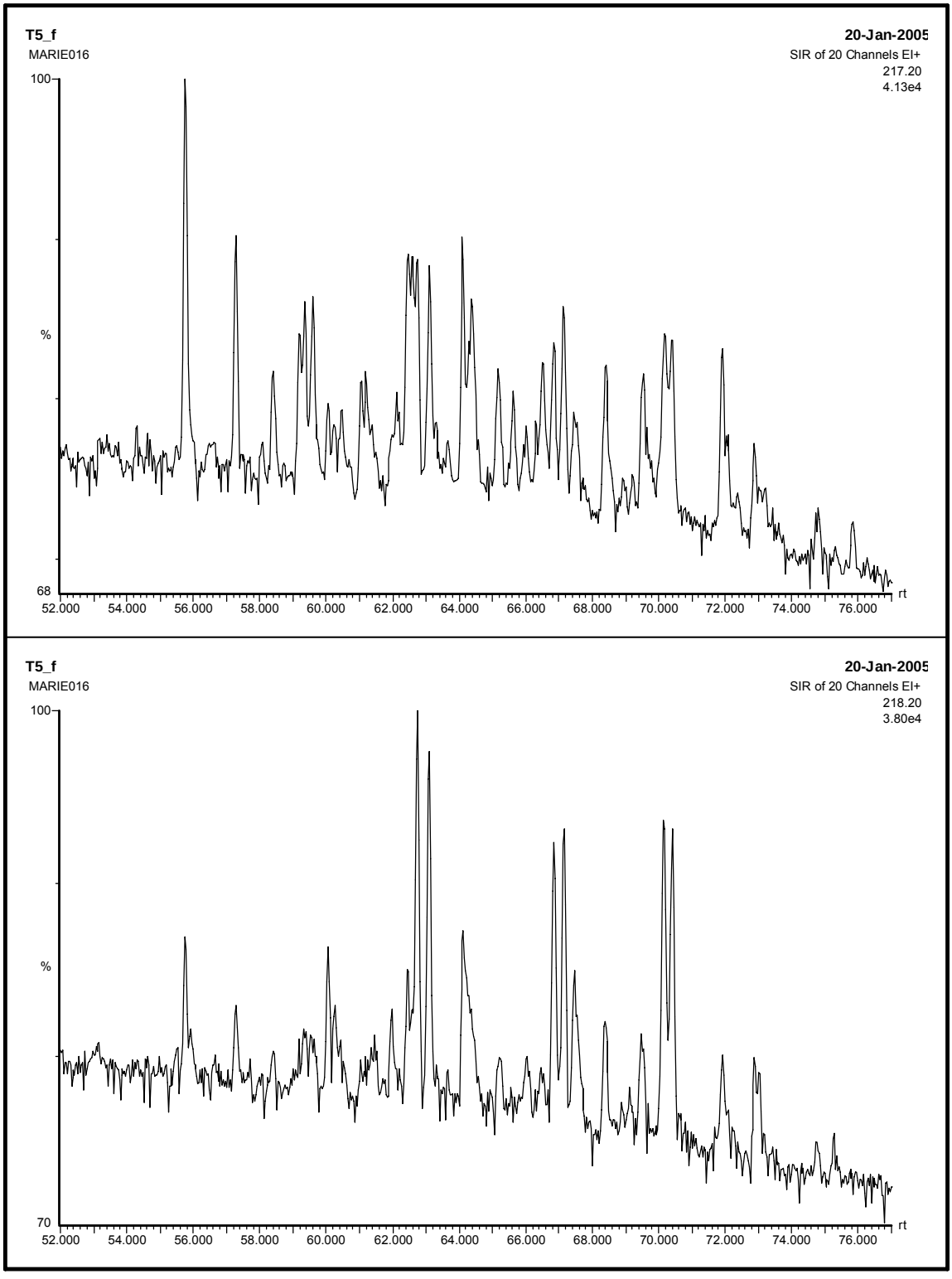
T5_f
MARIE016
20-Jan-2005
SIR of 20 Channels EI+
217.20
4.13e4
100
%
68
52.000
54.000
56.000
58.000
60.000
62.000
64.000
66.000
68.000
70.000
72.000
74.000
76.000
rt
T5_f
MARIE016
20-Jan-2005
SIR of 20 Channels EI+
218.20
3.80e4
100
%
70
52.000
54.000
56.000
58.000
60.000
62.000
64.000
66.000
68.000
70.000
72.000
74.000
76.000
rt

T5

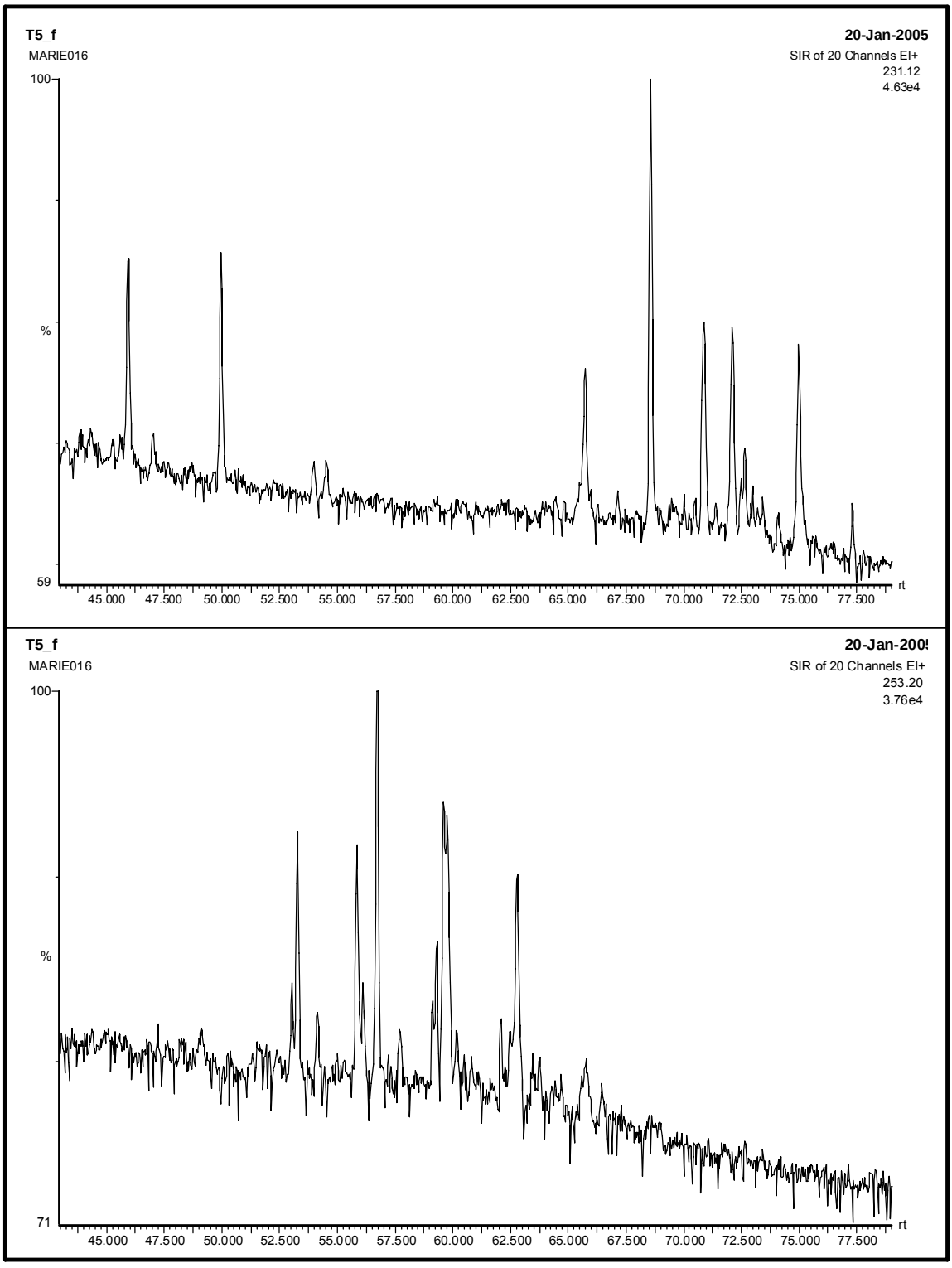
T5_f
MARIE016
20-Jan-2005
SIR of 20 Channels EI+
231.12
4.63e4
100
%
59
45.000 47.500 50.000 52.500 55.000 57.500 60.000 62.500 65.000 67.500 70.000 72.500 75.000 77.500
rt
T5_f
MARIE016
20-Jan-200
SIR of 20 Channels EI+
253.20
3.76e4
100
%
71
45.000 47.500 50.000 52.500 55.000 57.500 60.000 62.500 65.000 67.500 70.000 72.500 75.000 77.500
rt

T5

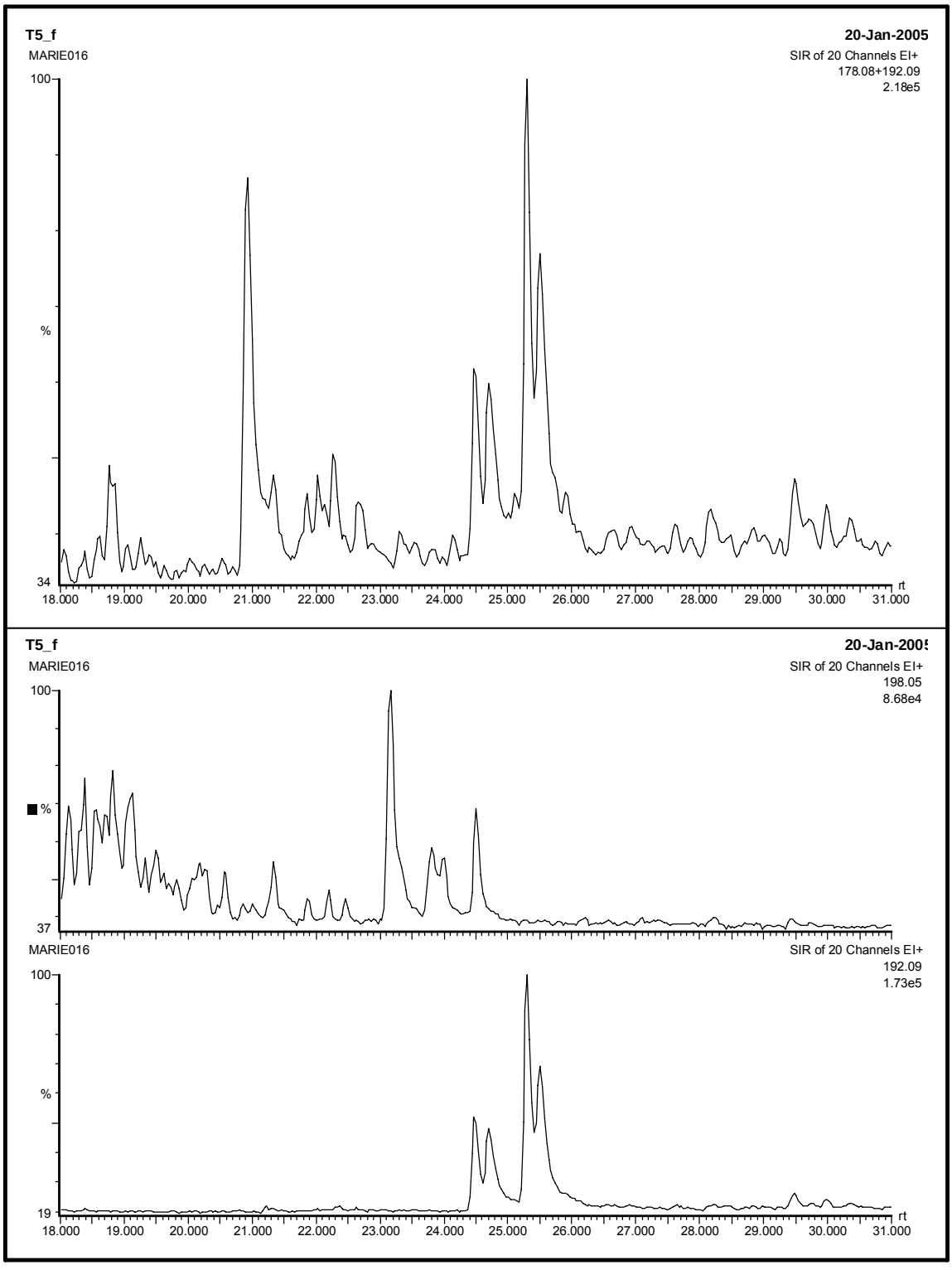
T5_f
MARIE016
20-Jan-2005
SIR of 20 Channels EI+
178.08+192.09
2.18e5
100
%
34
18.000 19.000 20.000 21.000 22.000 23.000 24.000 25.000 26.000 27.000 28.000 29.000 30.000 31.000
rt
T5_f
MARIE016
20-Jan-200
SIR of 20 Channels EI+
198.05
8.68e4
100
%
37
MARIE016
SIR of 20 Channels EI+
192.09
1.73e5
100
%
19
18.000 19.000 20.000 21.000 22.000 23.000 24.000 25.000 26.000 27.000 28.000 29.000 30.000 31.000
rt

Svale1

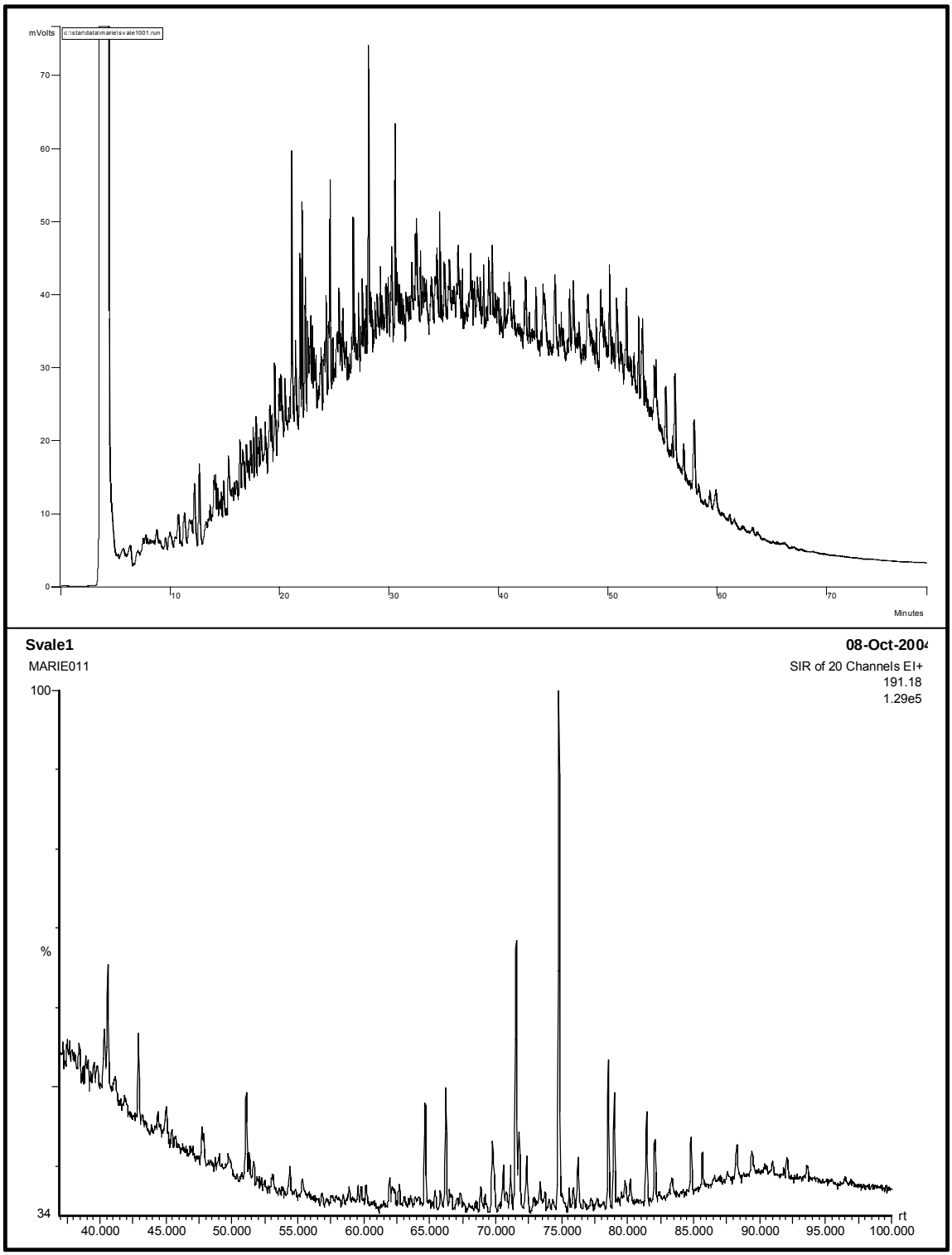
mVolts
c:\star\data\marie\svale1001.run
70
60
50
40
30
20
10
0
10
20
30
40
50
60
70
Minutes
Svale1
08-Oct-200
MARIE011
SIR of 20 Channels EI+
191.18
1.29e5
100
%
34
40.000
45.000
50.000
55.000
60.000
65.000
70.000
75.000
80.000
85.000
90.000
95.000
100.000
rt

Svale1

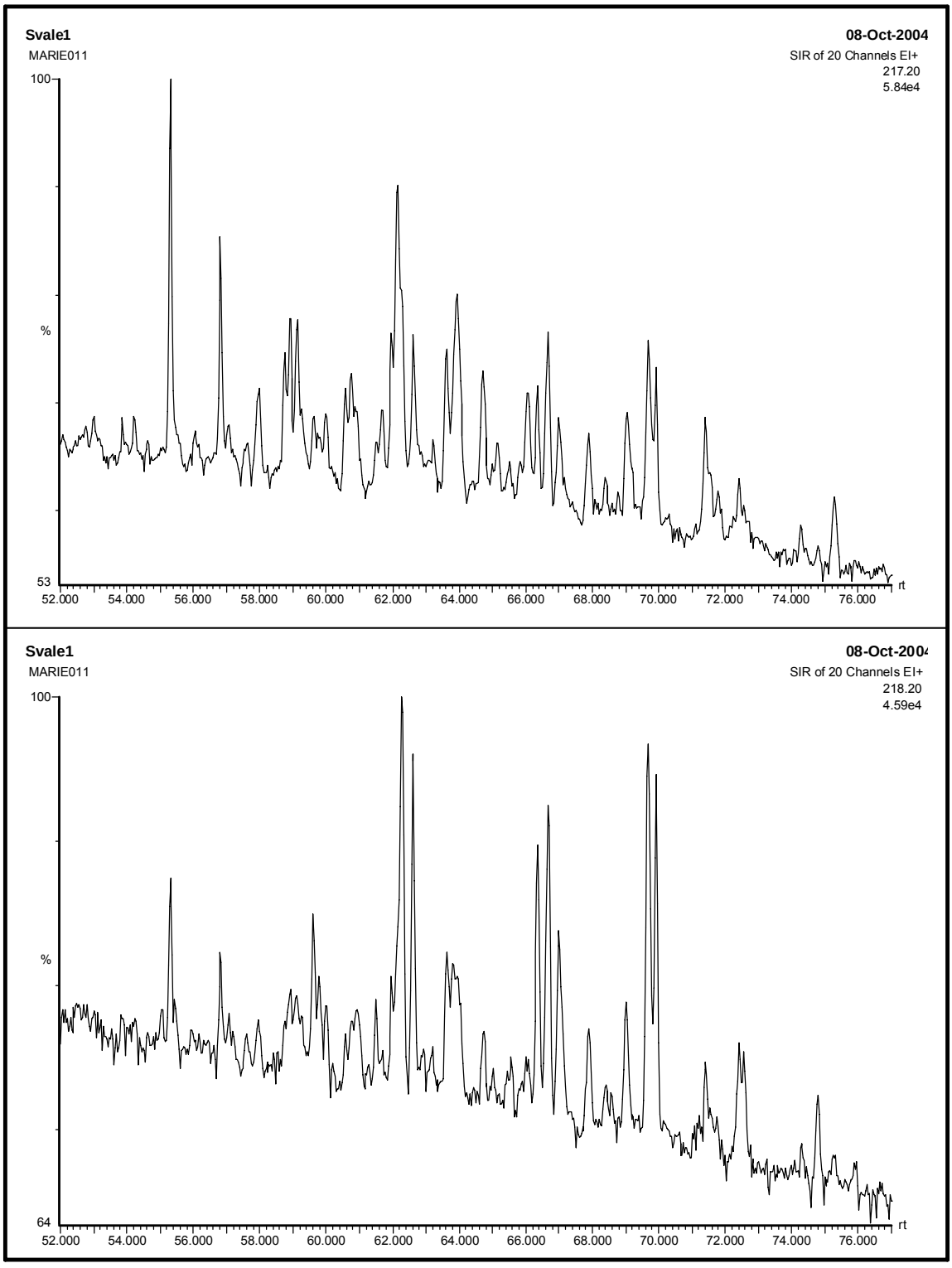
Svale1
MARIE011
08-Oct-2004
SIR of 20 Channels EI+
217.20
5.84e4
100
%
53
52.000
54.000
56.000
58.000
60.000
62.000
64.000
66.000
68.000
70.000
72.000
74.000
76.000
rt
Svale1
MARIE011
08-Oct-200
SIR of 20 Channels EI+
218.20
4.59e4
100
%
64
52.000
54.000
56.000
58.000
60.000
62.000
64.000
66.000
68.000
70.000
72.000
74.000
76.000
rt

Svale1

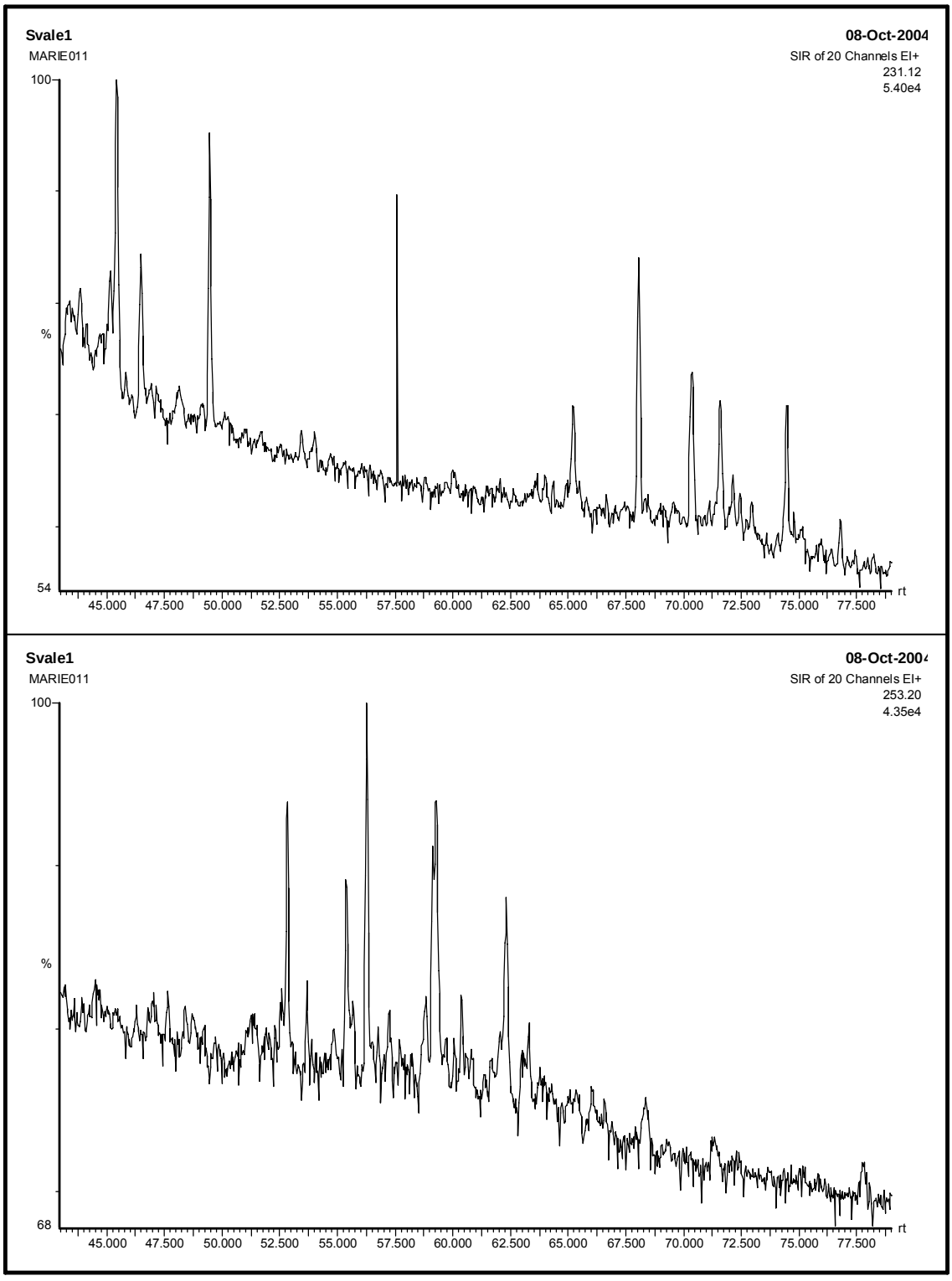
Svale1
MARIE011
08-Oct-2004
SIR of 20 Channels EI+
231.12
5.40e4
100
%
54
45.000 47.500 50.000 52.500 55.000 57.500 60.000 62.500 65.000 67.500 70.000 72.500 75.000 77.500
rt
Svale1
MARIE011
08-Oct-2004
SIR of 20 Channels EI+
253.20
4.35e4
100
%
68
45.000 47.500 50.000 52.500 55.000 57.500 60.000 62.500 65.000 67.500 70.000 72.500 75.000 77.500
rt

Svale1

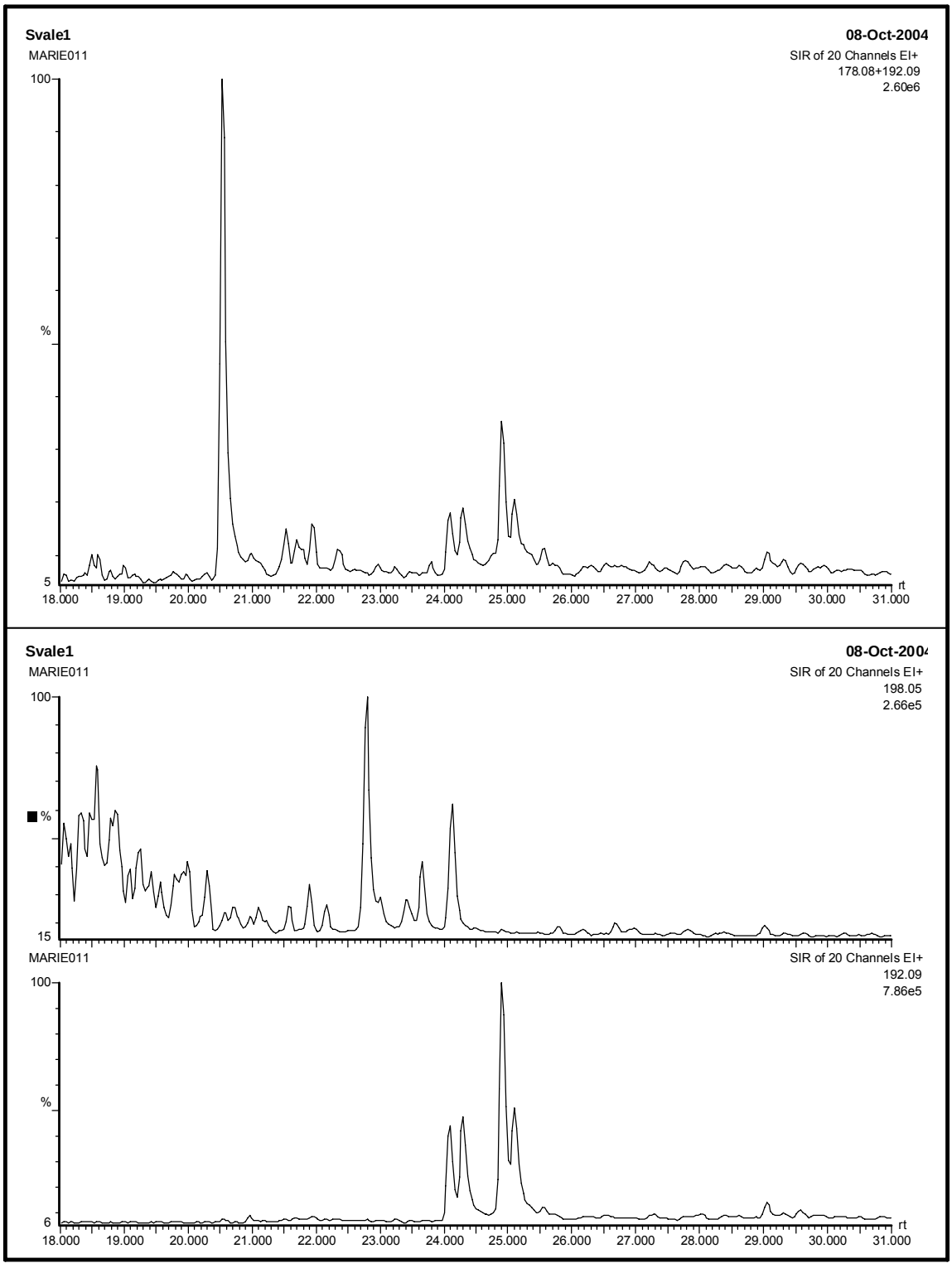
Svale1
MARIE011
08-Oct-2004
SIR of 20 Channels EI+
178.08+192.09
2.60e6
100
%
5
18.000 19.000 20.000 21.000 22.000 23.000 24.000 25.000 26.000 27.000 28.000 29.000 30.000 31.000
rt
Svale1
MARIE011
08-Oct-200
SIR of 20 Channels EI+
198.05
2.66e5
100
%
15
MARIE011
SIR of 20 Channels EI+
192.09
7.86e5
100
%
6
18.000 19.000 20.000 21.000 22.000 23.000 24.000 25.000 26.000 27.000 28.000 29.000 30.000 31.000
rt

Svale2

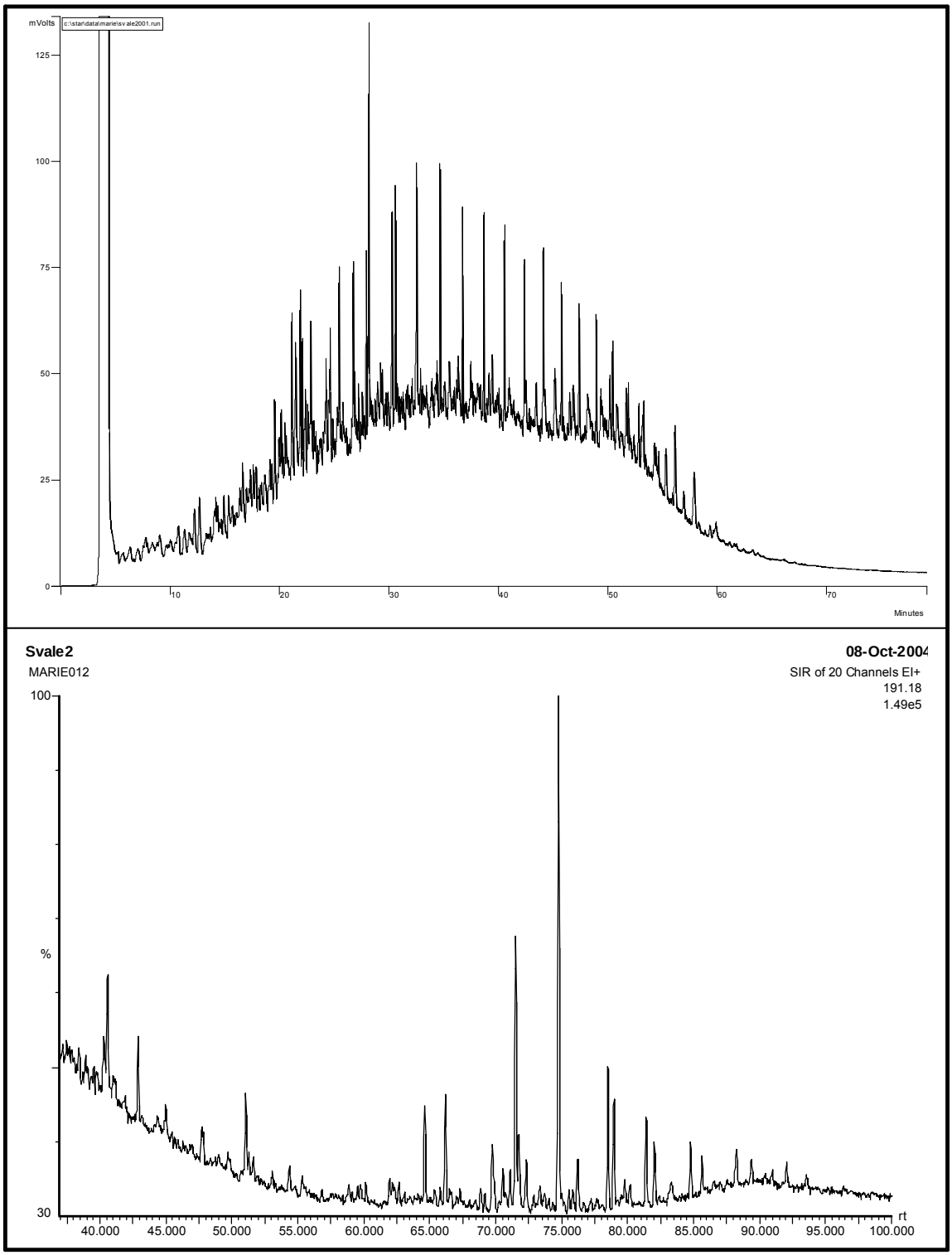
mVolts
c:\star\data\marie\svale2001.run
125
100
75
50
25
0
10
20
30
40
50
60
70
Minutes
Svale2
MARIE012
08-Oct-2004
SIR of 20 Channels EI+
191.18
1.49e5
100
%
30
40.000
45.000
50.000
55.000
60.000
65.000
70.000
75.000
80.000
85.000
90.000
95.000
100.000
rt

Svale2

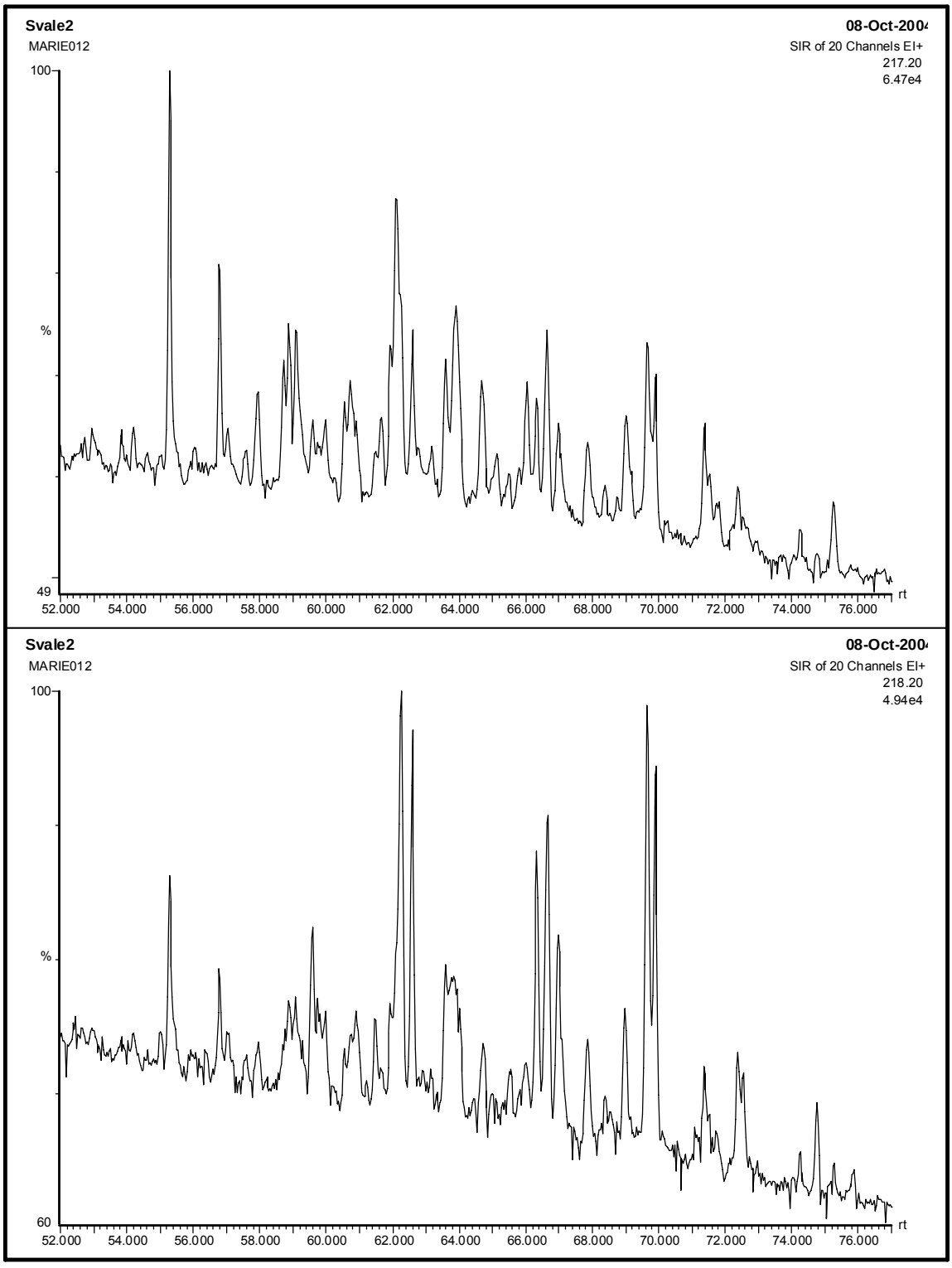
Svale2
08-Oct-200
MARIE012
SIR of 20 Channels EI+
217.20
6.47e4
100
%
49
52.000
54.000
56.000
58.000
60.000
62.000
64.000
66.000
68.000
70.000
72.000
74.000
76.000
rt
Svale2
08-Oct-200
MARIE012
SIR of 20 Channels EI+
218.20
4.94e4
100
%
60
52.000
54.000
56.000
58.000
60.000
62.000
64.000
66.000
68.000
70.000
72.000
74.000
76.000
rt

Svale2

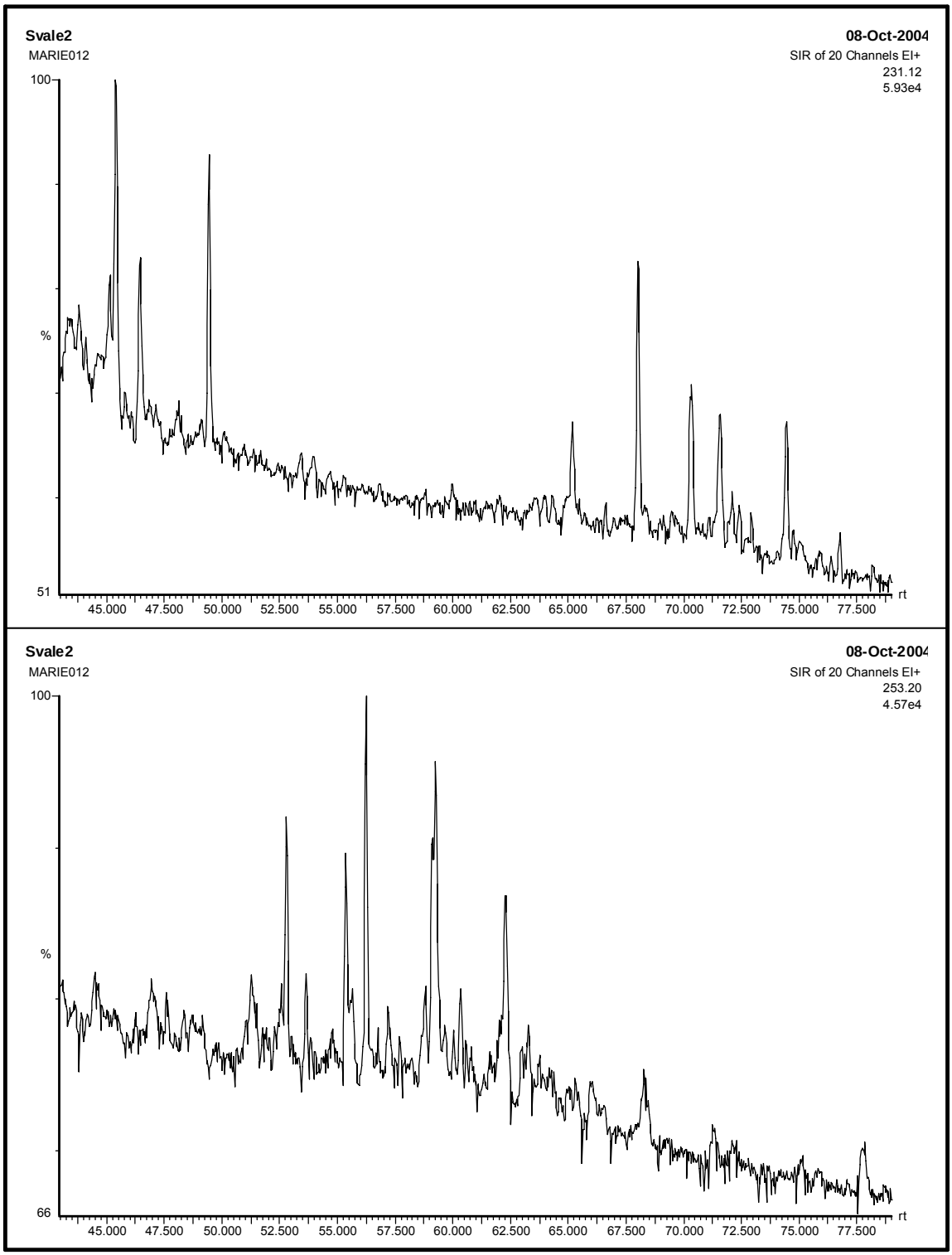
Svale2
MARIE012
08-Oct-2004
SIR of 20 Channels EI+
231.12
5.93e4
100
%
51
45.000 47.500 50.000 52.500 55.000 57.500 60.000 62.500 65.000 67.500 70.000 72.500 75.000 77.500
rt
Svale2
MARIE012
08-Oct-2004
SIR of 20 Channels EI+
253.20
4.57e4
100
%
66
45.000 47.500 50.000 52.500 55.000 57.500 60.000 62.500 65.000 67.500 70.000 72.500 75.000 77.500
rt

Svale2

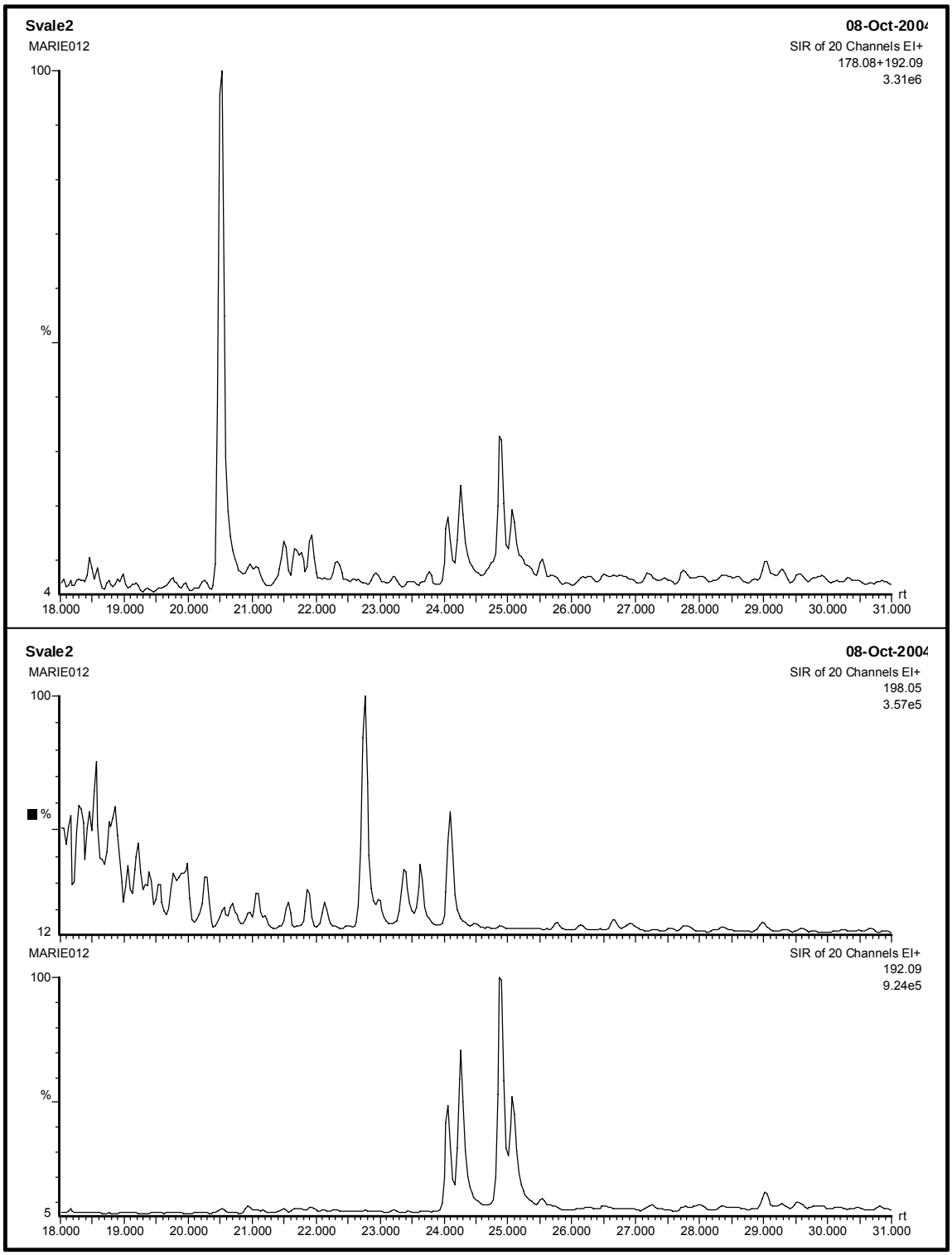
Svale2
08-Oct-200
MARIE012
SIR of 20 Channels EI+
178.08+192.09
3.31e6
100
%
4
18.000 19.000 20.000 21.000 22.000 23.000 24.000 25.000 26.000 27.000 28.000 29.000 30.000 31.000
rt
Svale2
08-Oct-200
MARIE012
SIR of 20 Channels EI+
198.05
3.57e5
100
%
12
MARIE012
SIR of 20 Channels EI+
192.09
9.24e5
100
%
5
18.000 19.000 20.000 21.000 22.000 23.000 24.000 25.000 26.000 27.000 28.000 29.000 30.000 31.000
rt

6507/7-2 DST2

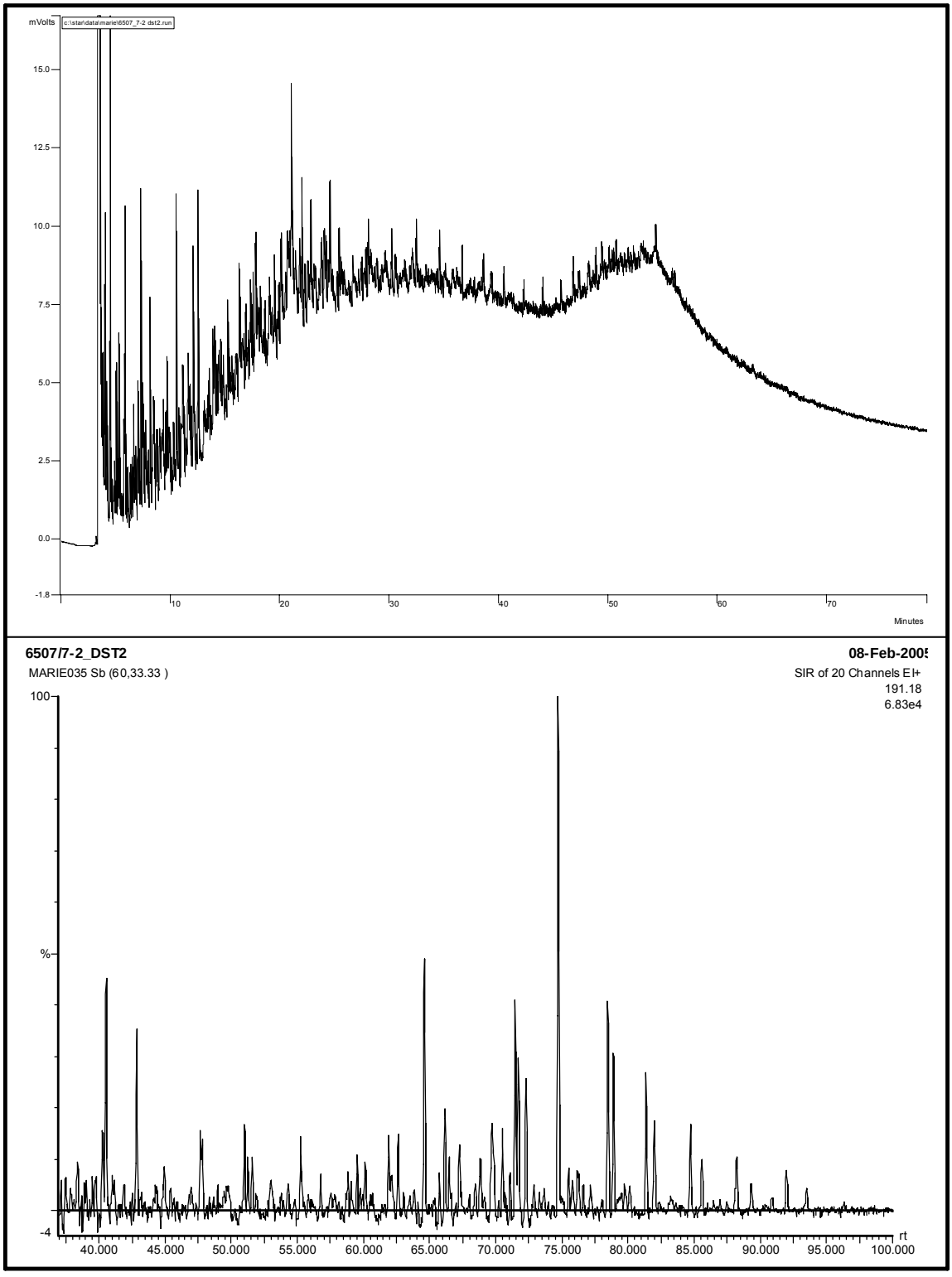
mVolts
c:\star\data\marie\6507_7-2 dst2.run
15.0
12.5
10.0
7.5
5.0
2.5
0.0
-1.8
10
20
30
40
50
60
70
Minutes
6507/7-2_DST2
08-Feb-2005
MARIE035 Sb (60,33.33)
SIR of 20 Channels EI+
191.18
6.83e4
100
%
-4
40.000
45.000
50.000
55.000
60.000
65.000
70.000
75.000
80.000
85.000
90.000
95.000
100.000
rt

6507/7-2 DST2

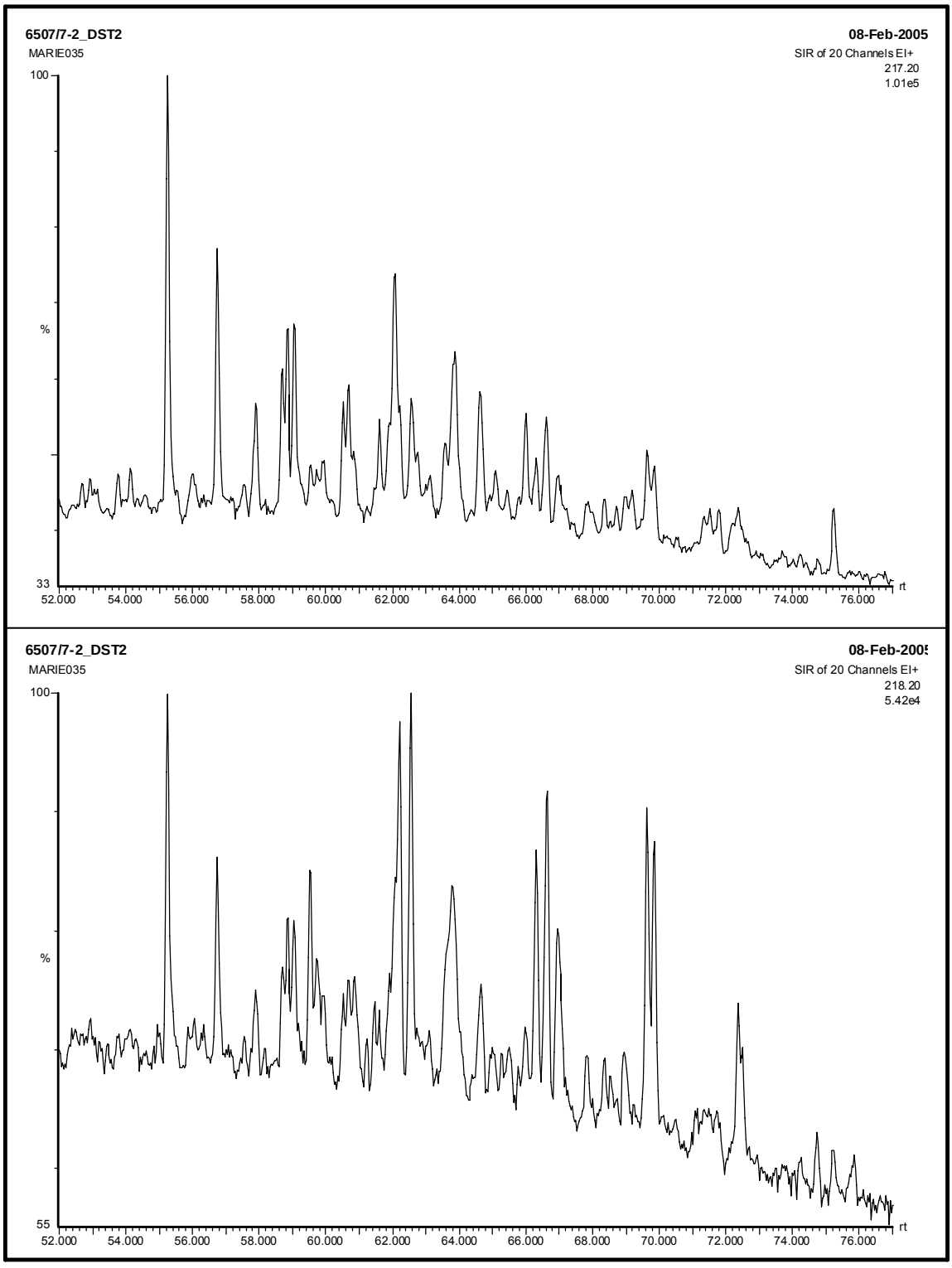
6507/7-2_DST2
MARIE035
08-Feb-2005
SIR of 20 Channels EI+
217.20
1.01e5
100
%
33
52.000
54.000
56.000
58.000
60.000
62.000
64.000
66.000
68.000
70.000
72.000
74.000
76.000
rt
6507/7-2_DST2
MARIE035
08-Feb-2005
SIR of 20 Channels EI+
218.20
5.42e4
100
%
55
52.000
54.000
56.000
58.000
60.000
62.000
64.000
66.000
68.000
70.000
72.000
74.000
76.000
rt

6507/7-2 DST2

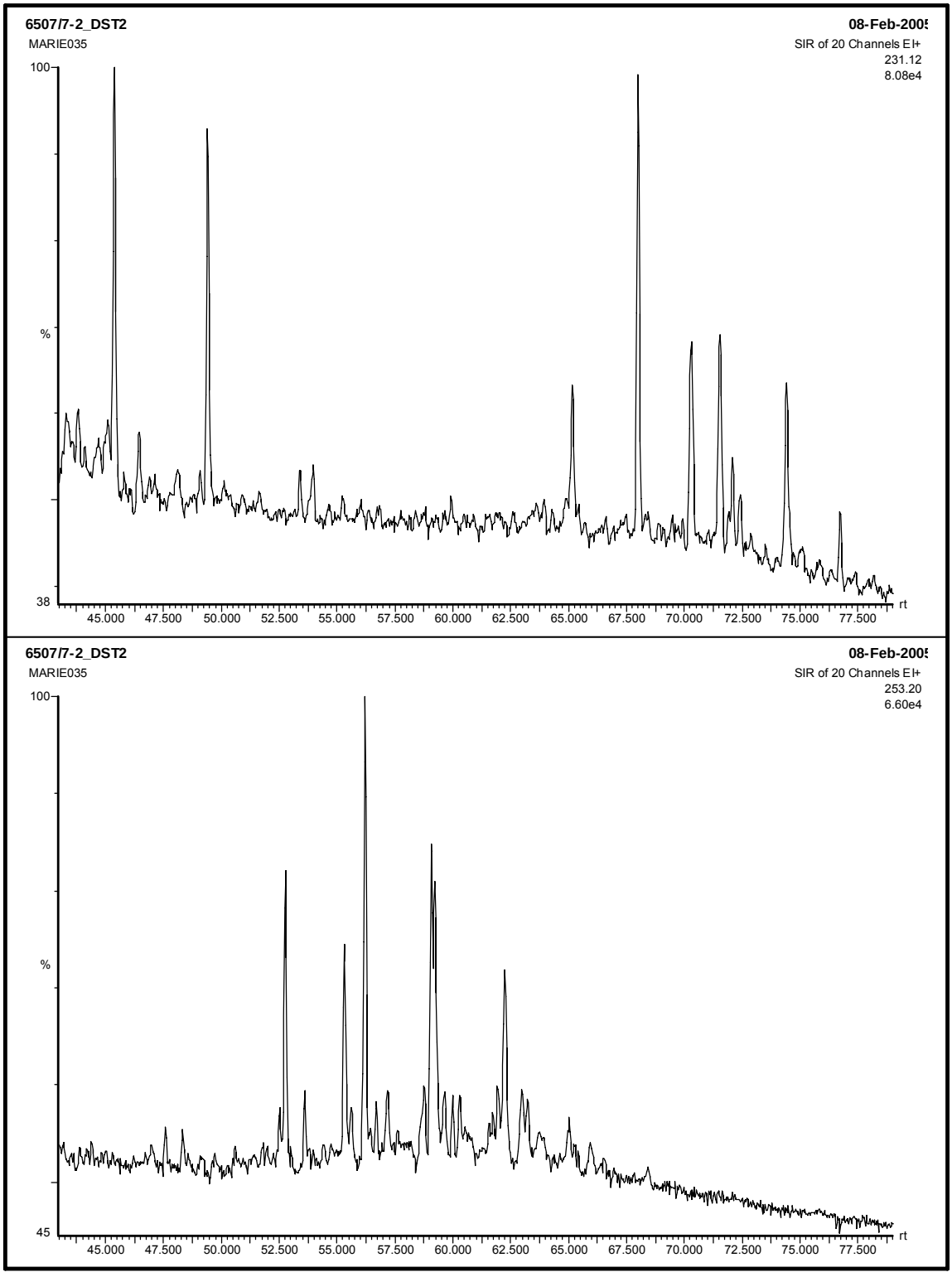
6507/7-2_DST2
MARIE035
08-Feb-200
SIR of 20 Channels EI+
231.12
8.08e4
100
%
38
45.000 47.500 50.000 52.500 55.000 57.500 60.000 62.500 65.000 67.500 70.000 72.500 75.000 77.500
rt
6507/7-2_DST2
MARIE035
08-Feb-200
SIR of 20 Channels EI+
253.20
6.60e4
100
%
45
45.000 47.500 50.000 52.500 55.000 57.500 60.000 62.500 65.000 67.500 70.000 72.500 75.000 77.500
rt

6507/7-2 DST2

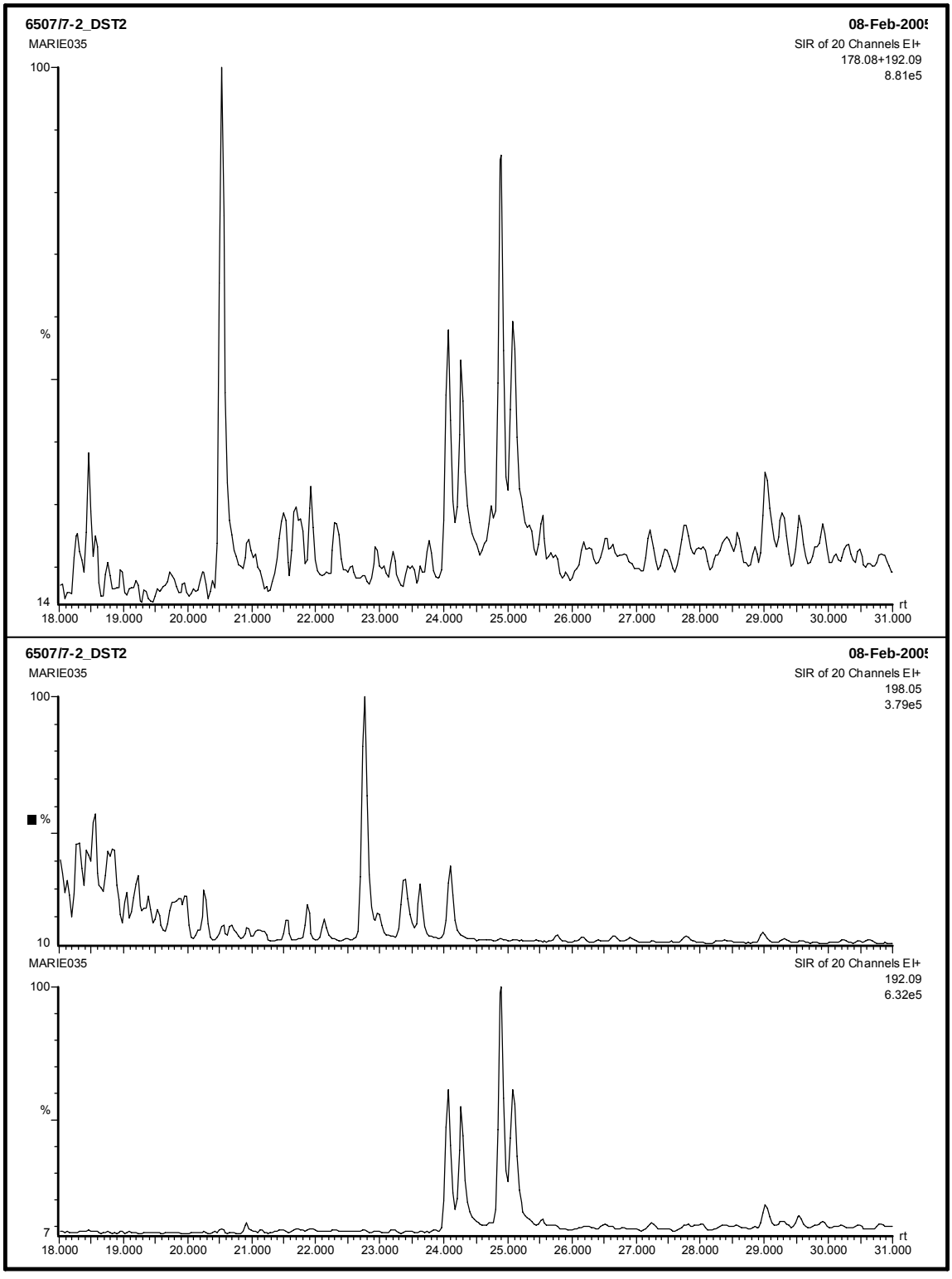
6507/7-2_DST2
08-Feb-200
MARIE035
SIR of 20 Channels EI+
178.08+192.09
8.81e5
100
%
14
18.000 19.000 20.000 21.000 22.000 23.000 24.000 25.000 26.000 27.000 28.000 29.000 30.000 31.000
rt
6507/7-2_DST2
08-Feb-200
MARIE035
SIR of 20 Channels EI+
198.05
3.79e5
100
%
10
MARIE035
SIR of 20 Channels EI+
192.09
6.32e5
100
%
7
18.000 19.000 20.000 21.000 22.000 23.000 24.000 25.000 26.000 27.000 28.000 29.000 30.000 31.000
rt

6507/7-4 DST1

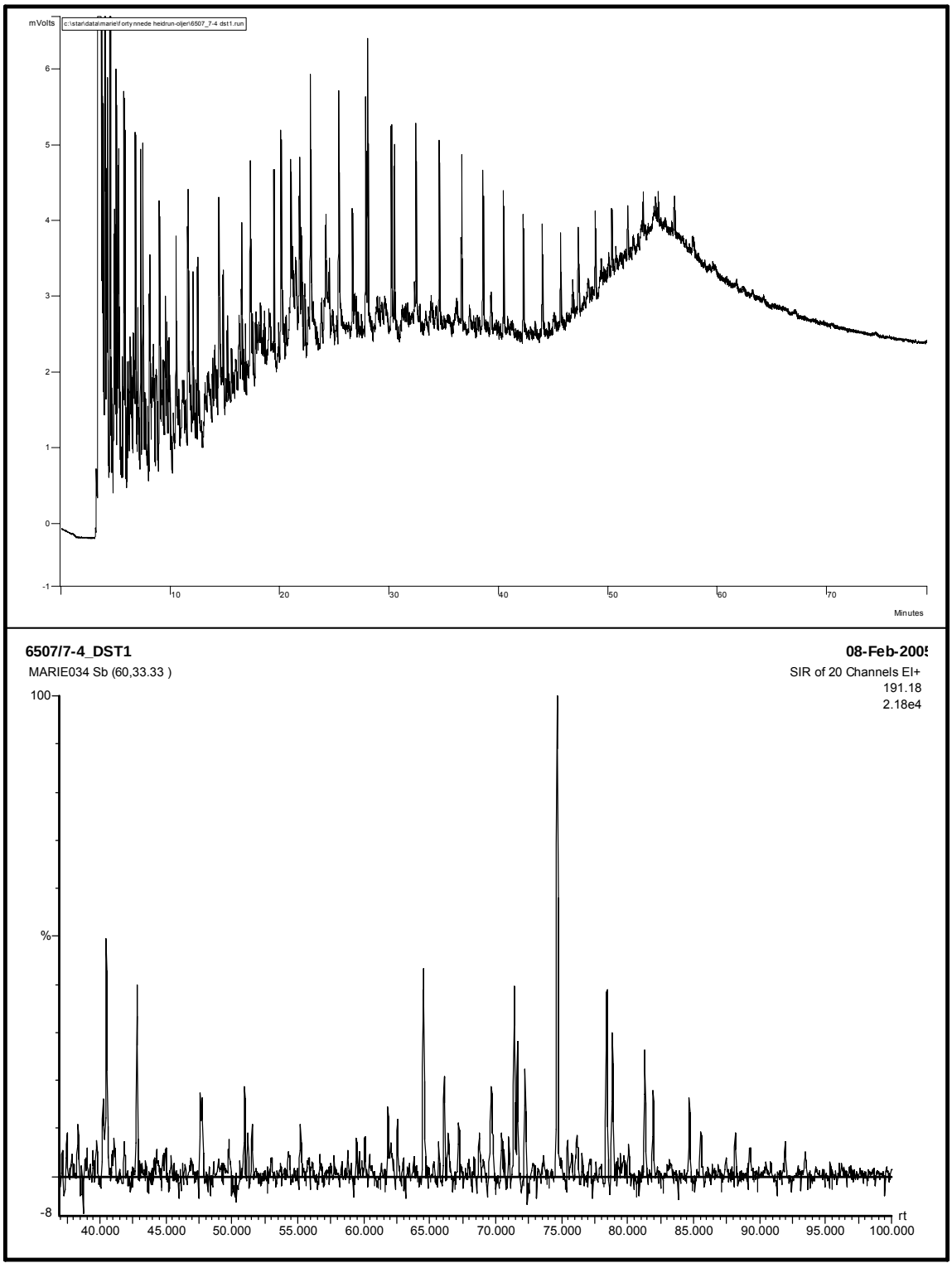
mVolts
c:\star\data\marie\fortynnede heidrun-oljer\6507_7-4 dst1.run
6
5
4
3
2
1
0
-1
10
20
30
40
50
60
70
Minutes
6507/7-4_DST1
MARIE034 Sb (60,33.33)
08-Feb-200
SIR of 20 Channels EI+
191.18
2.18e4
100
%
-8
40.000
45.000
50.000
55.000
60.000
65.000
70.000
75.000
80.000
85.000
90.000
95.000
100.000
rt

6507/7-4 DST1

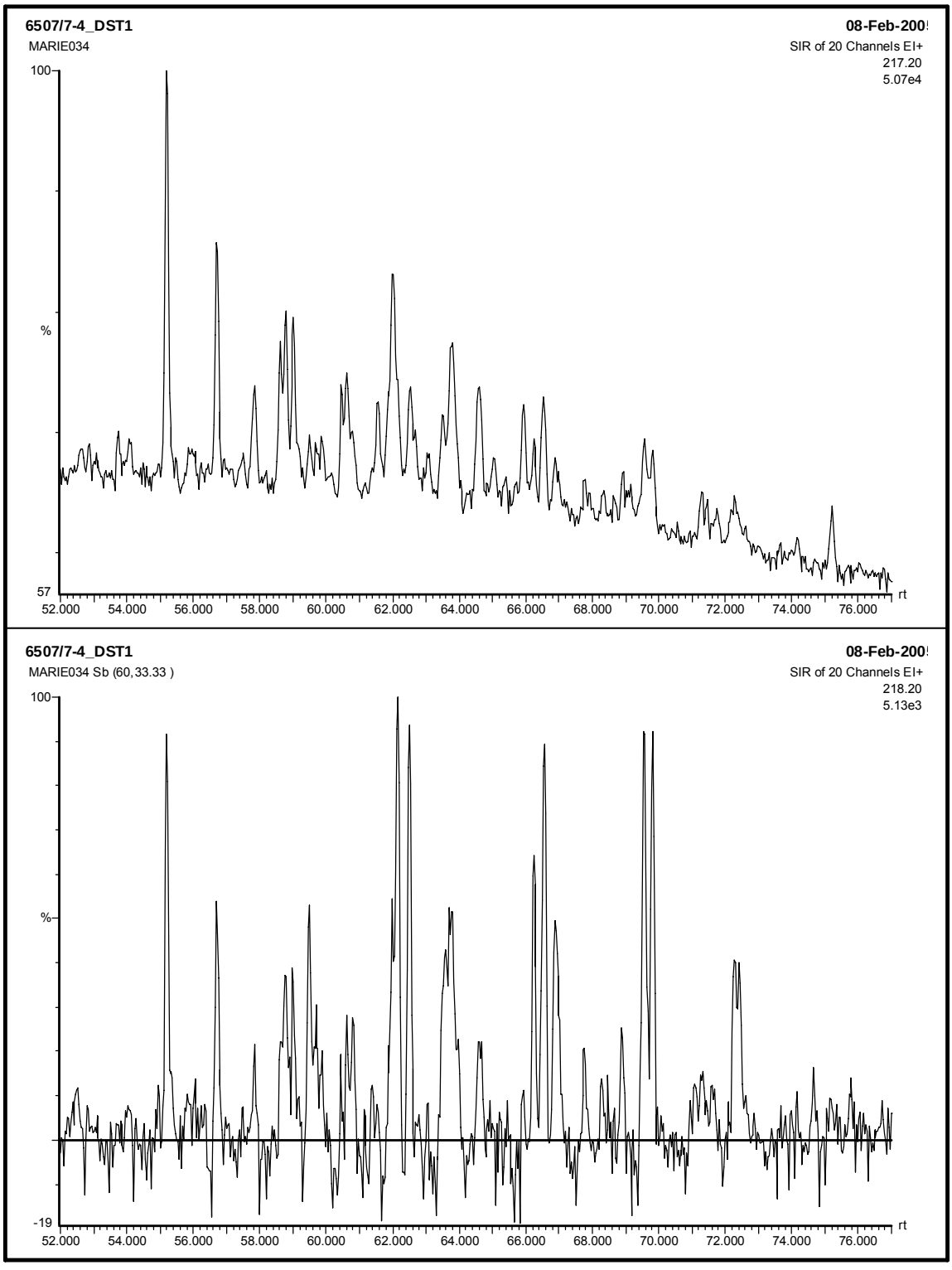
6507/7-4_DST1
MARIE034
08-Feb-200
SIR of 20 Channels EI+
217.20
5.07e4
100
%
57
52.000 54.000 56.000 58.000 60.000 62.000 64.000 66.000 68.000 70.000 72.000 74.000 76.000
rt
6507/7-4_DST1
MARIE034 Sb (60,33.33)
08-Feb-200
SIR of 20 Channels EI+
218.20
5.13e3
100
%
-19
52.000 54.000 56.000 58.000 60.000 62.000 64.000 66.000 68.000 70.000 72.000 74.000 76.000
rt

6507/7-4 DST1

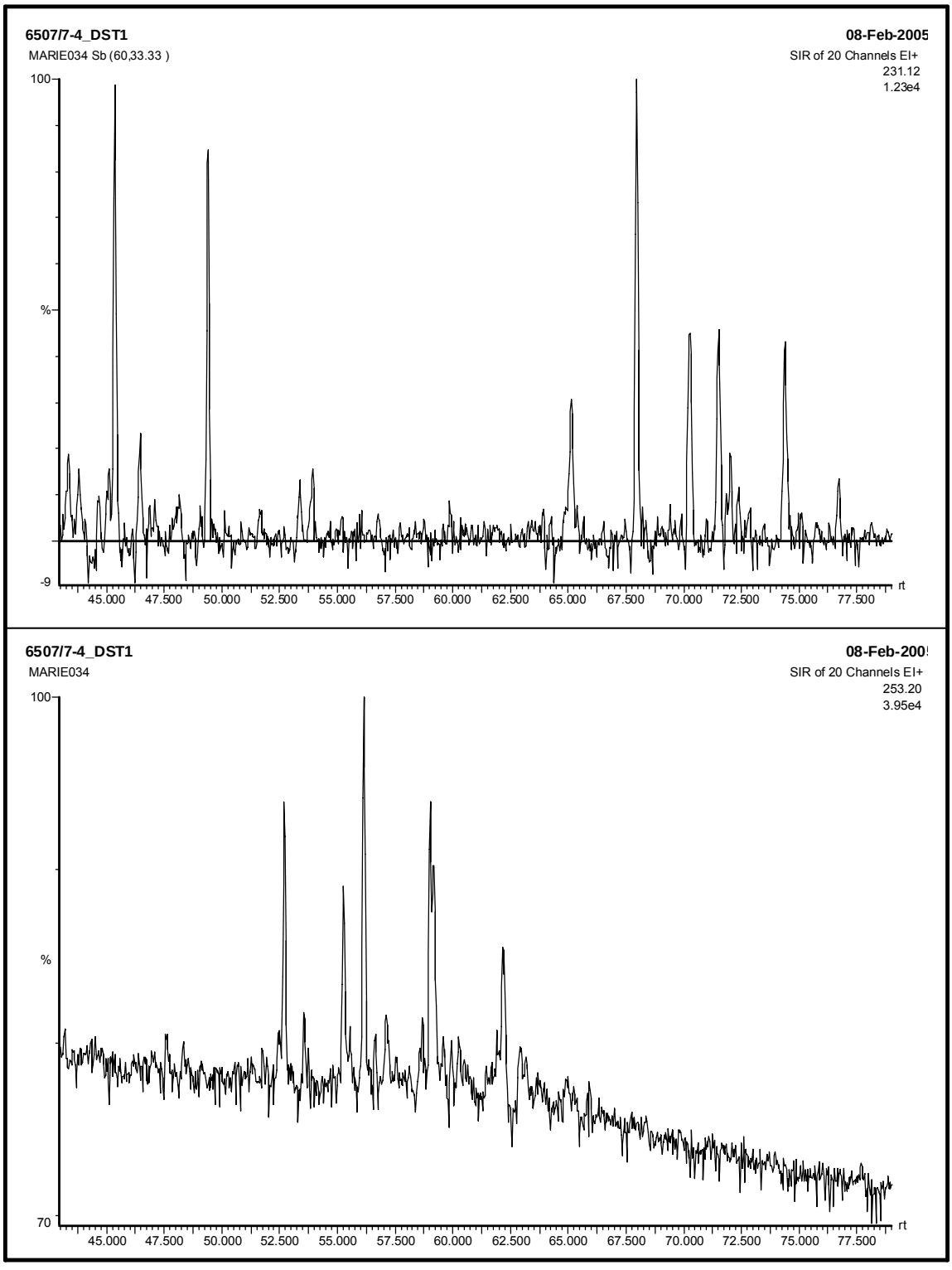
6507/7-4_DST1
MARIE034 Sb (60,33.33)
08-Feb-2005
SIR of 20 Channels EI+
231.12
1.23e4
100
%
-9
45.000 47.500 50.000 52.500 55.000 57.500 60.000 62.500 65.000 67.500 70.000 72.500 75.000 77.500
rt
6507/7-4_DST1
MARIE034
08-Feb-200
SIR of 20 Channels EI+
253.20
3.95e4
100
%
70
45.000 47.500 50.000 52.500 55.000 57.500 60.000 62.500 65.000 67.500 70.000 72.500 75.000 77.500
rt

6507/7-4 DST1

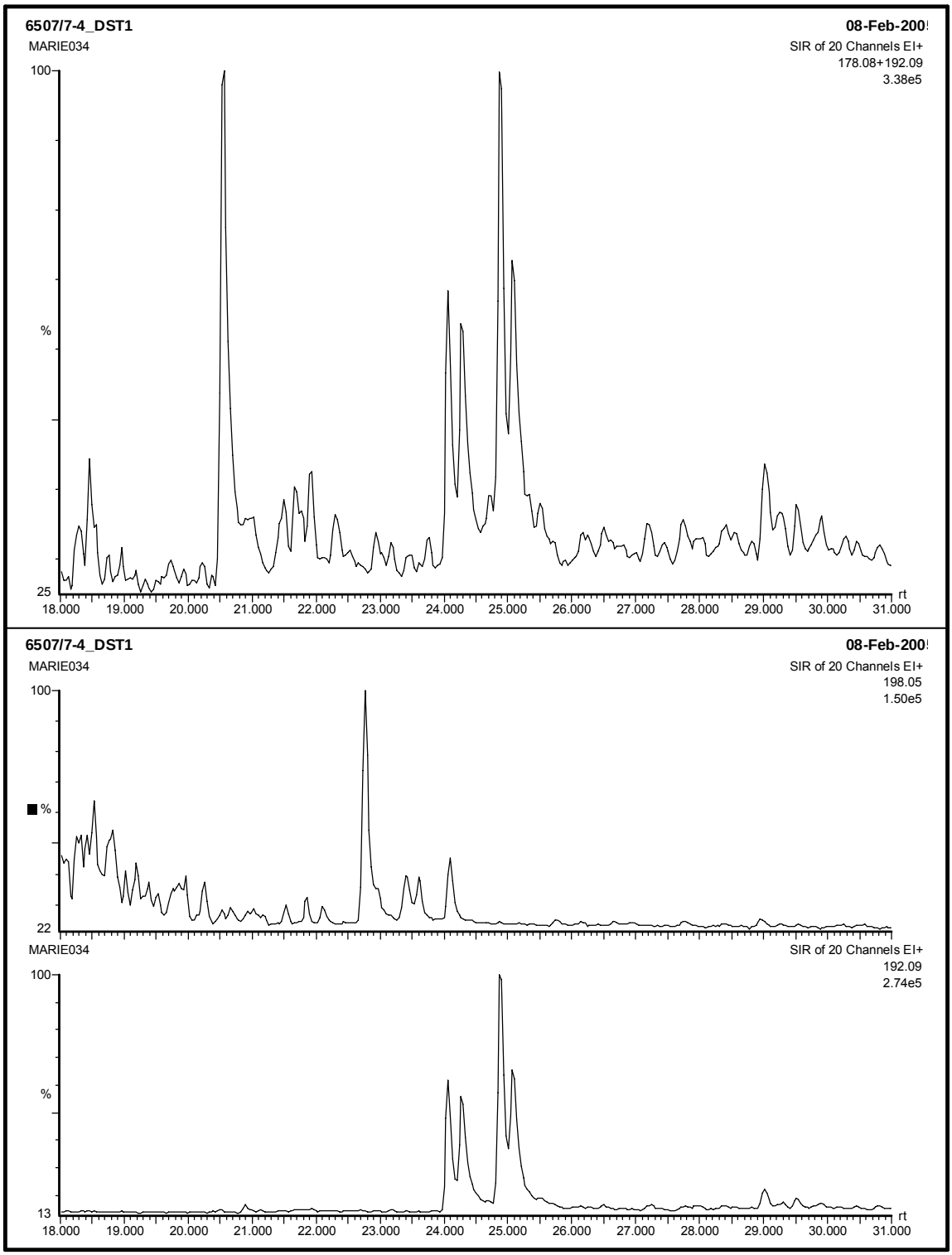
6507/7-4_DST1
08-Feb-200
MARIE034
SIR of 20 Channels EI+
178.08+192.09
3.38e5
100
%
25
18.000 19.000 20.000 21.000 22.000 23.000 24.000 25.000 26.000 27.000 28.000 29.000 30.000 31.000
rt
6507/7-4_DST1
08-Feb-200
MARIE034
SIR of 20 Channels EI+
198.05
1.50e5
100
%
22
MARIE034
SIR of 20 Channels EI+
192.09
2.74e5
100
%
13
18.000 19.000 20.000 21.000 22.000 23.000 24.000 25.000 26.000 27.000 28.000 29.000 30.000 31.000
rt

6507/7-4 DST3

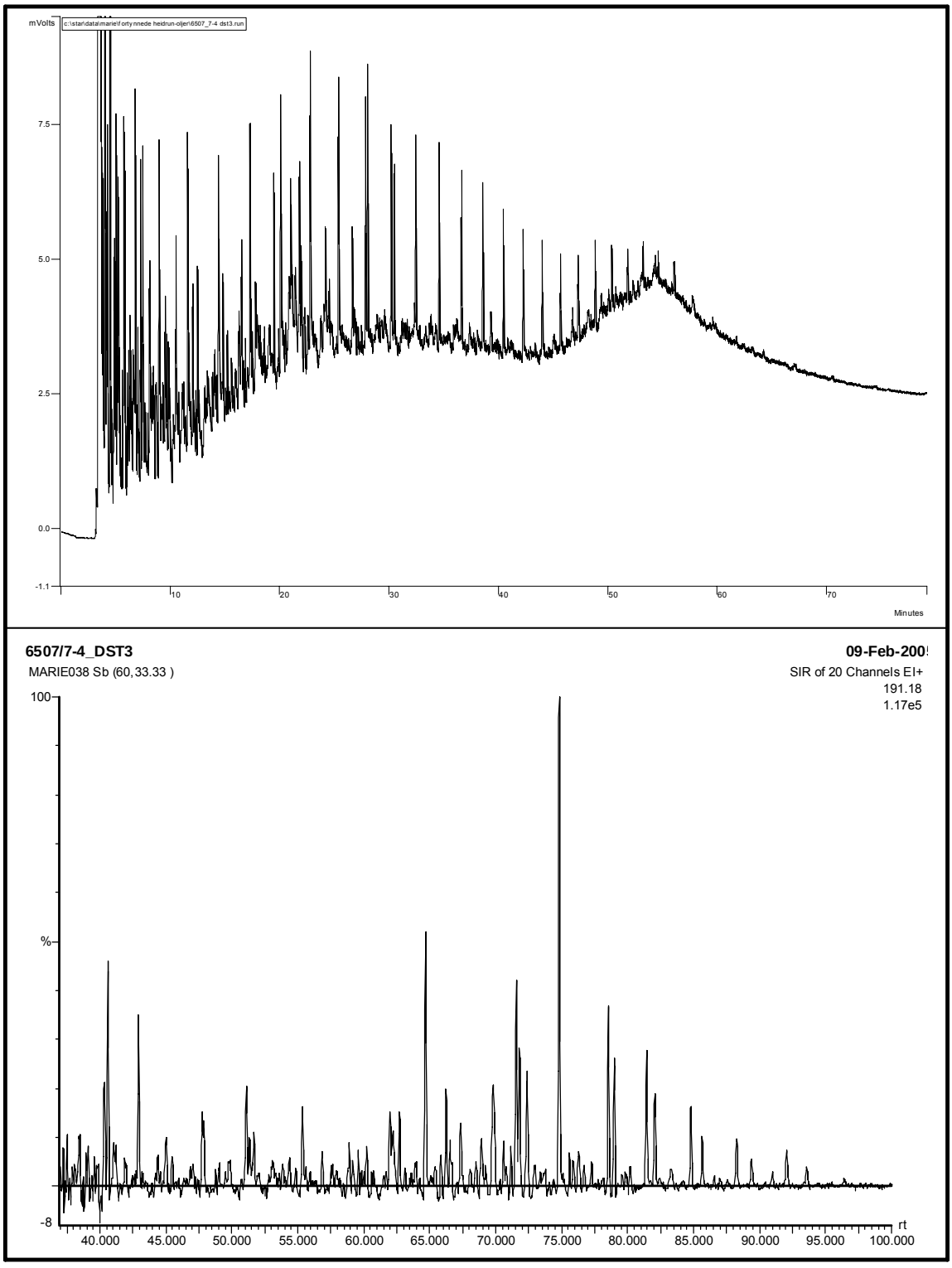
mVolts
c:\star\data\marie\Fortynnede heidrun-oljer\6507_7-4 dst3.run
7.5
5.0
2.5
0.0
-1.1
10
20
30
40
50
60
70
Minutes
6507/7-4_DST3
MARIE038 Sb (60,33.33)
09-Feb-200
SIR of 20 Channels EI+
191.18
1.17e5
100
%
-8
40.000
45.000
50.000
55.000
60.000
65.000
70.000
75.000
80.000
85.000
90.000
95.000
100.000
rt

6507/7-4 DST3

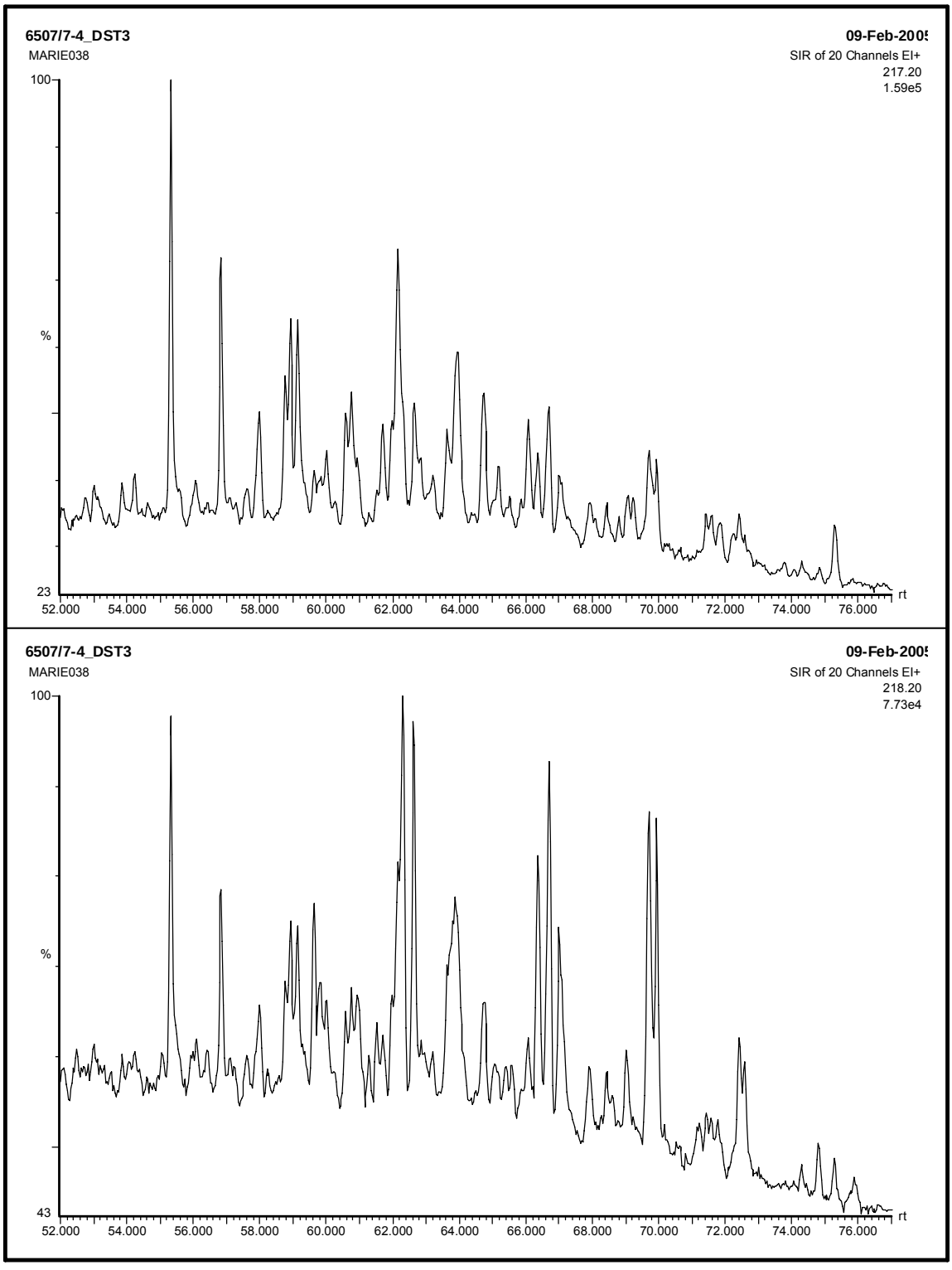
6507/7-4_DST3
MARIE038
09-Feb-200
SIR of 20 Channels EI+
217.20
1.59e5
100
%
23
52.000 54.000 56.000 58.000 60.000 62.000 64.000 66.000 68.000 70.000 72.000 74.000 76.000
rt
6507/7-4_DST3
MARIE038
09-Feb-200
SIR of 20 Channels EI+
218.20
7.73e4
100
%
43
52.000 54.000 56.000 58.000 60.000 62.000 64.000 66.000 68.000 70.000 72.000 74.000 76.000
rt

6507/7-4 DST3

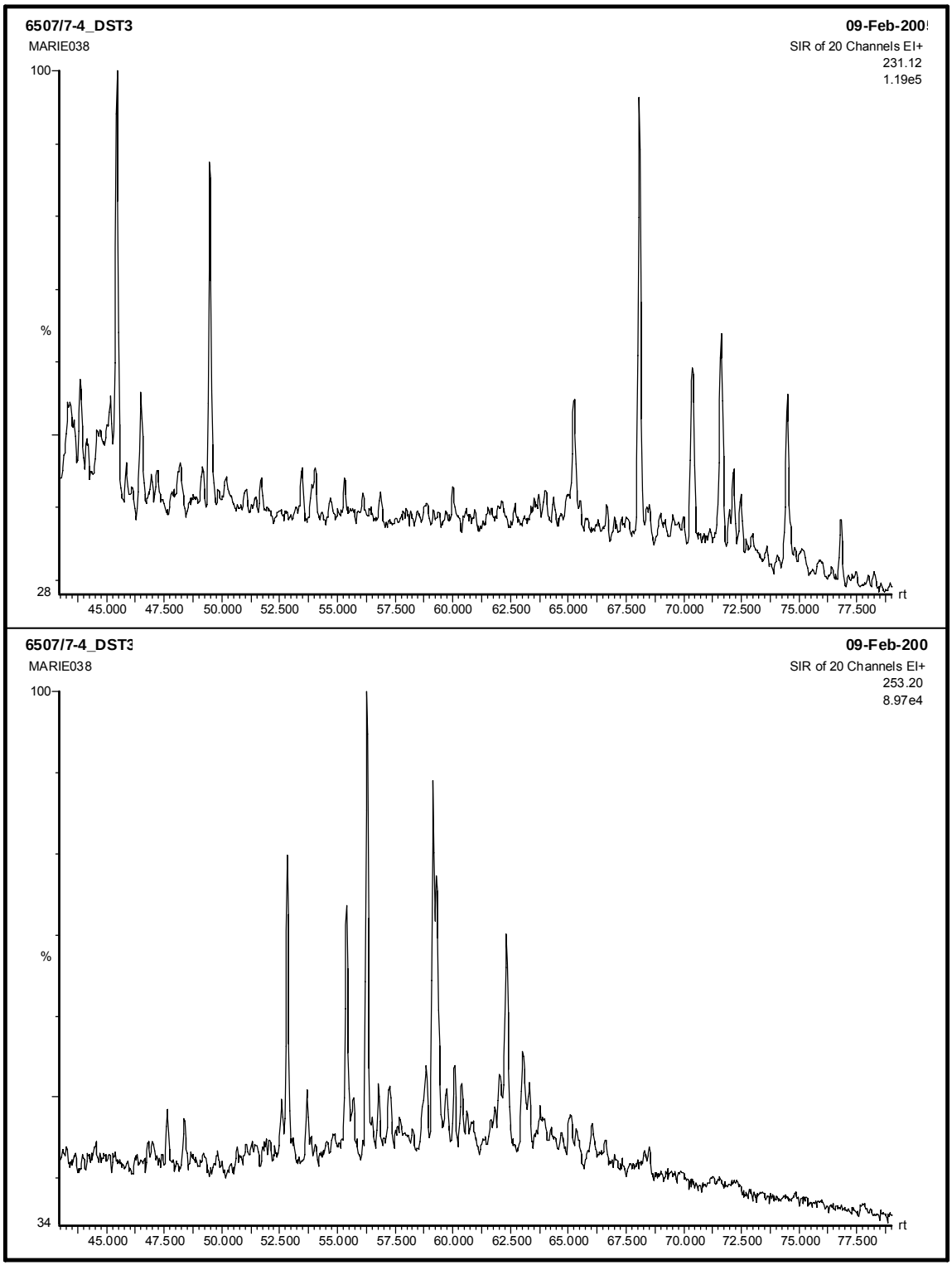
6507/7-4_DST3
MARIE038
09-Feb-200
SIR of 20 Channels EI+
231.12
1.19e5
100
%
28
45.000 47.500 50.000 52.500 55.000 57.500 60.000 62.500 65.000 67.500 70.000 72.500 75.000 77.500
rt
6507/7-4_DST3
MARIE038
09-Feb-200
SIR of 20 Channels EI+
253.20
8.97e4
100
%
34
45.000 47.500 50.000 52.500 55.000 57.500 60.000 62.500 65.000 67.500 70.000 72.500 75.000 77.500
rt

6507/7-4 DST3

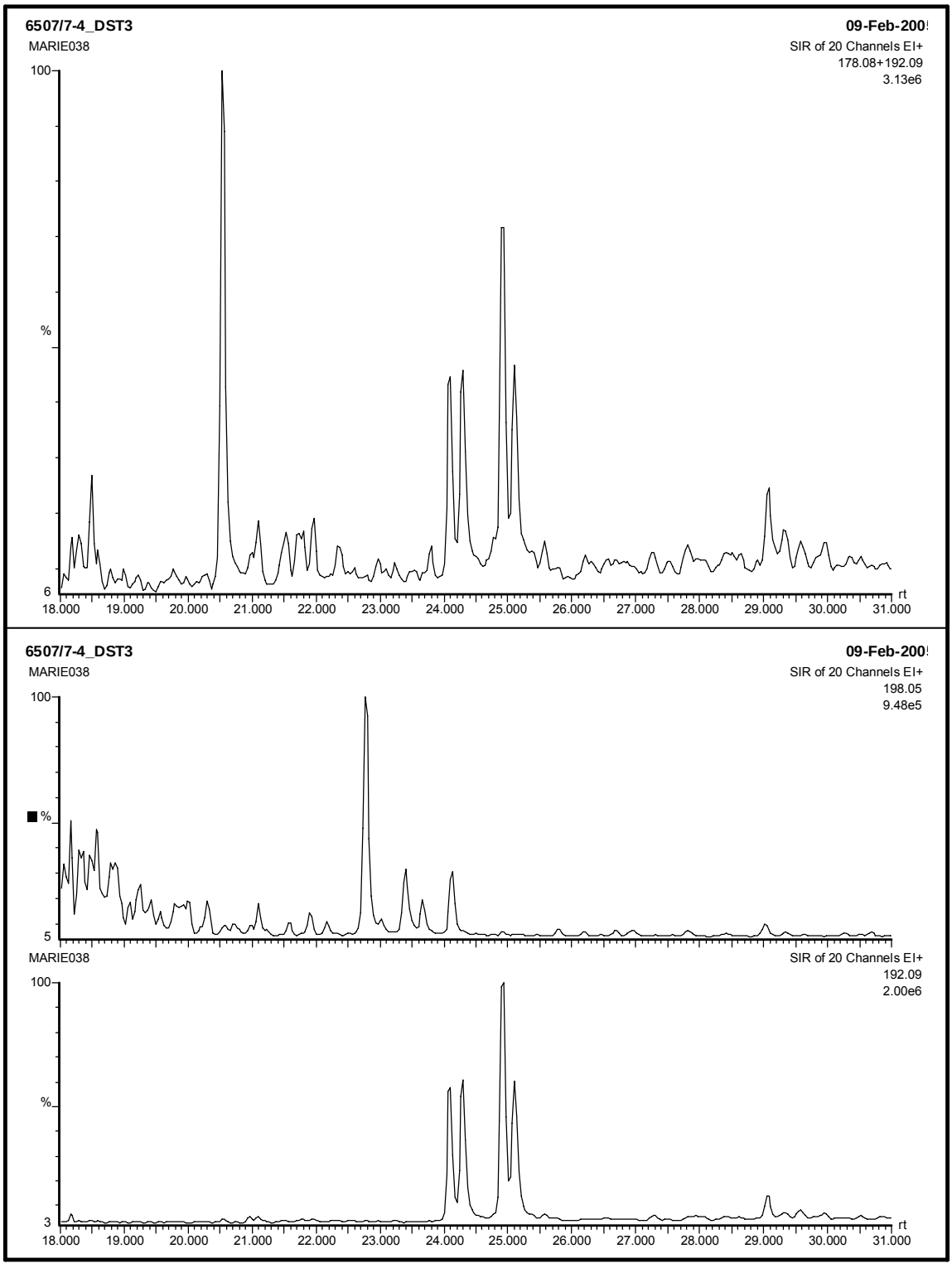
6507/7-4_DST3
09-Feb-200
MARIE038
SIR of 20 Channels EI+
178.08+192.09
3.13e6
100
%
6
18.000 19.000 20.000 21.000 22.000 23.000 24.000 25.000 26.000 27.000 28.000 29.000 30.000 31.000
rt
6507/7-4_DST3
09-Feb-200
MARIE038
SIR of 20 Channels EI+
198.05
9.48e5
100
%
5
MARIE038
SIR of 20 Channels EI+
192.09
2.00e6
100
%
3
18.000 19.000 20.000 21.000 22.000 23.000 24.000 25.000 26.000 27.000 28.000 29.000 30.000 31.000
rt

6507/7-5 DST2A

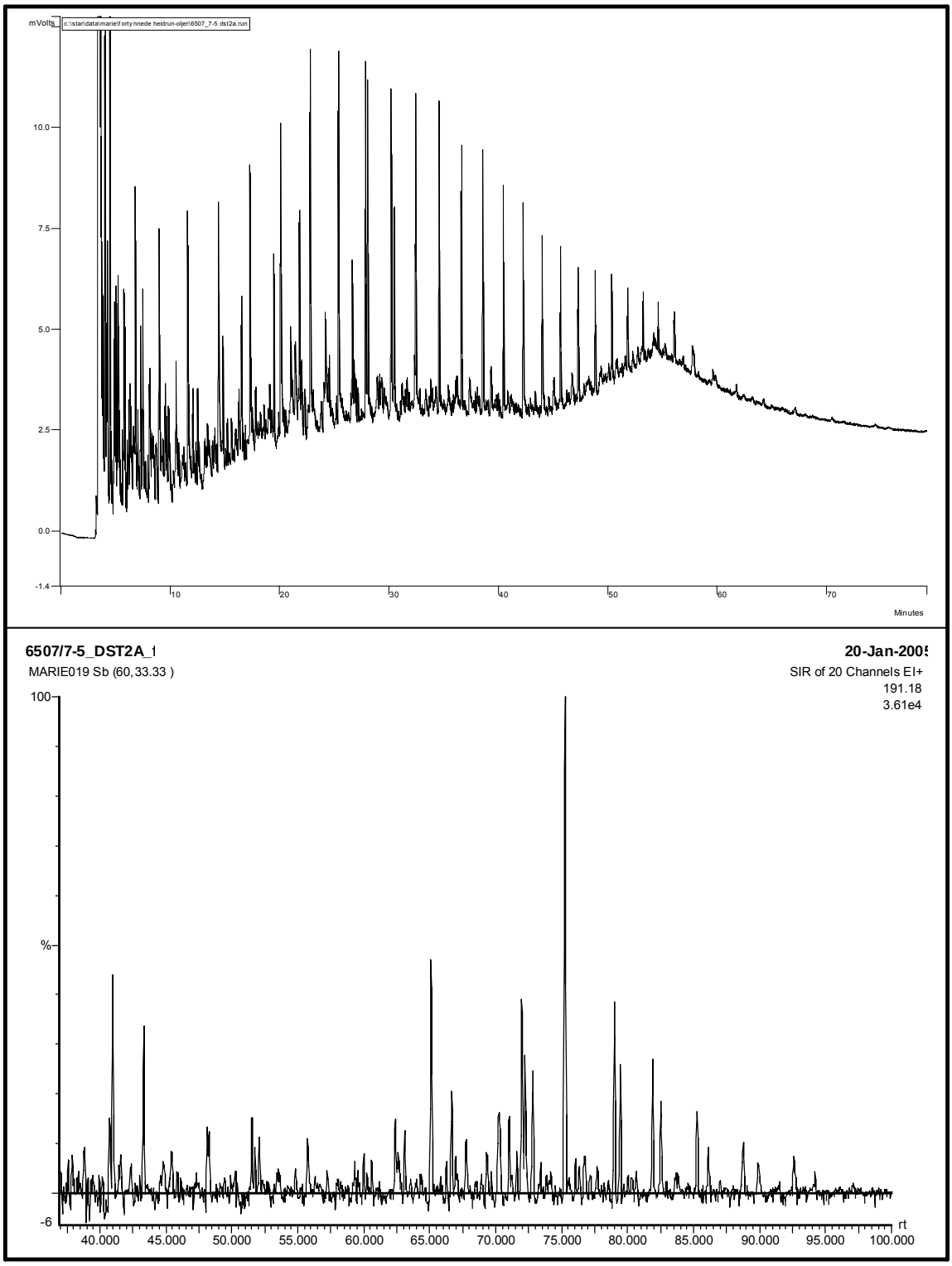

6507/7-5 DST2A

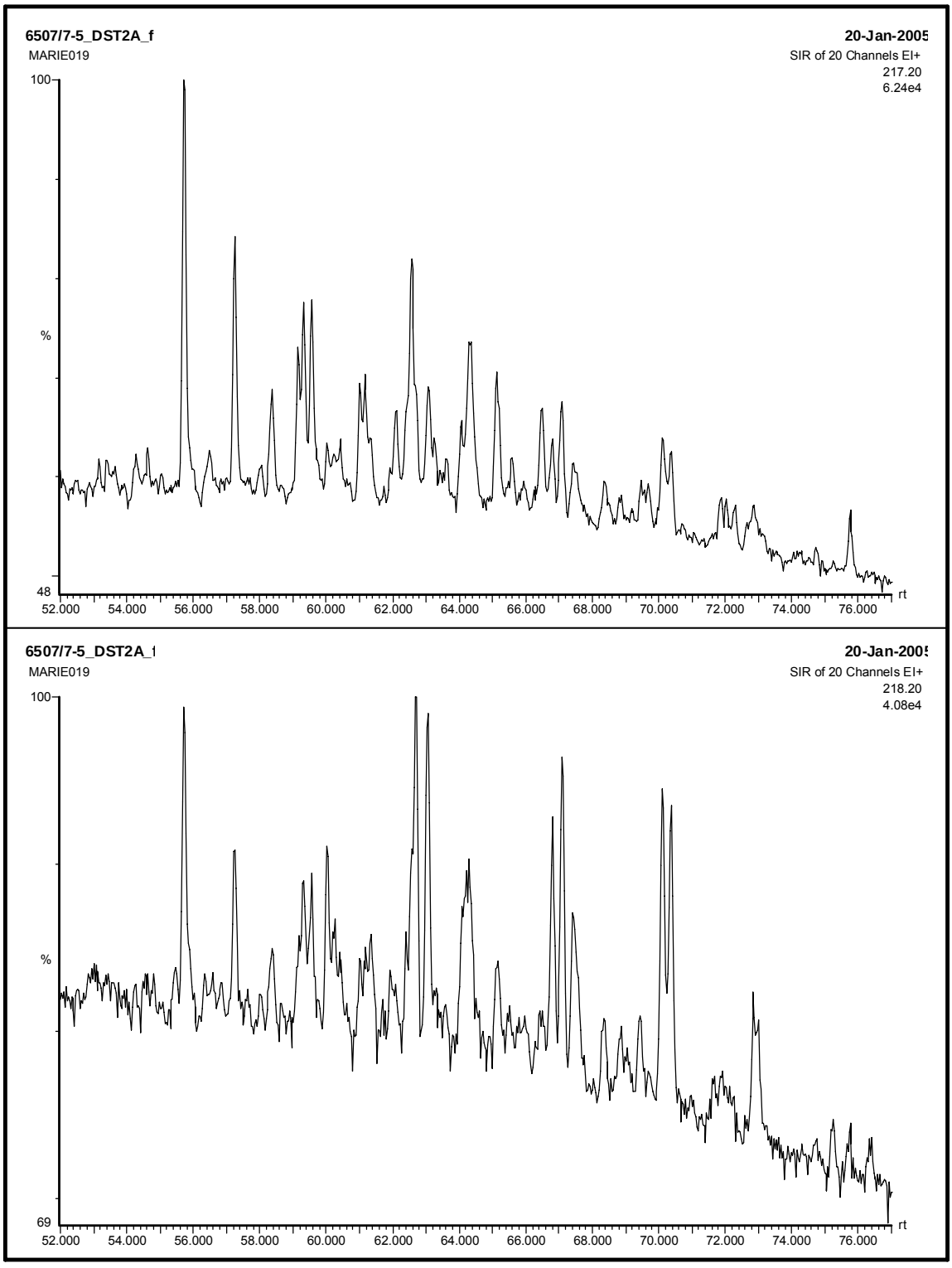

6507/7-5 DST2A

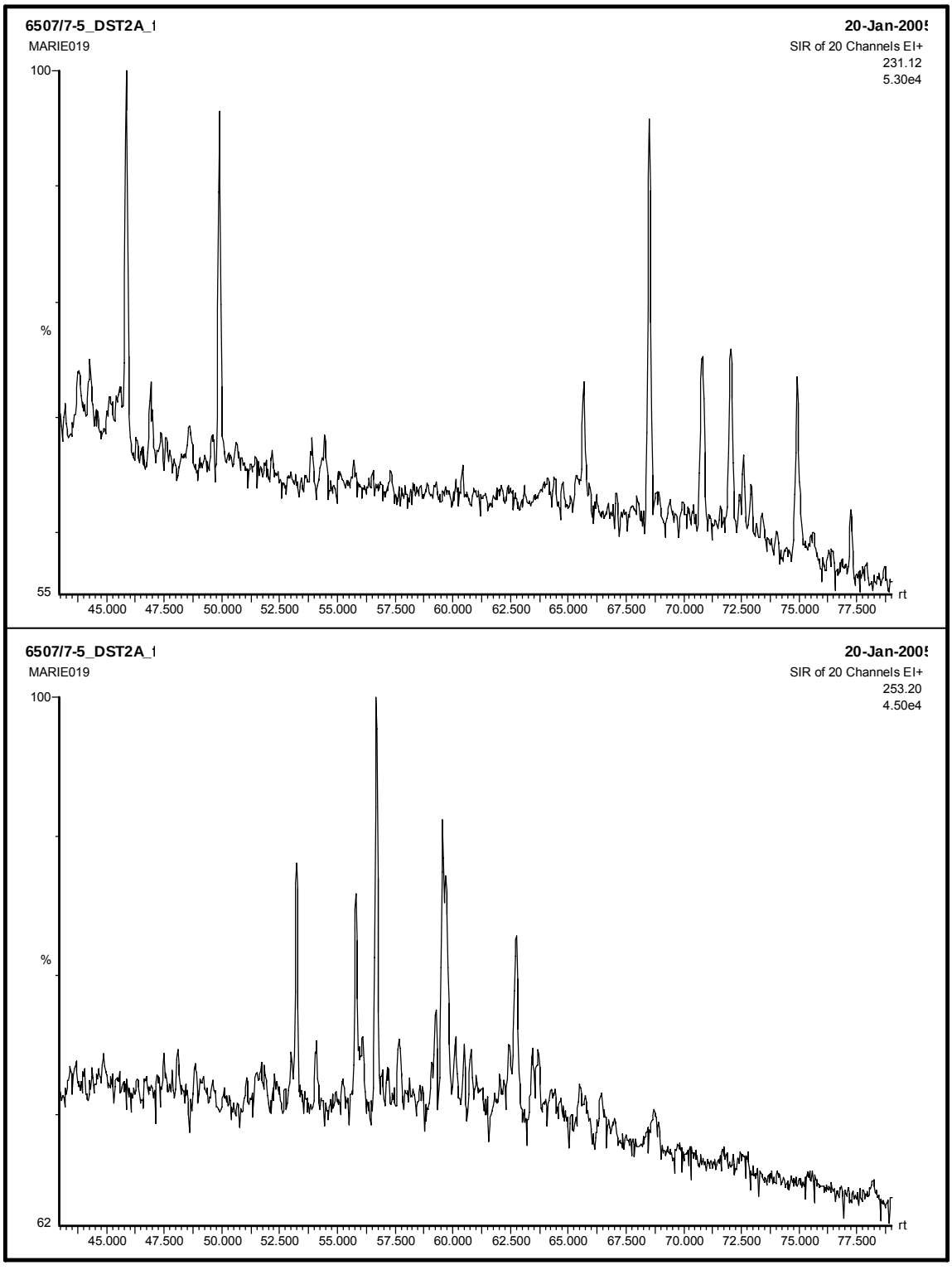

6507/7-5 DST2A

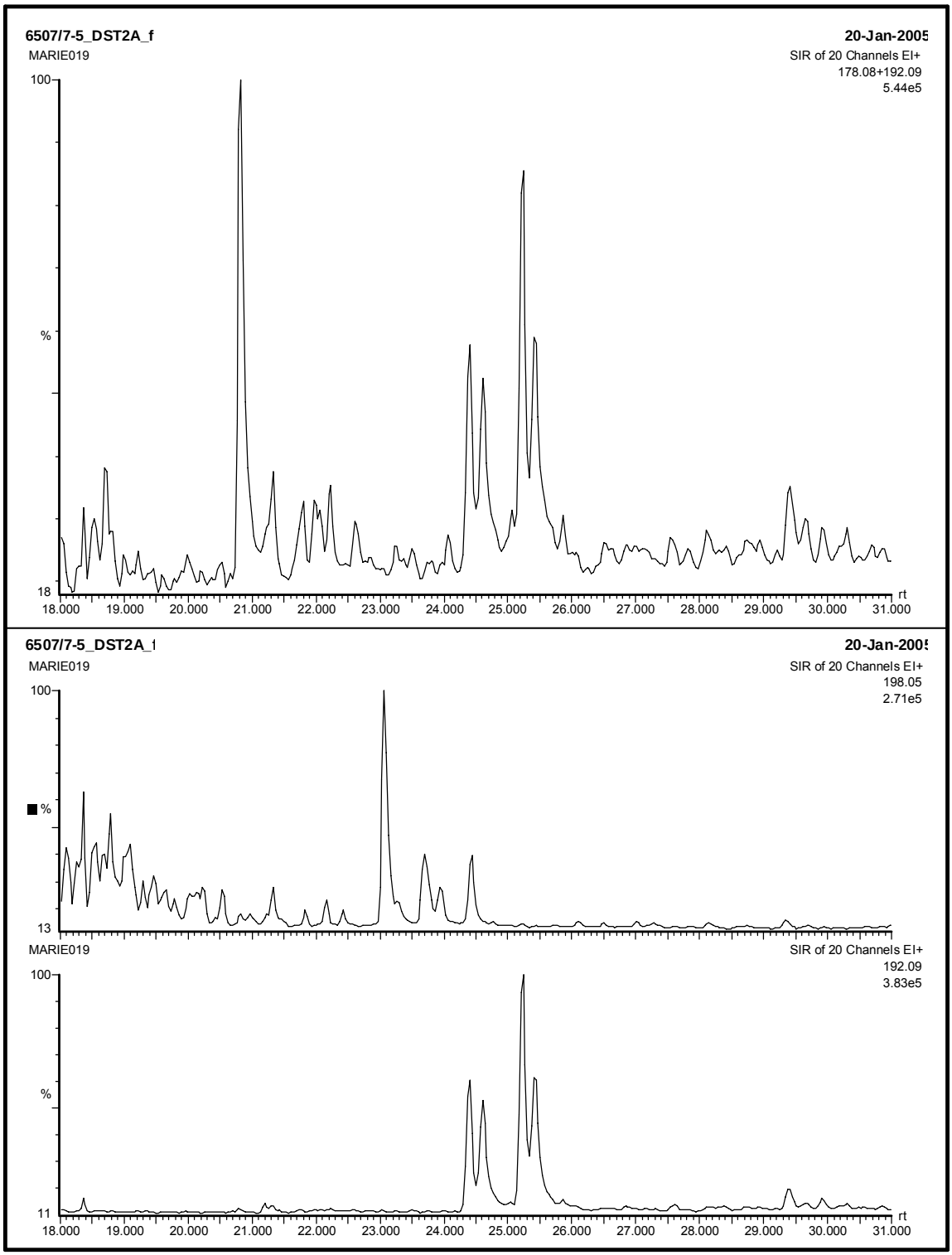

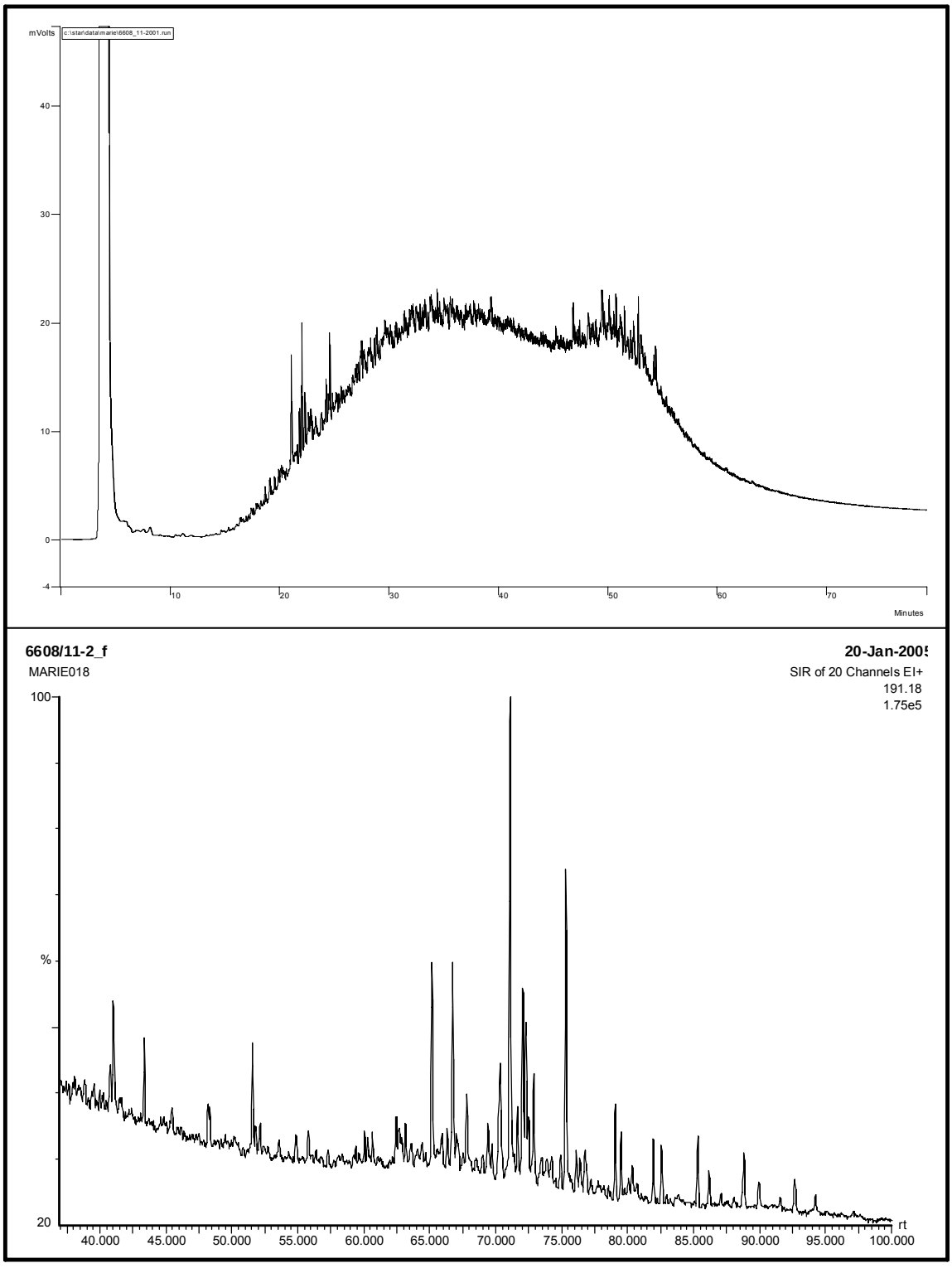
mVolts
c:\star\data\marie\6608_11-2001.run
40
30
20
10
0
-4
10
20
30
40
50
60
70
Minutes
6608/11-2_f
MARIE018
20-Jan-2005
SIR of 20 Channels EI+
191.18
1.75e5
100
%
20
40.000
45.000
50.000
55.000
60.000
65.000
70.000
75.000
80.000
85.000
90.000
95.000
100.000
rt

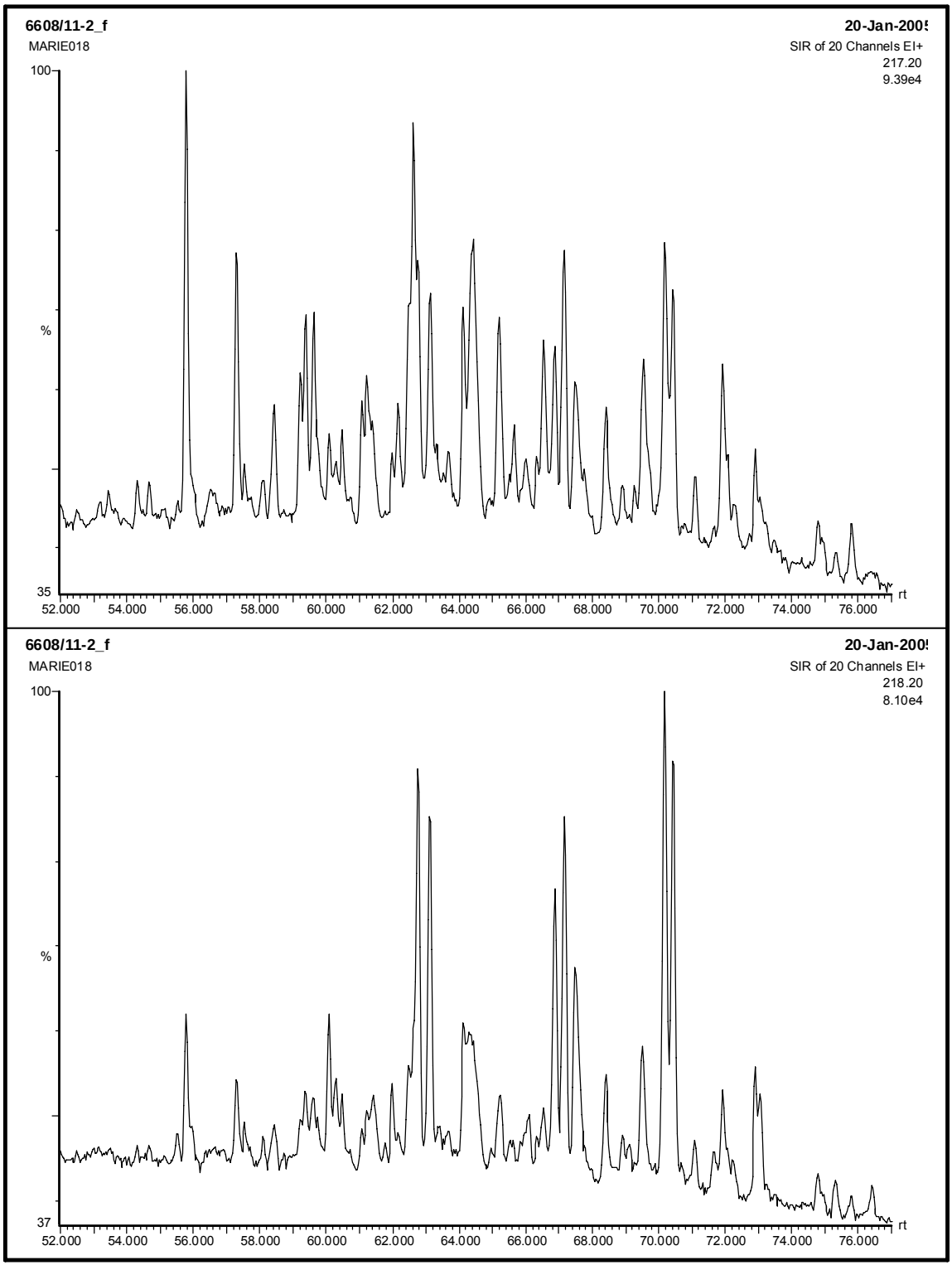
6608/11-2_f
MARIE018
20-Jan-200
SIR of 20 Channels EI+
217.20
9.39e4
100
%
35
52.000 54.000 56.000 58.000 60.000 62.000 64.000 66.000 68.000 70.000 72.000 74.000 76.000
rt
6608/11-2_f
MARIE018
20-Jan-200
SIR of 20 Channels EI+
218.20
8.10e4
100
%
37
52.000 54.000 56.000 58.000 60.000 62.000 64.000 66.000 68.000 70.000 72.000 74.000 76.000
rt

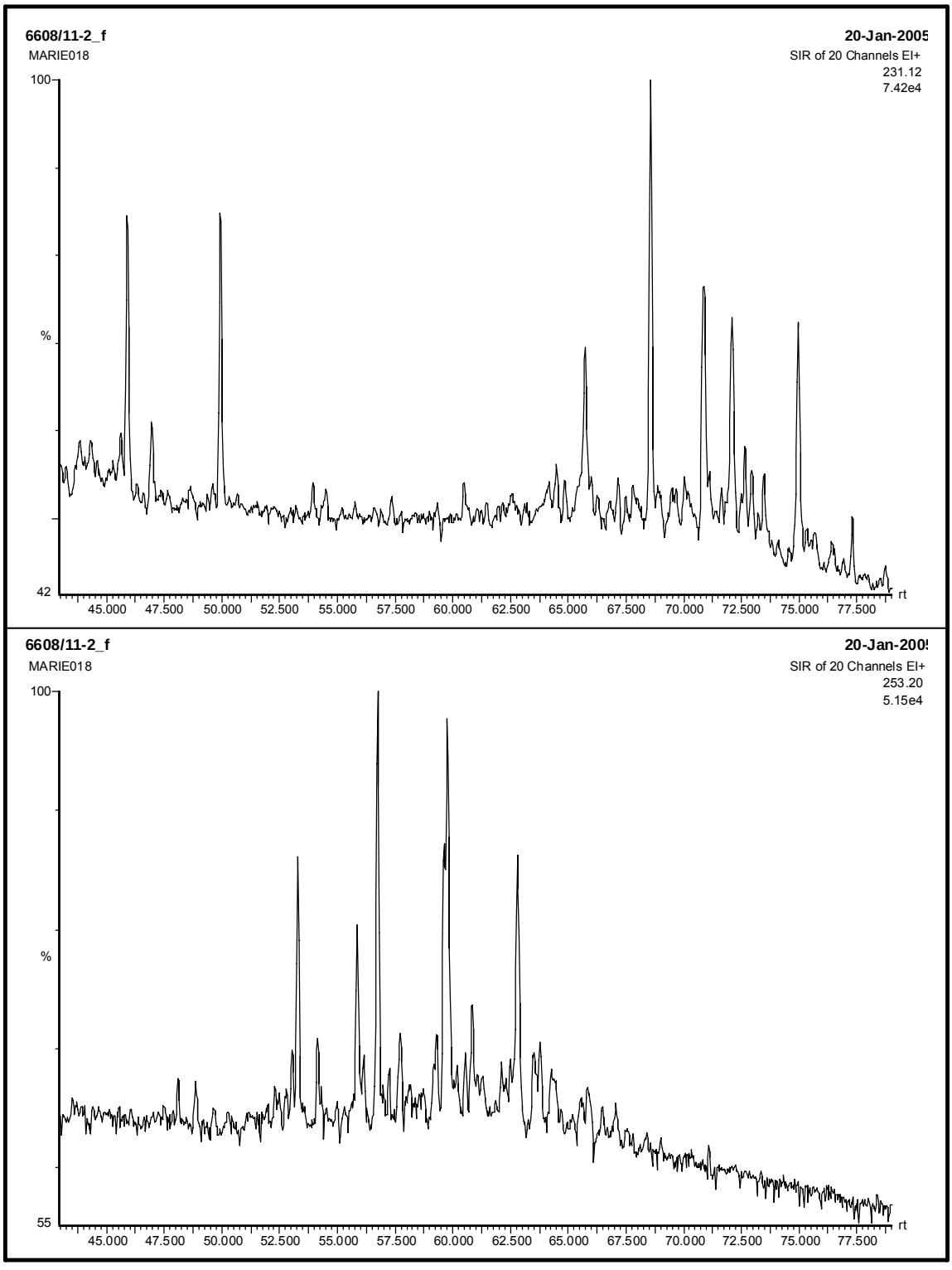
6608/11-2_f
MARIE018
20-Jan-2005
SIR of 20 Channels EI+
231.12
7.42e4
100
%
42
45.000 47.500 50.000 52.500 55.000 57.500 60.000 62.500 65.000 67.500 70.000 72.500 75.000 77.500
rt
6608/11-2_f
MARIE018
20-Jan-2005
SIR of 20 Channels EI+
253.20
5.15e4
100
%
55
45.000 47.500 50.000 52.500 55.000 57.500 60.000 62.500 65.000 67.500 70.000 72.500 75.000 77.500
rt

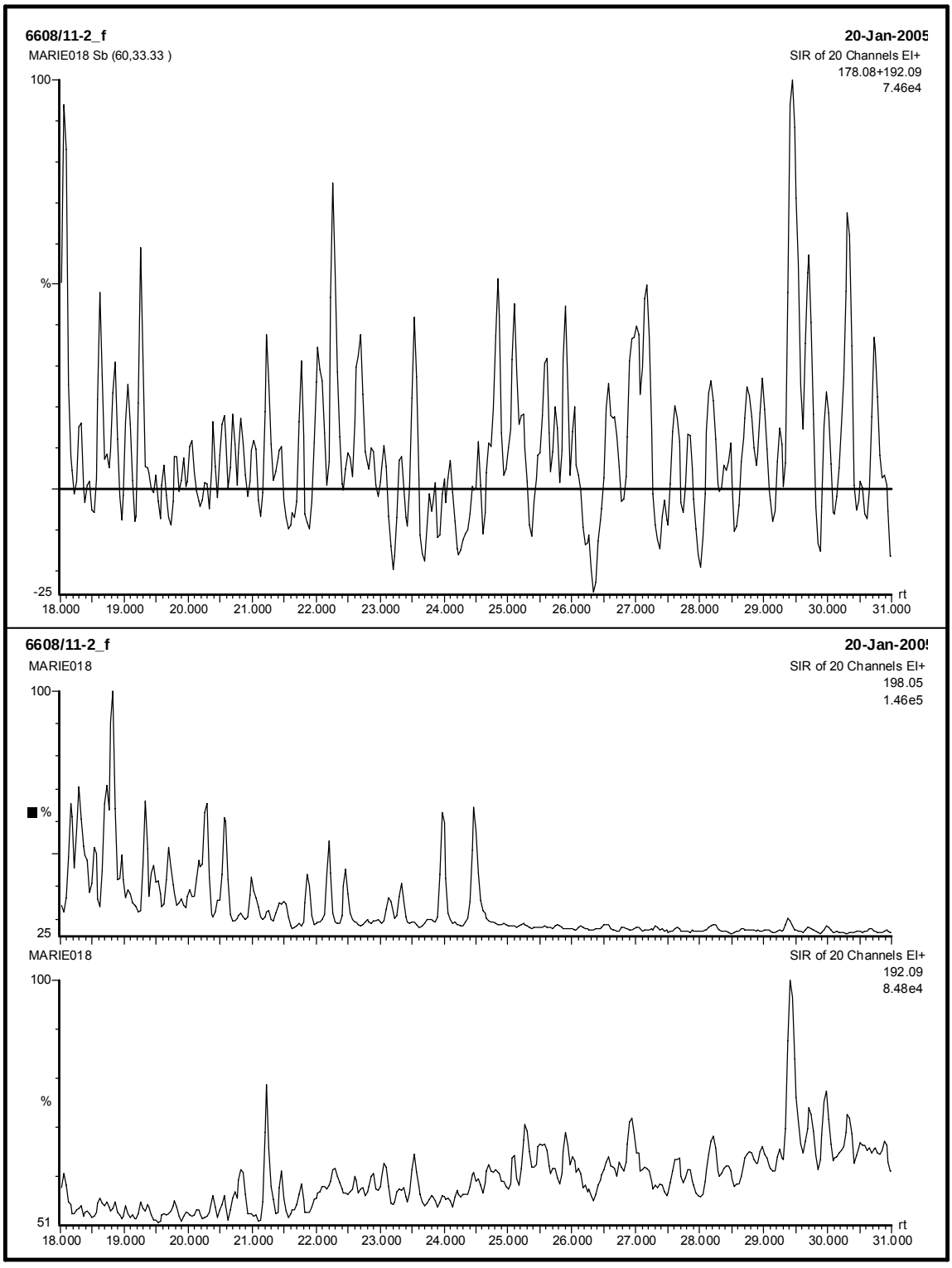
6608/11-2_f
20-Jan-2005
MARIE018 Sb (60,33.33)
SIR of 20 Channels EI+
178.08+192.09
7.46e4
100
%
-25
18.000 19.000 20.000 21.000 22.000 23.000 24.000 25.000 26.000 27.000 28.000 29.000 30.000 31.000
rt
6608/11-2_f
20-Jan-2005
MARIE018
SIR of 20 Channels EI+
198.05
1.46e5
100
%
25
MARIE018
SIR of 20 Channels EI+
192.09
8.48e4
100
%
51
18.000 19.000 20.000 21.000 22.000 23.000 24.000 25.000 26.000 27.000 28.000 29.000 30.000 31.000
rt

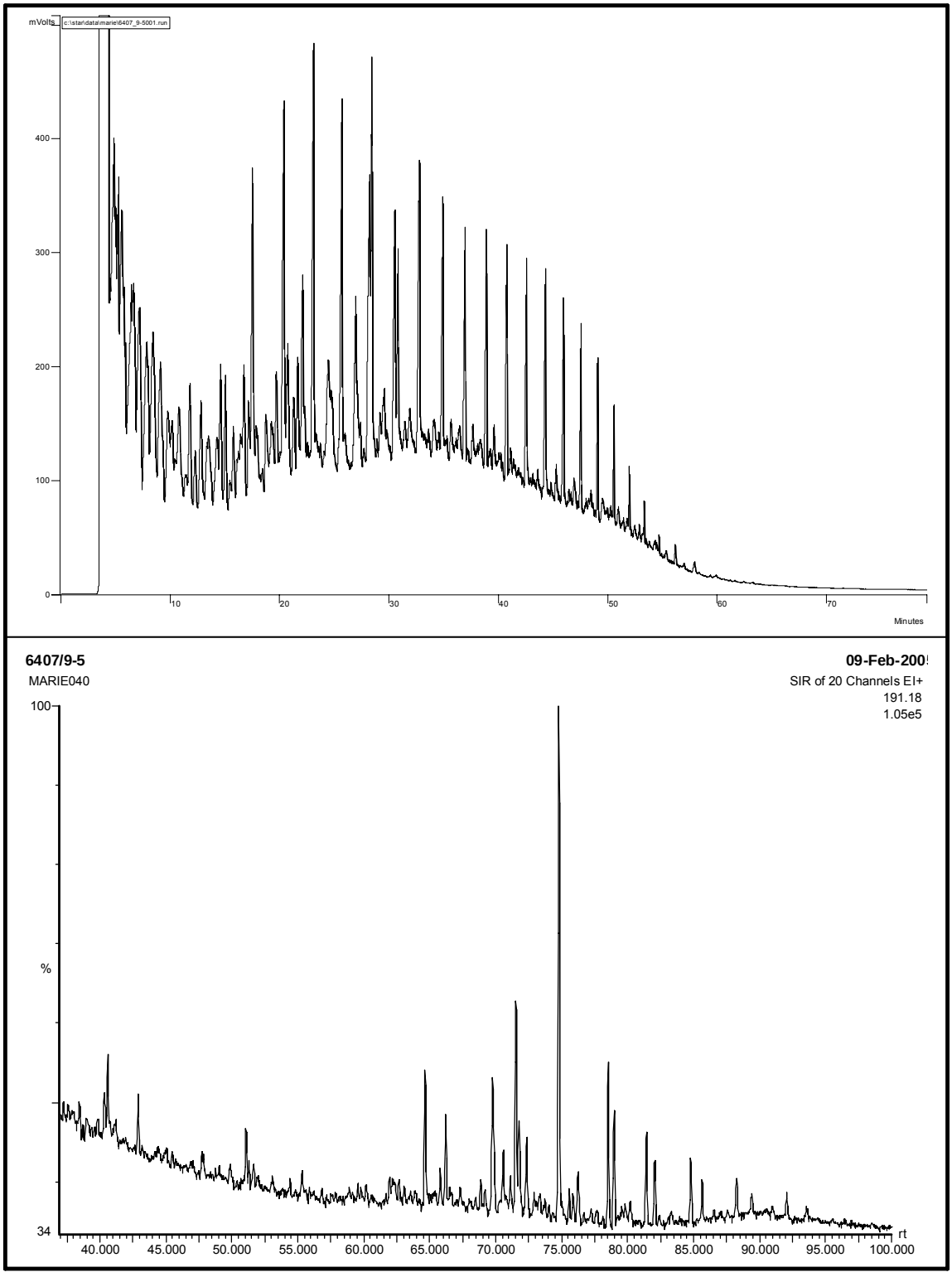
mVolts
c:\star\data\marie\6407_9-5001.run
400
300
200
100
0
10
20
30
40
50
60
70
Minutes
6407/9-5
MARIE040
09-Feb-200
SIR of 20 Channels EI+
191.18
1.05e5
100
%
34
40.000
45.000
50.000
55.000
60.000
65.000
70.000
75.000
80.000
85.000
90.000
95.000
100.000
rt

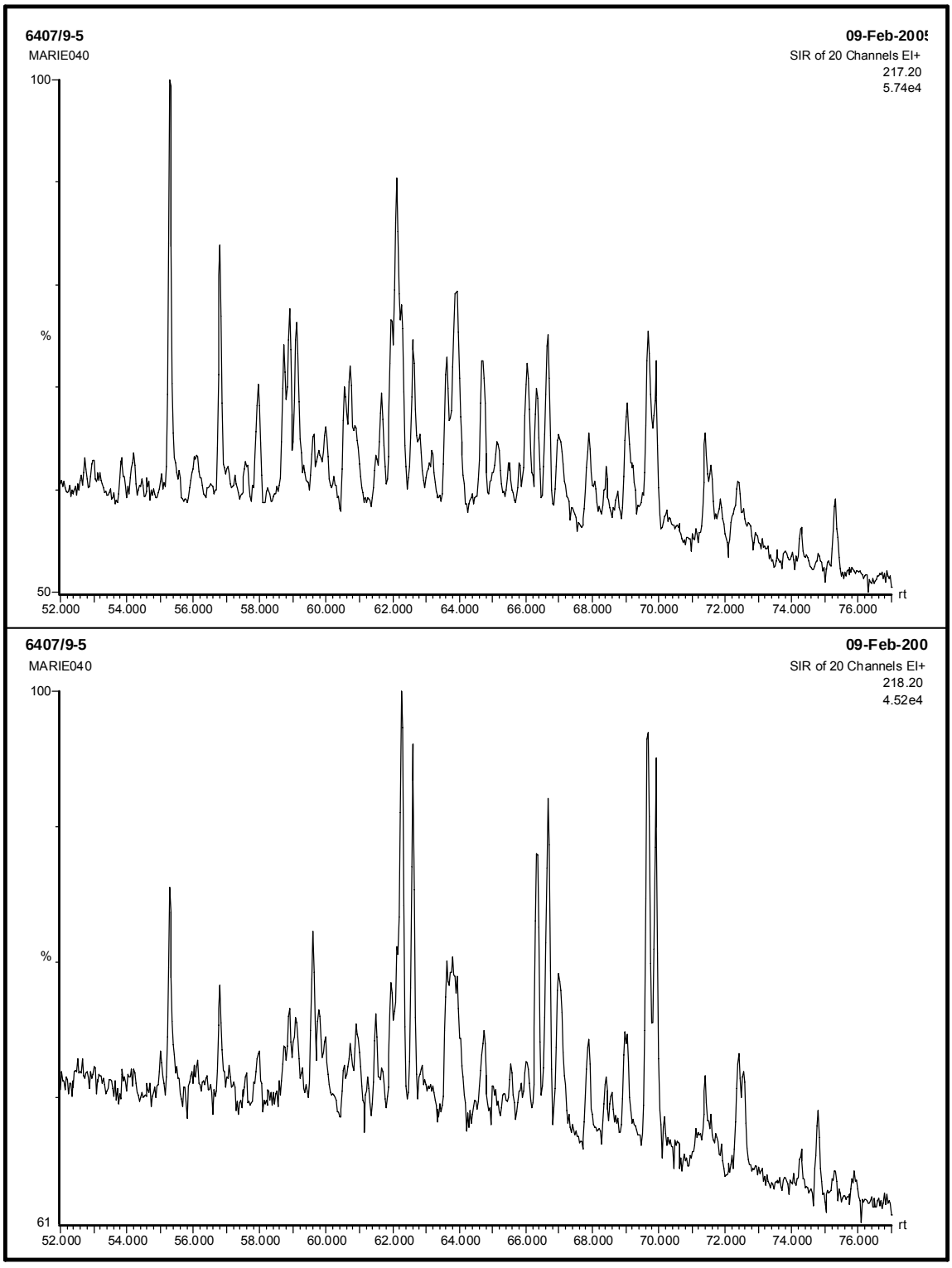
6407/9-5
MARIE040
09-Feb-200
SIR of 20 Channels EI+
217.20
5.74e4
100
%
50
52.000
54.000
56.000
58.000
60.000
62.000
64.000
66.000
68.000
70.000
72.000
74.000
76.000
rt
6407/9-5
MARIE040
09-Feb-200
SIR of 20 Channels EI+
218.20
4.52e4
100
%
61
52.000
54.000
56.000
58.000
60.000
62.000
64.000
66.000
68.000
70.000
72.000
74.000
76.000
rt

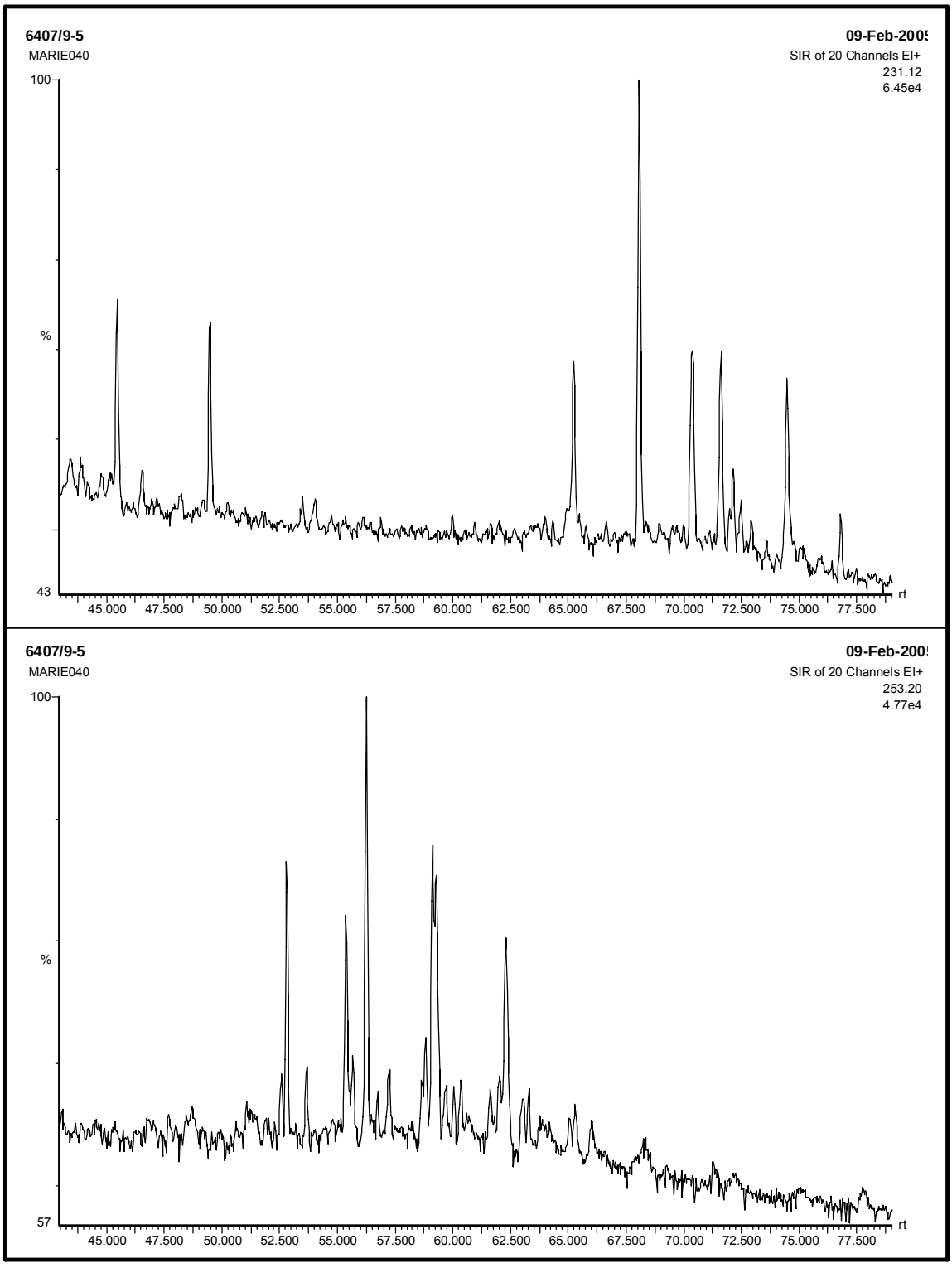
6407/9-5
MARIE040
09-Feb-200
SIR of 20 Channels EI+
231.12
6.45e4
100
%
43
45.000 47.500 50.000 52.500 55.000 57.500 60.000 62.500 65.000 67.500 70.000 72.500 75.000 77.500
rt
6407/9-5
MARIE040
09-Feb-200
SIR of 20 Channels EI+
253.20
4.77e4
100
%
57
45.000 47.500 50.000 52.500 55.000 57.500 60.000 62.500 65.000 67.500 70.000 72.500 75.000 77.500
rt

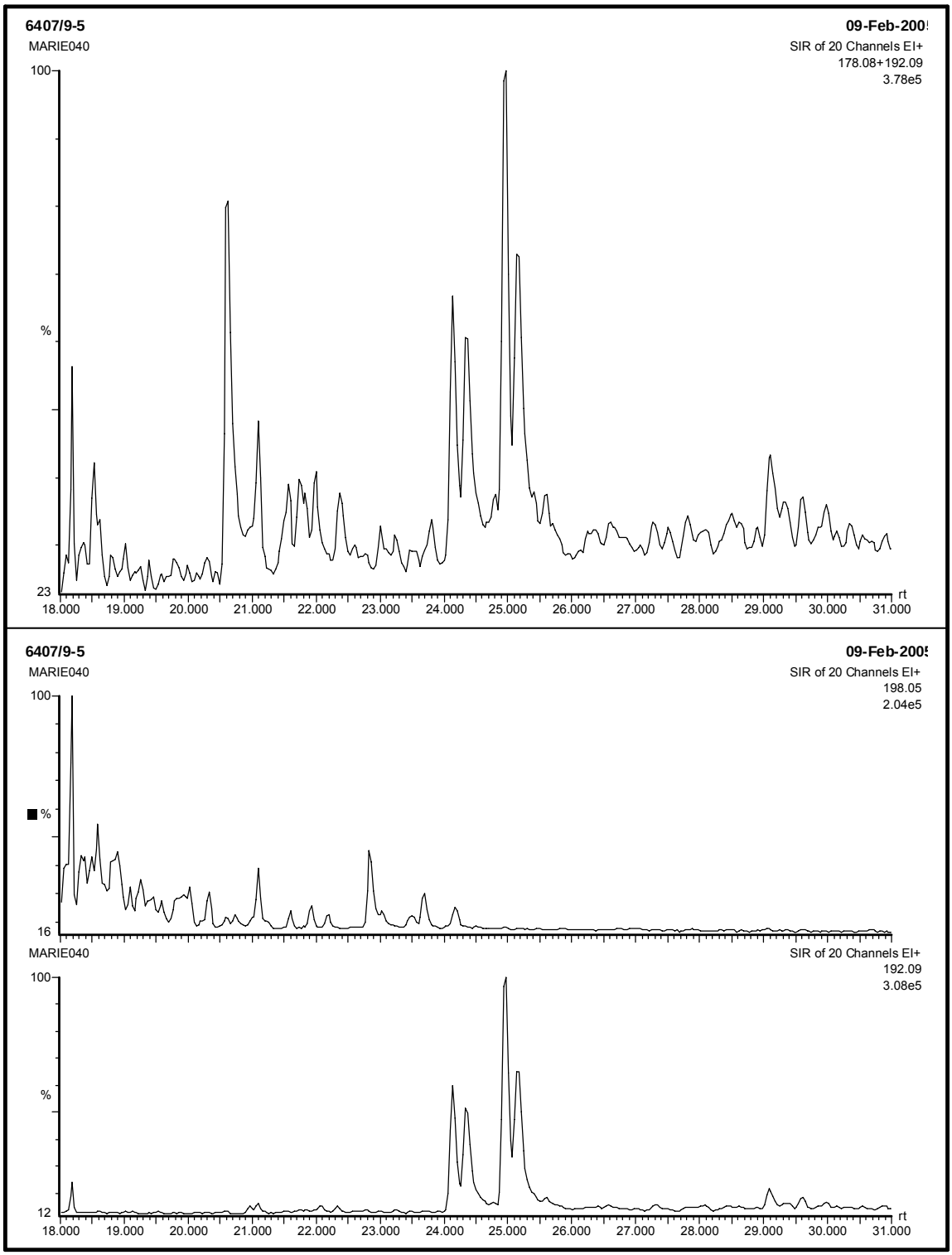
6407/9-5
09-Feb-200
MARIE040
SIR of 20 Channels EI+
178.08+192.09
3.78e5
100
%
23
18.000 19.000 20.000 21.000 22.000 23.000 24.000 25.000 26.000 27.000 28.000 29.000 30.000 31.000
rt
6407/9-5
09-Feb-200
MARIE040
SIR of 20 Channels EI+
198.05
2.04e5
100
%
16
MARIE040
SIR of 20 Channels EI+
192.09
3.08e5
100
%
12
18.000 19.000 20.000 21.000 22.000 23.000 24.000 25.000 26.000 27.000 28.000 29.000 30.000 31.000
rt

B IMP

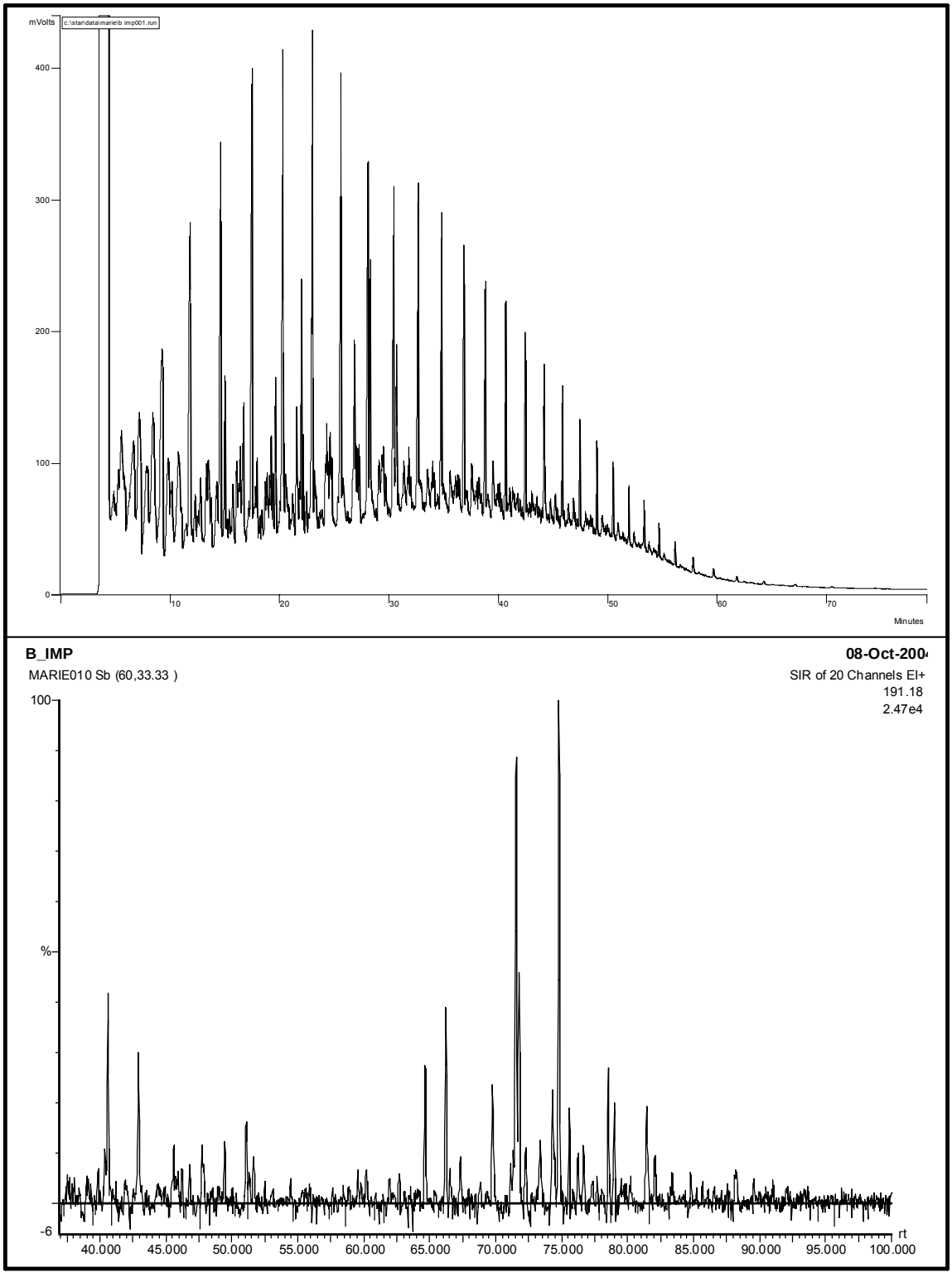
mVolts
c:\star\data\marie\b imp001.run
400
300
200
100
0
10
20
30
40
50
60
70
Minutes
B_IMP
08-Oct-200
MARIE010 Sb (60,33.33)
SIR of 20 Channels EI+
191.18
2.47e4
100
%
-6
40.000
45.000
50.000
55.000
60.000
65.000
70.000
75.000
80.000
85.000
90.000
95.000
100.000
rt

B IMP

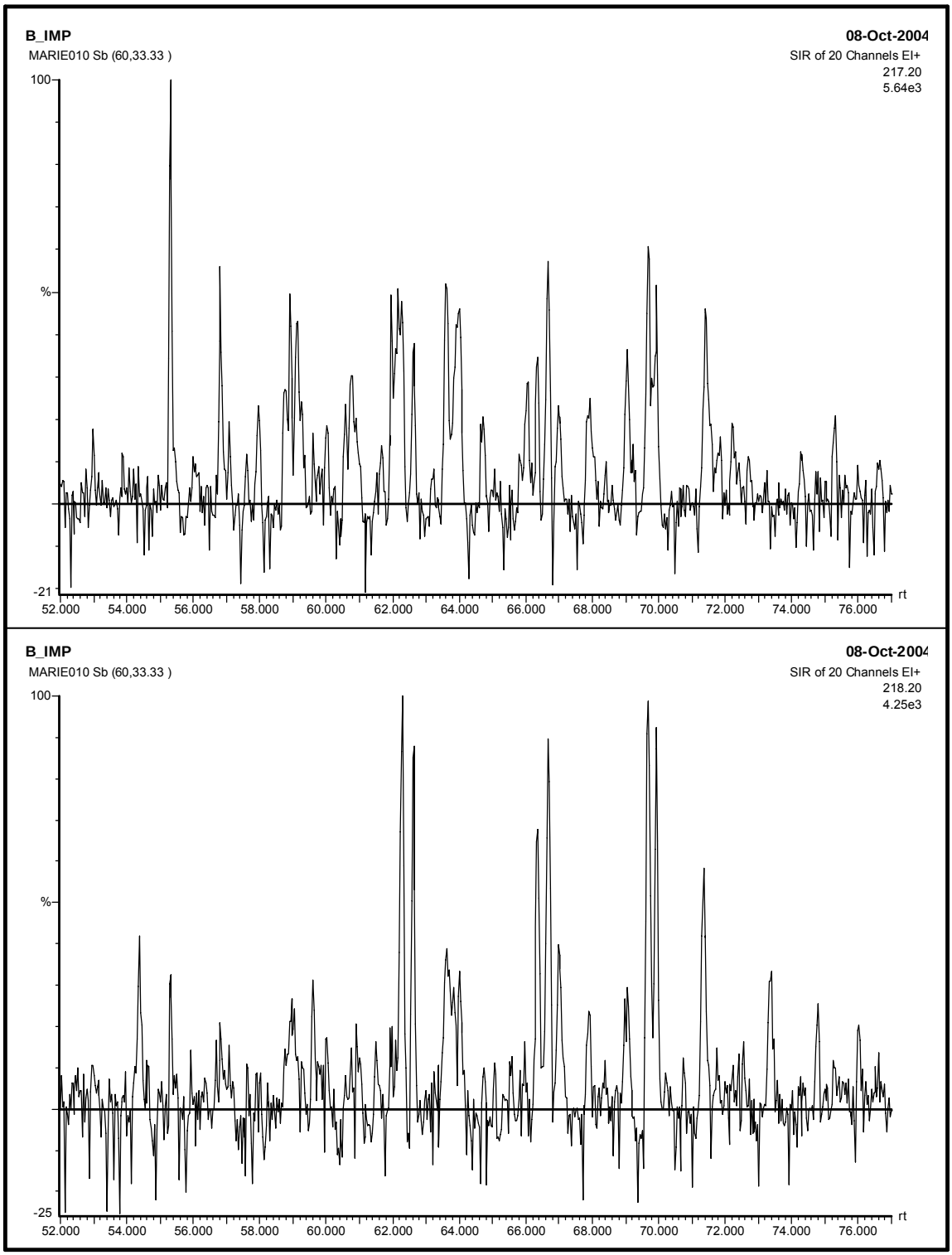
B_IMP
MARIE010 Sb (60,33.33)
08-Oct-2004
SIR of 20 Channels EI+
217.20
5.64e3
100
%
-21
rt
52.000
54.000
56.000
58.000
60.000
62.000
64.000
66.000
68.000
70.000
72.000
74.000
76.000
B_IMP
MARIE010 Sb (60,33.33)
08-Oct-2004
SIR of 20 Channels EI+
218.20
4.25e3
100
%
-25
rt
52.000
54.000
56.000
58.000
60.000
62.000
64.000
66.000
68.000
70.000
72.000
74.000
76.000

B IMP

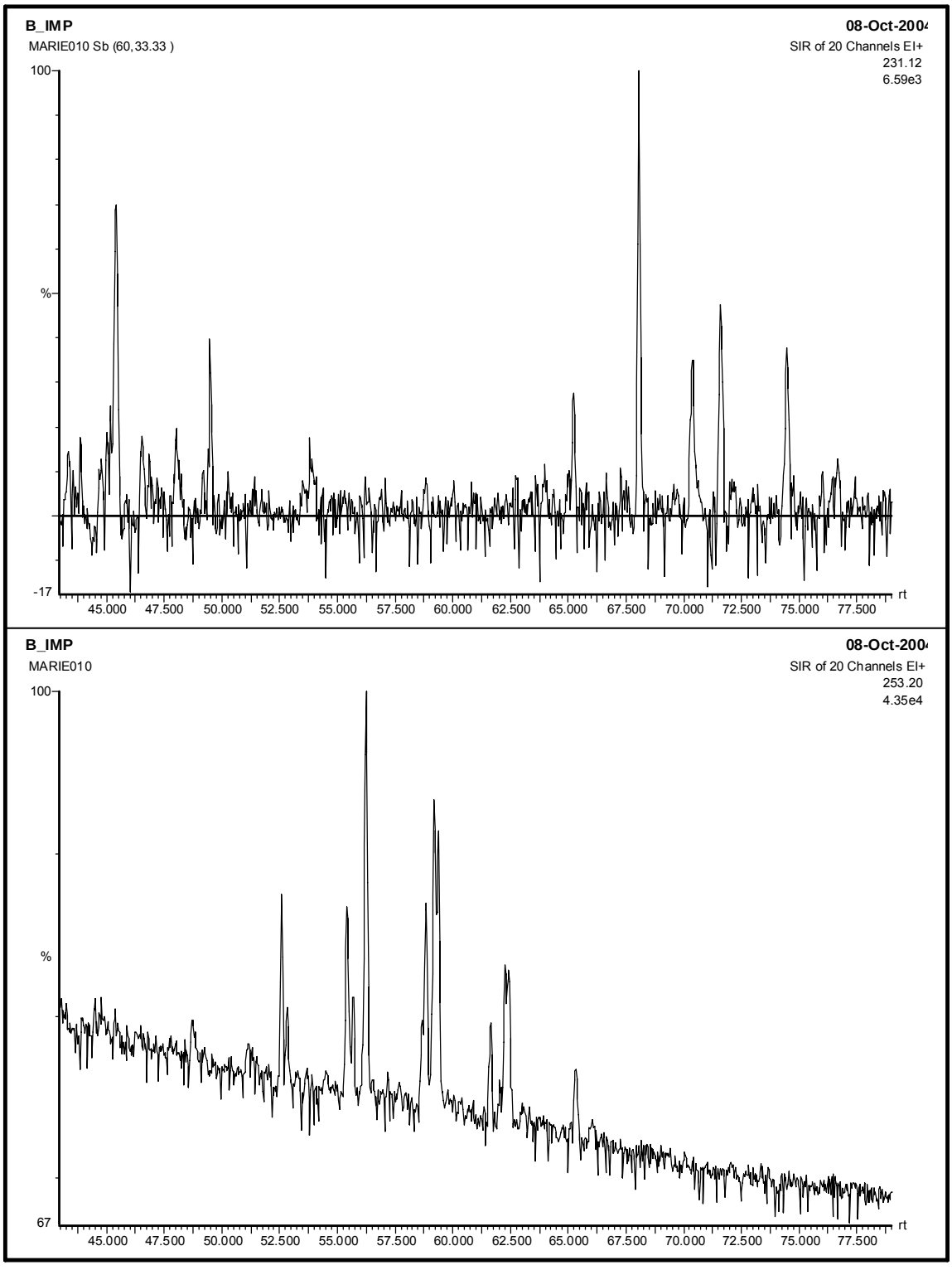
B_IMP
08-Oct-200
MARIE010 Sb (60,33.33)
SIR of 20 Channels EI+
231.12
6.59e3
100
%
-17
45.000 47.500 50.000 52.500 55.000 57.500 60.000 62.500 65.000 67.500 70.000 72.500 75.000 77.500
rt
B_IMP
08-Oct-200
MARIE010
SIR of 20 Channels EI+
253.20
4.35e4
100
%
67
45.000 47.500 50.000 52.500 55.000 57.500 60.000 62.500 65.000 67.500 70.000 72.500 75.000 77.500
rt

B IMP

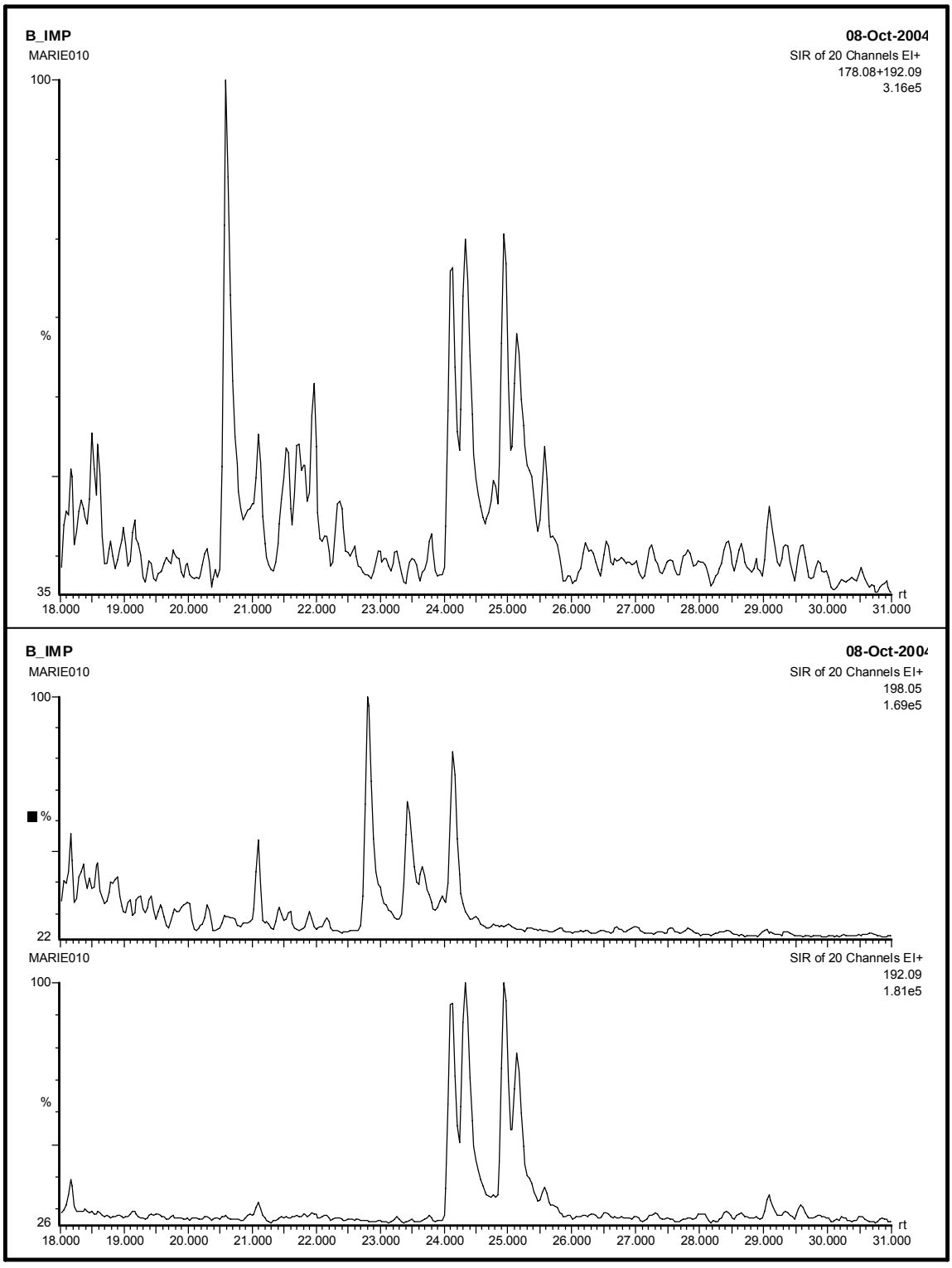
B_IMP
08-Oct-2004
MARIE010
SIR of 20 Channels EI+
178.08+192.09
3.16e5
100
%
35
18.000
19.000
20.000
21.000
22.000
23.000
24.000
25.000
26.000
27.000
28.000
29.000
30.000
31.000
rt
B_IMP
08-Oct-2004
MARIE010
SIR of 20 Channels EI+
198.05
1.69e5
100
%
22
MARIE010
SIR of 20 Channels EI+
192.09
1.81e5
100
%
26
18.000
19.000
20.000
21.000
22.000
23.000
24.000
25.000
26.000
27.000
28.000
29.000
30.000
31.000
rt

7/12-6 DST1

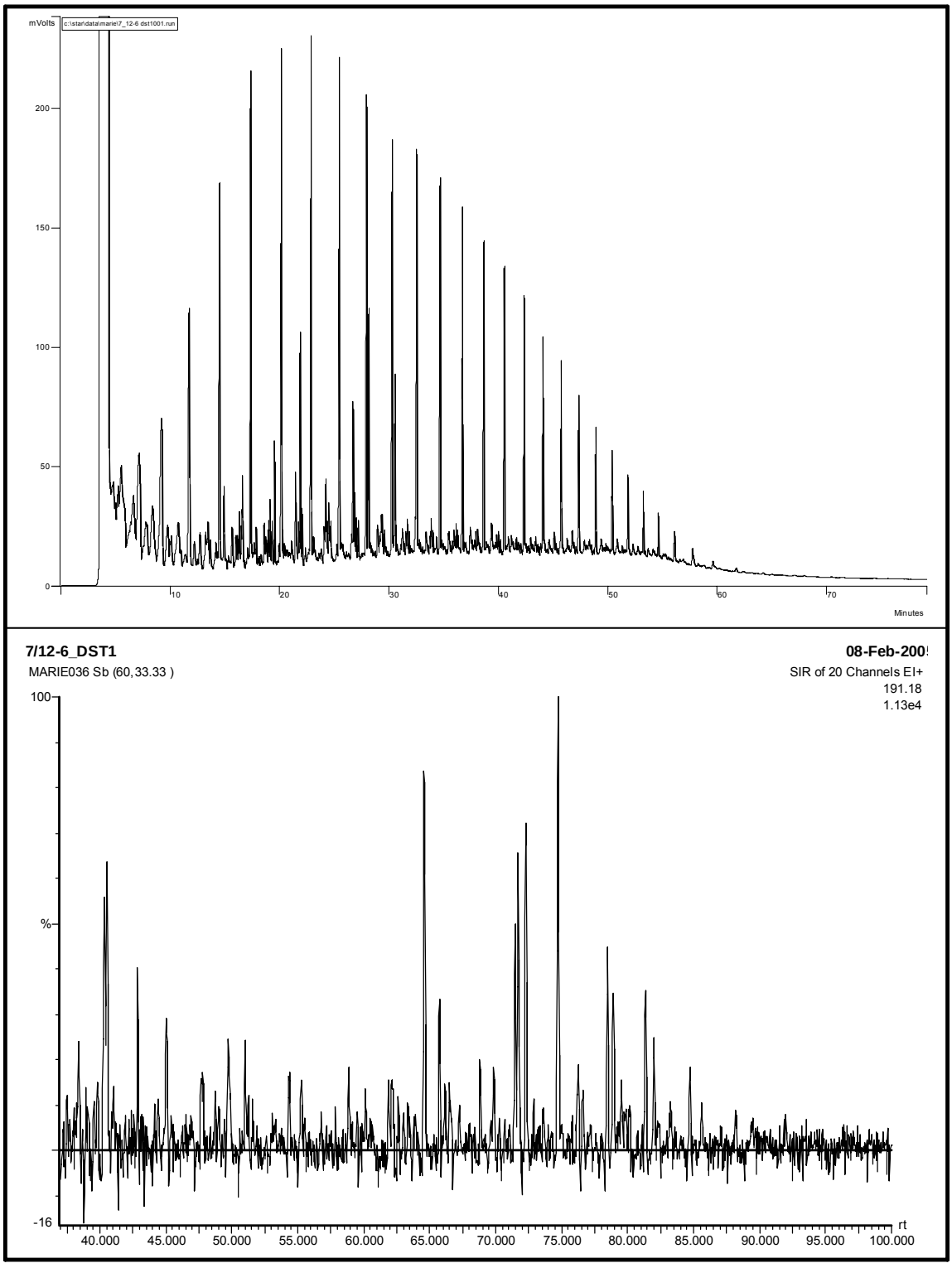
mVolts
c:\star\data\marie\7_12-6 dst1001.run
200
150
100
50
0
10
20
30
40
50
60
70
Minutes
7/12-6_DST1
MARIE036 Sb (60,33.33)
08-Feb-200
SIR of 20 Channels EI+
191.18
1.13e4
100
%
-16
40.000
45.000
50.000
55.000
60.000
65.000
70.000
75.000
80.000
85.000
90.000
95.000
100.000
rt

7/12-6 DST1

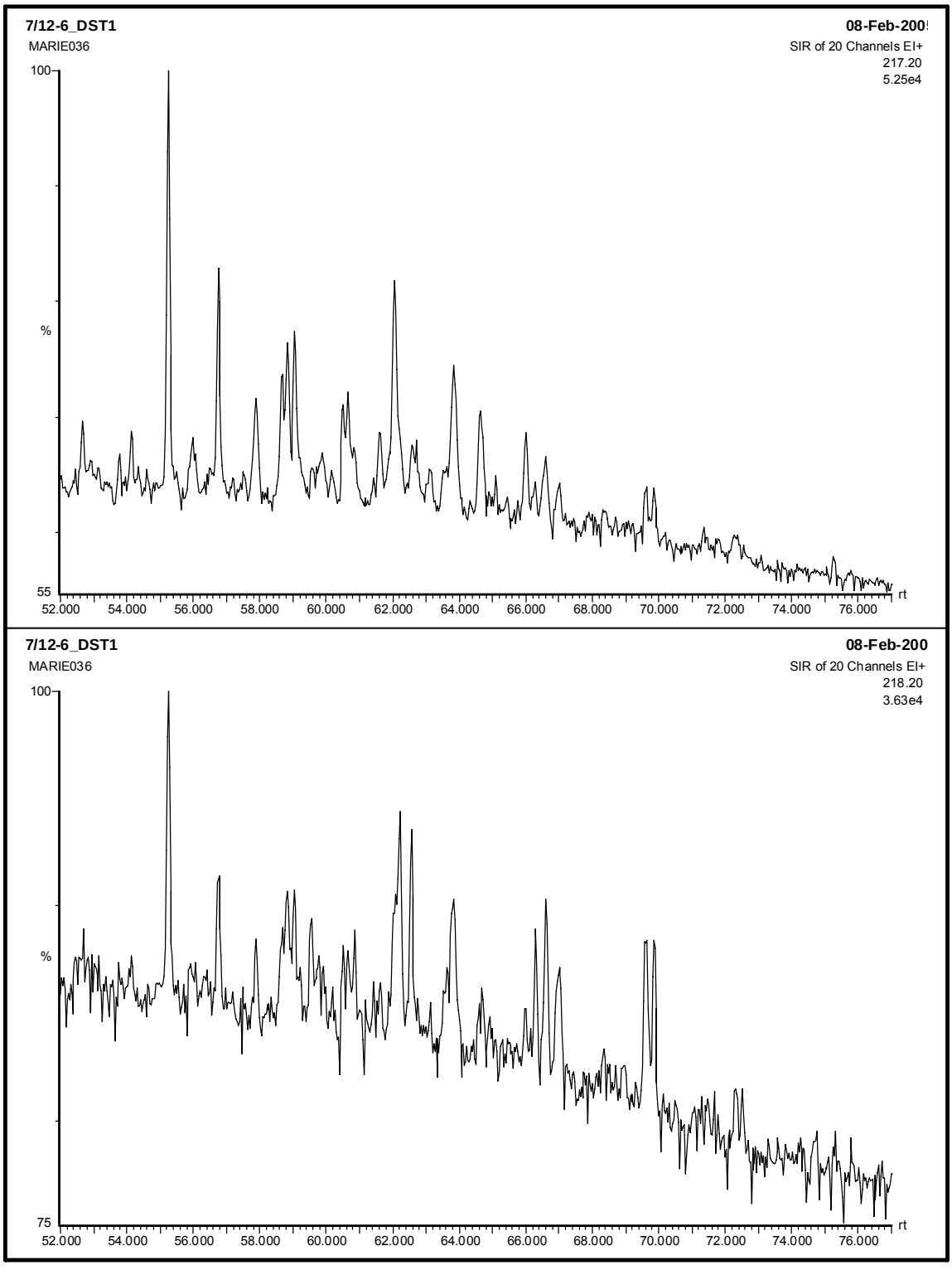
7/12-6_DST1
MARIE036
08-Feb-200
SIR of 20 Channels EI+
217.20
5.25e4
100
%
55
52.000
54.000
56.000
58.000
60.000
62.000
64.000
66.000
68.000
70.000
72.000
74.000
76.000
rt
7/12-6_DST1
MARIE036
08-Feb-200
SIR of 20 Channels EI+
218.20
3.63e4
100
%
75
52.000
54.000
56.000
58.000
60.000
62.000
64.000
66.000
68.000
70.000
72.000
74.000
76.000
rt

7/12-6 DST1

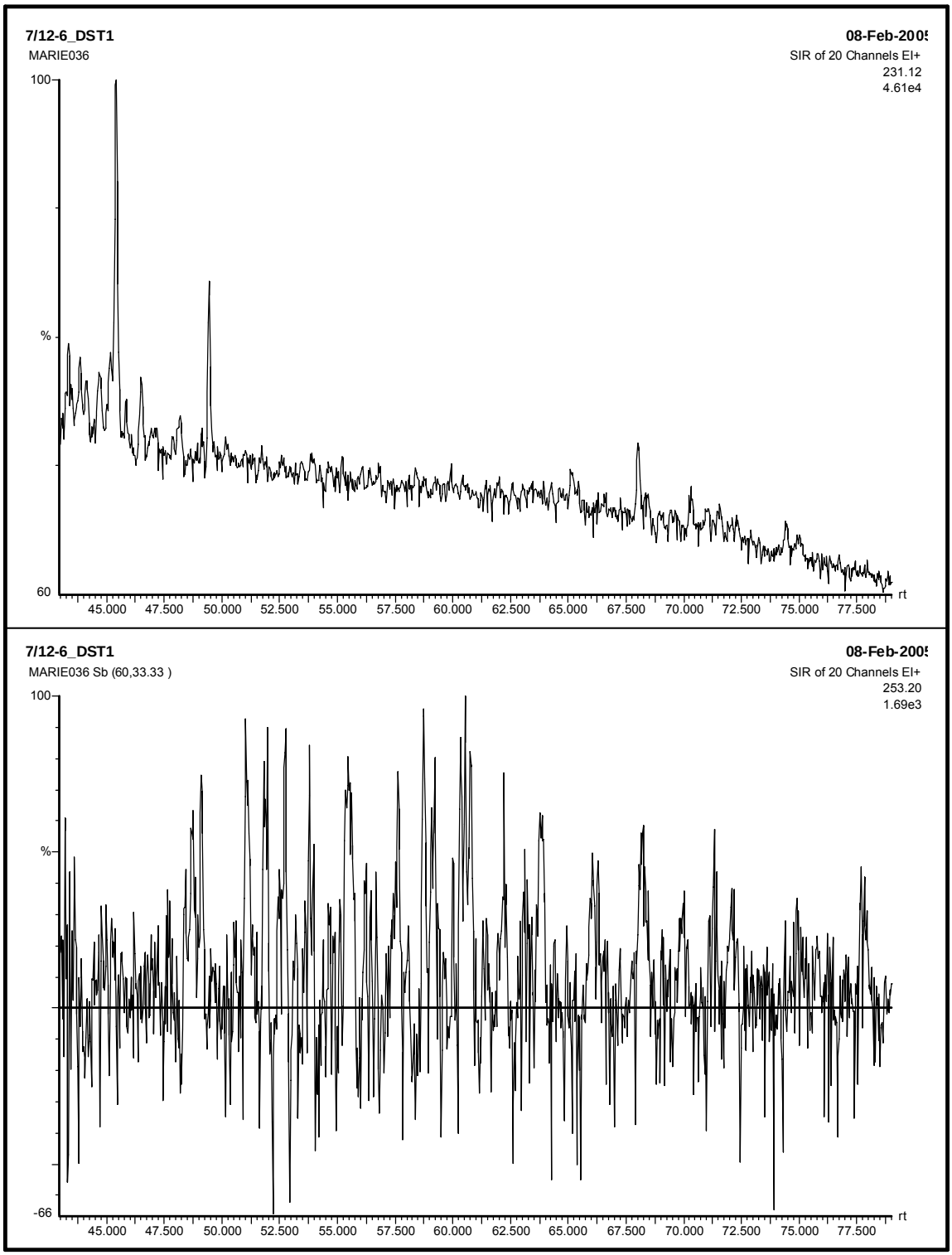
7/12-6_DST1
MARIE036
08-Feb-200
SIR of 20 Channels EI+
231.12
4.61e4
100
%
60
45.000 47.500 50.000 52.500 55.000 57.500 60.000 62.500 65.000 67.500 70.000 72.500 75.000 77.500
rt
7/12-6_DST1
MARIE036 Sb (60,33.33)
08-Feb-200
SIR of 20 Channels EI+
253.20
1.69e3
100
%
-66
45.000 47.500 50.000 52.500 55.000 57.500 60.000 62.500 65.000 67.500 70.000 72.500 75.000 77.500
rt

7/12-6 DST1

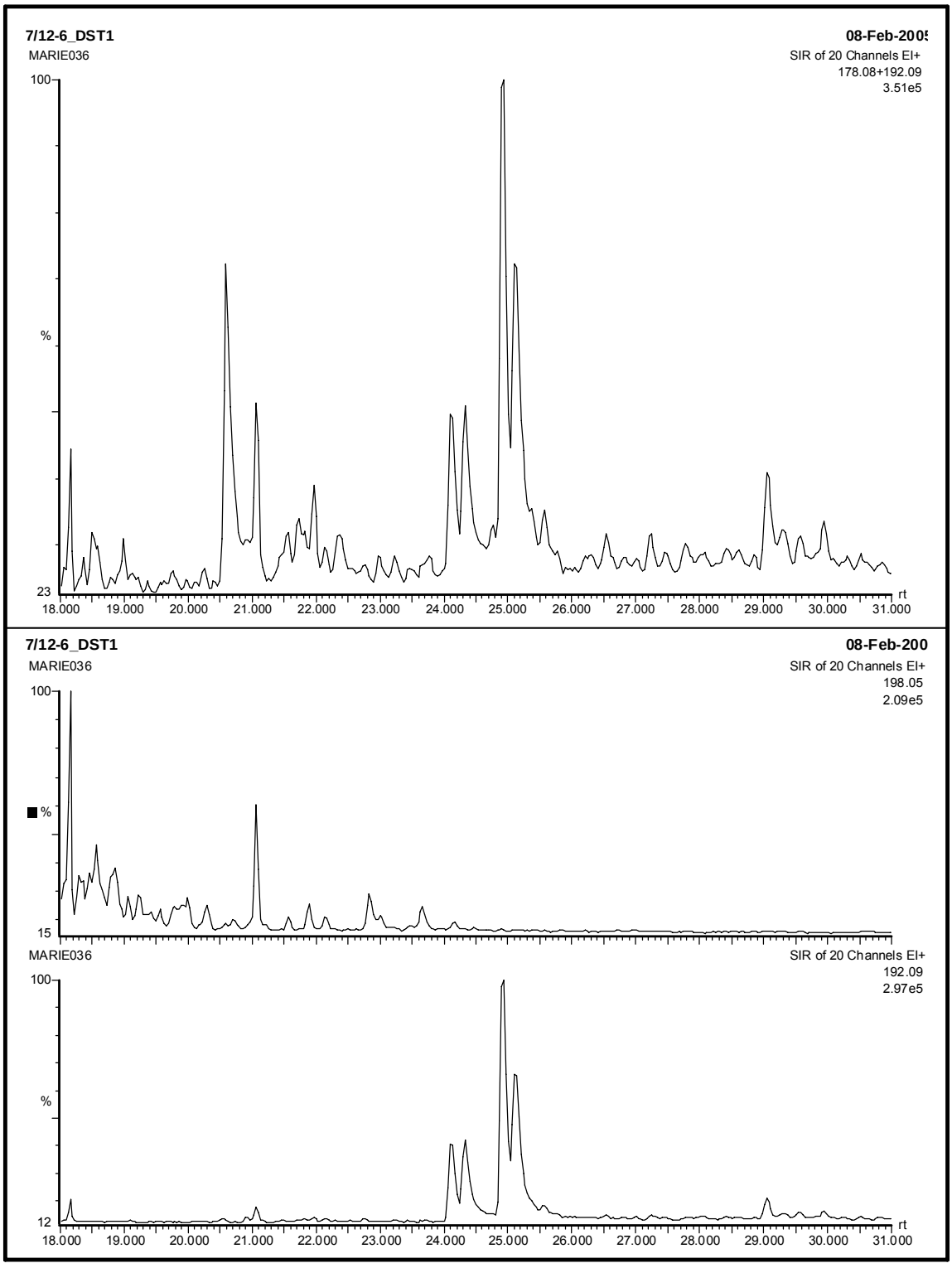
7/12-6_DST1
08-Feb-200
MARIE036
SIR of 20 Channels EI+
178.08+192.09
3.51e5
100
%
23
18.000 19.000 20.000 21.000 22.000 23.000 24.000 25.000 26.000 27.000 28.000 29.000 30.000 31.000
rt
7/12-6_DST1
08-Feb-200
MARIE036
SIR of 20 Channels EI+
198.05
2.09e5
100
%
15
MARIE036
SIR of 20 Channels EI+
192.09
2.97e5
100
%
12
18.000 19.000 20.000 21.000 22.000 23.000 24.000 25.000 26.000 27.000 28.000 29.000 30.000 31.000
rt

NSO-1

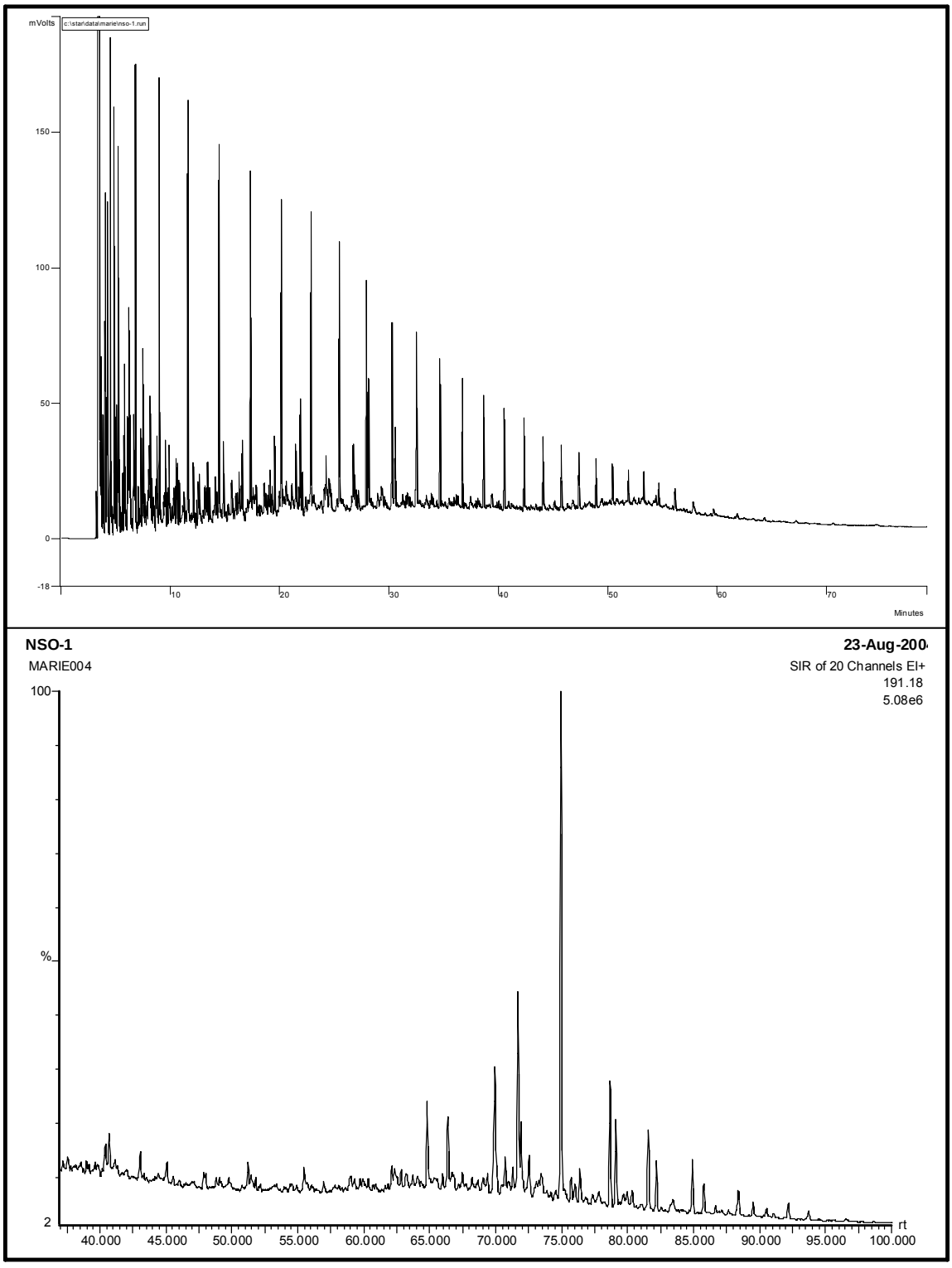
mVolts
c:\star\data\marie\nso-1.run
150
100
50
0
-18
10
20
30
40
50
60
70
Minutes
NSO-1
MARIE004
23-Aug-200
SIR of 20 Channels EI+
191.18
5.08e6
100
%
2
40.000
45.000
50.000
55.000
60.000
65.000
70.000
75.000
80.000
85.000
90.000
95.000
100.000
rt

NSO-1

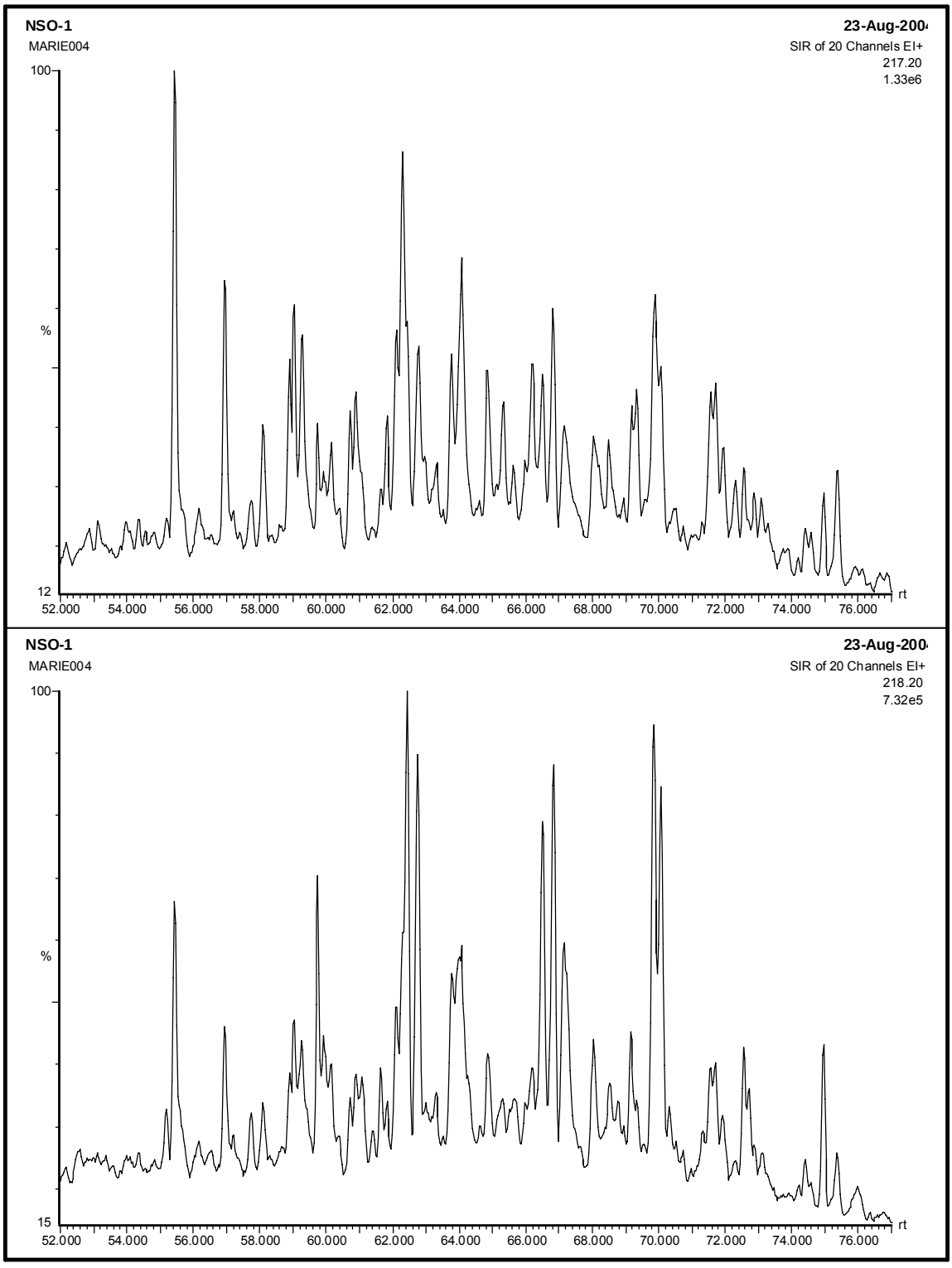
NSO-1
MARIE004
23-Aug-200
SIR of 20 Channels EI+
217.20
1.33e6
100
%
12
52.000
54.000
56.000
58.000
60.000
62.000
64.000
66.000
68.000
70.000
72.000
74.000
76.000
rt
NSO-1
MARIE004
23-Aug-200
SIR of 20 Channels EI+
218.20
7.32e5
100
%
15
52.000
54.000
56.000
58.000
60.000
62.000
64.000
66.000
68.000
70.000
72.000
74.000
76.000
rt

NSO-1

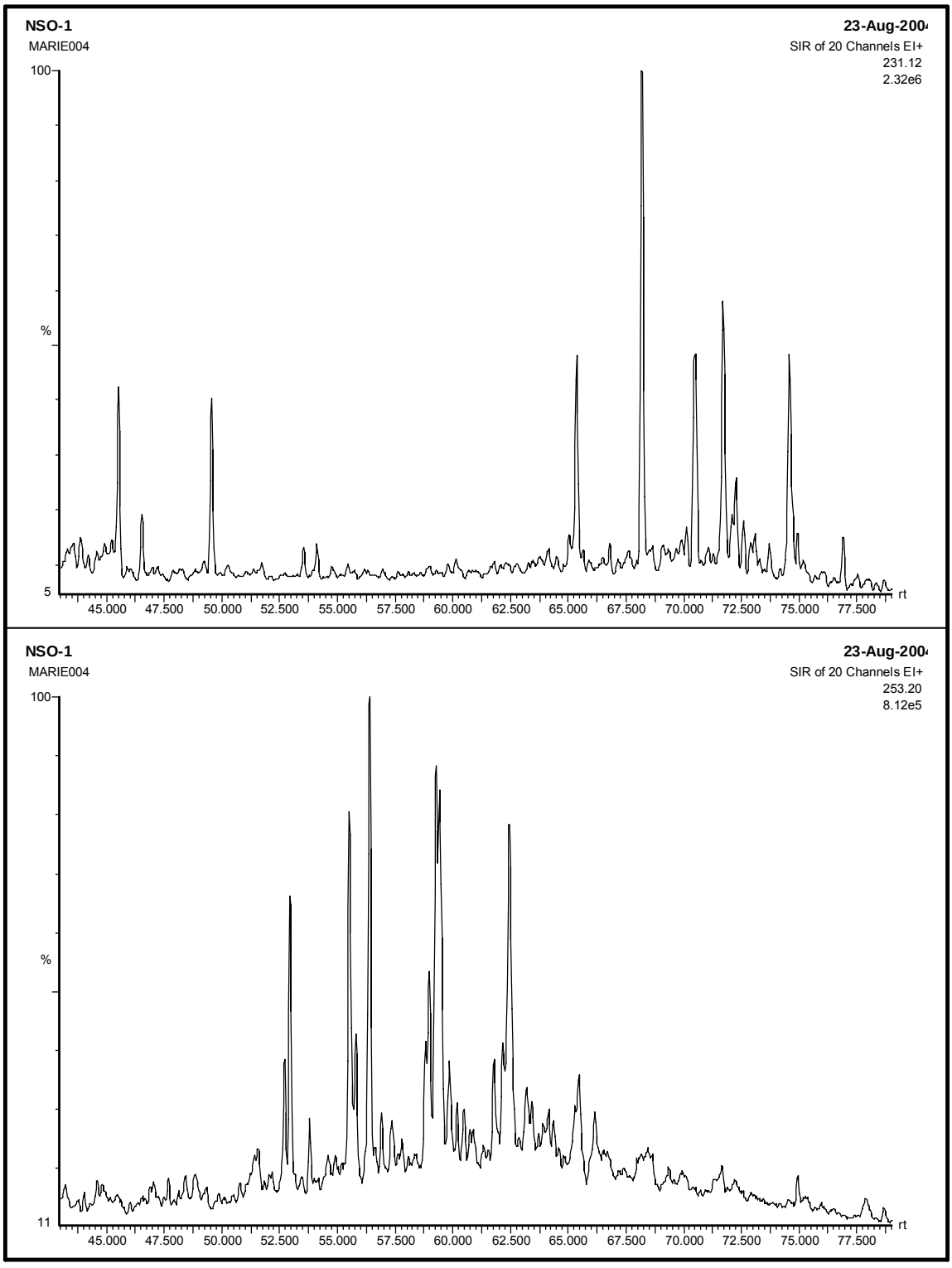
NSO-1
MARIE004
23-Aug-200
SIR of 20 Channels EI+
231.12
2.32e6
100
%
5
45.000 47.500 50.000 52.500 55.000 57.500 60.000 62.500 65.000 67.500 70.000 72.500 75.000 77.500
rt
NSO-1
MARIE004
23-Aug-200
SIR of 20 Channels EI+
253.20
8.12e5
100
%
11
45.000 47.500 50.000 52.500 55.000 57.500 60.000 62.500 65.000 67.500 70.000 72.500 75.000 77.500
rt

NSO-1

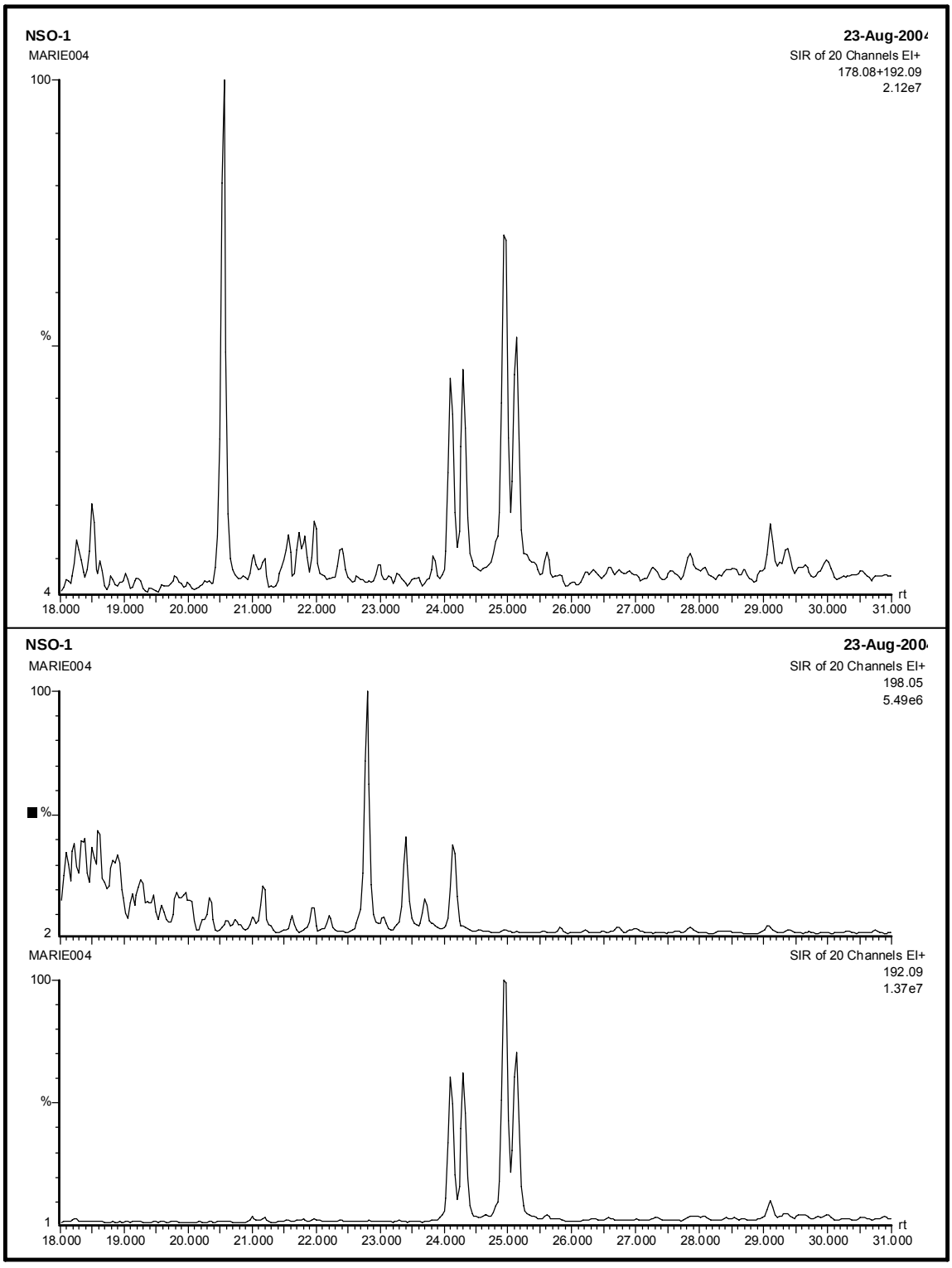
NSO-1
MARIE004
23-Aug-200
SIR of 20 Channels EI+
178.08+192.09
2.12e7
100
%
4
18.000 19.000 20.000 21.000 22.000 23.000 24.000 25.000 26.000 27.000 28.000 29.000 30.000 31.000
rt
NSO-1
MARIE004
23-Aug-200
SIR of 20 Channels EI+
198.05
5.49e6
100
%
2
MARIE004
SIR of 20 Channels EI+
192.09
1.37e7
100
%
1
18.000 19.000 20.000 21.000 22.000 23.000 24.000 25.000 26.000 27.000 28.000 29.000 30.000 31.000
rt